ICCG-10

TENTH INTERNATIONAL CONFERENCE ON CRYSTAL GROWTH

August 16 - 21, 1992
Sheraton Harbor Island Hotel
San Diego, California, USA

POSTER PRESENTATION ABSTRACTS

ICCG-10
POSTER PRESENTATION ABSTRACTS

INDEX

AD NUMBER	DATE	DTIC ACCESSION NOTICE
A256938	92	

1. REPORT IDENTIFYING INFORMATION

A. ORIGINATING AGENCY
MIT (Poster Presentation Abstracts)

B. REPORT TITLE AND/OR NUMBER
Third International Conference on Crystal Growth

C. MONITOR REPORT NUMBER
ARO 29062.1-MS-CF

D. PREPARED UNDER CONTRACT NUMBER
DAAL03-92-G-0042

2. DISTRIBUTION STATEMENT

A

REQUESTER:

1. *Put your mailing address on reverse of form.*
2. *Complete items 1 and 2.*
3. *Attach form to reports mailed to DTIC.*
4. *Use unclassified information only.*
5. *Do not order document for 6 to 8 weeks.*

DTIC:

1. *Assign AD Number.*
2. *Return to requester.*

DTIC Form 50 Mar 91 — PREVIOUS EDITIONS ARE OBSOLETE

DEFENSE LOGISTICS AGENCY
Defense Technical Information Center
Building #5, Cameron Station
Alexandria, Virginia 22304-6145

OFFICIAL BUSINESS
PENALTY FOR PRIVATE USE, $300

U.S. Army Research Office
ATTN: Technical Library
Post Office Box 12211
Research Triangle Park, NC 27709-2211

File Copy
OCC

ICCG-10

ORGANIZING COMMITTEES

	CHAIRPERSONS	COMMITTEE PERSONS
CONFERENCE CO-CHAIRMEN:	W.A. Bonner J.F. Wenckus	
TECHNICAL PROGRAM:	R.S. Feigelson R.F. Sekerka	Reviewers M. Brown, R. Brown, C. Bugg, B. Chai, T. Ciszek, S. Coriell, M. DiGiuseppe, E. Giess, M. Glicksman, R. Hopkins, A. Jordan, E. Monberg, P. Morris, G. Nancollas, K. Nassau, H. Olsen, J. Olson, F. Ponce, F. Rosenberger, L. Schneemeyer, D. Shaw, G. Sloan, G. Stringfellow, A. Witt.
LOCAL ARRANGEMENTS:	A.L. Gentile R.R. Monchamp	F.P. Doty, H. Olsen, L. Rothrock, B. Wechsler.
INDUSTRIAL EXHIBIT:	L. Colombo S. Samuelson	
FINANCE:	T. Kuech	
PROCEEDINGS EDITORS:	J.B. Mullin T. Surek	Subject Chairpersons (Partial List) J. Abell, I. Alexander, K. Barraclough, R. Belt, K. Bertness, G. Blom, M. Brown, B. Chai, K. Cheng, T. Ciszek, S. Coriell, R. DeMattei, J. Derby, A. Elliot, V. Fratello, E. Giess, M. Glicksman, R. Hopkins, D. Hurle, D. Kaiser, J. Kalejs, R. McConnell, A. McPherson, E. Monberg, P. Morris, D. Nason, M. Pusey, K. Ravi, R. Reynolds, F. Rosenberger, H. Schaake, L. Schneemeyer, F. Szofran
CORPORATE SPONSORSHIP:	F.A. Halden G.M. Loiacono	
GOVERNMENT SPONSORSHIP:	E.A. Giess A.F. Witt	
PUBLICITY:	M.A. DiGiuseppe J.C. Jacco	
PHOTO EXHIBIT:	R. Andrews P. Morris	
IOCG AWARDS:	B. Cockayne	
ACCOMPANYING PERSONS PROGRAM:	Arlene Bonner Patricia Brandle Madlyn Monchamp Aileen Wenckus	
CRYSTAL EXHIBIT:	R. Belt L.R. Rothrock	
ISSCG-8 COMMITTEE:	L. Boatner E. Bourret K.A. Jackson	
CONFERENCE SECRETARIAT	C. David Brandle	

INTERNATIONAL ADVISORY BOARD

BRAZIL: O.N. Mesquita
BULGARIA: D. Nenow
CANADA: F. Weinberg
CHINA: M.-H. Jiang and N.-B. Ming
CZECHOSLOVAKIA: B. Brezina
DENMARK: A.N. Christensen
FRANCE: R. Kern and B. Mutaftschiev
GERMANY: G. Kuhn, P. Rudolph, W. Tolksdorf and H. Wenzl
HUNGARY: J. Paltz
INDIA: P. Ramasamy
ISRAEL: L. Ben-Dor
ITALY: C. Paorici
JAPAN: H. Komatsu, T. Nishinaga and I. Sunagawa
KOREA: K.K. Orr
MEXICO: H. Riveros
ROMANIA: Z. Schlett
RUSSIA: A.A.Chernov, E.I. Givargizov and F.A. Kuznetsov
SPAIN: R. Rodriguez-Clemente
SWITZERLAND: D. Rytz
THE NETHERLANDS: P. Bennema, L.J. Giling and G.M. van Rosmalen
UNITED KINGDOM: K.G. Barraclough, B. Cockayne and P.M. Dryburgh
UNITED STATES OF AMERICA: G. Cullen, R.A. Laudise, G.H. Olsen, R. Reynolds and F. Rosenberger

INTERNATIONAL ORGANIZATION FOR CRYSTAL GROWTH

OFFICERS

President: B. Cockayne (ENGLAND)
Vice President: A.A. Chernov (RUSSIA)
Vice President: R.F. Sekerka (USA)
Secretary: M. Schieber (ISRAEL)
Treasurer: E. Kaldis (SWITZERLAND)
Past President: R. Kern (FRANCE)

IOCG EXECUTIVE COMMITTEE MEMBERS

K.W. Benz (GERMANY)
R.S. Feigelson (USA)
M.-H. Jiang (CHINA)
R.A. Laudise (USA)
T. Nishinaga (JAPAN)
C. Paorici (ITALY)
I. Sunagawa (JAPAN)
W.A. Bonner (USA)
D.T.J. Hurle (UK)
H. Komatsu (JAPAN)
B. Mutaftschiev (FRANCE)
V.V. Osiko (RUSSIA)
G.M. van Rosmalen (THE NETHERLANDS)
J.F. Wenckus (USA)

IOCG COUNCILORS REPRESENTING NATIONAL ORGANIZATIONS and GENERAL ASSEMBLY

FRANCE: A. Baronnet, J.J. Metois and B. Mutaftschiev
GERMANY: M. Krohn, G. Kuhn, P. Rudolph, W. Tolksdorf H. Walcher and H. Wenzl
HUNGARY: E. Lendvay
INDIA: P. Ramasamy and S.M.D. Rao
ISRAEL: A. Horowitz
ITALY: C. Paorici
JAPAN: T. Nishinaga, T. Ogawa and I. Sunagawa
KOREA: H. Kim, Y.S. Kim and K.K. Orr
RUSSIA: A.A. Chernov, P.P. Fedorov and F.A. Kuznetsov
SPAIN: R. Rodriguez-Clemente
SWITZERLAND: J. Hulliger and E. Kaldis
THE NETHERLANDS: J.W.M. van Kessel and J.A.M. Meijer
UNITED KINGDOM: P.M. Dryburgh, S.E.B. Gould and D.T.J. Hurle
UNITED STATES OF AMERICA: W. Bonner, C.D. Brandle and T. Surek

IUPAC: T.S. West
IUCr: A.I. Hordvik

GENERAL ASSEMBLY: P. Bennema, S. Kimura, O.N. Mesquita, N.-B. Ming, and D. Nenow

ICCG-10 CORPORATE SPONSORS

Airtron/Synoptics
AKZO
Allied Signal Corporation
Bertram Laboratories
Ceres Corporation
Cleveland Crystals
Crystal Associates Inc.
Crystal Technology Inc.
Crystal Systems
Deltronic Crystal Industries
DuPont Corporation
Eastman Kodak Company
Engelhard Industries
Epitaxx
Fujian Castech Crystals
Hewlett-Packard
Hughes Research Laboratories
Johnson Matthey Corporation
Keon Optics
Laser Diode Inc.
Magnesium Elektron Inc
MEMC Electronic Materials
Philips Laboratories
Quantum Technology
Saint Gobain
Sandoz Produkte AG Inc.
Texas Instruments, Inc.
Virgo Optics
Westinghouse S.T.C.
Zirconia Sales

US GOVERNMENT SPONSORS

Air Force Office of Scientific Research
Army Research Office
National Aeronautics and Space Administration
National Renewable Energy Laboratory
National Science Foundation
Oak Ridge National Laboratory
Office of Naval Research
Office of Naval Research - Europe
Wright Laboratories, Wright-Patterson Air Force Base

GUIDE TO POSTER TOPICS

"A" PAPERS	Fundamentals of nucleation and growth Crystal growth mechanisms Convection and segregation Morphological stability Dendrites and pattern formation
"B" PAPERS	Non-linear optic crystals Oxide crystal growth II-VI materials Laser materials (oxides and fluorides) Miscellaneous chalcogenides
"C" PAPERS	Silicon/germanium III-V bulk growth Wide bandgap materials (SiC, diamond, nitrides) Special techniques
"D" PAPERS	Halides Superconductors Special topics Refractory compounds Aqueous solution growth Biomaterials Industrial crystallization Gel growth


POSTER SESSION
NUMBER 1
TUESDAY
8:00 PM
EXHIBIT HALL

POSTER SESSION #1
EXHIBIT HALL
Tuesday 8:00 PM

A1
Nucleation Growth Model
S. M. Babu, R. Dhanasekaran and P. Ramasamy*
Anna University, India

A2
Effect of Additives on Nucleation Rate, Crystal Growth Rate and Induction Time in Precipitation
M. C. van der Leeden,* D. Kashchiev, and G. M. van Rosmalen
Delft University of Technology, The Netherlands; Institute of Physical Chemistry, Bulgaria

A3
Evolution of a Train of Interacting Steps in Surface Diffusion Field
M. Uwaha
Tohoku University, Japan

A4
Activation Process for Electrical Nucleation of NaAc Solution Studies by an X-Ray Diffraction and Voltammogram
T. Ohachi, Y.Iba, * M. Shindo and I. Taniguchi
Doshisha University, Japan

A5
Rate Expression for Nucleation of Ice by Particles Suspended in Water and Subjected to Electric Field
K. Thangaraj
Chikkanna Government Arts College, India

A6
Interfacial Thermodynamics of Non-Critical Clusters and Homogeneous Nucleation in Multi-Component Systems
K. Nishioka,* I. Kusaka, M. Okada, A. Mori, and T. Takai
University of Tokushima, Japan; California Institute of Technology, USA
Tokushima Technology Center, Japan; Kagawa University, Japan

A7
Nucleation Kinetics of Chloroform-Effect of Dipole-Dipole Interaction
F. J. Kumar,* D. Jayaraman, C. Subramanian, and P. Ramasamy
Anna University, India

A8
Complete Characterization of Epitaxial Systems from the Lattice Geometrical Point of View
P. Mock and H. Berger
Humboldt University of Berlin, Germany

A9
Determination of the Activity of the Dominating Dislocation Group from the Kinematical Measurements Using Statistical Methods
M. M. Mitrovic* and L. Petrusevski
University of Belgrade, Yugoslavia

A10
Grain Growth Mechanism in Al, Pb, Cd And Si
S. Kalainathan, R. Dhanasekaran and P. Ramasamy*
Anna University, India

A11
Varying Dislocation Growth Source Activity: (101) ADP Face
P. G. Vekilov* and Yu. G. Kuznetzov
Institute of Physical Chemistry, Bulgaria and Institute of Crystallography, Russia

A12
Step Kinetics and Dislocation Sources Activity in Electrocrystallization of Cubic Silver Faces
P. G. Vekilov* and C. Nanev
Institute of Physical Chemistry, Bulgaria

A13
Territory of a Two-Dimensional Nucleus as a Characteristic Scale of Surface Growing Under MBE Conditions
Y. Arima* and T. Irisawa
Gakushuin University, Japan

A14
Structural Feature of Surface in MBE Growth - Effect of Anisotropic Bonding and Diffusion
T. Irisawa* and Y. Arima
Gakushuin University, Japan

A15
Morphology and Growth Mechanism of New Shaped ZnO Crystals
M. Kitano,* T. Hamabe, S. Maeda, and T. Okabe
Matsushita Industrial Equipment Co., Toyama University, Japan

B1
Growth and Characterization of $KTiOAsO_4$ Crystals
P. A. Morris,* L. K. Cheng, J. D. Bierlein, J. B. Ings, R. F. Belt, and R. G. L. Barnes
DuPont Co. and Airtron/Litton, USA

B2
Defect Properties of Potassium Titanyl Phosphate (KTP)
L. J. O'Neill,* P. J. Halfpenny and J. N. Sherwood
University of Strathclyde, United Kingdom

B3
Crystal Growth And Morphology of Undoped and Nb, Al-Doped KTP Single Crystals
Y. Huang, B. N. Sun,* P. Han, and D. A. Payne
University of Illinois, USA

B4
Top Weighing TSSG Growth of Device Quality Crystals of KTP - Growth Optimisation and Kinetics
K. B. Hutton, R. C. C. Ward* and K. W. Godfrey
University of Oxford, United Kingdom

B5
Trivalent Cation Dopants in KTP: The Case of Cr3+
R. J. Bolt* and P. Bennema
University of Nijmegen, The Netherlands

B6
Growth Defects in β-BaB_2O_4 Crystal
W. Zhong, H. Hong, Z. Lu, T. Zhao, and S. Hua
Chinese Academy of Sciences, China

B7
Phases and Crystallization in the System Li_2O-B_2O_3-H_2O
K. Byrappa* and K. V. K. Shekar
University of Mysore, India

B8
Crystal Growth, Structure and Properties of $LiH_2B_5O_8$ and $Li_4H_2B_2O_6$ - New Superionic Borates
K. Byrappa* and K. V. K. Shekar
University of Mysore, India

B9
Czochralski Growth of Pure And Cd^{2+}, Nd^{3+} Doped Benzil $C_6H_5COCOC_6H_5$ Single Crystals
M. D. Aggarwal,* W. S. Wang and M. Tambwe,
Alabama Agr. & Mech. University, USA

B10
The Crystal Growth Behavior of the Organic Non-Linear Optical Material 2-(α-Methylbenzlamino)-5-Nitropyridine (MBANP)
P. J. Halfpenny,* R. I. Ristic and J. N. Sherwood
University of Strathclyde, United Kingdom

B11
Characterization of Defects on Organic Single Crystals by X-ray Topography
M. Tachibana, Q. Tang, A. Uedono, and K. Kojima
Yokohama City University, Japan

POSTER SESSION #1
EXHIBIT HALL
Tuesday 8:00 PM

B12
The Influence of an Interface Electric Field on the Behavior of Chromium during $LiNbO_3$ Single Crystal Growth
S. Uda* and W. A. Tiller
Stanford University, USA

B13
The Influence of an Interface Electric Field on the Distribution Coefficient of Chromium in $LiNbO_3$
S. Uda* and W. A. Tiller
Stanford University, USA

B14
Optical Determination of the Congruent Composition of $LiNbO_3$ Crystals
I. Baumann,* D. Krabe, P. Rudolph, and R. Schalge
Telefilter GmbH Teltow, Germany

B15
Growth of Cr:LiCAF Crystals by Bridgman Technique
L. Chen, C. Huang and S. Zhao
Research Institute of Synthetic Crystals, China

B16
Crystal Growth and Properties of Complex Fluoride Crystals of Cubic Perovskite
Y. Zhang, S. Ren and J. Zhang
Chinese Academy of Sciences, China

B17
Crystal Growth and Characterization of Fluorides with Elapasolite Structure
J.P. Chaminade, J.G. Grannec, A. Tressaud, I.N. Flerov, A.I. Kruglik and K.S. Alexander
Laboratoire de Chimie du Solide du CNRS, Universite de Bordeaux, France

B18
Growth by LPE of Nd:YAG Single Crystals Layers for Waveguide Laser Applications
B. Ferrand,* D. Pelenc, I. Chartier, and Ch. Wyon
CEA-DTA/LETI/DOPT, France

B19
Growth and Stoichiometry Problems of ZnSe for High Power Laser Optical Components
E. Krause,* A. Fissel and H. Hartmann
Central Institute for Electron Physics, Germany

B20
The Growth of Alexandrite Crystals
X. Ma,* Y. Shen, G. Wu, R. Zhu, J. Xu, and X. Zhang
Shanghai Institute of Optics, China

B21
Growth and Optical Characterization of Trivalent Titanium Doped Chrysoberyl (Ti^{3+}:$BeAlO_4$)
K. Yamagishi,* Y. Nobe, Y. Anzai, Y. Yamaguchi, and H. Takei
Mitsui Mining & Smelting Co. Ltd., Japan

B22
Czochralski Growth of Mg_2SiO_4:Cr^{4+} in Oxiding Atmosphere
P. Pan,* H. Zhu, S. Yan, Y. Chai, S. Wang, and Y. Hou
Shanghai Institute of Ceramics, China

B23
Growth of High-Quality Ti:Al_2O_3 Crystals for Solid-State Laser Applications
C. P. Khattak* and F. Schmid
Crystal Systems, Inc., USA

B24
Laser Quality Ti:Sapphire Crystal Growth by Czochralski
S. Yin,* Q. Qin, J. Xu, D. Zhou, X. Huang, and H. Tang
Anhui Inst of Optics & Fine Mechanics, China

B25
Investigation of LNA Single Crystals
T. Xu,* W. Peng, Q. Zheng, and C. Huang
South/West Inst. of Technical Physics, China

B26
Growth of Nd:YAG Crystals Free from Dislocation and Core
T. Xu,* Z. Wu, W. Peng, Z. Zheng, Z. Xiao, J. Zhou, S. Zhang, and S. Xie
South/West Inst. of Technical Physics, China

B27
Growth and Laser Properties of Neodymium Doped CNGGG Crystals
M. Timoshechkin
Academy of Sciences, Russia

B28
Si and Mg Doped GGG Crystals
M. Gobbels, S. Kimura, K. Langer, and E. Woermann
Institut fur Kristallographie, Germany

B29
The Growth of $LaMgAl_{11}O_{19}$:Nd Large Crystals with High Quality
G. Wu, X. Ma,* J. Xu, X. Zhang, and Y. Shen
Shanghai Institute of Optics, China

B30
The Growth of $BeAl_6O_{10}$:Cr (BHA:CR) Crystals
X. Ma,* P. Pan, G. Wu, and Z. Hu
Shanghai Institute of Optics, China

C1
Silicon Carbide Control in EFG System
S. Rajendran,* M. Larrousse, B. Bathy, and J. P. Kalejs
Mobil Solar Energy Corporation, USA

C3
Facet Formation in Silicon Single Crystals Grown by VMFZ Method
M. Kimura,* H. Arai, and H. Yamagishi
Shin-Etsu Handotai Co. Ltd., Japan

C4
In Situ Observations of Surface Flow of Silicon Melts During the CZ Growth Process
Y. Shiraishi
Kimura Metamelt Project, Japan

C5
Observation of Mass Transport in Silicon Melts During CZ Growth by Fluoroscopic Technique
A. Yokotani
Osaka University, Japan

C6
Detection of Micro-Precipitates in Si Crystal Related to the Crystal Growth Mechanism
K. Moriya* and K. Hirai
Mitsui Mining & Smelting Co. Ltd., Japan

C7
Study of Low-Temperature Epitaxy of Silicon Grown on its 7x7 Superlattice Surface by Observing Intensity Profile in LEED
Y. Shigeta and K. Maki*
Yokohama City University, Japan

C8
In-situ RHEED Study of Growth Processes in the Initial Stage of Ge Films on (311)Si Surfaces by Gas Source MBE
Y. Yasuda,* Y. Koide, S. Zaima and K. Itoh
Nagoya University, Japan

C9
Growth of Heavily Doped SiGe from Metallic Solutions
A. Borshchevsky* and J.-P. Fleurial
Jet Propulsion Laboratory, USA

POSTER SESSION #1
EXHIBIT HALL
Tuesday 8:00 PM

C10
Sequential Etching of Gallium Arsenide
P. E. R. Nordquist,* R. L. Henry and R. J. Gorman
Naval Research Laboratory, USA

C11
Growth and Characterization of (100) and (111) Semiinsulating and Semiconducting GaAs Single Crystals
P. Santhanaraghavan,* K. Sankaranarayanan, J. Kumar, S. Anbukumar, and P. Ramasamy
Anna University, India

C12
Growth of Large-Diameter, Low Dislocation Density Gallium Arsenide Single Crystals
V. A. Antonov, M. A. Boolekov, and T. I. Markova
NPO "Elma", Russia

C13
GaSb Solution Growth by the Solute Feeding Czochralski Method
A. Watanabe, A. Tanaka,* and T. Sukegawa
Shizuoka University, Japan

C14
A Novel Technique for Czochralski Growth of GaSb Single Crystals
P. G. Mo, H. Z. Tan, L. X. Du, and X. Q. Fan
Academy of Sciences of China, China

C15
Growth of $Al_xGa_{1-x}Sb$ Bulk Materials
G. Bischopink* and K. W. Benz
Albert-Ludwigs-Universitat Freiburg, Germany

C16
Optical and Electrical Characterization of $Al_xGa_{1-x}Sb$ Crystals Grown by the Travelling Heater Method
B. K. Meyer,* G. Bischopink, K. W. Benz, W. Kramer, and G. Pensl
Technical University Munich, Germany

C17
Crystal Growth of GaInAsSb Mixed Crystals by a Rotary Bridgman Method
Y. Hayakawa,* T. Ozawa, M. Ando, T. J. Anderson, P. H. Holloway, B. Pathangey, and M. Kumagawa
Shizouka University, Japan

C18
Growth And Characterization of InGaAs Bulk Crystals by Liquid Phase Electro-Epitaxy
M. Yanagase, S. Tanaka,* K. Hiramatsu, and I. Akasaki
Nagoya University, Japan

C19
Wetting of III-V Melts on Materials for Crucibles
T. Duffar,* I. Harter, P. Dusserre, N. Eusthatopoulos, and J. P. Nabot
DEM/SESC, France

D1
The Hot-Forging Investigation of BaF_2 Crystals
H. Zhong, C. Huang and W. Li
Research Inst of Synthetic Crystals, China

D2
Investigation of the Scintillation Properties of Barium Fluoride Crystal
Y. N. Zheng,* S. X. Ren, T. B. Zhang, and Y. Z. Zhu
Beijing Glass Research Institute, China

D3
The Radiation Damage of Rare Earth Ions Doped Barium Fluoride Crystals
G. Chen,* H. Xiao, S. Q. Man, S. X. Ren, and J. Q. Zhang
Beijing Glass Research Institute, China

D4
Growth of Meruric Iodide Using the Temperature Oscillation Method: Relationship Between Growth Parameters and Crystal Quality
M. D. Serrano, M. T. Santos, A. Martinez, E. Dieguez,* A. Ibarra, and M. Gonzalez
University Autonoma de Madrid, Spain

D5-VIDEO PRESENTATION
Vapor Growth of Large Mercuric Iodide Crystals
M. Zha, M. Piechotka and E. Kaldis
Eidgenossische Technische Hochschule, Switzerland

D6
Radiative/Conductive Inhibition of the Growth Rate in Vapor Growth of Mercuric Iodide Crystals
E. Kaldis,* M. Piechotka and A. Roux
Eidgenossische Technische Hochschule, Switzerland

D7
Laser Controlled Nucleation of α-HgI_2 Crystals from the Vapor Phase
M. Piechotka,* M. Zha and E. Kaldis
Eidgenossische Technische Hochschule, Switzerland

D8
Processing α-Mercuric Iodide by Zone Refining
A. Burger,* S. H. Morgan, D. O. Henderson, Y. Biao, K. Zhang, E. Silberman, D. Nason, L. van den Berg, C. Ortale-Baccash, and E. Cross
Fisk University, EG&G/EM, USA

D9
Growth and Characterisation of Gel Grown Crystals of Lead Chlorobromide
P. Sagayaraj, S. Sivanesan, F. D. Gnanam, and R. Gobinathan
Anna University, India

D10
Complex Interaction of Some Transition Metal Ions and the Growing Potassium Halogenide Crystals
D. Dragonova
University of Sofia, Bulgaria

D11
In-situ Crystal Growth Study of Fullerenes
M. Verheijen, H. Meekes, P. Bennema, and G. Meijer
University of Nijmegen, The Netherlands

D12
The Research Interferential Effect of Crystal Films
W. Zhu and X. Yang
Research Inst of Synthetic Crystals, China

D13
Study on 3-Component Fibonacci Ta/Al Multilayer Films Grown by Magnetron Sputtering
R. W. Peng, A. Hu, and S. S. Jiang
Nanjing University, China

D14
Formation Mechanism of Smoke Quartz
W. Zhong, S. Hua, and E. Shi
Chinese Academy of Sciences, China

D15
Separation in Metallic Melts
S. Sprenger, J. Proschmann, T. Strangfeld, and H. Bach*
Ruhr-Universitat Bochum, Germany

D16
Prediction of the Existence Region of Some III-V Binary Compounds
C. A. Galeazzi* and C. Pelosi
MASPEC Institute, Italy

POSTER SESSION #1
EXHIBIT HALL
Tuesday 8:00 PM

D18
Studies on Recrystallization by Acoustic Emission
A.P. Cook and A.P. Wade
University of British Columbia, Canada

D19
Single Crystals of TaB, Ta_3B_4, Ta_2B_3 and TaB_2, as Obtained from High-Temperature Metal Solutions, and Their Properties
S. Okada,* K. Kudou, I. Higashi, and T. Lundstrom
University of Uppsala, Sweden

D20
Crystal Growth of Boron-Rich Solids of Al-M-B (M=Li,Be,Mg) System from High-Temperature Aluminum Solutions
I. Higashi,* M. Kobayashi, S. Okada, K. Hamano, and T. Lundstrom
University of Uppsala, Sweden

D21
Thermal Conductivity and Thermoelectric Power of Float Zone Grown VCx and $Ti_{1-y}V_yC_x$ Single Crystals
C. P. Beetz,* Jr., D. F. Cummings, and W. J. Precht
Advanced Technology Materials, Inc., USA

D22
Growth of Uranium-Titanium (U_2Ti) Compound in a High Vacuum
T. Shikama,* A. Ochiai, Y. Suzuki, and K. Suzuki
Tohoku University, Japan

D23
Study on the Magnetostrictive Crystal of $Tb_{0.27}Dy_{0.73}Fe_{1.95}$:Mn
Q. Li, Y. Chang,* R. Yuan, S. Huang, and D. Jin
Wuhan University of Technology, China

D24
Growth of $Tb_xDy_{1-x}Fe_{2-w}$ Magnetostrictive Crystals without Contamination
Q. Li, Y. Chang,* R. Yuan, S. Huang, and D. Jin
Wuhan University of Technology, China

D25
Crystal Growth of the Transition Metal Silicides $MoSi_2$ And WSi_2
A. N. Christensen
Aarhus University, Denmark

D26
Nitrogen Induced Phase Transformation of Thin Film of Tantalum
Y. Akagi,* Y. Okamoto, Y. Nakamura, and M. Koba
Sharp Corporation, Japan

SESSION 1A

ELECTROCRYSTALLISATION - NUCLEATION GROWTH MODEL

A1

S. Moorthy Babu, R. Dhanasekaran and P. Ramasamy
Crystal Growth Centre
Anna University, Madras-25, India

Nucleation phenomenon during electrocrystallisation of elemental and compound semiconductors has been studied to understand the kinetics and mechanisms involved in the initial stages and further growth of electrodeposits. The existing models are based on either nucleation and growth or random adsorption process [1-3]. The present model is developed based on the formation of nucleation by two dimensional nucleation and the growth by the Birth and Spread model. The model describes the activation of the nuclei and their growth by direct incorporation. The growth process depends on the rate constants, concentration of the individual species and potential. The effect of medium and double layer is ignored. The expressions for nucleation rate and current density have been derived in terms of overpotential, surface tension etc. The total current density is the sum of the individual current densities and is determined for each potential. Hence, voltammogram has been constructed. The fractional surface coverage of the electrode has been determined using the Avrami's theorem and the modified overlap process. The results are discussed.

[1] R. Greef, R. Peat, L.M. Peter, D. Pletcher and J. Robinson, "Instrumental Methods in Electrochemistry," Ellis Horwood, Chichester, 1985.
[2] L. Durai, R. Dhanasekaran and P. Ramasamy, *J. Crystal Growth*, 79 (1986) 783.
[3] B. Bhattacharjee and S.K. Rangarajan, *J. Electroanal. Chem.* 302 (1991) 207.

EFFECT OF ADDITIVES ON NUCLEATION RATE, CRYSTAL GROWTH RATE AND INDUCTION TIME IN PRECIPITATION

A2

M.C. van der Leeden[1], *D. Kashchiev*[2] *and G.M. van Rosmalen*[1]
[1]Delft Technical University, Laboratory for Process Equipment,
Leeghwaterstraat 44, 2628 CA Delft, The Netherlands
[2]Bulgarian Academy of Sciences, Institute of Physical Chemistry,
Sofia 1040, Bulgaria

Recently [1,2], the effect of 0.01125 ppm of a random copolymer of maleic acid and vinyl sulphonic acid (PMA-PVS) on $BaSO_4$ precipitation was investigated, using a combined analysis of the induction times in both seeded and unseeded precipitation. This additive appeared to retard growth and to stimulate nucleation of $BaSO_4$. The process of primary nucleation of $BaSO_4$ under the prevailing experimental conditions was concluded to be heterogeneous, in view of the determined relatively low σ-values of 40±2 and 50±2 mJm^{-2} in the absence and presence of PMA-PVS, respectively. The growth was found to proceed by the mechanism of 2D surface nucleation (birth and spread model).

The effect of minor amounts of additives on the precipitation kinetics of mineral salts is in general attributed to their preferential adsorption on the mineral surface. According to the equilibrium adsorption theories, adsorption leads to a decrease of the nucleus surface specific free energy σ and specific edge free energy κ. In the presence of PMA-PVS, however, higher values for σ and κ than in the absence of the additive were determined.

To explain the increase of σ and κ, a theory is proposed where the additives behave as active centres for 3D and 2D nucleation in addition to the original heterogeneous nucleation sites, and do not adsorb onto the nuclei formed on both types of active centres. For this reason, σ and κ of the nuclei formed are independent of the additive concentration, although they can be different for the nuclei formed on additive molecules and those formed on the original active centres. General expressions are derived for the nucleation rate, the rate of crystal growth for the birth and spread mechanism, and the induction time in unseeded precipitation in the presence of additives.

Induction times in unseeded $BaSO_4$ precipitation are measured as a function of the PMA-PVS concentration and interpreted by the proposed theory. It can be concluded that this theory describes fairly well the obtained experimental data.

1. M.C. van der Leeden, D. Verdoes, D. Kashchiev and G.M. van Rosmalen, in: Advances in Industrial Crystallization (eds. J. Garside, R.J. Davey and A.G. Jones) Butterworths, 1991, p.31.
2. M.C. van der Leeden, D. Kashchiev and G.M. van Rosmalen. submitted for publication in J. Colloids and Interface Sc.

A3

EVOLUTION OF A TRAIN OF INTERACTING STEPS IN SURFACE DIFFUSION FIELD

Makio Uwaha
Institute for Materials Research, Tohoku University
2-1-1 Katahira, Aoba-ku, Sendai 980, Japan

Steps on a crystal growing from a vapor interact via interference of the diffusion field of adsorbed atoms. This interaction leads to bunching of steps as well as the reduction of the growth velocity. We study time evolution of a train of parallel straight steps, which are interacting also with direct forces such as the elastic interaction.

The velocity of a straight step is the sum of the diffusion current from the lower side of the step and that from the upper side. A general formula of the velocity is given as a function of the step distances, the interaction strength and the kinetic coefficients of the step.

If the attachment kinetics from the lower side of the step is faster than that from the upper side, the interference of the diffusion field gives rise to an effective attraction under sublimation. As is well-known this attraction ensures the stability of an equidistant step train under growth and leads to an instability under sublimation if steps have no direct interactions.[1] With the repulsive direct interaction of steps, however, the step train is stable even under sublimation. There is a critical underpressure below which the instability occurs. This critical value depends on the kinetic coefficients as well as the interaction strength.

Similarly, there is a critical underpressure below which two repulsive steps can form a bound state. In this case two distant steps repel each other, but two close steps form a stable bound state. If there is a third step at a distance in the lower side of the bound pair, this step collides with the pair and forms a new pair with one of the members. As a result, the step at the highest level expelled from the bound state, which looks like billiards.

Time evolution of a train of many steps will be also analyzed, and the relation to experimental observations will be discussed.

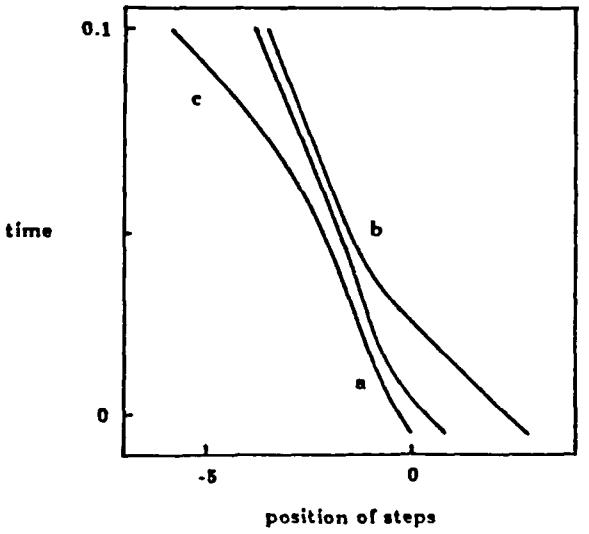

Figure 1. A typical time evolution of three steps: a) Nearby steps first form a stable bound pair, b) The third step collides with the pair and forms a new pair, c) The first step is expelled.

1. P. Lennema and G.H. Gilmer, in Crystal Growth: An Introduction ed. P. Hartman (North-Holland, Amsterdam, 1973) 263.

ACTIVATION PROCESS FOR ELECTRICAL NUCLEATION OF NaAc SOLUTION STUDIED BY AN X-RAY DIFFRACTION AND VOLTAMMOGRAM

A4

Tadashi Ohachi, Y. Iba, Masao Shindo and Ichiro Taniguchi
Department of Electrical Engineering
Doshisha University, Kyoto 602, Japan

NaAc solution is one of key materials FOR heat storage, because of its large heat of fusion at a suitable temperature (264J/g or 340J/cm^3 at 58.3 °C) and its large supercooling. Electrical nucleation of sodium acetate trihydrate (NaAc; $NaCH_3COO \cdot 3H_3O$) is observed by an activated Cu-Hg amalgam electrode[1]. The activation process by the electrical treatment of ac voltage (0.5V) of 60Hz with dc bias voltage (-1.5V vs. SCE) is studied by an X-ray diffraction measurements and cyclic voltammograph in this report.

The application of negative potential against an SCE is important. An ac voltage superimposed dc bias voltage is effective for the activation. The composition of an original amalgam electrode and an activated electrode is determined as $Cu_{15}Hg_{11}$ by powder diffraction patterns, which were measured by Philip's PW1877 system using Cu radiation and step scanning mode of 0.01 deg/sec between 5 to 90 deg in 2 θ.

Cyclic voltammogram measurement is studied using current voltage characteristics between amalgam electrodes are measured by a SOLATRON 1286 with a three-electrode system using SCE in a saturated KC1 solution. An aqueous solution of 55 wt% $NaCh_3COO$ at about 60 °C and scanning speed of 0.2 V/sec between -1.8 to 0.2 V are used for the measurement. Positive polarity means applying positive voltage to an amalgam electrode against SCE.

For the electrical nucleation below 33.3 °C step potential is applied with 0.05 V increment for 30 sec up to +1.0 or -1.5 V by the same SOLATRON system used for the voltammogram measurement. The observation of the nucleation processes is made by a video camera. The electrical nucleation occurred in both polarities for Cu-Hg activated electrodes. The nucleation potential area about 0.7 and -0.75 V for positive and negative polarity. The value of negative polarity is much smaller than positive one.

[1] T. Ohachi, M. Hamanaka, H. Konda, S. Hayashi, I. Taniguchi, T. Hashimoto and Y. Kotani, *J. Crystal Growth* 99(1990)72.
[2] T. Ohachi, M. Shindo and I. Taniguchi, Proc. of 4th Topical Meeting on Crystal Growth Mechanism (Tokyo Univ, 1991) ed. T. Nishinaga p. 25.

RATE EXPRESSION FOR NUCLEATION OF ICE BY PARTICLES SUSPENDED IN WATER AND SUBJECTED TO ELECTRIC FIELD

A5

K. Thangaraj
Head, Department of Physics
Chikkanna Government Arts College, Tiruppur (India)

The critical free energy for the formation of a nucleus can be written as

$$\Delta G^* = \frac{16\pi}{3} \frac{f(\sigma)f(v)}{(\Delta G_v + ce^2)^2}$$

where f(σ depends on the interfacial free energies and f(v) on the shape of the embryo and ce^2 is the strain energy. In the case of heterogeneous nucleation of ice by particles suspended in water, the nucleation rate

$$J = \frac{kT}{h} n_c 4\pi\gamma^2 \exp\left(-\frac{\Delta g}{kT}\right)\exp\left(-\frac{\Delta G^*}{kT}\right)$$

where T is the nucleation temp. and n_c the no. of water molecules/unit area of the surface and Δg the activation energy for self diffusion across the liquid-solid boundary. This expression is modified incorporating correction for the number of active sites on the surface of the particle and change in the activation energy when the suspension is placed in an electric field. Assuming that hydrophilic sites are provided by foreign atoms on the surface the expression becomes,

$$J^* = \frac{kT}{h} 4\pi\gamma^2 n_c n_o \exp\left(\frac{-\Delta g + f(z)}{kT}\right)\exp\left(-\frac{2\Delta G^*}{kT}\right)$$

where n_o is the total number of foreign atoms on the surface and f(z), the change due to interaction energy due to electric field. The expression is tested with available experimental results.

A6

INTERFACIAL THERMODYNAMICS OF NON-CRITICAL CLUSTERS AND HOMOGENEOUS NUCLEATION IN MULTI-COMPONENT SYSTEMS

K. Nishioka, I. Kusaka[1], M. Okada[2], A. Mori and T. Takai[3]
Faculty of Engineering, University of Tokushima
[1]Now at Department of Chemical Engineering, California Institute of Technology
[2]Tokushima Technology Center
[3]Faculty of Education, Kagawa University

Interfacial thermodynamics is extended to non-critical clusters in vapor for multi-component systems. This extension is required to clarify the uncertainty over whether or not the size and composition dependence of interfacial tension must be taken into account in taking the extremity condition of the reversible work to derive the size and the composition of a critical nucleus. It is found that the differential of interfacial tension does not arise in the extremity condition due to the Gibbs-Duhem relation derived for a system of a non-critical cluster and the vapor in equilibrium under an additional constraint which maintains the number of molecules in a cluster. Extension of interfacial thermodynamics to non-critical clusters is essential also in deriving the governing equation for transient nucleation processes, since the unknown detachment rate of a monomer to a cluster must be replaced by the attachment rate by employing the principle of detailed balance. However, for this procedure be justified, relaxation time required for the molecular distribution to achieve the equilibrium distribution in a cluster must be much shorter than the interval between attachment or detachment of a monomer. This problem is studied by molecular dynamics simulation as well as by theoretical consideration.

A7

NUCLEATION KINETICS OF CHLOROFORM - EFFECT OF DIPOLE-DIPOLE INTERACTION

F. Joseph Kumar, D. Jayaraman, C. Subramanian and P. Ramasamy
Crystal Growth Centre
Anna University, Madras - 25, India

There is considerable current interest on homogeneous nucleation theory due to the size dependence of surface energy and the dipole-dipole interaction effect for polar substances. But the simultaneous effect of both these phenomena on the nucleation parameters have not been studied so far.

For a spherical droplet a surface dipole is oriented at a finite angle with its nearest neighbours, the angle being a function of the radius of the droplet [1]. The increase in surface potential energy due to non parallel orientation is obtained as

$$\int_0^{2\theta} \mu^2 \sin 2\theta \, c \, j_s/2x^3 \, d\theta = 2\mu^2/x^3$$

The work of formation of a droplet due to condensation of supersaturated vapour is equated to the product of surface area of the droplet and the sum of the surface energy of a plane interface, the change of surface energy corresponding to that radius and the increase in surface energy due to the dipole-dipole interactions [2].

$$\int_0^r (P_2 - P_1)dv_2 = [\sigma_\infty + d\sigma(r)/dr \cdot r + \mu^2/2\pi x^3 r^2] \cdot A$$

The expression for curvature dependence of surface tension is obtained as

$$\sigma(r) = \exp[-\delta_\infty/r(1 + \delta_\infty/2r)] \, [\sigma_\infty + \mu^2/4\pi x^3 r^2 \, (1 - \delta/3r)]$$

Accordingly the expression for critical radius gets modified. The above corrections are incorporated in the classical nucleation theory and the nucleation parameters are calculated for the polar material Chloroform having dipole moment 1.02D. If the dependence of surface free energy on curvature on y is considered the critical supersaturation required at a particular temperature is lowered, however the dipole-dipole interaction effect enhances its value. The net result is that our theoretical predictions agree well with the experimental results [3].

[1] F.F. Abraham, "Homogeneous Nucleation" (Academic Press) 1974 186.
[2] F. Joseph Kumar, D. Jayaraman, C. Subramanian and P. Ramasamy, *J. Materials Science Letters*, 10 (1991) 608.
[3] Katz et al, *J. Chem. Phys.*, 65 (1976) 382.

COMPLETE CHARACTERIZATION OF EPITAXIAL SYSTEMS FROM THE LATTICE GEOMETRICAL POINT OF VIEW

A8

P. Möck, H. Berger
Institut für Kristallographie und Materialforschung
Humboldt Universität, Invalidenstraße 110, 0-1040 Berlin, Germany

From the lattice geometrical point of view epitaxial systems are commonly characterized by the laws of overgrowth (i.e. (hkl of substrate || (h'k'l') of deposit, [uvw] of substrate || [u'v'w'] of deposit). But there is a lot of experimental evidences on various epitaxial systems that the laws of overgrowth fail in general because an epitaxial misorientation exists [1]. So the development of a new description tool for epitaxial systems is recommended.

The complete characterisation of epitaxial systems is performed by means of transformation matrices which transforms the (direct or reciprocal) lattice of the substrate to the (direct or reciprocal) lattice of the deposit. These transformation matrices can be divided into five factors: the scalar of the volume change, the deformation tensors of substrate and deposit, the rotation matrix of the ideal orientation relationship (which have the same information content as the laws of overgrowth) and the rotation matrix of the epitaxial misorientation [2]. These factors can be correlated to the epitaxial growth conditions. The symmetry group of the epitaxial sample, the symmetry group of their physical properties and the admissible line defects at the interface can be calculated from the transformation matrices. Additional peaces of information concerning the lattice geometry can also be derived from the transformation matrices.

A complete characterization from the lattice geometrical point of view of the epitaxial system CdTe on GaAs (slightly misorientated from (001)) using x-ray techniques is described in [3].

[1] Aindow, M., Pond, R.C.: Phil. Mag A63, 667 (1991).
[2] Möck, P., Berger, H.: Proc. 3rd International Symposium on Trends and New Applications in Thin Films, Strasbourg, 1991.
[3] Möck, P., Hedel, R., Berger, H.: Z. Krist. Suppl. 199 (1991).

DETERMINATION OF THE ACTIVITY OF THE DOMINATING DISLOCATION GROUP FROM THE KINEMATICAL MEASUREMENTS USING STATISTICAL METHODS

A9

M.M. Mitrovic
Faculty of Physics, P.O. Box 550, 11001 Belgrade, Yugoslavia
Lj. Petruševski
Faculty of Architecture and Institute of Mathematics
Bulevar revolucije 73/II, 11001 Belgrade, Yugoslavia

Measuring the dependence of linear growth rate of crystals (R) on relative supersaturation σ of the solution is very difficult due to growth rate dispersion. Namely, it is well know that, under same condition of supersaturation and temperature (T) different crystals of the same material grow at different rates. BCF theory [1] anticipates this dispersion through various values of the activity of the dominating dislocation group (ε) for the face. Due to numerous parameters whose local fluctuations can cause the change of crystal growth rate, as well as due to errors in measuring rate, it is difficult to distinguish the crystals that grow with similar ε. Therefore it is not easy to separate groups of crystals that grow with different σ from the histograms of distributions of crystal growth rates [2,3], and it is even more difficult to determine reliably ε for a small number of the observed crystals [4]. Fluctuations of growth parameters and measuring errors result in normal distribution of growth rates around the average value which depends on external conditions and ε. Distributions of growth rates of all crystals growing under the same conditions can be described by normal, gamma and log-normal distribution [2,3], depending on conditions of crystal growth. Separation of crystal groups that grow with the same ε from all the crystals comes down to separation of groups of crystal with normal growth distributions from all the crystals whose growth dispersion is described by some of the mentioned distributions. Aiming at that, the statistical criterions have been determined in order to separate groups of crystals growing with the same ε. By analyzing the dependence of $R(\sigma,T,\varepsilon)$ for Rochelle salt and $MnCl_2 \cdot 4H_2O$ crystals, several parameters from which depends the growth rate of the mentioned crystals in [010] and normal to the (100) plane direction, respectively, have been determined.

1. U.K. Burton et al., Phil. Trans. Roy. Soc. (London) 243 (1951) 299.
2. M.M. Mitrovic, *J. Crystal Growth* 55 (1987) 411.
3. M.M. Mitrovic and R.I. Ristic, *J. Crystal Growth* 112 (1991) 160.
4. R.J. Davey, et al., *J. Crystal Growth* 47 (1979) 1.

A10

GRAIN GROWTH MECHANISM IN Al, Pb, Cd AND Si

S. Kalainathan, R. Dhanasekaran and P. Ramasamy
Crystal Growth Centre
Anna University, Madras - 600 025, India

A kinetic model has been investigated to determine the grain growth mechanism in Al, Pb, Cd and Si during the process of annealing. The expressions have been derived to evaluate the grain size and size distribution as a function of annealing time and annealing temperature. Computer simulation technique has been applied to determine the numerical values of the grain boundary self diffusion of atoms. Graphs have been drawn for the grain size and size distribution as function of annealing time and temperature using our numerical findings. Our theoretically predicted values have been compared with the available experimental results. It is observed that the grain size and size distribution increase with annealing time and temperature in all the cases of present investigations. The model has been extended to the grain growth phenomenon in heavily doped polycrystalline silicon doped with P, As and B during device fabrication and also extended to the case of Al_2O_3:ZrO_2. The numerically simulated values of grain size as a function of annealing time, temperature and dopant concentration of the dopants are in good agreement with experimental values. The grain size distribution of grain size in the polycrystalline matrix has been reported first time in the literature for the different experimental conditions of annealing processes.

A11

VARYING DISLOCATION GROWTH SOURCE ACTIVITY; (101) ADP FACE

P.G. Vekilov
Institute of Physical Chemistry, Sofia 1040, Bulgaria
Yu.G. Kuznetzov
Institute of Crystallography
USSR Academy of Sciences, Moscow 117333, Russia

Michelson interferometry and X-ray topography were applied to study in situ growth kinetics on dislocation sources with changing activity. The growth source activity varied due to changing of the number of dislocations and its linear dimensions or to closely approaching the crystal edge. To vary the size of the critical two-dimensional nucleus ρ_c independently of supersaturation the experiments were carried out under two different pH of the mother solution. Different Cr^{3+} concentrations were added to observe impurity effects.

It is shown that the dislocation source consists of parallel dislocations and splits if the distance between a pair of dislocations d does not satisfy the condition $d<2\pi\rho_c$. On the contrary, dislocations that follow the above conditions always form a joint growth source. When this condition is violated a group of dislocations with positive or zero summary Burgers vector splits from the growth source. At lower temperatures (27°C) this leads to changing of the mean step height and, hence, of the step kinetic coefficient according to an earlier described correlation. Different types of $R(d)$ curves appear if the growth source activity changes.

In the close vicinity (~1μm) of the crystal edge of activity of the growth source sharply drops due to the two-dimensional Gibbs-Thomson effect. This measurements helped us to independently confirm the numerical coefficient of dislocation spiral rotation (=19), and the free surface energy of the step riser. If the only dislocation source present on the face is in the vicinity of the edge its growth is governed by the adjacent prism face - "dependent growth." A formula to describe it is proposed.

STEP KINETICS AND DISLOCATION SOURCES ACTIVITY IN ELECTROCRYSTALLIZATION OF CUBIC SILVER FACES

A12

P.C. Vekilov and Chr. Nanev
Institute of Physical Chemistry
Sofia 1040, Bulgaria

A laser Michelson interferometer was attached to an inverted microscope, thus achieving magnification of about 100 times. This set-up was applied to study in situ the electrochemical growth of cubic silver faces from 6N $AgNO_3$ solution on dislocations after the classical capillary method.

Measurements of the normal growth rate, dislocation hillock slope, tangential step velocity and current density as a function of the crystallisation overvoltage were performed. Dislocation sources pass from the studied face to the adjacent octahedral faces and vice versa The most active dislocation source present on the face leads growth. At higher current densities crystal edges are in better diffusion conditions and that is why the leading dislocation source is usually situated close to the edges. At higher hillock slopes ($>5x10^{-3}$) a decrease of the effective step kinetic coefficient is observed most probably due to bulk diffusion step field overlap. In pure solutions the accumulation of uncontrollable impurities with time leads to a decrease in the step kinetic coefficient β up to 4 times. In the presence of a drop of 1:3 HNO β is constant with time, but is ~7 times lower than in pure solutions.

Hillock slope/overvoltage curves enabled us to determine the summary Burgers vector $b_\perp$ and the linear dimensions of the dislocation sources leading growth. For single dislocations the slope is a linear function of the overvoltage. Complex dislocation sources had 2, 3, and 8 times higher $b_\perp$ and this helped us to determine the free surface energy of the step riser on the (100) Ag face without suppositions of the step height. The values 130 erg/cm^2 in the pure solutions and 110 erg/cm^2 in the presence of HNO_3 were found.

TERRITORY OF A TWO-DIMENSIONAL NUCLEUS AS A CHARACTERISTIC SCALE OF SURFACE GROWING UNDER MBE

A13

*Yoshiyasu Arima and Toshiharu Irisawa**
Department of Physics and *Computer Center
Gakushuin University, 1-5-1 Mejiro, Toshima-ku, Tokyo 171, Japan

In MBE growth process, no evaporation occurs because of sufficiently low temperature of the substrate and extremely large incident beam flux, Nevertheless, the surface grows layer by layer with keeping its flatness. We have shown[1] that the important parameter to decide the growth mode in such condition is the waiting time τ_c of an adatom before capture by another adatoms, not the life time τ_s of an adatom. Moreover, the diffusion length λ_c in time τ_c coincides with the mean distance between neighboring nuclei, i.e. the diameter of the territory of a nucleus.

In order to evaluate the characteristic length λ_c of growing surface generated by Monte Carlo simulation, we calculated the space-dependent correlation function $G(r)$ of the local surface height. It takes a minimum with a negative value at the distance r^* which corresponds the radius of territory[2]. In the initial stage of growth from the full-flat surface, we find good agreement in r^* with a half of λ_c which is estimated by the theory[1]. In addition, the depth of the minimum value of G(r) changes periodically corresponding to the layer by layer growth.

On the vicinal surface, we can decide whether the nucleations occur on the terrace or not by evaluating the correlation in height between at the step and on the middle of terrace. Then, we find that when λ_c exceeds about 1.3 times of the distance between neighboring steps, the nucleation does not occur on the terrace, and therefore, the oscillation of the surface structure disappears. Thus, the condition that the step flow growth mode appears is given as $\lambda < \lambda_c = (D_s/J)^{1/4}$ in agreement with our theory, where D_s and J are the surface diffusion coefficient and the incident beam flux, respectively.

[1] T. Irisawa, Y. Arima and T. Kuroda, *J. Crystal Growth* 99(1990)491.
[2] Y. Arima and T. Irisawa, *J. Crystal Growth*, in press.

A14

STRUCTURAL FEATURE OF SURFACE IN MBE GROWTH - EFFECT OF ANISOTROPIC BONDING AND DIFFUSION -

*Toshiharu Irisawa and Yoshiyasu Arima**
Computer Center and *Department of Physics
Gakushuin University, 1-5-1 Mejiro, Toshima-ku, Tokyo 171, Japan

Recently, the surface structures are studied in detail by using STM (scanning tunnel microscopy). Then, it is reported that the formation of the extremely anisotropic cluster on Si (001) surface[1], and the difference of the step structure for the step direction on GaAs (001) vicinal surface[2]. However, it is not clear that which is the main reason of these anisotropy, the anisotropy of bonding or that of the surface diffusion of adatoms.

In MBE growth process, no evaporation occurs because of sufficiently low temperature of the substrate and extremely large incident flux. Nevertheless, the surface grows layer by layer with keeping its flatness detected as the oscillation of intensities of RHEED[3]. We have shown[4] that the important parameter to decide the growth mode in such condition is the waiting time τ_s of an adatom before capture by another adatoms, not the life time ts of an adatom. By using Monte Carlo simulation, we also confirmed the periodic changes of surface structure.

In order to investigate more realistic system including the anisotropy of the bond energy and that of the surface diffusion, we carried out Monte Carlo simulation taking account of these anisotropy in MBE growth conditions. When the bond energies are anisotropic in lateral direction on surface, we found in agreement with the experimental observations[1,2] that the two-dimensional cluster tends to expand in the direction of stronger bond, and the steps perpendicular to that direction become rough on the vicinal surface. On the other hands, the anisotropy of surface diffusion hardly yield those anisotropic structure of surfaces.

[1] Y.W. Mo, J. Kleiner, M.B. Webb and M.G. Lagally, *Phys. Rev. Lett.* 66(1991)2001.
[2] M.D. Pashley, K.W. Haberen and J.M. Gaines, *Appl. Phys. Lett.* 58(1991)406.
[3] J.J. Harris and B.A. Joyce, *Surf. Sci.* 108(1981)L90.
[4] T. Irisawa, Y. Arima and T. Kuroda, *J. Crystal Growth* 99(1990)491.

A15

MORPHOLOGY AND GROWTH MECHANISM OF NEW SHAPED ZnO CRYSTALS

*Motoi Kitano, Takeshi Hamabe, Sachiko Maeda and Toshio Okabe**
Matsushita Ind. Equip. Co., Inazu, Toyonaka, Osaka 561, Japan
*Depart. of Physics, Toyama Univ., Gofuku, Toyama 930, Japan

We reported a new method to grow large and uniform tetrapod-like ZnO crystals by growing the octahedral nuclei inside an oxide layer formed intentionally on the surface of Zn powder (ZnO/Zn powder) and developing their legs on its alternate four faces of the nucleus after expelled out of the oxide layer.

In this paper we report a new shaped ZnO crystal by using the same method but adding Sn-Zn alloy powder to ZnO/Zn powder. The mixed powder was burned in an electronic furnace heated from 900 to 980°C, to which air was supplied at a regulated flow-rate. A SEM micrograph of the typically unique crystals obtained is shown in fig. 1. The crystal has four long and four short legs which are united at a same junction and make an equal angle of 78° to each other. The top surface of the short legs constitutes two or three portions as seen in fig. 1, which grow longer to make a bundle of needle crystals as seen in fig. 2. The crystallographic polarity of the top surfaces of legs as well as the facets of the octahedral nucleus was determined by chemical etching method. From the results shown in fig. 3 and 4, the additional short legs would grow on the four oxygen faces of an octahedral nucleus while the long legs grow on its four zinc faces. The reflection diffraction by 200 keV TEM could identify the Zn_2SnO_4 crystalline thin layer only on the top surfaces of the short legs. The present observation suggests that the short legs of multi-legs-form ZnO crystals develop on oxygen faces by VLS mechanism with tin acting as an agent while the long legs grow on zinc faces by VS mechanism as in the case of the legs of the tetrapod-like ZnO crystals.

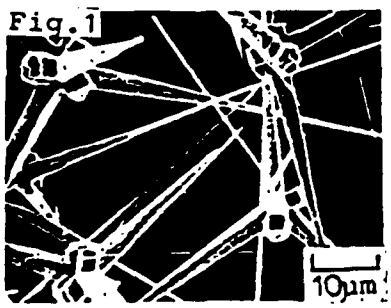

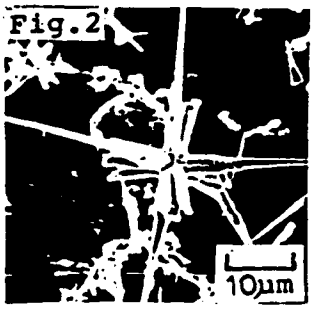

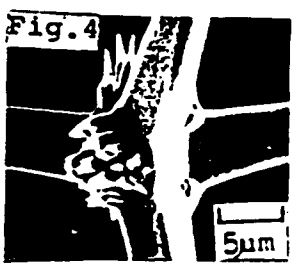

SESSION 1B

GROWTH AND CHARACTERIZATION OF $KTiOAsO_4$ CRYSTALS

B1

P.A. Morris, L.K. Cheng and J.D. Bierlein
DuPont Company, Experimental Station, Wilmington, DE 19880
J.B. Ings and R.F. Belt
Airtron, Morris Plains, NJ 07950
R.G.L. Barnes
Johnson Matthey Electronics, Royston, Hertfordshire SG8 5HE England

Recent work has shown that $KTiOAsO_4$ (KTA) exhibits significantly higher nonlinear and electro-optic coefficients than $KTiOPO_4$ (KTP).[1] KTA is isomorphic to KTP and therefore also has the one-dimensional ionic conduction properties of KTP, which allow the formation of well-defined waveguide structures. KTA crystals have previously been grown via the flux technique using both K_2O-As_2O_5[2] and K_2WO_4-$KAsO_3$-Li_2WO_4 fluxes[1,3] but few comparisons have been made regarding the properties of these crystals and the optimum process for the growth of KTA crystals has not been established.

Large crystals grown using the K_2WO_4-$KAsO_3$-Li_2WO_4 flux have previously been reported to contain optical inhomogeneities which are considered to be due to the incorporation of W impurities into the crystals.[3] This material has also been observed to contain domain structures which can deleteriously affect their optical performance. Earlier crystals grown using the K_2O-As_2O_5 flux contained relatively large concentrations of Si, Al and Fe impurities, which were found to be present in the arsenate precursors.[4] A reduction in the ionic conductivity of these crystals, relative to KTP flux grown at similar temperatures, was observed and attributed to the Si and Al contents. The effects of the impurities in these crystals on the other properties of KTA were not addressed.

To determine the optimum growth conditions for KTA, crystals have been grown using both the K_2O-As_2O_5 and K_2WO_4-$KAsO_3$-Li_2WO_4 flux techniques. In addition, crystals have been grown using the K_2O-As_2O_5 flux process with 3-9's and 5-9's pure arsenate precursors. The properties of these crystals, as well as KTA crystals grown by hydrothermal techniques[5] are discussed. The properties of specific interest include the nonlinear coefficients, optical homogeneity, domain content, damage susceptibility and ionic conductivity.

1. J.D. Bierlein, H. Vanherzeele, A.A. Ballman, *Appl. Phys. Lett.*, **54**, 783 (1 989).
2. T.E. Gier, U.S. Patent No. 4,231,838 (4 November 1980).
3. L.K. Cheng, J.D. Bierlein, A.A. Ballman, *J. Crystal Growth*, **110**, 697 (1991).
4. P.A. Morris, Materials for Nonlinear Optics, (Am. Ch. Soc., Washington, DC, 1991) p. 380.
5. J.B. Ings, R. Belt, 10th Int. Conf. on Crystal Growth, San Diego, CA (1992).

DEFECT PROPERTIES OF POTASSIUM TITANYL PHOSPHATE (KTP)

B2

L.J. O'Neill, P.J. Halfpenny and J.N. Sherwood
Department of Pure and Applied Chemistry
University of Strathclyde, 295 Cathedral Glasgow G1 1XL UK

Potassium titanyl phosphate (KTP) has emerged in recent years as an outstanding material for a range of non-linear optical applications. Substantial variations in optical performance, however, are not uncommon between apparently similar crystals. This phenomenon has also been observed for a number of other non-linear optical materials. Differences in the nature and density of crystallographic defects are potentially important, though largely unexplored, factors in this respect.

We present here a detailed examination of the structural defects present in flux grown crystals of KTP using x-ray diffraction topographic methods in combination with chemical etching. Both bulk and surface defect structures are considered. The influence of crystal growth conditions upon the nature, density and distribution of imperfections is discussed, together with an evaluation of their significance with respect to the non-linear optical performance of crystals of KTP.

B3

CRYSTAL GROWTH AND MORPHOLOGY OF UNDOPED AND Nb, Al-DOPED KTP SINGLE CRYSTALS

Y. Huang, B.N. Sun, P. Han and D.A. Payne
Department of Material Science and Engineering, Material Research Laboratory, and
Beckman Institute, University of Illinois at Urbana-Champaign, Urbana, IL 61801

Single crystals of potassium titanyl phosphate $KTiOPO_4$ (KTP) were grown from high temperature solutions using $K_6P_4O_{13}$ as the flux. Seeded and spontaneous nucleation techniques were used. The crystal habits were found to be dependent on the nucleation conditions as well as the presence of dopants. Higher cooling rates and higher supersaturations reduced the morphological importance of the {100} faces. The results are discussed in terms of features of the crystal structure. The effects of Nb and Al on morphology are reported.

Surface striations along [010] were observed on the {100} faces of KTP crystals, which were grown at larger driving force. A transition from 2D to quasi-1D nucleation for growth mechanism is proposed for the most important {100} habit faces.

B4

TOP WEIGHING TSSG GROWTH OF DEVICE QUALITY CRYSTALS OF KTP - GROWTH OPTIMISATION AND KINETICS

K.B. Hutton, R.C.C. Ward and K.W. Godfrey
Clarendon Laboratory, University of Oxford
Parks Road, Oxford OX1 3PU UK

A top-seeded solution growth technique incorporating crystal weighing has been developed for the study and optimisation of the growth of device quality crystals of the nonlinear material KTP. The weighing facility forms part of a computerised data acquisition system which allows the complete growth process to be monitored and controlled, including the crucial first stage of seed melt-back and regrowth. Studies have been undertaken of the crystal growth of KTP from the KTP/K_6 potassium phosphate solution system by slow cooling in the temperature range 1000-800°C.

KTP crystals grow with characteristic habit faces under conditions of large supersaturation and high fluid flow, where the maximum stable growth rate is likely to be limited by interface kinetic factors. The effects on the growth of the various experimental parameters - including supersaturation, temperature profile, seed orientation, and accelerated seed rotation conditions - are analysed in this paper. Crystal quality has been assessed using X-ray topography and impurity levels determined by microprobe analysis. It is shown that crystals free of solvent inclusions and with very low dislocation densities are produced by this method, suitable for optical applications such as SHG devices and waveguides.

B5

TRIVALENT CATION DOPANTS IN KTP: THE CASE OF Cr^{3+}

R.J. Bolt
RIM Lab. for Solid State Chemistry
University of Nijmegen, Toernooiveld, 6525 ED Nijmegen, Holland

Crystals of $KTiOPO_4$ were grown, containing different concentrations Cr^{3+}. The results were studied with microscopy, Instrumental Neutron Activation Analysis (INAA) and microprobe. Chromium builds in preferentially in certain growth sectors of KTP like {100} and to an even stronger measure {101}.

GROWTH DEFECTS IN β-BaB_2O_4 CRYSTAL

B6

Zhong Weizhuo, Hong Huicong, Lu Zhiping, Zhao Tiande and Hua Sukun
Shanghai Institute of Ceramics, Chinese Academy of Science
1295 Ding Xi Road, Shanghai 200050, China

In present work the growth defects in BaB_2O_4 crystals grown by the temperature from the flux are investigated by using X-ray topography and Micrography. The used crystals were grown on the $(000\bar{1})$ face of positive polar axis C and $(000\bar{1})$ face of negative polar axis C respectively. The investigated sample crystals were oriented along $\{11\bar{2}0\}$, $\{10\bar{1}0\}$ and $\{0001\}$ directions. The defects in the crystal are planar ones, and distributed along positive rhombic faces R $\{10\bar{1}2\}$ and negative polar faces r$\{01\bar{1}2\}$ and S$\{11\bar{2}2\}$, and sometimes along hexagonal prism faces a $\{10\bar{1}2\}$. There are two kinds of inclusions. One consists of solid particales or something with cotton-like structures, another one has a negative crystal structure with regular geometric shape, such as trigonal cone and hexagonal prism. After analyzing the crystallization morphology of β-BBO crystals, we have come to the conclusion that the negative crystals are the appearance of simple forms of trigonal cone and hexagonal prism and its formation which has a kind of internal growth mechanism is due to the temperature oscillations or the supercooling in the melt during the growth. The results of electronic probe analysis have shown that the inclusion contains Si^{4+}, Al^{3+}, Na^{+}, Mg^{2+}, Ca^{2+}, K^{+} and so on. Sometimes the inclusions are distributed regularly along some groups of faces. For instance, the inclusions in the crystal grown in the direction of $\{01\bar{1}0\}$ along Y axis often have hexagonal symmetry and radial distribution and the orientation is consistent with the one of $\{11\bar{2}2\}$ faces.

PHASES AND CRYSTALLIZATION IN THE SYSTEM Li_2O-B_2O_3-H_2O

B7

K. Byrappa and K.V.K. Shekar
The Mineralogical Institute, University of Mysore
Manasagangotri, Mysore-570 006, India

Borates have attracted great attention of Materials' Scientists owing to their variety of applications in the modern technology, particularly after the successful application of transitional metals rare earth borates as miniature laser materials. Today Lithium triborate is the best available nonlinear optical material. Similarly lithium tetraborate is the well known piezoelectric material. The study of borate systems began in 1930's with Li_2O-B_2O_3 system. However, very little is known even today about the Li_2O-B_2O_3-H_2O system. Moreover, the study of borate systems has been carried out in an open system using flux method. Hence, the present authors have made an attempt for the first time to study Li_2O-B_2O_3-H_2O system under hydrothermal conditions. The work has resulted in the discovery of several new borates for the first time and it is predicted that most of these new borates are the potential technological materials. The study of the system Li_2O - B_2O_3-H_2O has resulted in the crystallization of the following phases: $Li_4B_7O_{12}Cl$, $Li_2B_4O_7$, $Li_3B_5O_8(OH)_2$, LiB_3O_5, $Li_4H_2B_2O_6$, $H_2LiB_5O_9$ etc. The composition diagram of the system Li_2O - B_2O_3 - H_2O will be given. Also, the important properties of these phases will be discussed in brief.

B8

CRYSTAL GROWTH, STRUCTURE AND PROPERTIES OF $LiH_2B_5O_9$ AND $Li_4H_2B_2O_6$ - NEW SUPERIONIC BORATES

K. Byrappa and K.V.K. Shekar
The Mineralogical Institute, University of Mysore
Manasagangotri, Mysore-570 006, India
S. Gali and A. Cardenas
Department de Crystal.lografia i Diposits Minerals
Universitat de Barcelona, Facultat de Geologia
Marti i Franques s\n 08028 Barcelona, Spain

Borates form an important group of technological materials in the recent years, particularly after the discovery of lithium triborate as the best nonlinear optical material. The present authors have discovered several new phases in the system Li_2O-B_2O_3-H_2O under hydrothermal conditions. In this paper the authors report the crystal growth of $LiH_2B_5O_9$ and $Li_4H_2B_2O_6$ - the two new borates under hydrothermal conditions. The crystal structures of these new borates have been refined using Philips PW 1100 single crystal X-ray diffractometer. Both crystallize in the monoclinic system and the cell parameters are as follows: $LiH_2B_5O_9$, $P2_1/a$, a = 13.576 (4), b = 9.077(4), c = 5.543(3) Å, β = 91.47°, V = 682.8(4) $Å^3$, $Li_4H_2B_2O_6$, C2/c, a = 8.374, b = 4.977, c = 6.205 Å, β = 114.8°, V = 234.75 $Å^3$.

Here, the authors have discussed the crystal structures with reference to the properties. The crystal chemistry of the borates indicate the potential electrical conductivity. Hence, the authors have carried out the impedance measurements for these compounds which indicate high lithium ionic conductivity in the order of 10^{-2} (ohm, cm)$^{-1}$ at about 300°C.

B9

CZOCHRALSKI GROWTH OF PURE AND Cd^{2+},Nd^{3+} DOPED BENZIL $C_6H_5COCOC_6H_5$ SINGLE CRYSTALS

M.D. Aggarwal, W.S. Wang and M. Tambwe
Department of Physics
Alabama A&M University, Normal, Al 35762

A modified Czochralski Crystal growth system for the growth of benzil ($C_6H_5COCOC_6H_5$) single crystals has been designed and fabricated. Single crystals of benzil (10x10x20 mm^3) of optical quality have been grown successfully from melt by this technique. Angle tuned second harmonic generation of Nd:YAG laser radiation at λ_ω=1.06μm with a conversion efficiency $n = I_{2\omega}/I_\omega$ = 0.4% has been demonstrated using a 5 mm thick crystal sample. We also used a Nd:YAG pulse laser to measure the radiation damage threshold as 159 MW/cm2 (c-axis) and 239 MW/cm2 (a-axis) under the conditions that laser pulse width is 10 ns. The nonlinear coefficients and damage thresholds of benzil indicate that benzil is not an ideal nonlinear optical material. The poor nonlinearity of benzil may be due to a crystal structure symmetry of the compound including the two benzene rings. In recent years, several new organometallic complex crystals, having high nonlinear efficiency and high laser damage thresholds have appeared in the literature. Using simple organic conjugated radicals and the halogens as ligands with a metallic ion for the formation of the complex crystals, it is possible to clearly illustrate the effect of radical structure arrangement on the nonlinear optical efficiency. For the above mentioned reasons, we attempt to improve on nonlinear optical properties of benzil. Cd^{2+} and Nd^{3+} doped benzil material has been prepared. The Czochralski and the modified Bridgman-Stockbarger techniques will be used for growing doped benzil single crystals and results will be presented.

THE CRYSTAL GROWTH BEHAVIOUR OF THE ORGANIC NON-LINEAR OPTICAL MATERIAL 2-(α-METHYLBENZYLAMINO)-5-NITROPYRIDINE (MBANP)

B10

P.J. Halfpenny, R.J. Ristic and J.N. Sherwood*
Department of Pure and Applied Chemistry
University of Strathclyde, 295 Cathedral Street, GLASGOW G1 1XL, UK

Over the past decade a wide range of polar organic materials has been developed for non-linear optical applications. Many of these exhibit figures of merit several orders of magnitude greater than their inorganic counterparts and have substantially higher laser damage thresholds. While the considerable potential of such materials has been clearly demonstrated, a significant obstacle to their development and the full exploitation of this potential has been the difficulty encountered in the growth of large high quality crystals.

2-(α-methylhenzylamino)-5-nitropyridine (MBANP) is amongst the most promising of these highly efficient organic NLO materials with potential applications for frequency conversion in the near infrared. MBANP, however, exhibits many of the problems commonly associated with the crystal growth of organic NLO materials. In particular, its poor thermal stability at the melting point preclude growth from the melt. Furthermore, the growth behaviour from solution is complex, with a strongly supersaturation dependant crystal habit, unstable growth or zero growth rate of certain faces, depending upon growth parameters. Although growth of large high quality crystals of MBA from solution has been achieved, this behaviour poses considerable difficulties.

The results of a detailed study of the crystal growth kinetics MBANP crystals from methanol solution are presented. The supersaturation and temperature dependence of the growth behaviour of the major faces have been examined, in particular the transition from zero growth to rapid unstable growth in the polar <010> direction. These results are considered in the context of the highly polar nature of MBANP and possible causes of the anomalous growth behaviour are discussed.

*Permanent Address: Institute of Physics, P.O. Box 57, Belgrade, Yugoslavia.

CHARACTERIZATION OF DEFECTS IN ORGANIC SINGLE CRYSTALS BY X-RAY TOPOGRAPHY

B11

Masaru Tachibana, Qi Tang, Akira Uedono** and Kenichi Kojima*
Department of Physics and *Graduate School of Integrated Science
Yokohama City University, 22-2 Seto, Kanazawa-ku, Yokohama 236, Japan

Recently, much attention have been paid on organic crystals owing to their attractive properties, such as optical non-linearity, super-conduction and so on. The growth of large organic single crystals with high-quality is one of the important subjects for basic research and applications of their properties. The understanding of the properties of defects in the growth crystals are indispensable for the improvement of crystal quality. X-ray topography is one of the most powerful methods for characterizing the defects in large and nearly perfect organic crystals.

We will report on the growth of organic single crystals from various methods and the characterization of the defects in growth crystals by X-ray topography.

As an example, the investigation for benzophenone crystals is summarized as follows. The nearly perfect benzophenone single crystals have been grown by Czochralski method. The dislocations introduced during the crystal growth have been examined using Lang technique and synchrotron radiation technique of X-ray topography. The double images of single dislocations were found on the topographs taken in some reflection planes. The dislocation images were analyzed by means of the kinematical theory. Consequently, the Burgers vector of predominant grown-in dislocations was determined to be [001](7.88 Å). This preferred Burgers vector of the grown-in dislocations is the general aspect in Czochralski-grown benzophenone single crystals.

We will also present on the growth of other organic crystals and the assessment of their perfection.

**Present address: Faculty of Engineering, University of Tokyo, Hongo, Bunko-ku, Tokyo 113, Japan.

B12

THE INFLUENCE OF AN INTERFACE ELECTRIC FIELD ON THE DISTRIBUTION COEFFICIENT OF CHROMIUM IN LINbO3

Satoshi Uaa and William A Tiller
Department of Materials Science and Engineering
Stanford University, Stanford, CA 94305-2205, USA

The effective solute partitioning of chromium was investigated on single crystals of $LiNbO_3$ grown by the laser-heated pedestal growth (LHPG) technique. Electric field effects at the interface influence this solute partitioning leading to an electric field-dependent effective solute distribution coefficient, k_E. The origin of these electric field effects in $LiNbO_3$ was nicely confirmed by D'yakov *et al*[1] that an electric field generated via a temperature gradient is associated with a thermoelectric power while an additional electric field is growth rate associated via a charge separation effect. The LHPG technique made it possible to explore these field effects by controllably changing the growth velocity (V) and the temperature gradient (G_S, G_L) near the interface over a wide range. The strong thermoelectric power generated in both the solid and liquid yields an extremum point in the potential curve at an interface. By applying the BPS theory to our experimental data, we found that a higher temperature gradient, leading to a higher thermoelectric power, yields a larger k_E (Fig 1) and a larger k'_{E0} which is the intercept value at V=0 for constant G_L in Fig 1. By plotting k'_{E0} vs. the temperature gradient, G_L, we find the phase diagram solute partition coefficient to be $k_0 \approx 3.65$, represented by an intercept value at G_L=0 in Fig 2. It is theoretically shown that the same considerations can he applied to all ion partitioning at a solid-liquid interface.

[1] V.A. D'yakov, D.P. Shumov, L.N. Rashkovich, A.L. Aleksandrovskii, *Izvestiya Akademii Nauk SSSR. Seriya Fizicheskaya* **49**, 2418-2420 (1985). (UDC 548.55).

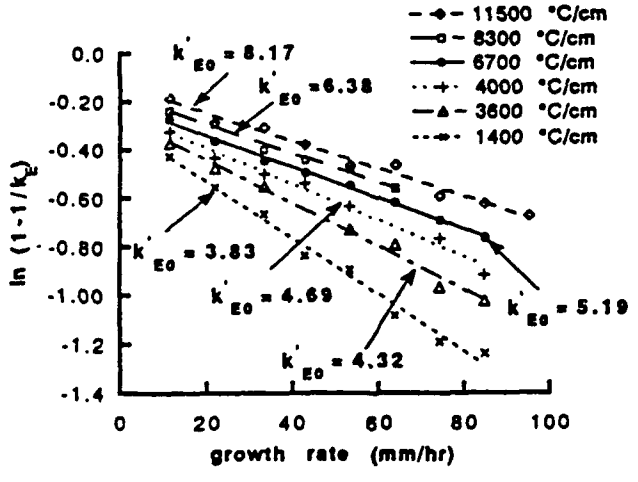

Figure 1

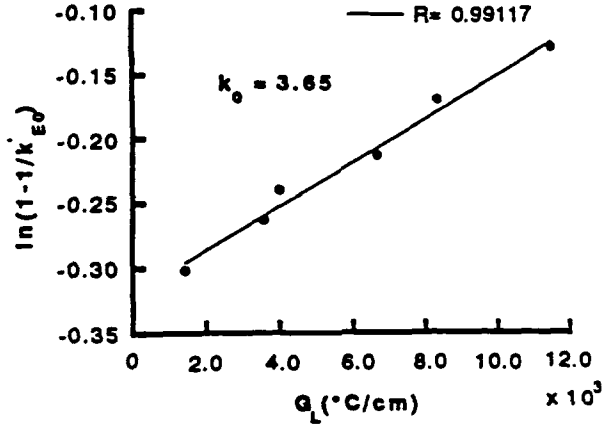

Figure 2

THE INFLUENCE OF AN INTERFACE ELECTRIC FIELD ON THE BEHAVIOR OF CHROMIUM DURING $LiNbO_3$ SINGLE CRYSTAL GROWTH

B13

Satoshi Uda and William A Tiller
Department of Materials Science and Engineering, Stanford University
Stanford, CA 94305-2205, U.S.A

The role of thermoelectric power and/or charge separation-generated electric fields upon Cr-doped $LiNbO_3$ crystal growth by the laser-heated pedestal growth (LHPG) technique is treated by investigating both steady-state and initial transient solute redistribution based on the concept of a field-modified partition coefficient, k_{E0} and an effective growth velocity, Y_E. This (V_E, k_{E0}) transformation technique is very useful for simplifying the interface conservation condition as a boundary condition when one needs to solve a differential equation including field effect terms and these often make this condition very complex without such a modification. This simplification comes from the fact that V_E includes all the electric field terms and k_{E0} then has a simple form $k_{E0}=k_{E0}$ (V/V_E). The V_E is extended to V_{EL} and V_{ES}, for the liquid and the solid, respectively, when one deals with the diffusion of a solute of interest both in the liquid and solid. The magnitude of these electric field effects is dominated not only by the strength of the field but also by the solute diffusion coefficient in the phase considered since the electric field effect is always a combination of the strength of the field and the diffusivity of the solute upon which the field operates. In order to clarify the effect of these electric fields, we designed a specific experiment where one sees an interesting solute depletion phenomena found for the Cr^{3+} ion in the solid immediately behind the interface. A high diffusion coefficient for Cr^{3+} in the liquid and a very low diffusion coefficient for Cr^{3+} in the solid, combined with the electric field operating in the liquid, leads to a strong pulling force on the Cr^{3+} from the solid through the interface into the liquid. This generates a deep solute depletion region in the solid behind the interface. An analytical solution to this depletion phenomena is given and the quantitative agreement between theory and experiment is shown.

OPTICAL DETERMINATION OF THE CONGRUENT COMPOSITION OF $LiNbO_3$ CRYSTALS

B14

*I. Baumann, D. Krabe**, P. Rudolph* and R. Schalge****
Telefilter tft GmbH TFE, Material Research and Technology
*Humboldt-University Berlin, Dep. of Crystallography and Material Science
**Lennéstr. 82, 0-1500 Potsdam, Germany
***Sophienstr. 25, 0-1130 Berlin, Germany

The birefringence of $LiNbO_3$ varies due to the compositional variation of the extraordinary refractive index ne [δn_e = -(1.1 - 1.6 x 10^{-4}) / C 01 – [illegible] Li_2O] [1]. Optical applications demand a homogeneity of the refractive indices and birefringence of 5 - 7 x [illegible] To find the exact congruent composition to ensure identical properties throughout the whole crystal boule is therefore an important task in crystal growth.

We solved this problem with an orthoscopic test equipment [2,3] which reveals the relative course of n_e parallel to the growth direction by means of an interference pattern over the whole crystal. The course of the interference fringes shows a typical feature depending on the deviation from the congruent composition (see fig.1). Assuming a linear dependence of δn_e from the Li_2O content in $LiNbO_3$, we can use Pfann's segregation equation to describe the change of the birefringence as result of compositional segregation.

The congruent composition of [00.1] grown $LiNbO_3$ was determined with 48.470 ± 0.005 mol-% Li_2O. Local appearing optical inhomogeneities especially in the range of g<0.1 due to compositional variations will be discussed as result of an incomplete mixing in the melt, the evaporation loss of a melt constituent and a change in the convective stream pattern in the melt during crystal growth.

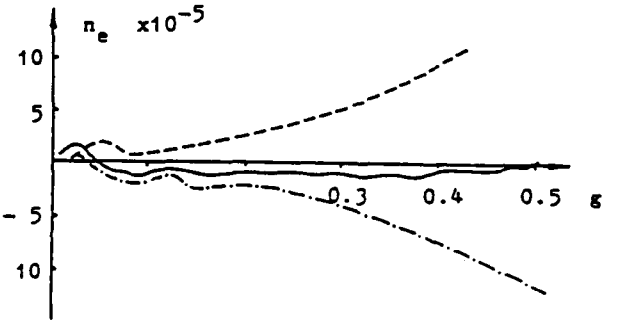

Li_2O-content: 48.46 mol-%, 48.47 mol-%, 48.48 mol-%

Figure 1. Variation of n_e parallel to the growth direction

[1] J.R. Carruthers et al., *Applied Optics* 13/10 (1974) 2333.
[2] R.L. Byer et al., *J. Appl. Phys.* 41/6 (1970) 2320.
[3] R. Schalge, C. Barta, Int. Symp. on Mercury (I) - Halides Liblice 17.-19.10.1976 p.31.

B15

GROWTH OF Cr:LiCAF CRYSTALS BY BRIDGMAN TECHNIQUE

Lisen Cheng, Chaoen Huang and Shuqing Zhao
Research Institute of Synthetic Crystals
P.O. Box 733, Beijing, 100018, P.R. China

Cr:LiCAF (chromium doped colquiriite) crystals have been grown by various techniques including top-seed crystal, Czochralski and melting-zone techniques. But center scattering and other defects always appears in the as-grown crystals, and it almost impossible to get tension-free crystals by the above mentioned usual crystal growth techniques.

Formation mechanisms of center scattering in Cr:LiCAF crystals have been analyzed in our laboratory. To remove the center scattering in the crystals and the tension produced during crystal growth, we purified the source materials for Cr:LiCAF crystal growth, and selected Bridgman method to grow the crystals. In our experiments, a two-zone heating furnace was designed and the effects of temperature distributions in the furnace on the quality of as-grown crystals were studied systematically.

Under the optimum growth conditions obtained from the experiments, center scattering free crystals of Cr:LiCAF have been got in our laboratory.

B16

CRYSTAL GROWTH AND PROPERTIES OF COMPLEX FLUORIDE CRYSTALS OF CUBIC PEROVSKITE

Y. Zhang, S. Ren** and J. Zhang***
*Current address: Wainer Str. 4, w-7939 Schwedi-Hoerenhausen, Germany
**Beijing Glass Research Institute, 100062, Beijing, China

In order to develop new tunable solid state lasers and color center lasers, we studied the crystal growth and properties of complex fluoride crystals of cubic perovskite. The crystals of pure $KMgF_3$ and $KZnF_3$, and those doped with Ni^{2+}, Eu^{2+}, and Cr^{3+}, etc., have been grown by the Bridgman-Stockbarger method. The raw material must be dehydrated, purified and fluorinated very carefully. Flat solid-melt interface crystals of laser quality have been successively grown with specially designed graphite crucibles. With Li^{1+} for charge compensation, $KZnF_3$ crystals doped with one atomic percent of Cr^{3+} have been grown with sizes up to D30 x L50 mm without crack. The optical, spectral, color center, and laser properties of these crystals have been measured and will be presented in comparison with Cr^{3+}:GSGG.

B17

CRYSTAL GROWTH AND CHARACTERIZATION OF FLUORIDES WITH ELPASOLITE STRUCTURE

J. P. Chaminade, J. Grannec and A. Tressaud
Laboratoire de Chimie du Solide du CNRS, Université de Bordeaux I, 33405 - Talence Cedex, France
I.N. Flerov, A.I. Kruglik and K.S. Alexandrov
L.V. Kirensky Institute of Physics, 66036 - Krasnoyarsk, USSR

Fluorides of general formula A_2BMF_6, where A and B are monovalent metal ions and H is a trivalent cation, belong to a wide family of crystals whose structures derive from that of the elpasolite (K_2NaAlF_6 prototype structure, Fm3m with z=4). The structural arrangement corresponds to that of the perovskite with an additional cationic ordering between the smaller monovalent cations B and trivalent cations H in the octahedral sites [1,2].

These materials have been proposed as attractive ionic host crystals for optical applications: lasers, detectors or scintillators. The present work deals with the crystal growth of Rb_2KMF_6 compounds with M = Fe, Ga, Y, In by Bridgman method.

Commercial products KF and RbF were dehydrated under vacuum. MF_3 trifuorides were synthesized from the corresponding chlorides or oxides under an HF flow up to 1000°C or under an F_2 stream up to 600°C depending on the material. The crystal-growth equipment was built up of two independent furnaces separated by an insulating zone. The temperature of each furnace has been separately programmed. The biconical shaped crucibles were sealed under dry argon atmosphere and set in the crystal growth apparatus. Initially heated to $T = T_F + 50$ K in the upper furnace, the crucible was moved down to the cooler furnace at a rate of 0.15 mm/h to 1.5 mm/h with a thermal gradient of 2.5 K/mm. The temperature was then lowered to room temperature at a rate of 10 K/h to minimize any thermal stresses.

Single crystals of 3 cm long, 1 to 1,5 cm diameter were obtained without visible inhomogeneities. They were cut into slices or cubes along the different crystallographic orientations. X-ray diffraction, calorimetric and optical properties were investigated. As an example, Rb_2KInF_6 which is cubic at room temperature undergoes two successive phase transitions at about 284 K and 265 K, as already observed for Rb_2KScF_6.

[1] K.S. Aleksandrov and S.V. Misyul', *Sov. Phys. Crystallogr.*, 26, 612, (1981).
[2] A. Tressaud, S. Khairoun, J.P. Chaminade and M. Couzi, *Phys. Stat. Sol.* a) 98, 417 (1986).

GROWTH BY LPE OF Nd:YAG SINGLE CRYSTALS LAYERS FOR WAVEGUIDE LASER APPLICATIONS

B18

B. Ferrand, D. Pelenc, I. Chartier and Ch. Wyon
CEA - DTA/LETI/DOPT - 85 X - 38041 Grenoble Cédex - France

This paper is concerned with the growth of Nd:YAG layers by Liquid Phase Epitaxy for waveguide laser applications. Layers were grown on (111) YAG substrates from a saturated PbO/B_2O_3 flux using the horizontal dipping. Films with thickness up to 100 µm and with Nd concentration up to 15% have been obtained. Influence of melt composition on growth conditions were discussed. Good quality films have been grown at low supersaturation ($\Delta T < 20°C$) and at a temperature higher than 1000°C, to prevent lead contamination. Some substitutions were studied with the purpose of optimizing the waveguide properties. Samples were prepared with Nd concentration of about 1.5% and substitutions with gallium, in order to increase the refractive index and with lutetium, in order to adjust the lattice mismatch.

By cutting and polishing such samples, we have fabricated planar waveguides on which very low threshold laser operation have been performed at 1.064 µm using R6G dye laser and GaAlAs diode laser as pump source [1].

[1] D.P Shepherd, S.J Field, D.C. Hanna, A.C Large. A.C Tropper, I. Chartier, B. Ferrand, D. Pelenc, "Very low threshold laser operation of an epitaxially grown Nd:YAG Waveguide," Submitted to CLEO 92.

GROWTH AND STOICHIOMETRY PROBLEMS OF ZnSe FOR HIGH POWER LASER OPTICAL COMPONENTS

B19

E. Krause, A. Fissel and H. Hartmann
Institut für Kristallzüchtung, 0-1086 Berlin, FRG

ZnSe is one of the most important materials for high power CO_2-laser components. For the growth of thick layers (up to 1 cm) we use a modified low pressure chemical vapour deposition process. We start from the pure elements and avoid the commonly used highly toxic hydrogen selenide gas. The chemical reaction takes place at total pressures around 6 Torrs and growth temperatures between 480-810°C. Deposition rates vary between 30-120 µm/h. The transport controlled growth regime required optimization of stream line patterns across the glassy carbon substrates of 120x200 mm dimensions.

To this end we used powder patterns produced in the region of homogeneous nucleation under otherwise real deposition conditions. The main problems we are dealing with result from varying gas phase concentrations and distributions of the Se-Polymers (Se_2-Se_{14}). The large influence of growth stoichiometry - expressed by the partial pressure ratio Zn/Se_x - on the growth phenomena of the polycrystalline layers and on their crystallographical, mechanical, optical properties is also connected with that problem.

We present results to growth morphology (columnar, cellular structure), mechanical stress distributions and optical measurements (transmission, defect luminescence, colour cathodoluminescence) related to effects of deviation from stoichiometry during growth. On the base of these results we try to understand the large differences in laser induced damage threshold found by testing the material.

A main result was the finding of the deterioration of morphological features as well as physical properties under Zn excess during growth. Best properties and highest laser damage resistance was found for slight Se-excess (3-5%).

THE GROWTH OF ALEXANDRITE CRYSTALS

B20

Ma Xiaoshan, Shen Yafang, Wu Guangzhao, Zhu Rude, Xu Jun and Zhang Xinmin
Shanghai Institute of Optics and Fine Mechanics PRC

In this paper, we will discuss two problems for the growing of alexandrite crystals. This two problems had puzzled us for a long time. One of them is the 'melt aging' which was named by R.C. Linares some decades ago. The strange phenomenon, melt aging is such that no one can grow transparent alexandrite crystal from aging melt. The mechanism of melt aging formation is suggested. A novel process is designed to overcome the melt aging. The second problem is a novel kind of inclusions have been found in alexandrite crystals. This kind of inclusions is parallel to <100> direction and takes majority part of the inclusions. Studies in the formation of such inclusions and the necessary ways to eliminate them are, therefore, essential in the improvement of the optical quality of laser crystals. We study and propose a mechanism for the inclusions formation. After studying high quality crystals have been grown with good reproducibility.

B21

GROWTH AND OPTICAL CHARACTERIZATION OF TRIVALENT TITANIUM DOPED CHRYSOBERYL (Ti^{3+}:$BeAl_2O_4$)

*K. Yamagishi, Y. Nobe, Y. Anzai, Y. Yamaguchi and H. Takei**
Corporate R&D Center, Mitsui Mining & Smelting Co., Ltd, Ageo 362, Japan
*Institute for Solid State Physics, Tokyo University, Tokyo 106, Japan

Trivalent titanium ion doped chrysoberyl (Ti^{3+}:$BeAl_2O_4$) is a promising crystal for tunable laser. Many titanium doped oxide and fluoride crystals are known to have two difficulties when applied as a tunable laser crystal; control of the valency state of titanium and an unrecognizable absorption center in the lasing wavelength of the trivalent titanium ion in the crystals.

We grew titanium ion doped chrysoberyl crystals using Czochralski method under different growth atmospheres (H_2 + H_2O or H_2 + CO_2) to control the valence state of titanium ion. The distribution coefficient showed remarkable change near $logPO_2$ = -9 (Fig. 1), which is close to the phase equilibrium condition between the trivalent and tetravalent titanium ions as calculated from the standard energy of formation. The valence state of titanium was almost trivalent (more than 95%) in crystals grown in an atmosphere where the oxygen partial pressure was between $logPO_2$ = -9 and -12. Optical absorption spectra of all the grown crystals did not exhibit an absorption due to the divalent titanium ion.

We grew subsequently iron ion doped crystals, off-stoichiometry crystals and high titanium doped chrysoberyl crystals. Czochralski method was used to grow the low transition metal doped chrysoberyl crystals, and floating zone method was used to grow the off-stoichiometry and high titanium doped crystals. All the titanium doped chrysoberyl crystals showed strong optical absorption between 400 ~ 650 nm caused by the trivalent titanium ion, and weak absorption between 350 ~ 1,900 nm, which was within the lasing wavelength region. The weak absorption coefficient was found to be proportional to the square of the titanium ion concentration and was independent of both the dopant level of the iron ion and the BeO/Al_2O_3 stoichiometry. To decrease this weak absorption, titanium and boron co-doped crystals were grown. No weak absorption was observed in these crystals and the strong absorption was not affected.

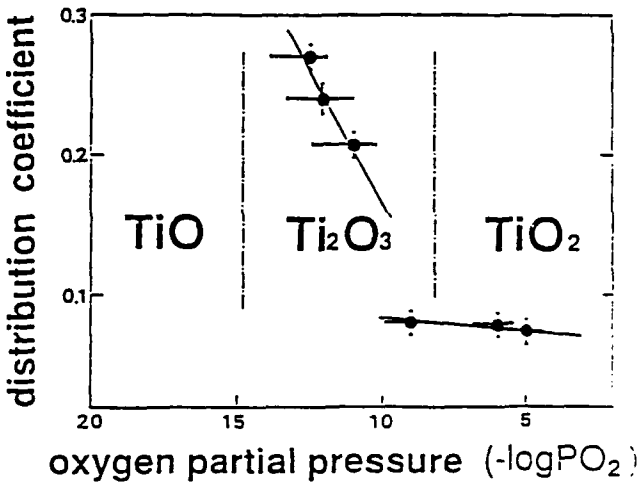

Figure 1. Oxygen partial pressure dependence of distribution coefficient.

CZOCHRALSKI GROWTH OF $Mg_2SiO_4:Cr^{+4}$ IN OXIDIZING ATMOSPHERE

B22

Pan Peicong
Shanghai Institute of Ceramics, Academia Sinica
Home Address: Room 103, 306 Ta Cheng Road, Jia Ding County
Shanghai 201800, P.R.China
Zhu Hongbing, Yan Shenghui, Chai Yao, Wang Shiting and Hou Yingchun
Shanghai Institute of Optics and Fine Mechanics, Academia Sinica
Shanghai 201800, P.O.Box 800216, P.R.China

The tetravalent chromium ions doped forsterite ($Cr^{4+}:Mg_2SiO_4$) is a newly developed tunable laser crystal centered at 1.2um. Many people have reported that the relative concentration of Cr^{+4} ions in Mg_2SiO_4 depends on the growing atmosphere and an oxidizing atmosphere may partially transforms the Cr^{3+} into Cr^{4+}.

In our experiment, Cr^{+4} doped forsterite crystals were grown by Czochralski method with use of rf-heating and Ir crucible under oxidizing atmosphere. Large single crystals of $Mg_2SiO_4:Cr^{4+}$ up to 25 mm in maximum diameter and 80 mm long were grown. By comparing the absorption around 1.0 um, the relationship between the oxygen partial pressure of the growth atmosphere and the relative concentration of Cr^{+4} was determined. Our experiments indicated that a summit concentration of Cr^{+4} is obtained in the crystals grown from nitrogen with 15% oxygen.

Everybody knows that iridium reacts with oxygen in an oxidizing atmosphere in high temperature. Our experiments also showed that this reaction is susceptible to occurrence between 800°C and 1400°C. A minimal oxidation of iridium can be obtained if the oxygen gas was not flowed into chamber of furnace until the temperature of Ir crucible was increased above 1400°C. In the cooling process, the oxygen gas should be pumped before the temperature was dropped down to 1400°C. To protect the Ir crucible from oxidizing, another method has been used successfully. The outer surface and a small part of inner surface of Ir crucible was covered with a coating of zircite ceramics about 0.5 mm in thickness by Plasma Jet Method. But the coating only can be used once and should be renewed in next growth. As a result, Ir consumption in every growth 30 of hours was reduced from 12.5g to 4.0g.

In this paper, the other growth technique and properties of Cr^{+4} doped forsterite crystal is also introduced.

GROWTH OF HIGH-QUALITY $Ti:Al_2O_3$ CRYSTALS FOR SOLID-STATE LASER APPLICATIONS

B23

C.P. Khattak and F. Schmid
Crystal Systems, Inc., Salem, MA 01970

Lasing action in titanium-doped sapphire ($Ti:Al_2O_3$) was demonstrated in 1982. The emission for this widely tunable material spans from 660 nm to 1200 nm, peaking at 800 nm. There is no excited-state absorption; therefore $Ti:Al_2O_3$ has the potential as an efficient tunable solid-state laser.

The Heat Exchanger Method (HEM) was developed for the growth of $Ti:Al_2O_3$ boules. During initial development a broad parasitic absorption centered at 800 nm limited the performance of the material for laser applications. This parasitic absorption was associated with Ti^{3+} - Ti^{4+} pair formation. Emphasis was placed on growing crystals under a reducing atmosphere to minimize Ti^{4+} formation. Currently 10 cm diameter $Ti:Al_2O_3$ boules of high quality are grown for laser applications. Characterization of the material has shown that the parasitic absorption is undetectable even in 8 cm long rods.

The low segregation coefficient of titanium in sapphire results in gradation of Ti concentration within the boule. Laser rods are therefore cored perpendicular to the growth direction so that the dopant Variation within the rod is minimized. Crystal growth, characteristics of the material and laser applications will be discussed.

B24

LASER QUALITY Ti:SAPPHIRE CRYSTAL GROWTH BY CZOCHRALSKI

Yin Shaotang, Qin Qinhai, Xu Jiangfong, Zhou Dongfang, Huang Xiouhua and Tang Honggao
Anhui Institute of Optics and Fine Mechanics
Academia Sinica, Hefei, P.R. China

Ti: sapphire is a phonon-terminated laser crystal with excellent thermal, physical and optical properties, and its broadest lasing band form 660 to 1100nm promises the future in many fields of application.

The Ti:sapphire crystal was grown by the Czochralski method. The reason which causes macroscopic defects in the crystal was discussed. The raw material was carefully selected and purified. The defects has been significantly reduced by controlling liquid flow, temperature field, crucible size and other growth parameters. The crystal size grown has reached φ30 x 120mm without precipitates, bubbles and other defects.

The main problem for device application is the residual infrared absorption existed in Ti:sapphire crystal. In an oxidizing atmosphere partial Ti^{3+}can be easily turned to Ti^{4+} which results in high residual infrared absorption during growth or annealing. Accordingly the crystal has to be grown and annealed at high temperature in a reducing atmosphere. The coefficient of residual infrared absorption at 800nm of the crystal grown in our laboratory is below $0.01cm^{-1}$. The main absorption coefficient at 490nm can be controlled from 0.5 to $25cm^{-1}$. The figure of merits can reach above 200.

The crystal was lased pumping by double-frequency of YAG laser with high efficiency, tunable range from 670 to 1020nm and frequency doubling from 340 to 500nm. The lasing of Ti:sapphire has also been demonstrated pumping by PS-pulse-YAG laser or flash lamp.

The Ti:sapphire crystal with laser quality and high FOM for laser application has been grown by the Czochralski method in our laboratory.

B25

INVESTIGATION OF LNA SINGLE CRYSTALS

Xu Tianhua, Peng Weiqing, Zheng Qimeng and Huang Changming
South-West Institute of Technical Physics
Chengdu, Sichuan 610015, P.R.C.

LNA single crystals were grown along the orientation perpendicular to the crystalline c axis using Czochralski technique by RF heating. The tested ranges of the components in the formula

$$(La_{1-x}ND_x)_{1+w}Mg_{1+y}Al_{11+z}O_{18+\frac{3}{2}w+y+\frac{3}{2}z}$$

were: w = -0.0 ~ 0.1, x = 0.15 ~ 0.25, y=-0.50 ~ 0.10, z = -0.05 ~ 0.5. The results have shown that it is favorable for growth and qualities of the crystals when y= -0.65 ~ 0.70 and the crystals are rich in Al(several per cent).

The crack and the cleavage along (00.1) are related mainly with the temperature distribution and the high steps of (00.1) appearing during enlargement of the shoulder, but they can be avoided by using a special structure of the thermal field and slowing down the rate of forming shoulder. There exists usually a 'core effect' in LNA crystal with convex interface; vertical step-like microscopic morphology of (00.1) at the convex end of the crystal when the crystal is pulled out of the melt rapidly, especially when the corresponding temperature gradient is small. Such a growth mechanism is considered to be the main cause of the "fog-like" scatterer and lamination.

When the crystal is grown at a high rotation rate, the conversion of the interface shape similar to that of YAG resulted from the transition of the liquid flow was observed. At that time, the diameter of the crystal increases rapidly and the temperature oscillates violently; the interface becomes flat and the "core effect" ends. For this purpose, the "Controlled Conversion of Solid/Liquid Interface" developed by us in the investigation of YAG was tested and the "core effect," the defects in the region below interface conversion, the "water ripple" and "fog-like" scatterers were eliminated. It is believed that application of this method is of special significance and effect to the growth of crystals having a growth mechanism similar to that of LNA. Since the crystal grows with flat interface, the growing front advances simultaneously, what makes it possible to avoid the troubles associated with the step-like growth.

We have grown large crystal of comparatively good quality, 28mm in diameter and 190mm in length. The laser rod size is up to ϕ7 x 135mm. And an output of 7.73J and 30w were obtained with a LNA laser rod having 6 mm in diameter and 94 mm in length.

GROWTH OF Nd:YAG CRYSTALS FREE FROM DISLOCATION AND CORE

B26

Xu Tianhua, Wu Zihe, Peng Weiqing, Zheng Qimeng, Xiao Zhongchao, Zhou Jianmin, Zhang Shengxiu and Xie Sanwen
South-West Institute of Technical Physics
Chengdu, Sichuan Province 610015, P.R.C.

A new method called "Controlled Conversion of Solid/Liquid Interface" developed by us for growth of Nd:YAG crystals free from dislocation and core is reported. In the process of developing the technique, investigations were carried out of the relationship between the interface conversion and the growth parameters, such as rotation rate, diameter of crystal and temperature distribution, the influence of the conversion on the temperature stability near the interface, the breakdown of the interface and the dislocations caused by constitutional supercooling as well as the law of the dislocation extending.

When the crystal is grown at a fixed high rotation rate, the "spontaneous conversion" of the solid/liquid interface from convex to flat usually happens due to transition of the natural convection to the forced one, which leads to constitutional supercooling and dislocation breeding. Under the conditions of proper selection of the seed and the structure of the thermal system we should first allow the crystal to grow at a low rotation rate until it becomes equi-diametral; then, increase the rotation rate to a necessary level to make the interface flipping and flatting; use artificial re-melting to eliminate the defect region resulted from the unstable growth during the conversion and keep the diameter uniform before and after the conversion, finally, make the crystal grow with a flat interface when the system has stabilized.

The dislocations in the prepared samples were investigated by means of etching method and birefringence observation. And some Nd:YAG crystals up to 22-27mm x 120-150mm free from dislocation and core have been grown by using this method with a satisfactory repeatability. The method has been used in the growth of YAG respectively doped with Nd, Er or Tm by RF or resistance heating, and it is undoubted that the method can be also used in growth of other refractory oxide crystals, such as GGG and YAP.

GROWTH AND LASER PROPERTIES OF NEODIMIUM DOPED CNGGG CRYSTALS

B27

M. Timoshechkin
General Physics Institute, Academy of Sciences
117942, Vavilov Street 38, Moscow, USSR

The application of garnets in laser devices is well known because of the good combination of optical, spectra-emission and thermo-mechanical properties. In our paper we report crystal growth data, growth defects formation in Chochralski grown from platinum crucibles crystals of calcium-niobium-gallium-germanium garnet (CNGGG) which are of interest for use in efficient solid state lasers. The influence of crystal growth conditions, melt composition, some structural defects and optical inhomogeneities on laser properties are estimated. As a result, high optical quality Nd doped CNGGG crystals were grown and laser rods 5 mm in diameter and 60 and 75 mm long were fabricated and tested. The laser rods demonstrated efficiency more then 1.4% which was as high as that for high quality Nd:YAG laser rods in the same test conditions.

B28

Si AND Mg DOPED GGG SINGLE CRYSTALS

M. Göbbels[1], *S. Kimura*[2], *K. Langer*[3] *and E. Woermann*[1]

[1]Institut für Kristallographie, RWTH Aachen, Jägerstraße 17/19, D-5100 Aachen, Germany

[2]National Institute for Research in Inorganic Materials, Namiki 1-1, Tsukuba, Ibaraki 305, Japan

[3]Institut für Mineralogie und Kristallographie, TU Berlin, Ernst-Reuter-Platz 1, D-1000 Berlin 12, Germany

There is a wide range of application for GGG ($Gd_3Ga_5O_{12}$) single crystals as laser host materials and substrates for magnetic bubble devices. Due to impurities, especially Si, in the starting oxides color centers are formed in the GGG crystal.

Several GGG single crystals with different doping levels of Si, Mg and Si+Mg were grown by the floating-zone method. The actual doping level was checked by chemical and spectroscopical analysis. The color centers were activated by annealing at 1673 K in argon, hydrogen or oxygen atmospheres respectively followed by a Xe-lamp irradiation. The transmission spectra of the crystals were measured.

The absorption bands corresponding to the activated color center can be correlated with the respective dopant and the type of activation (table 1). In case of Si+Mg-doping the Si-color center formation is eliminated.

Table 1. Color centers and the corresponding activation

	Si-doped GGG	Mg-doped GGG
Annealing in H_2	Absorption band at 320 nm after additional irradiation.	Decrease of absorption at 240-310 nm. Increase of absorption at 240-310 nm due to addiitional irradiation.
Annealing in O_2	Decrease of absorption at 240-310 nm.	Absorption at 240-310 nm increases.
Annealing in Ar	Absorption band at 420 nm	No influence on the absorption.

B29

THE GROWTH OF $LaMgAl_{11}O_{19}$:Nd LARGE CRYSTALS WITH HIGH QUALITY

Wu Guangzhao, Ma Xiaoshan, Xu Jun, Zhang Xinmin and Shen Yafang

Shanghai Institute of Optics and Fine Mechanics, PRC

Kahn et al[1] postulated that $LaMgAl_{11}O_{19}$:Nd (LMA:Nd) maybe a good laser crystal for high power laser output and growed large crystals for the first time. Aubert et al 2) and others have grown LMA:Nd crystals by Czochralski technique. Coeure[3] claimed that LMA:Nd is a very good laser crystal for high power output and laser fusing usings. But there are two main difficulties for crystal growth with high quality. The material with stoichiometric composition cannot melt congruently and the crystals as grown always cleave along the (001) plane. We have analyse the inclusions in LMA:Nd crystals with electron probe. The analytical data show that the inclusions are formed by the main component composition variation and no solute tails formed by constituent supercooling have been found. Crystals grown from melt with suitable composition are good and no inclusion have been found in it. After studying the morphlogical important order experimentally and calculating this order with PBC theory[4], it is found the attachment energy of (001) is much less than the others. We cannot avoid the cleavage property of LMA:Nd crystal unless change the attachment energy of (001), but it is possible to change the thermofield to avoid the cleavage of crystals due to the thermal stress. So proper thermofield is designed and high quality crystals free from cleavage and inclusions have been grown with this proper designed thermofield. The dimension of the crystal is 20mm in diameter and 130mm in length. Crystals more larger than this can be grown if the crucible and furnace is large enough. Laser performance show 16W Cw laser output have been obtained.

B30

THE GROWTH OF $BeAl_6O_{10}$:Cr (BHA:Cr) CRYSTALS

MA Xiaoshan, Pan Peicong, Wu Guangzhao and Hu Zhiwei

Shanghai Institute of Optics and Fine Mechanics, PRC

Chen Minqin

Fudan University, PRC

After considering of the requirements for a good Cr^{3+} doped tunable laser crystal, our research has been centering on the development of BHA:Cr, a novel Cr^{3+} doped tunable laser crystal. We growed this crystals for the first time in 1986. The crystal structure are determined and the fluorescent spectra in relation to the crystal structure have been studied also.

SESSION 1C

SILICON CARBIDE CONTROL IN EFG SYSTEM

C1

S. Rajendran, M. Larrousse, B. Bathy and J.P. Kalejs
Mobil Solar Energy Corporation

Thin walled octagonal tubes of Silicon are produced by Edge defined Film-fed Growth process. In this process molten silicon, contained in a graphite crucible, rises through an octagonal die due to capillary action and forms a solid/melt meniscus with a hollow octagonal seed. The octagon tube is pulled up and silicon pellets are fed into the crucible continuously.

The total length of the silicon tubes grown from a single die is limited by the amount of silicon carbide precipitate formed in the capillary slot. Modelling the mass transport and the precipitation of the carbon dissolved in molten silicon revealed that the amount of silicon carbide precipitate depends on the temperature of the silicon melt entering the capillary feed slot.

Magnetic and thermal models of the EFG system developed earlier [1], with commercially available software, were used to determine the parameters that impact the temperature of the silicon melt. The modelling results showed that the silicon melt temperature can be lowered by reducing the height of the die-tip.

A new die-tip was designed incorporating these concepts and other requirements needed to make the crystal growth process robust. The new die-tip has been determined to be functional and the total length of tubes grown from a single die has increased substantially.

The presentation will discuss the salient results on the mass transfer aspects of carbon in silicon melt, compare the magnetic and the thermal model results of the EFG growth system with the old die-tip and the new die-tip. Further, the photomicrographs of the die slots showing the silicon carbide precipitation in the old and the new die-tip designs will be presented.

1. S. Rajendran, C.C. Chao, D.P. Hill, J.P Kalejs and V. Overbye, *J. Crystal Growth* 109 (1991) 82-89.

C2

THE PROGNOSTICATION OF OXYGEN CONCENTRATION IN A LARGE SILICON CRYSTAL GROWN BY CZOCHRALSKI PULLING METHOD UNDER MAGNETIC FIELD USING AN ELECTRONIC COMPUTER

A.I. Pogodin
Chemical-Mettallurgical Plant, Podolsk, USSR
I.V. Starshinova
Institute of Rare Metal Industry, Moskow, USSR

This paper describes prediction of oxygen concentration in silicon crystal (diameter 100-150 mm, weight 20-30 kg) by Czochralski pulling under magnetic field with variation of its magnitudes (B) crystal and crucible rotation rates (W_s, W_c). The prediction was made on the basis of the mathematical simulation of hydrodynamics, heat transport and oxygen transport in the melt. The model considered a rotating in a crucible for a melt that conducts both heat and electricity using the Navier-Stoks equation and the Bussinesk approximation, employing a finite difference method for the initial boundary conditions. The boundary conditions for the temperature were given from the experiment investigation effect of the temperature variations at the crucible walls. The computer program of the numerical simulation was made using IBM PC/AT-386. The values of B, W_s, W_c were defined in the computation which give fixed oxygen concentration in a large silicon crystal.

For instance, Fig. 1a shows oxygen concentration (N_o) in an initial part of the crystal (diameter 100 mm) when B rises from 0 to 0,5 T (Tesla) and W_s=0, W_c=0 (crucible diameter 330 mm, weight of the melt 22 kg). The fluid flow patterns were calculated for the points 1, 2, 3 on the curve N_o=f(B) in Fig. 1a are illustrated in Fig. 1b. The functional dependences N_o =f(B) for different values of W_s, W_c are similar to that on Fig. 1a.

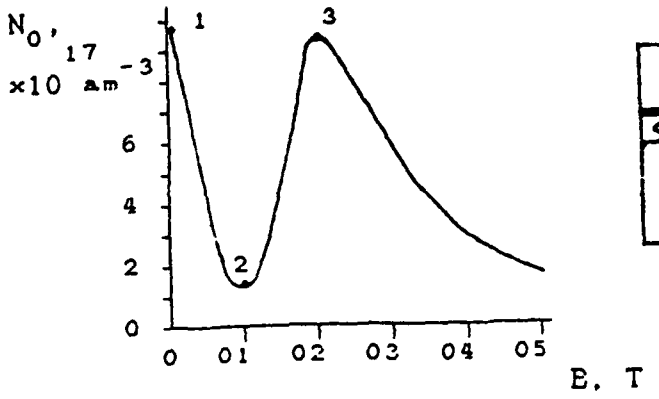

Figure 1a

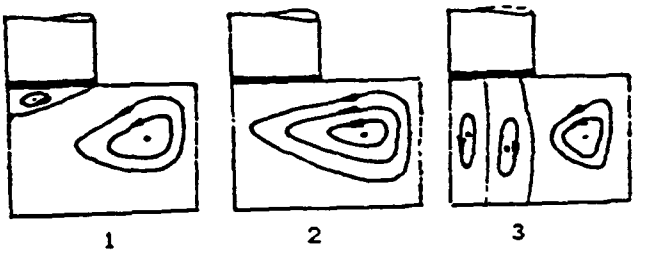

Figure 1b

C3

FACET FORMATION IN SILICON SINGLE CRYSTALS GROWN BY VMFZ METHOD

M. Kimura, H. Arai and H. Yamagishi
Isobe R&D Center, Shin-Etsu Handotai Co., Ltd.
Isobe 2-13-1, Annaka, Gunma, Japan

A fluctuation of electric resistivity in silicon single crystals by method gives a serious problem on the characteristics of discrete devices. However, it is expected that such fluctuation can be reduced by the suppression effect of a magnetic field on the motion of silicon melt. In this report, we investigated a method in vertical magnetic fields (VMFZ) for silicon single crystals of larger diameter than 3".

In the experiments, silicon single crystals were pulled in the direction of <111> axis in vertical magnetic fields up to 0.1 Tesla. Phosphorus was doped in the crystals as n-type dopant impurities. The strength of the applied magnetic field was increased at interval of 200mm during one growth process. Wafers were sliced from each ingot parallel or perpendicular to its growth axis. The distribution of the electric resistivity was measured by 4-probe method. Growth striation patterns were revealed by striation etching technique. A distribution of RF power generated by induction coil was measured by thermo-couples.

In the results, the radial profile of the electric resistivity significantly changed according to the magnetic field. The electric resistivity decreased at the center of the wafer in strong magnetic field. Such crystals were obtained in the magnetic field of more than 0.075T and 0.05T for the crystals of 3" and 4" diameter, respectively. The striation patterns indicated that this phenomenon was due to the formation of growth facets. Moreover, the facet region enlarged as the field strength increased. We considered the mechanism of the facet formation as follows. The RE power by induction coil had a maximum value at a radial position where the electric resistivity started decreasing. This result suggests that the flow pattern in the molten zone was separated at its position by vertical magnetic field. ID the inner core regions, the heat from the melt surface may be transferred mainly by thermal conduction. This leads the descent of the melt temperature near the growing interface. Accordingly, the facet occurs at the center of the interface when its shape varies from concave to convex toward the melt. We also considered the drastic change of the electric resistivity due to the facet formation as follows. In the facet region, monatomic sheet will grow at a rate independent of the speed of movement of the isotherms. Such sheet growth can occur after a nucleation at the enough supercooling of the melt. On the other hand, in the off-facet region, the growth rate of the monatomic sheet is controlled by the rate of movement of the isotherms because no nucleation is required. Therefore, such growth speed is much faster on the facet than the off-facet. Here, the faster the sheet grows, the more the impurities such as phosphorus are incorporated in crystal. So, the electric resistivity is lower in the facet region than the off-facet region.

C4

IN-SITU OBSERVATION OF SURFACE FLOW OF SILICON MELT DURING CZ GROWTH PROCESS

Yutaka Shiraishi
Kimura METAMELT Project, ERATO, JRDC
Tsukuba Research Consortium, 5-9-9 Tokodai, Tsukuba Ibaraki 300-26, Japan

The heat and mass transfer phenomena of silicon melts in the crucible of a Czochralski puller have been investigated theoretically and experimentally by many researchers [1,2,3]. Many theories and suggestions have been made about the macroscopic bulk flow of silicon melts. However there are no reports on either the experimental or theoretical aspects of transfer phenomena around the periphery of growing silicon crystals.

This paper is concerned with the in-situ observation of the surface flow of molten silicon during the growth process, with the goal of clarifying the most significant melt parameter for crystal growth.

To accurately study the surface flow of melts, we selected SiC powder (1 mm diameter) as a tracer for use during crystal growth. We did analyses under conditions close those used in actual commercial crystal growth. The diameters of the silica crucible and silicon crystal were 350 mm and 100 mm, respectively, with a melt depth of 100 mm. We observed the surface flow while changing the rotate speeds of the crucible and crystal.

We obtained the following results.

1. We could clearly see the paths of the tracers (Fig. 1) and were able to confirm the spoke pattern.
2. The tracers gather near the meniscus around the crystal and in the dark fields of the spoke pattern.
3. The surface flow pattern showed different behavior in the area just around the periphery of crystal as compared to other areas. It is notable that near the meniscus the tracers move toward the crystal against the forced convection caused by crystal rotation.

These results suggest that the surface flow caused by Marangoni convection just around the crystal is the most important parameter that determines the crystal quality (such as oxygen concentration). In addition, the surface flow at a position 10 to 170 mm from the edge of the crystal strongly depend on crystal and/or crucible rotation. Furthermore, the spoke pattern indicates the instability of the bulk flow. The surface flow of silicon melts will be discussed based on the results of *in-situ* observation and the computer simulations.

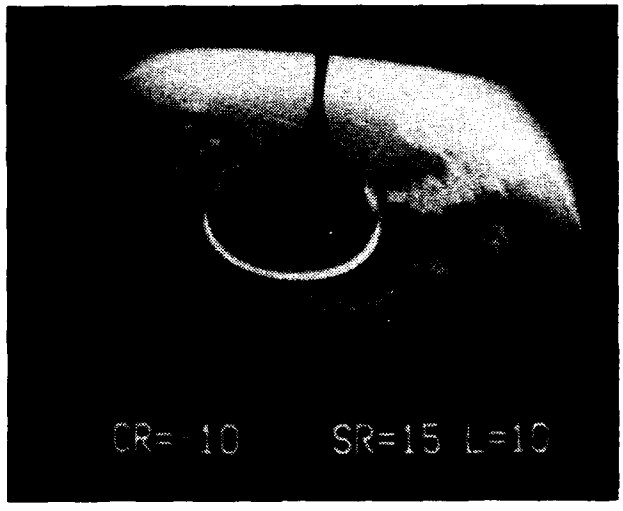

Figure 1

[1] K. Kakimoto, M. Eguchi, H. Watanabe and T. Hibiya, *J. Crystal Growth* 88 (1988) 365.
[2] P. A. Ramachandran, M. P. Dudukovic and D. Dorsey, *J. Electrochem. Soc.*, 137(1990) 3229.
[3] K. M. Kim and W. E. Langlois, Semiconductor Silicon 1990, eds. H. R. Huff and J. Chikawa (The Electrochem. Soc., Pennington, 1990), p.81.

C5

OBSERVATION OF MASS TRANSPORTATION IN SILICON MELT DURING Cz GROWTH BY FLUOROSCOPIC TECHNIQUE

Atsushi Yokotani, Noriyuki Yoshimoto and Shigeyuki Kimura
Kimura METAMELT Project, ERATO
Research Development Corporation of Japan
Tsukuba Research Consortium, 5-9-9 Tohkohdai
Tsukuba, Ibaraki 300-26, Japan

The quality of silicon (Si) crystals grown by the Czochralski (Cz) method is strongly affected by the mass transport process in the melt. Especially. the transportation of oxygen dissolved in the Si melt is very important to grow large high quality Si crystals for ultra high density memory devices. It has been demonstrated that an x-ray fluoroscopy is useful for observation of convection in the Si melt during the growth using a small scaled apparatus [1]. We designed and constructed a new Cz growth system with the x-ray fluoroscope, which is intended for more practical use in order to investigate the behavior of oxygen in the melt and oxygen concentration in grown crystals.

The experimental setup are schematically shown in Fig. 1. A chamber made of aluminum was used in order to reduce an unnecessary absorption of the x-ray. A silica crucible of 178 mm in diameter was used. The anode of the point x-ray source was made of tungsten. The maximum acceleration voltage and current were 150 kV and 3 mA, respectively. The projected image of the melt was detected by a combination of an x-ray image intensifier with 300 mm aperture and a TV camera. The flow pattern of the melt was visualized by using tungsten tracers of which diameter were 1 mm coated by silica and carbon. For a crucible of this size, it is very difficult to identify small particles of the tracers because of a limitation of resolution of the x-ray image intensifier. Therefore, we used a video image processor for enhancement of the image of the particles in the melt. Starting material of 3 kg was charged and heated by a carbon heater under 1 atm of pure argon.

Figure 2 shows an obtained image of the melt. The motion of the tracers in the melt was successfully observed. A Si crystal of 75 mm diameter was grown under this condition. The distribution of oxygen concentration in the grown crystal was measured by an FT-IR method. It was found that the oxygen concentration in the crystal changed corresponding with change the flow pattern of the melt as crystal growing. The detailed mechanism of the transportation of oxygen in the melt will be discussed related to the flow pattern which is controlled by hydrodynamic properties of the melt.

[1] K. Kakimoto *et. al., J. Crystal Growth* **88** (1988) 365.

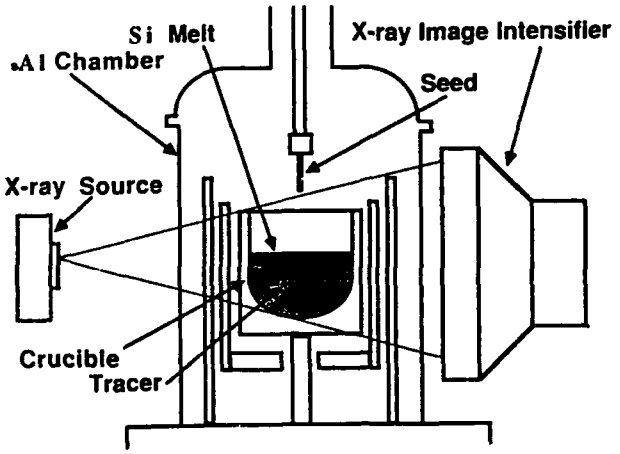

Figure 1. A schematic drawing of experimental setup.

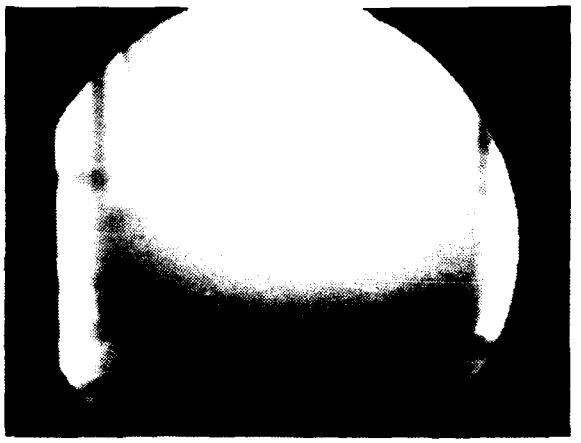

Figure 2. X-ray transmitted image of Si melt.

C6

DETECTION OF MICRO-PRECIPITATES IN SI CRYSTAL RELATED TO THE CRYSTAL GROWTH MECHANISM

Kazuo Moriya and Katsuyuki Hirai
Corporate R & D Center
MITSUI Mining & Smelting Co., LTD.
1333-2 Haraichi, Ageo-shi, Saitama-ken 362 Japan

Defects in heat treated (100) Si wafers grown by the CZ method were detected by laser scattering tomography. Then it was found by observing many samples that there are many linkage relationships among the micro-precipitates in the crystal. From 3-dimensional observation, it was determined that these linkage relationships are due to the as-grown defects which were related to the configuration of the crystal growth interface.

The crystal growth mechanism on (100) interface of a Si wafer was estimated by using new growth model (two types of kink) and it was concluded that this surface is not a pure adhesive growth surface and that there is a probability that a cobble texture will be formed on the solid-liquid interface.

Periodic defects distribution is accidentally observed on vertical cross section in IG (Intrinsic Gettering) treated CZ Si wafer. This evidence means almost all of precipitates in heat-treated wafer is related to the crystal growth originated defects, because it is difficult to image that such regularity is generated by homogeneous nucleation of oxide.

C7

STUDY OF LOW-TEMPERATURE EPITAXY OF SILICON GROWN ON ITS 7 x 7 SUPERLATTICE SURFACE BY OBSERVING INTENSITY PROFILE IN LEED

Yukichi Shigeta and Kunisuke Maki
Department of Physics, Yokohama City University
Seto, Yokohama, Kanagawa 236, Japan

Low-temperature epitaxial growth (LTEG) of Si film was performed on 7 x 7 superlattice surface of Si(111) substrate held at temperatures below 300°C. The surface structure was studied by observing the intensity profile on (0,0) and (1,0) rods in LEED. The following two features on the LTEG can be pointed out from LEED observation. (1) The epitaxial growth occurs in films deposited at thicknesses below a certain value, d_c [1]. The value increases with increasing the substrate temperature (T_s) and with decreasing the growth rate of film(R) [2]. (2) The epitaxial film is composed of two epitaxially grown grains: One grain has 111 surface, and the other has $\overline{111}$ surface [1]. This was judged from deviating the intensity ratio of (1,0) to (0,0) rods from unity. The former is called normal (N-) epitaxial grain, and the latter faulted (F-) epitaxial grain.

It was also found out that the intensity ratio approaches unity drastically for Si film grown at R = 0.12 nm/min while it is kept at 2.5 for Si film deposited at R = 3.0 and 0.3 nm/min [2]. The former is due to the decrease in the number density of F-epitaxial grains during Si film growth which will be followed by rearranging Si atoms on the reversed stacking sequence to the normal stacking of diamond structure. Furthermore the full width at half maximum (FWHM) of the profile changes with R, which was observed when incident electrons were satisfied with the surface wave resonance (SWR) condition for both epitaxial grains. Since the FWHM depends on which surface wave was formed, we reach a view that surface morphology of Si film changes with R [3]. In particular the FWHM decreases with decreasing R and increasing T_s under the SWR condition for F-epitaxial grain. This implies that surface and interface structural relaxations could occur at low R for good epitaxial relation in case of LTEG of Si on Si (111) substrate. Some activated process required for the relaxation of interface structure will be examined.

[1] Y. Shigeta and K. Maki, Japan. *J. Appl. Phys.*, 29, 2092 (1990).
[2] K. Maki, Y. Shigeta and T. Kuroda, *J. Crystal Growth*, in print (1991).
[3] For some results, Y. Shigeta, To be published to Japan. *J. Appl. Phys.*

C8

IN-SITU RHEED STUDY ON GROWTH PROCESSES IN THE INITIAL STAGE OF Ge FILMS ON (311)Si SURFACES BY GAS SOURCE MBE

Y. Yasuda, Y. Koide, S. Zaima and K. Itoh
Department of Crystalline Materials Science, School of Engineering
Nagoya University, Furo-cho, Chikusa-ku, Nagoya 464-01 Japan

The film growth of Ge on Si substrates has attracted much attention because of potential applications of Ge/Si heterostructures to electronic and photonic devices. We have reported that {311}-faceted islands are formed at the final step in the initial stage of the epitaxial growth of Ge films on (100)Si and (811)Si substrate surfaces [1]. In the present paper, we have investigated the growth process in the initial stage of Ge films grown on (311)Si substrate surfaces by Gas source MBE using GeH_4.

The growth of Ge films was performed under conditions of GeH_4 pressure between $1x10^{-5}$ and $6x10^{4}$ Torr and substrate temperatures between 400 and 700°C. The film growth process and the surface structure were in-situ observed by RHEED.

It has been found that the (311)Si surface thermally cleaned at 1200°C has a 3x2 structure consisting of the threefold periodicity in the $[3\bar{1}01]$ direction and the twofold one in $[\bar{2}33]$ at room temperature and, however, that this structure changes to a 3x1 structure by elevating the substrate temperature to 400-700°C.

The growth mode of Ge films on the (311)Si surfaces at substrate temperatures between 400 and 600°C is Stranski-Krastanov type, and the following features on the growth process consisting of two growth steps have been found.

(1) At the first step of growth, two-dimensional layers having a 1x2 surface superstructure are epitaxially grown on the (311)Si-3x1 surface.

(2) At the second step of growth, pyramid-shaped islands with {111} facets and the (311) facets are formed at 400 and 450°C and, on the other hand, plate-shaped islands with (311) facets are grown at 500 and 600°C. It is noted that Ge islands grow flatly at higher temperatures above 500°C, which is considered to be due to the desorption of hydrogen from GeH_4 on the growing surface.

These results indicate that a characteristic growth mechanism exists in the Ge growth on (311)Si-=3x1. We have also examined the substrate temperature dependences of the size of the 1x2 domains and the occupation area of the Ge islands and have found various interesting phenomena on the growth kinetics. We will discuss on the growth mechanism by considering the atomic arrangement on the surface, the film growth kinetics and the kinetics of GeH4 decomposition reaction.

[1] Y. Koide and Y. Yasuda et al., Jpn. *J. Appl. Phys.* **28**(1989)L690; *J. Crystal Growth* **99**(1990)254; *J. Appl. Phys* **68**(1990)2164; N. Ohshima and Y. Yasuda et al., *Appl. Phys. Lett.* **57**(1990)2434;. *Appl. Surface Sci.* **48/49**(1991) 69.

C9

GROWTH OF HEAVILY DOPED SiGe FROM METALLIC SOLUTIONS

Alex Borshchevsky and Jean-Pierre Fleurial
Jet Propulsion Laboratory/California Institute of Technology, USA

Liquid phase epitaxy (LPE) and travelling solvent method (TSM) have been used to grow heavily doped Si-Ge solid solutions. LPE has been found suitable for near equilibrium growth of single-crystalline layers of silicon-rich Si-Ge alloys at temperatures substantially lower than for binary melts. The retrograde nature of the solid solubility of most dopants used in heavily doped Si-Ge has been investigated in order to select processing temperatures adequate for high dopant(s) concentrations into the grown layers. Necessary ternary and quaternary phase diagrams, previously calculated, were used extensively for these experiments. Differential thermal analysis of some of the resulting layers supported the diagrams computations. III and V elements were used as dopants and their interaction in Si-Ge matrix is discussed. Direct compositional measurements proved great enhancement of one dopant solid solubility in presence of another. Electrical properties of the layers were measured between room temperature and 1000°C. The TSM recrystallization of silicon-rich Si-Ge solid solutions was performed at 800-900°C temperature range in sealed quartz ampoules moving at 0.4-0.6 mm/day rate. The growth resulted in polycrystalline ingots with cross-sections of the grains of about 5-7 mm. Electrical and thermal properties of TSM bulk samples were measured from room temperature up to 1000°C.

C10

SEQUENTIAL ETCHING OF GALLIUM ARSENIDE

Paul E. R. Nordquist, Richard L. Henry and Robert J. Gorman
U.S. Naval Research Laboratory, Washington, DC, USA 20375-5000

The Abrahams and Buiocchi (AB) etch and the NaOH-KOH eutectic etch are commonly used to reveal crystalline defects in GaAs. The eutectic etch reveals (as does the KOH etch) those dislocations intersecting the plane of the surface, while the AB etch reveals dislocations and precipitates (e.g. As) and, because of its "memory effect", allows a three dimensional evaluation of crystalline perfection. By using first the AB etch and then the eutectic etch on the same polished piece of GaAs it is possible to obtain more information than can be gotten by either etch used separately. Branching dislocations, linear defects and loops can be identified. Sequential etching and the intercalibration of the two etches gives additional information on the directionality of defects and permits resolution of differences in etch pit density found by the separate etches.

We report results of sequential etching experiments done on GaAs grown by the Vertical Zone Melt (VZM) method. The nature and density of defects revealed by these etching procedures are discussed and correlated with process growth variables. The etching behavior of VZM-grown material will be compared with that of LEC-grown material.

C11

GROWTH AND CHARACTERISATION OF (100) AND (111) SEMIINSULATING AND SEMICONDUCTING GaAs SINGLE CRYSTALS

P. Santhanaraghavan, K. Sankaranarayanan, J. Kumar, S. Anbukumar and P. Ramasamy
Crystal Growth Centre, Anna University, Madras-600 025, India

The past few years have seen the emergence of Gallium Arsenide technology from research laboratory to production floor and boule masses have increased to the multi-kilogram range, with diameter 5-10 cm. This has been accompanied by drastic development in device fabrication technology - from signal stage device to integrated circuits of considerable complexity - for digital and analogue applications. In this paper, we present the LEC technique for growing bulk single crystals of GaAs and the subsequent process of making ingots into polished wafers suitable for device fabrication. Several GaAs crystals (semi insulating and n type) weighing 1 kg and 2 inch dia were grown using the High Pressure Puller. Growth runs were carried out both by using polycrystalline charges and also from elemental materials using either the [100] or [111] oriented seeds. The resistivity, mobility and carrier concentration data of the crystals grown reveal their suitability for device fabrication. The defect investigations were made by FTIR, PL and DLTS studies. The dislocation density revealed by molten KOH etchant shows that the EPD is in the range of 10^4 - 10^5 cm^2. A comparative study is made with molten KOH and A/B etchants.

Fluctuations of threshold voltage of MESFET fabricated in a wafer are investigated. MESFET of gate length 2 μm and width 10 μm were fabricated. The channel layer was made by Si ion implantation and the preceeding annealing was done with SiN_4 capping. Gates and ohmic contacts were made of Au:Ge and Ti/Pt/Au respectively. The MESFET threshold voltage was found to depend strongly on the dislocation variation in any single wafer.

C12

GROWTH OF LARGE-DIAMETER, LOW DISLOCATION GALLIUM ARSENIDE SINGLE CRYSTALS

V.A. Antonov, M.A. Boolekov and T.I. Markova
NPO "ELMA", 103460 Moscow, USSR

The new modification of FEC technique for growing 3 inch diameter low dislocation density GaAs single crystals use for manufacturing UHSICs has been developed. The main feature of the technique is high value of crystal diameter/crucible diameter ratio, it is more than 0.8. The technique offered allows to solve the problem of crystal shape stabilization under conditions of low temperature gradients and to grow the crystals with average dislocation density less then $5x10^3$ cm^{-2} with high yield without doping with hardened impurities. Semi-insulating GaAs single crystals Cr-doped under low pressure and undoped under high pressure have been grown by this technique. Electrophysical properties of crystals grown and their dislocation structure features have been studied. The crystals are characterized by high uniformity of electrophysical parameters along the crystal length and dislocation density decrease from the seeding part to the tail of the crystal.

GaSb SOLUTION GROWTH BY THE SOLUTE FEEDING CZOCHRALSKI METHOD

C13

Akiyoshi Watanabe, Akira Tanaka and Tokuzo Sukegawa
Research Institute of Electronics, Shizuoka University
3-5-1 Johoku, Hamamatsu 432, Japan

The most important problem in growing a homogeneous alloy bulk is how to keep the composition of the growth solution constant during the growth. To realize this condition, we have proposed the modified CZ method, in which a GaInSb pseudo-binary alloy can be pulled up at constant temperature by supplying the GaSb source material spontaneously into the GaSb-InSb pseudo-binary solution according to the crystal growing. To establish this technique, we performed a GaSb pulling from Ca-rich binary solution containing a GaSb source in the bottom.

The cylindrical GaSb polycrystalline source of 15mm diameter placed in the hole centered in the bottom of the carbon crucible of 30mm diameter and 10mm depth. Ga-rich solution of about 40g saturated with Sb at 640°C was loaded on the source. The top surface of the solution was adjusted to the same level of the top of the crucible and maintained at that level during the growth by pushing up the source to fill up the level lowering arising from the source consuming. The crucible placed in N_2 ambient was heated to 660°C by the electric furnace. Then, the GaSb seed crystal rotated at 60rpm was dipped into the solution and pulled up at the rate of 1-2mm/h. The relative position of the furnace to the crucible was adjusted so as to establish the temperature gradient to keep the rates of growth and supply in a state of balance.

In this manner, the GaSb, for example, of about 10g could be grown from the solution in which Sb content was 25atm%. All through the growth, the temperature was held constant at 660°C in this case. This means that the GaSb source dissolved into the solution at the bottom, moved to the upper portion of the solution and segregated as the grown crystal in steady state. Thus, the solute feeding technique was established in Ga-Sb system.

The knowledge obtained here is useful for developing the preparation techniques of not only the alloy bulks but also the high quality compound bulks.

A NOVEL TECHNIQUE FOR CZOCHRALSKI GROWTH OF GaSb SINGLE CRYSTALS

C14

P.G. Mo, H.Z. Tan, L.X. Du and X.Q. Fan
Shanghai Institute of Metallurgy, Chinese Academy of Sciences
865 Chang Ning Road, Shanghai 200050, China

As is known, the main difficulty encountered in growing GaSb crystals by CZ method is the appearance of a thin oxide film (scum) on the melt surface. This film impairs the seeding and promotes twinning during the crystal growth process. In view of the problem, a novel upper-lower crucible technique for synthesis and growth of GaSb has been developed. The remarkable feature of this method is that only one-step growth cycle is needed for growing from the scum-free melt in pure H_2 instead of the two- step growth cycle as reported by Sunder et al (1986) and Moravec et al (1989).

The key element of the technique is the design of the equipment which keeps the scum on the residual melt surface after GaSb melt synthesizing and homogenizing in the upper crucible, so that the clean melt flows into the lower crucible. The equipment design strategy will be presented. Using this technique, GaSb single crystals with clean metallic sheen can be grown from the scum-free melt in the lower crucible immediately by the conventional CZ method.

Undoped and Te-doped, <100> and <o> "device quality" GaSb single crystals with diameter 5cm and a mass of 600-1000g have been grown with relatively high yield (>70%). In generally, the etch pit density of the as-grown crystals is less than $10^3 cm^{-2}$. The room temperature electrical properties of undoped and Te doped crystals are similar with the published data, however, the higher electron carrier concentrations with higher mobilities at 77K of Te doped crystals are also to be found.

In addition, the generation of twinning during crystal growth and the segregation behavior of Te are briefly described.

C15

GROWTH OF $Al_xGa_{1-x}Sb$ BULK MATERIAL

G. Bischopink and K.W. Benz
Kristallographisches Institut und
Freiburger Material-Forschungszentrum, Universität Freiburg
Hebelstraße 25, D-7800 Freiburg, Fed. Rep. of Germany

The ternary alloy $Al_xGa_{1-x}Sb$ offers a wide range of applications in long wavelength optoelectronics. Up to now this material has been grown as thin layers mainly by LPE or MBE. We describe the growth of homogenous bulk $Al_xGa_{1-x}Sb$ single crystals with the Travelling Heater Method (THM) from a mathematical model, based on the time dependent transport equation for each dissolved compound in the solution zone.

Single crystals of the ternary III-V compound $Al_xGa_{1-x}Sb$ with a diameter up to 25 mm a length of more than 25 mm and an AlSb solid composition x in the range of 0.1 to 0.8 have been successfully grown.

The growth temperature ranged from 543°C to 630°C. As seed material we used GaSb with (111)B or (100) orientation. The crystals were grown with a Ga rich as well as a Sb rich solution zone. The feed material was realized with polycrystalline (Al,Ga)Sb. To control our theoretical description and to analyze the shape of the growing interface we induced time markers in form of striations of the type I which are related to fluctuations of the Al composition. From the measured microscopic growth velocity we calculated the material transport coefficient of Sb and Al in Ga solution and of Ga and Al in a Sb solution. In the case of the Sb transport coefficient in a Ga solution the extrapolation from LPE data corresponds with our experimental values, whereas the Al transport coefficient shows smaller values than expected at temperatures higher than 550 °C.

To characterize the (Al,Ga)Sb material, detailed measurements of the radial and axial Al solid composition were made by x-ray microprobe analysis. With a spatially resolved photoluminescence (SRPL) with laser spot diameter of 5 µm and cathodoluminescence (CL), we measured the Al solid composition inside macrosteps at the interface seed - grown crystal. The Al content inside a macrostep is about 0.2-0.4% higher than outside the macrostep. CL and SRPL mappings measured at different wavelengths will be shown. Detailed information about the structure of ternary feed material, growth parameters and the solid distribution of the grown crystals will be given.

C16

OPTICAL AND ELECTRICAL CHARACTERIZATION OF $Al_xGa_{1-x}Sb$ CRYSTALS GROWN BY THE TRAVELLING HEATER METHOD

B.K. Meyer, G. Bischopink, K.W. Benz*, W. Kramer and G. Pensl***
Physikdepartment, E 16, Technical University Munich, 8046 Garching, Germany
*Kristallographisches Institut, University Freiburg, Hebelstr.28, 7800 Freiburg, Germany
**Angewandte Physik, University Erlangen, Staudtstr.7, 8520 Erlangen, Germany

$Al_xGa_{1-x}Sb$ with a crossover from direct to indirect gap at about $x>0.4$ can offer a new and interesting material for optoelectronic applications in the near-infrared region (0.81 to 1.69 eV). AlSb is equally important for application in tunneling devices such as AlSb-InAs-AlSb superlattices. Very little is known about intrinsic.

Bulk $Al_xGa_{1-x}Sb$ single crystals with various AlSb solid compositions were grown by the Travelling Heater Method (THM) on GaSb substrates. The crystals were grown with a Ga rich as well as a Sb rich solution zone (undoped or doped with Te).

We report in this investigation on results obtained by electrical characterization (DLTS, Halleffect, photoconductivity) and optical spectroscopy (photoluminescence). Deep centers (DX center) and shallow centers (Γ and X conduction band derived donors) were investigated, their structural properties depending on the composition range (studied from $0 < x < 0.54$) will be presented and discussed.

CRYSTAL GROWTH OF GaInAsSb MIXED CRYSTALS BY A ROTARY BRIDGMAN METHOD

C17

Y. Hayakawa, T. Ozawa, M. Ando, T.J. Anderson, P.H. Holloway*, B. Pathangey* and M. Kumagawa*
Research Institute of Electronics, Shizuoka University
Johoku 3-5-1, Hamamatsu-shi, Shizuoka 432, Japan
*University of Florida, Gainesville, FL 32611, USA

A GaInAsSb quaternary mixed crystal is a very promising material for the substrate, because the lattice constant (a) and energy gap (Eg) can be controlled independently in the range of 5.653 Å < a < 6.478 Å, and 0.10 eV < Eg < 1.428 eV at room temperature. It is however, very difficult to grow single crystals with large size. This is because there are several problems such as (1) the constitutional supercooling is easy to occur at the growth interface, (2) the lattice constant between the seed and the grown crystals is different, (3) the composition ratio in the solution is changed during the growth of crystals, and (4) the miscibility gap exists.

We have developed a new growth method called Rotary Bridgman method to grow III-V mixed crystals. This is similar to the conventional Bridgman Method, but the relative motion is given between a grown crystal and the source solution by rotating a growth ampoule. We have investigated the effect of ampoule rotation on the quality of GaInAsSb mixed crystals by comparing the Rotary Bridgman method with the Horizontal Bridgman method.

A $Ga_{1-x}In_xAs_ySb_{1-y}$ single crystal (x = 0.24-0.25, y = 0.99) of 2 mm thick was grown by the Rotary Bridgman method. The In composition was uniform both along and across the growth directions. On the other hand, the thickness of the single crystal grown by the Horizontal Bridgman method was maximum 1 m and the growth interface was not smooth. The In composition was higher in the lower part than in the upper part of the crystal. These results indicated that the Rotary Bridgman method was superior to the Horizontal Bridgman method on the standpoint of the homogeneity and the single crystalline state.

GROWTH AND CHARACTERIZATION OF InGaAs BULK CRYSTALS GROWN BY LIQUID PHASE ELECTRO-EPITAXY

C18

M. Yanagase, S. Tanaka, K. Hiramatsu and I. Akasaki
Department of Electronics, Nagoya University
Furo-cho, Chikusa-ku, Nagoya 464-01, Japan

It is important to grow homogeneous ternary bulk crystals for preparing a variety of epitaxial structures without lattice matching to a binary semiconductor. Liquid phase electro-epitaxy (LPEE) method is known as a solution growth technique in which the growth is controlled only by the electric current flowing across the liquid-solid interface while the growth temperature is maintained constant. Thus high-quality bulk crystals having uniform alloy composition should be obtained by LPEE.

Bulk growth of InGaAs by LPEE technique was carried out on (111)A-oriented GaAs substrates in a vertical boat at the growth temperature of 780°C. Metallic Indium of about 2.5g were loaded in the boat. The growth area was 5mmx6mm. Polycrystalline GaAs lumps were used as a source material.

We have obtained successfully 2mm-thick $In_xGa_{1-x}As$(x~0.07) bulk crystals on (111)A GaAs substrates, for the first time, for the growth of 30 hours and at a current density of 12 A/cm^2. Electron-probe microanalysis showed that the compositional fluctuation along the growth direction do not exceed 1%. The full width at half maximum of the double crystal X-ray rocking curve (XRC) measured for a (333) reflection on the surface of the 2mm-thick InGaAs bulk crystal was as narrow as about 70 sec. However, the shape of the XRC was asymmetrical and was dependent on the position along the surface. In this paper, detailed properties of LPEE grown InGaAs bulk crystals will be presented in connection with the growth condition.

C19

WETTING OF III-V MELTS ON MATERIALS FOR CRUCIBLES

T. Duffar, I. Harter, P. Dusserre, N. Eusthatopoulos and J.P. Nabot
CEA/DTA/CEREM/DEM, Section d'Etudes de Ia Solidification et de la cristallogenèse, Centre d'Etudes Nucléaires, 85X, 38041 Grenoble Cedex, France

The interaction behavior of III-V melts with materials for crucibles is studied by sessile drop experiments in the idealised cases of GaSb and InSb melts on glassy carbon, silica, sapphire, boron nitride and aluminum nitride substrates.

The experiments are performed under static vacuum in sealed silica ampoules and the method has been validated by comparison with published results for materials which accept dynamic vacuum. Special care has been given to the quality of the residual gases in the cell and to the roughness and cleanliness of the substrates. By these means, we obtained a great reproducibility of the results.

From the shape of the drop, we calculated the surface tension of the melt and its contact angle on the substrate. These values were used in order to compute the adhesion work. The obtained results where in good agreement with the published values of surface tension of GaSb and InSb.

The contact angles were in the range 100° to 135° and typical of non-reactive systems. The work of adhesion varies in a factor three from boron nitride to aluminum nitride. For the low values of this work of adhesion (on BN and C), only van der Waals interactions can be taken into account, but for the high values (on AlN, Al_2O_3 and SiO_2) it is necessary to take into account chemical interactions. Attempts to use Li's theoretical model to compute the effect of the antimony composition on the wetting behavior have shown that this model is a very useful tool to predict the surface parameters in III-V melts.

SESSION 1D

THE HOT-FORGING INVESTIGATION OF BaF_2 CRYSTALS

D1

Zhong Hongwu, Huang Cun xin and Li Wei
Research Institute of Synthetic Crystals, Beijing,China

This is the first report for BaF_2 crystals investigated by hot-forging technique. Grain growth were observed by using optical microscope, scattering grains are some tiny crystals of regular shape under high temperature hot-forging, there are some veiling regions observed in the forged crystals. The temperature effect on stress-strain curves for crystal forging was studied. The IR and UV transmission curves of crystals were measured, the results show that two absorption peaks (3600 cm^{-1} and 1400 cm^{-1}) appeared in curves for the crystals forged in lower vacuum. The UV transmission of forged crystals is lower than that of single crystals. The property measurements show that the mechanical strength and thermal shock resistance of forged crystals are superior to that of single crystals.

INVESTIGATION OF THE SCINTILLATION PROPERTIES OF BARIUM FLUORIDE CRYSTAL

D2

Y.N. Zheng, S.X. Ren
Beijing Glass Research Institute, Beijing, 100062
T.B. Zhang, Y.Z. Zhu
Institute of High Energy Physics, Academia Sinica, 100039

The scitillation property of Barium Fluoride crystals on different growth condition were studied. Our experiment results showed that the higher the ultraviolet transmission rate the larger must the optical output be. This kind of relationship is due to the purity of starting materials as well as the crystal structure perfection.

THE RADIATION DAMAGE OF RARE EARTH IONS DOPED BARIUM FLUORIDE CRYSTALS

D3

G. Chen, H. Xiao, S.Q. Man, S.X. Ren and J.Q. Zhang
Beijing Glass Research Institute
Dongdadi 1, Chongwenmenwai, Beijing 100062, P.R. China

It is importment to improve the ability of radiation resistance of BaF^2 crystal for its using as detector in high energy physics experiments such as the SSC. Most rare earth ions doping will influence the radiation damage of BaF_2 crystals just with ppm weight doped. These elements are Ce, Pr, Nd, Eu, Tb, Dy, Ho, Er, Tm, Yb. Other elements doped samples, such as Y.La, Lu doped, are not found evident difference comparing with undoped sample. Ce, Pr, Nd, Sm doped samples make higher absorption in range after irradiated. On the other hand, Eu^{3+} and Yb^{3+}, being doped in BaF_2 crystals, will get an electron each one to reduce the content of color centres that can make absorption in UV range. Therefore, the good transmission crystals are gotten after irradiated by γ-ray. Unfortunately, these elements will lead to new absorption in ultraviolet range after samples irradiated. But there are indications that other elements are also helpful to radiation resistance. Their absorption peaks in ultraviolet range influence hardly the luminous export of the fast component of BaF_2 crystals after irradiated, and the crystals have good transmission in UV range except for some small absorption peaks. The further research are being carried out now.

D4

GROWTH OF MERCURIC IODIDE USING THE TEMPERATURE OSCILLATION METHOD: RELATIONSHIP BETWEEN GROWTH PARAMETERS AND CRYSTAL QUALITY

M.D. Serrano, M.T. Santos, A. Martinez and E. Dieguez
Dpto. Física Aplicada, Univ. Autónoma, 28049 Madrid, Spain
A. Ibarra and M. Gonzalez
CIEMAT, Av. Complutense 22, 28040 Madrid, Spain

The Temperature Oscillation Method (T.O.M.) has been used in the past to obtain HgI_2 bulk crystals. In this work we present the relationship between the crystal growth parameters and the crystal quality.

Seven different T.O.M. equipments have been built and working simultaneously in order to modify as much as possible growth parameters. Each T.O.M. equipment has been made of transparent furnace with one to three lateral heater elements and with two more furnaces, one in the bottom of the growth ampoule and the other one inside the cold finger. Several thermocouples or PT100 sensors located at different places have been used to control the temperature. Each T.O.M. equipment was placed in a nearly closed transparent box, with a temperature stability better than ±0.1°C.

The following parameters have been studied: starting materials, ampoule with/without rotation, crystallization and source temperatures, ratio between the crystallization area in the ampoule and the cold finger area, air flux in the cold finger, etc.

The crystals have been analyzed by DSC measurements, transition temperature, optical measurements and detector performance.

D5

VAPOUR GROWTH OF LARGE MERCURIC IODIDE CRYSTALS (VIDEO PRESENTATION)

M. Zha, M. Piechotka and E. Kaldis
Laboratorium für Festkörperphysik, ETH Hönggerberg,
CH-8093 Zurich, Switzerland

Vapour growth of α-HgI_2 crystals, since it proceeds at low temperatures (approx. 115°C), offers an excellent opportunity to perform in situ observation of the growth process. We have been using a 3 chip CCD video camera (Sony DXP-730P) with a 24-fold zoom and resolution 736x581 pixels corresponding to a linear resolution of ±50 μm. The camera was combined with a video tape recorder for analog image storage as well as with a computer and an image digitizer for the numerical processing (on line growth rate measurements).

In the film, various aspects of the vapour growth of α-HgI_2 crystals will be presented, among them:

(a) growth apparatus

(b) nucleation process; elimination of nuclei using a laser beam

(c) growth mechanism of various faces (movement of steps)

(d) anisotropy of the growth resulting from the thermal anisotropy of the crystals

(e) influence of the nonstoichiometric components in the gas phase and that of the thermal field on the morphology of the crystals

(f) visualization of striations in large crystals using scattering of a laser beam.

RADIATIVE/CONDUCTIVE INHIBITION OF THE GROWTH RATE IN VAPOUR GROWTH OF MERCURIC IODIDE CRYSTALS

D6

*E. Kaldis, M. Piechotka and A. Roux**
Laboratorium für Festkörperphysik, ETH Hönggerberg
CH-8093 Zurich, Switzerland
*Institut de Mechanique des Fluides, 1, Rue Honnorat, F-13003 Marseille, France

The decrease in the linear growth rate of large α-HgI_2 crystals growing from the vapour phase under constant apparent undercooling has been recently investigated in a series of articles (see [1] and references there). To understand the vapour growth mechanism of large (>500 g) single crystals it is necessary to elucidate this phenomenon, which is accompanied with changes in the crystal morphology and perfection.

The high reproducibility of the size vs. time curves upon growth/evaporation (i.e. thermal) cycling of a given α-HgI_2 crystal [1] points out to a thermal origin of the phenomenon. α-HgI_2 crystals, with their very low and anisotropic thermal conductivity (0.4/2.0 W/m•K, $\parallel$ /$\perp$ to the c-axis, respectively) due to the layered structure, may build indeed an increasing thermal barrier to the dissipation of the condensation heat as their size increases. The thermal anisotropy results with different kinetics of (001) and (100) faces when they leave the cooling finger area, beyond which the heat dissipation limits the growth rate. However, at the crystal size of several cm, still an apparent undercooling up to 10 K, is necessary to keep the crystal at the zero growth/evaporation rate. This temperature gradient exists although no condensation heat is evolved at the vapour/crystal interface under these conditions. The numerical modeling of the thermal field inside our growth furnaces showed indeed, that taking into account thermal conductivity only, both in the vapour as well as in the solid phase, no conditions can be simulated under which the crystal stops to grow. On the other hand, taking into account also the *radiative heat transfer to the crystal*, the observed stop of the growth at constant undercooling can be simulated with increasing crystal dimensions. This *unexpected result* (the growth proceeds at temperature as low as 115°C) lead us to the conclusion that the geometrical arrangement and the temperature of the heating zones above the growing crystal play an important role in the kinetics of the growth and influences the final habit of large α-HgI_2 crystals.

1. M. Isshiki, M. Piechotka and E. Kaldis, *J. Crystal Growth* 102 (1990) 344.

LASER CONTROLLED NUCLEATION OF α-HgI_2, CRYSTALS FROM THE VAPOUR PHASE

D7

M. Piechotka, M. Zha and E. Kaldis
Laboratorium für Festkörperphysik, ETH Hönggerberg,
CH-8093 Zurich, Switzerland

Vapour growth has been established as the only technique to grow large, spectrometer quality α-HgI_2 crystals. The crystals nucleate on a flat glass plate (pedestal) with no restriction (a capillary or a cone) for the natural selection of nuclei. The requirement of having a possibly large homogeneous cooling spot (cold finger), when the crystal is already several cm large, is exactly opposite to the demand of possibly localized small cold spot during the nucleation phase. In addition, nuclei of the yellow β-HgI_2 phase are simultaneously formed and must be eliminated. Up to now, temperature reversal has been used for the nuclei selection. With this method, a good nucleus could be selected within a couple of weeks, depending on the properties of starting material and the skills of the experimenter. The novel method developed in our laboratory allows for a vast decrease of the time spent for selection of nuclei. The method takes advantage of the fact that the solid phase of mercuric iodide strongly absorbs the wavelength of the Ar laser (488 and 514 nm), whereas neither its vapour nor the ampoule walls do so. A simple system has been built consisting of a high resolution 3 chip CCD video camera, Ar laser and optics for the manual adjustment of the laser beam along the pedestal. An important feature of the method is that cleaning of the preferential nucleation centers on the glass plate from mercuric iodide by the laser irradiation is very efficient (no memory effects). One can also continuously irradiate a deliberate location at the pedestal to suppress the parasitic nucleation during the growth phase. The main limitation to this technique is that the nuclei to be removed must not exceed the diameter of the laser beam (approximately 0.5 mm), otherwise they cannot be completely removed even by scanning the beam across the surface.

D8

PROCESSING α-MERCURIC IODIDE BY ZONE REFINING*

A. Burger, S.H. Morgan, D.O. Henderson, Y. Biao, K. Zhang and E. Silberman
Department of Physics, Fisk University, Nashville, Tennessee 37208
D. Nason, L. van den Berg, C. Ortale-Baccash and E. Cross
EG&G Energy Measurements Inc., Santa Barbara Operations, Goleta, California 93117

The purification of α-mercuric iodide material, which is grown as a single crystal by physical vapor transport at EG&G/EM, Santa Barbara Operations, for gamma ray spectrometer, photocell and X-ray detector applications, has been modified to include zone refining. Zone refining has been included for evaluation as a final step in the materials preparation process (denoted as 4XMXS), which has consisted of synthesis from aqueous solutions of potassium iodide and mercuric chloride, several vacuum sublimations, a melting and unidirectional resolidification, and a closed system sublimation. A zone refiner has been constructed which features two coupled zones, adjustable ampule inclination, facility for ampule rotation, zone translation speeds up to 10 mm/min, and an ampule capacity of up to 1 kg. These evaluation studies have typically used ampules of 10 - 20 mm diameter and 100 - 250 mm length, with 64 zone passes at speeds of 10 - 100 mm/hr. Several analytical methods are being used for the evaluation of zone refining, including anion chromatography, differential scanning calorimetry (DSC), total carbon analysis, and infrared spectroscopy. Samples are extracted and homogenized from the extreme rear, center and extreme front (direction of zone travel) of a refined ingot. The central 80% (approximately) of the ingot is used to grow crystals for the evaluation of detector quality. Anion chromatography results indicate a residual chloride ion level of a few ppm in 4XMXS material, and zone refining produces concentrations of typically 20 - 40 ppm in the front and generally more than an order of magnitude lower in the center and rear, depending on the particular refining conditions. Impurity concentrations of sulfate, nitrate, phosphate and fluoride ions are generally less than 1 ppm, with no significant redistribution from zone refining. Differential scanning calorimetry results show a systematic lowering of the freezing point (2-3°C) and the $\alpha \rightarrow \beta$ phase transition temperature (4-6°C) in the front sections as compared to the center or rear. Diffuse reflectance and total carbon measurements are under way. Zone refining appears to have beneficial effect on the growth of single crystals of α-mercuric iodide by physical vapor transport. The spontaneous nucleation and the growth of void-free crystals are easier with zone-refined material, and there is less ampule residue. Early results indicate zone refining has a beneficial effect on photocell performance, but beneficial effects on gamma-ray detector performance have not yet been realized.

*This work was performed under the auspices of the U.S. Department of Energy under Contract No. DE-AC08-88 NV10617.

D9

GROWTH AND CHARACTERISATION OF GEL GROWN CRYSTALS OF LEAD CHLOROBROMIDE

P. Sagayaraj, S. Sivanesan, F.D. Gnanam and R. Gobinathan
Alagappa College of Technology, Anna University, Madras -25, India

Single crystals of mixed halides of lead have drawn much attention in the past because of their photoluminescence, structural morphology and ionic conductivity. In the present paper, we report on the growth aspects of PbClBr crystals grown by gel technique at room temperature. The experiments were conducted using silica gel, employing straight tubes and U tubes. The growth of crystals have been carried out using a modified two-stage chemical reaction. In the first stage, an intermediate material in the form of colloidal precipitate is formed in the gel medium and in the second stage suitable nutrients are allowed to diffuse into the gel and react with the colloidal precipitate to produce crystals. Long luminescent needles of PbClBr crystals up to 6 cm have been harvested. Figure shows the photograph of the grown crystal. The effect of gel density, neutral gel, concentration of reactants and pH value have been investigated and discussed. The grown crystal is characterised by X-ray, SEM and chemical analysis.

COMPLEX INTERACTION OF SOME TRANSITION METAL IONS AND THE GROWING POTASSIUM HALOGENIDE CRYSTALS

D10

B. Draganova
University of Sofia, Faculty of Chemistry

In spite of the numerous investigations there is no clarity so far about the crystal - impurity interaction. The reason lies in the extreme complexity of these interactions - the polyfunctional dependence of the surface and volume stages of the process on the parameters of the state and the nature of the components. Not last the reason for the lack of clarity is in the fragmentarity of the investigations.

A systematic study of the equilibrium incorporation and than of the crystal growth of the potassium halogenides KX in the presence of some transition metal ions let us differentiate two basic types of interaction:

1. Interaction of growing KX crystals with d^{10} ions (d^{10} and $d^{10}s^2$). Two different mechanisms (I and II) of interaction are proposed, the second of which is two-dimensionally condensational and habit changing. However, both of these act as passivating the K growth. The results on the lead and cadmium ions fit into different theoretical laws since they are not full electron analog.
2. Interaction of growing K crystals with d^n ions. Three of more mechanisms of interaction have been proposed. All but the first one are two-dimensional condensational. Only the third is usually habit changing. All but the first are activating and passivating, i.e. they start with clear maxima in the growth rate. This is an important peculiarity of the d^n ions, connected to a certain degree with the dislocation growth mechanism. Temperature effects differ: only exothermic, partially exo- and endo-thermic or only endothermic. The growth rate maxima are also a complex temperature and concentration functions.

As a whole the present report is meant to illustrate the great variety of type and direction of effects in the impurity - growing K crystals interaction and the possibility, although with difficulties, to describe them by well known theoretical laws.

IN SITU CRYSTAL GROWTH STUDY OF FULLERENES

D11

M. Verheijen, H. Meekes and P. Bennema
Laboratory of Solid State Chemistry
G. Meijer
Department of Molecular and Laser Physics,
University of Nijmegen, The Netherlands

Recently, Krätschmer et al [1] discovered a method to synthesise C_{60} and higher carbon number fullerenes in macroscopic amounts. Since this discovery a lot of efforts have been made to improve the purity of these materials and to produce single crystals both from the pure material as from derived compounds and to study the physical and chemical properties of these substances. Growth techniques used varied from solution growth (in several organic liquids) to vapour phase growth. In most cases the starting material was produced in an arc between two carbon electrodes in a suitable buffer gas and afterwards purified by means of chromatographic separation. The disadvantage of solution grown crystals is the building in of solvant molecules. Therefore, we decided to use vapour growth in order to study the growth properties and morphology of these fullerenes. The techniques used for the observations were interference optical microscopy and scanning electron microscopy. We present results on the macroscopic morphology of fullerenes and we will explain these results in terms of a periodic bond chain analysis using intermolecular potentials as described in literature. Furthermore we will report on some in-situ growth observations, which were performed in order to study the growth kinetics.

[1] W. Krätschmer, L.D. Lamb, K. Fostiropoulos and D.R. Huffman, *Nature* 347(1990)354-358.

D12

THE RESEARCH OF INTERFERENTICAL EFFECT OF CRYSTAL FILMS

Zhu Wenyuan and Yang Xueming
R.I.S.C., P.O. Box 733, Beijing 100018 China

Alternative coating SiO_2 and ZrO_2 crystal films were deposited on the plastic base by using vacuum coating technology.

The thickness of each layer is controlled by exactly designed program so that we make it separated from base easily and have outstanding interferentical effect. Description of this article emphasize coating technology and measurement of optical property of crystal films. This material can be mixed with any coatings to be used in the field which need interferentical effect.

D13

STUDY ON 3-COMPONENT FIBONACCI TA/AL MULTILAYER FILMS GROWN BY MAGNETRON SPUTTERING

R.W. Peng, A. Hu and S.S. Jiang
National Laboratory of Solid State Microstructures
Nanjing University, Nanjing 210008, People's Republic of China

A new class of quasiperiodic superlattice structures called 3-component Fibonacci structures (3CFS) is studied both theoretically and experimentally. These structures are produced by the substitution rule $A \rightarrow AC$, $C \rightarrow B$ and $B \rightarrow A$. The ratios among the thicknesses of building blocks A, B, C are chosen to be characteristic irrational ξ and η, which satisfy the equations: $\eta^2+\eta-1=0$ and $\xi^2=\eta$. The projection method is applied to deal with the spectrum and indexing problem of their diffraction. Then the diffraction peak positions are analytically found to be located at the wave vector $q(n_1,n_2,n_3) = 2\pi D^{-1}(n_1+n_2\xi+n_3\eta)$, where the average superlattice wavelength $D=d_A+d_B\xi+d_c\eta$ and $n_i(i=1,2,3)$ are integers. The 3-component Fibonacci Ta/Al multilayer films are fabricated by two-target magnetron sputtering. The X-ray diffraction peaks of these quasiperiodic superlattices at low and high angles can be labelled by n_1, n_2 and n_3. Furthermore, the experimental results are in good agreement with the numerical calculations using the model for compositionally modulated multilayers. Some possible applications of these structures are discussed.

D14

FORMATION MECHANISM OF SMOKE QUARTZ

Zhong Weizhuo, Hua Sukun and Shi Erwei
Shanghai Institute of Ceramics, Chinese Academy of Science
1295 Ding Xi Road, Shanghai 200050, China

In this article the formation and its mechanism of the colour centre of Al^{3+} in the quartz has been investigated. It offers the model of structure of Al^{3+} in the quartz and discusses the relation between Al^{3+} distribution in the quartz and crystal growth habit.

When the Al^{3+}-doped quartz crystal is irradiated by the γ-ray radiation, its electric properties will be deteriorated. When it is used to make the filters or the oscillators, the equivalent resistance is increased. This irradiation damage and the formation mechanism of the smoky quartz have already been widely concerned. In order to study the form of Al^{3+} in the solution, its aggregation and distribution in the quartz and the relationship to the crystal growth habit, some experiments on the effect of the impurity of Al^{3+} in the synthetic quartz have been carried out.

SEPARATION IN METALLIC MELTS

D15

S. Sprenger, J. Proschmann, T. Strangfeld and H. Bach
Institut für Experimentalphysik, Ruhr-Universität, D-4630 Bochum, FRG

The separation in monotectic systems depends on physical-chemical properties of the elements as well as on kinetic parameters. For better understanding of the mechanism in metallic phase diagrams we investigated the lanthanides as model systems. They change their properties only in small steps. In general the divalent rare earths form monotectic systems with the trivalent ones, but elements of the same valence are miscible. Our efforts were concentrated on the ternary system Eu-La-Sm. It was determined by differential thermal analysis (DTA). The binary systems Eu-La and Eu-Sm have a miscibility gap in the melt, La-Sm has not. Besides a section from a monotectic to a miscible phase diagram was investigated: $Eu_{50}La_{50}$-$La_{50}Sm_{50}$.

We observed a change of the specific heat in the melt - higher in temperature than the binodal or the liquidus. This effect was confirmed by measurements of the magnetic susceptibility. We suppose it indicates a variation of the short range order which may be responsible for the separation.

This 'structure' in the melt is caused by the electronic configuration, similar parameters as in the solid state: valence and atomic radius.

This work was financially supported by the German Ministry of Research and Development (BMFT) in the frame of the microgravity research program under contract 01 QV 88189.

PREDICTION OF THE EXISTENCE REGION OF SOME III-V BINARY COMPOUNDS

D16

C.A. Galeazzi and C. Pelosi
MASPEC Inst./CNR, Via Chiavari 18/A.43100 Parma (Italy)

Point defects play a very important role in conditioning the most interesting properties of both elemental (Si, Ge) and binary semiconductors such as mobility, lifetime, luminescence efficiency, etc.; even if this topic may have impact on the materials technological development it is worth to say that, till now, a clear identification of different types of point defects which according to classical literature are named interstitials and vacancies and in the case of binary compounds antisites., is lacking.

In this communication, we use the Bragg-Williams model to study the formation of some Ga-containing binary compound and it will be shown that the generation of antisite point defects is intrinsically inherent with the ordering process, implicitly assuming that the antisites are the most common defects.

Since the melting temperatures of binary III-V are much lower than the critical ones, the model assumed here is very accurate and the existence region may be calculated by imposing that the chemical potentials of the same elements in the liquid and solid phase are equal. The thermodynamic constants of the sphalerite phase are obtained from the experimental characteristics of III-V compounds, namely the concentrations of antisite defects (in several case they give origin to electrical levels in the forbidden band) is tightly connected to interaction parameter and, at the congruent melting point, the chemical potentials of the two elements forming the binary compound are obtained.

It will be shown that according to the theoretical statement the presence of antisite defects is intrinsically connected to the formation of a binary ordered compound and this fact can explain the defects concentration ratio in between elemental and binary semiconductors; moreover the properties of binary compounds (such as existence region and therefore point defect concentration) are also dependent on the thermodynamical properties of the adjacent liquid phase.

Finally a comparison between the usual method employed to give the crystal lattice disorder, i.e. the quasichemical reaction systems and the one we propose here and we apply it to the III-V family of Ga-containing compounds.

D17

FORMATION OF SECONDARY TWINS IN TWINS IN THIN FILMS

Saiyu Maruyama
Osaka College, Hirao, Mihara, Minamikawachi, Osaka 587, Japan

For the investigation on the mechanical properties of thin films, particularly on the mechanical twinning, silver films epitaxially oriented in (001), and colloidal gold lamellae oriented in (111) have been prepared.

By applying them tensile stress, broad twin bands are produced. During broadening, two kinds of secondary twins are formed in them so as to accommodate the rotational moment, like double slip.

In (001) silver films, under the tensile stress along <110>, (111) primary twins are formed. The first kind secondary twins which have a $(11\bar{1})_t$ twin plane different from the primary one are found in the latter. (The subscript t refers to the twin lattice.)

If we know the twin plane K_1, and the direction of η_2 (intersection between the plane of shear and the second undistorted plane K_2), we can calculate the indices of an arbitrary plane transformed after primary or secondary twinning, by the use of transformation matrix. For the primary twin, $K_1=(111)$ and $\eta_2=[112]$ under [110] tension. The film surface is transformed into $(110)_t$, and rotated by 19.5°. In the secondary twin, $K_1=(11\bar{1})_t$, = $\eta_2=[12\bar{1}]_t$, then the film surface is $(11\bar{3})_m$, which is unrotated by 6°. These are identified by electron microscopy and diffraction.

The second kind secondary twins are found in (111) laminar colloidal gold. Under some tensile stress, (111) twins occur. The twinning shears revealed at the crystal edges are variable and much larger than that calculated. High resolution lattice image elucidates that the twin band is not homogeneous but is composed of twin(s) and matrix(ces). The latter is not the remnant but the secondary twin of the second kind. That is, (111) K_1 plane remains unchanged, whereas the twinning shear η_1, and therefore η_2 change. The secondary twin is formed by shear given by reactive normal stress of the primary twinning, from specimen substrace (Mylar sheet). As the twin plane K_1 is unchanged, the secondary twin bears detwinning in orientation. The primary and secondary twinning shear components normal to the surface are substractive, while those parallel to the surface are additive. This explains why the twinning shears observed are so large and variable.

D18

STUDIES OF RECRYSTALLIZATION BY ACOUSTIC EMISSION

A.P. Cook and A.P. Wade
Department of Chemistry, University of British Columbia
2036, Main Mall, Vancouver, B.C., Canada V6T 1Z1

Numerous and intense bursts of acoustic energy are emitted from many compounds during recrystallization from saturated solutions. These broad-band, high frequency (50 kHz - 700 kHz) signals are readily detected using piezoelectric transducers. The recrystallization of both organic (benzoic acid) and inorganic (ionic salts of 1st row transition metals, alkali metals, and inorganic polymers) compounds has been monitored using acoustic emission. Previous work in this research group has centered on the effect of the concentration of reagents on the acoustic emission from a recrystallizing system, but little work has been done on the relationship between the number and rate of acoustic bursts and the crystal morphologies formed. This work seeks to address this issue.

The chemical system chosen for study was potassium bromide recrystallizing from aqueous solution at ambient temperature. Solutions were prepared which contained varying concentrations of lead nitrate dopant (0-32000 ppm) and the change in the acoustic emission behaviour was monitored as the number of acoustic events per unit time, as well as changes in the frequency content of the signals. All the experiments were carried out on the surface of a broad-band piezoelectric transducer (Bruel and Kjaer model 8312) and normalized to the mass of crystals produced. Simultaneously, microscope video imaging with magnifications between x100 and x300 was used to follow the growth of the crystals visually. The images were stored on a PC/AT microcomputer and a "near real-time" pixel sum calculation used to correlate the growth of the crystals with the number of acoustic events observed. The crystals were also grown in agar gels and their resulting structures analyzed for a change in the degree of branching, as it is hypothesized that one source of the acoustic emission signals is from crystal fracture during growth. Microscopic structural changes across the system were studied using scanning electron microscopy and again correlated with the changes in the observed acoustic emission.

D19

SINGLE CRYSTALS OF TaB, Ta_5B_6, Ta_3B_4 AND TaB_2, AS OBTAINED FROM HIGH-TEMPERATURE METAL SOLUTIONS, AND THEIR PROPERTIES

Shigeru Okada and Kumo Kudou
Department of Applied Chemistry, Kanagawa University
Rokkakubashi Kanagawa-ku, Yokohama 221, Japan
Iwami Higashi
The Institute of Physical and Chemical Research
Wako, Saitama 351-01, Japan
Torsten Lundström
Institute of Chemistry, University of Uppsala
Box 531, S-751 21 Uppsala, Sweden

The binary borides of the transition metals are of great interest to applications due to their unique properties[1]. In the tantalum-boron system the intermediate phases Ta_2B, Ta_3B_2, TaB, Ta_5B_6, Ta_3B_4 and TaB_2 have been reported[1,2,3]. Recently we have prepared TaB, Ta_5B_6, Ta_3B_4 and TaB_2 single crystals from tantalum metal and boron powder using an aluminum-flux method[2,3]. In the present paper, we report experimental conditions for growing the TaB, Ta_5B_6, Ta_3B_4 and TaB_2 single crystals in relatively large size. The crystals were examined by X-ray diffraction and chemical analysis. Densities and Vickers microhardness of the crystals were measured and oxidation at high temperature in air was studied.

The starting materials were tantalum metal powder (purity, 99.9%) crystalline boron powder (purity, 99.9%), and aluminum chips (purity, 99.996%). Mixtures of these materials in various atomic-ratios (B/Ta=0.5~3.0 Al/Ta=3.35~217.96) were placed in an alumina crucible. The synthesis of crystals was carried out in a tantalum element resistance furnace, heated in an argon atmosphere at 1650°C for 5 h, and then cooled slowly to room temperature. The crystals grown were separated from the solidified mixture by dissolving the solvent aluminum metal with 6-mol/dm^3 hydrochloric acid. The unit cell dimensions and chemical compositions of the obtained crystals are given in Table 1.

1. B. Aronsson et al., "Borides, Silicides and Phosphides," Methuen, London (1965).
2. S. Okada et al., Nippon Kagaku Kaishi (1985) 1535.
3. S. Okada et al., Bull. Chem. Soc. Jpn., 63 (1990), 687.

Table 1. Lattice constants and chemical composition.

Compound	Atomic ratio B/Ta	a(Å)	Unit cell dimension		V (Å^3)	Chemical Composition B/Ta
			b (Å)	c (Å)		
TaB	1.0	3.280(1)	8.670(3)	3.156(2)	89.73(13)	0.94
Ta_6B_6	1.2	3.1385(10)	22.609(7)	3.2865(8)	233.20(12)	–
Ta_3B_4	1.33	3.2914(8)	13.994(3)	3.1327(6)	144.29(8)	1.29
TaB_2	2.0	3.097(1)	–	3.242(2)	31.10(3)	1.81
TaB_2	2.5	3.086(1)	–	3.262(2)	31.07(4)	1.93
TaB_2	2.8	3.076(1)	–	3.275(2)	30.99(4)	2.02
TaB_2	3.0	3.076(1)	–	3.275(2)	30.99(4)	1.88

D20

CRYSTAL GROWTH OF BORON-RICH SOLIDS OF Al-M-B (M = Li, Be, Mg) SYSTEM FROM HIGH-TEMPERATURE ALUMINUM SOLUTIONS

Iwami Higashi and Masayoshi Kobayashi
The Institute of Physical and Chemical Research, Wako, Saitama 351-01, Japan
Shigeru Okada and Kenya Hamano
Department of Applied Chemistry, Kanagawa University,
Rokkakubashi Kanagawa-ku, Yokohama 221, Japan
Torsten Lundström
Institute of Chemistry, University of Uppsala, Box 531, S-751 21 Uppsala, Sweden

Boron-rich solids consisting of B_{12} icosahedra are of great interest because of their unique properties which in many cases are of potential technological importance[1,2]. In our previous works[3,4,5], we performed preparation and structure analysis of the icosahedral B_{12} compounds of Al-M-B (M = Li, Be, Mg) system. In the present paper, we describe the crystal growth of these ternary compounds and related materials.

Each of the starting mixtures of Al, M and B with the required composition was placed in an Al_2O_3 crucible and heated in an argon atmosphere using a vertical Al_2O_3 tube furnace equipped with SiC resistors. The temperature of the furnace was raised to 1500°C, kept for 3 h and then cooled to room temperature at a rate of about 10°C/min. The crystals grown in the solidified mixture were separated by dissolving the excess metal solvent Al with hydrochloric acid. The crystals, obtained by this method and characterized by single-crystal structure analysis, were $AlLiB_{14}$, $AlMgB_{14}$ and $Al_{1.1}Be_{0.6}B_{22}$. Crystal chemistry and mechanical properties of these materials will be presented.

1. V.I. Matkovich, Ed., Boron and Refractory Borides (Springer, Berlin, 1977).
2. D. Emin, T. Aselage, C.L. Beckel, I.A. Howard and C. Wood, eds., Boron-Rich Solids (Am. Inst. Phys., New York, 1986).
3. I. Higashi, Y. Takahashi, *J. Less-Common Metals* 81 (1981) 135.
4. I. Higashi, J. Solid State Chem. 32 (1980) 201.
5. I. Higashi and T. Ito, *J. Less-Common Metals* 92 (1983) 239.

D21

THERMAL CONDUCTIVITY AND THERMOELECTRIC POWER OF FLOAT ZONE GROWN AND VC_x AND $Ti_{1-y}V_yC_x$ SINGLE CRYSTALS

C.P. Beetz, Jr., D.F. Cummings and W.I. Precht
Advanced Technology Materials, Inc., Danbury, CT 06810
F.R. Chien and S.R. Nutt
Division of Engineering, Brown University, Providence, RI 02912

We have measured the thermal conductivity, electrical resistivity and thermopower of VC_x and $Ti_{1-y}V_yC_x$ single crystals grown by the float zone technique and have examined the crystals using TEM. We will present results for VC_x (x=0.80 and x=0.88) and $Ti_{1-y}V_yC_x$ alloy crystals having two different compositions measured over the temperature range 300-10°K. The VC_x is an interesting system that has been shown to exhibit an ordered superlattice arrangement of carbon vacancies. The purpose of this study is to examine the influence of the ordered vacancy array on the thermal conduction processes. The thermal conductivity measurements have been made using a classical heater and sink technique. At low temperatures T<100°K, the heat is predominantly carried by lattice vibrations however scattering by carriers that do not participate in the heat conduction seems to be a limiting factor. The mechanisms limiting the low temperature thermal conduction and the influence of carbon vacancy ordering will be discussed. Above ~100°K, the conduction has a significant electronic component that increases with temperature. In this temperature regime, the conduction is limited by carbon vacancy, alloy and Umklapp scattering processes in the crystals. The temperature dependence of the thermoelectric power and electrical resistivity will also be discussed and correlated with the results from TEM.

This work was partially supported by the Naval Weapons Center at China Lake, CA.

GROWTH OF URANIUM-TITANIUM (U_2Ti) COMPOUND IN A HIGH VACUUM

D22

Tatsuo Shikama, Akira Ochiai, Yoshimitu Suzuki and Kenji Suzuki
The Oarai Branch, Institute for Materials Research,
Tohoku University, Oarai, Ibarakiken, 311-13 Japan

Recently, actinide compounds are attracting attention in the field of solid state physics. It is anticipated that they will realize very interesting electronic and magnetic properties due to their unique 5f-electron configurations. However, their interesting intrinsic properties will be easily concealed by small amount of impurities. So, the growth of highly-pure crystals is essential to study their interesting electronic properties.

Here, we are trying to develop highly-pure and well-qualified uranium compounds. Uranium is chemically very active and it interacts quite easily not only with gaseous environments but also with solid crucibles used for melting its compounds. Also, it is not so easy to obtain highly pure uranium metal as a raw material. We developed a r.f.-heating zone-refining apparatus with a water-cooled copper hearth, which will operate in a high-vacuum. Also, we purified the uranium metal by the zone-refining and the electrotransportation in a high vacuum. Using the developed apparatus and the purified uranium, we tried to grow a highly pure crystal of uranium-titanium compound, U_2Ti. U_2Ti is thought to have interesting electronic properties as it is the compound between the so-called 5f and 3d elements. Also, U_2Ti has been studied as a hydrogen-storage material. However, U_2Ti is the line compound and congruent but with a solid solution phase of β-Ti and γ-U at 1171K. So, the conventional melting techniques are not applicable to grow its single crystal of high quality.

In this study, the exact amount of the highly-pure uranium metal and a highly-pure titanium of 99.9at% was melted in a high vacuum. The formed ingot of about 120mm long and about 8mm in diameter was zone melted several times. Then, the ingot was zone heated to the temperature of about 1220-1370K, just above the phase-boundary temperature. The 6 passes of the zone heating was carried out along the ingot with the speed of 0.2mm/min in a vacuum of about $1x10^{-8}$Pa. Then, the ingot was kept to be heated at 1040K for about 30 days on the water-cooled hearth by 140mm long r.f. coil in a dynamic vacuum of $1x10^{-8}$Pa. The results of characterization of the grown crystal will be reported.

STUDY ON THE MAGNETOSTRICTIVE CRYSTAL OF $Tb_{0.27}Dy_{0.73}Fe_{1.95}$:Mn

D23

Li Qiang, Chang Yiling, Yuan Runzhang, Huang Shaohua and Jin Dejiang
Advanced Material Research Institute
Wuhan University of Technology, Wuhan, China

$Tb_{0.27}Dy_{0.73}Fe_{1.95}$ crystal possesses very excellent magnetostrictive properties when mixing with Mn during the process of crystal growth. This paper reports the crystal growth of $Tb_{0.27}Dy_{0.73}Fe_{1.95}$:Mn, the effect of Mn on its magnetostrictive properties (λ_s, d_{33}, μ_T, k_{33} etc.), and the method of controlling the amount of Mn during the process of crystal growth.

GROWTH OF $Tb_XDy_{1-X}Fe_{2-W}$ MAGNETOSTRICTIVE CRYSTALS WITHOUT CONTAMINATION

D24

Li Qiang, Chang Yiling, Yuan Runzhang, Huang Shaohua and Jin Dejiang
Advanced Material Research Institute
Wuhan University of Technology, Wuhan, China

$Tb_XDy_{1-X}Fe_{2-W}$ ($0.2<X_{0.3}$, $0<W<0.1$) is a new kind of excellent magnetostrictive material with the high λ_s at room temperature. We have got Large-Size (10 ~ 15mm in diameter) $Tb_XDy_{1-X}Fe_{2-W}$ single crystals completely without contamination by using magnetic levitation cold crucible in CZ technique. In the growth of crystals by this method, the starting materials Tb (>99.95%wt), Dy (>99.98%wt, Fe (>99.99%wt) were used to synthesize the precursor alloy of 80 ~ 100g and a RF power of 15 ~ 20KW. A pulling speed of 5 ~ 10mm/h and a rotation rate of 10 ~ 20r/min were chosen. The single crystal of $Tb_XDy_{1-X}Fe_{2-W}$ grows under such conditions usually with the direction of <111> or <112>.

D25

CRYSTAL GROWTH OF THE TRANSITION METAL SILICIDES $MoSi_2$ AND WSi_2

Axel Norlund Christensen
Department of Inorganic Chemistry
Aarhus University, DK-8000 Aarhus C, Denmark.

Single crystals of the transition metal silicides $MoSi_2$ and WSi_2 were grown in a floating zone growth mode from polycrystalline preforms of the compounds. The preforms were made from stoichiometric mixtures of powders of the metals and silicon, which were pressed isostatically to rods at room temperature and sintered in an ambient helium atmosphere. The rods had the approximate dimensions: Length 10 cm, diameter 1 cm. The floating zone growth was performed in a crystal growth unit for 10 MPa gas pressure,[1] at the conditions: RF heating, ambient atmosphere 1 MPa He, growth rate 5 mm h^{-1}.

$MoSi_2$ and WSi_2 are tetragonal, space group *I4/mmm* with the unit cell dimensions $MoSi_2$: a = 3.200(5), c = 7.861(5) Å, WSi_2: a = 3.212(5), c = 7.890(5) Å.[2] Guinier photographs were taken of samples of the crystals with a Nonius Guinier camera using $CuK\alpha_1$ radiation (λ = 1.5406 Å) and silicon (a = 5.4305 Å) as an internal standard. The positions of the reflections on the films were measured with a fotometer, and the tetragonal space group was confirmed with the unit cell parameters, $MoSi_2$: a = 3.2048(3), c = 7.8471(11) Å, WSi_2: a = 3.2133(6), c = 7.8267(15) Å.

Laue photographs of the crystals showed an excellent crystal quality. The growth direction of $MoSi_2$ was close to the [110] direction, and that of WSi_2 was close to the direction [100]. Discs of the crystals were cut with spark erosion after the planes (100), (110) and (001), polished with diamond paste and used in angle-resolved photoemission studies of the electronic band structures of $MoSi_2$ and WSi_2.

1. Castonguay, R.A., Technical Specialities and Services Co., P.O. Box 9, Salem, MA 01970, U.S.A.
2. Zachariasen, W.H., Z.Phys. Chem. 128 (1927) 39.

D26

NITROGEN INDUCED PHASE TRANSFORMATION OF THIN FILM OF TANTALUM

Y. Akagi, Y. Okamoto, Y. Nakamura and M. Koba
Materials Research and Analysis Division, Corporate RED Group
SHARP Corporation, Tenri, Nara 632, Japan

Tantalum thin metal film has been used in an electronic application such as a fine electrode because of highly stable properties against chemical processes. Among two kinds of polytypes, α and β phases, nonequilibrium tetragonal β phase (high resistivity of 200μΩ cm) only appears in a thin films less than 500nm when prepared by sputtering method, while a thick foil or bulk form consists of low resistive cubic α phase (20μΩ cm). Studies are still being continued to distinguish whether β phase is an allotrope of bcc Ta or an impurity-stabilized tantalum phase. On the other hand, in order to stabilize a cubic α phase in α phase in a thin film form, nitrogen-doping method has been positively used to promote the transformation of tantalum from β to α phase, but the resistivity still remains relatively higher value around 800 μΩ cm.

In this paper, X-ray and TEM observations carried out to reveal the structural origin for the phase transformation will be reported in a nitrogen-doped tantalum film prepared by sputtering method. From an X-ray diffraction, phase relation in a film with the doping of nitrogen was determined and distinctive orientation relative to a substrate was observed. From TEM observation of doped film, superlattice fringe image was clearly observed in addition to the fundamental lattice image of tantalum. The presence of a superstructure indicates an ordered solid solution of nitrogen in tantalum. In addition to the above structural study, following experimental criteria to induce phase-transformation and further to realize a low resistive film will be reported in a thin film less than 500nm. Nitrogen concentration in a film required for the phase transformation was found to be 10^{21} atoms/cm^3. Detailed structural information of the columnar grain of nitrogen induced α tantalum and the distribution of its preferred orientation surely contribute to make clear the metal-ceramic interface, and also play an important role for the further reduction of resistivity of a thin film.


POSTER SESSION
NUMBER 2
TUESDAY
8:00 PM
EXHIBIT HALL

POSTER SESSION #2
EXHIBIT HALL
Tuesday 8:00 PM

A16
Free Surface Energy and Burgers' Vector of the Growth Sources on (101) ADP Face
P. G. Vekilov, Yu. G. Kuznetsov, and A. A. Chernov*
Institute of Crystallography, Russia

A17
The Wandering of Steps and the Terrace Width Distribution on Clean Si (lll)
C. Alfonso, J. M. Bermond, J. C. Heyraud,* and J. J. Metois
CRMC2-CNRS, France

A18
The Interaction of Particles with an Advancing Solid-Liquid Interface in Aluminum Based Composites
C. Schvezov* and Y. Fasoyino
Universidad Nacional de Misiones, Argentina; University of British Columbia, Canada

A19
Concentration Dependencies of the Distribution Coefficient at Equilibrium Incorporation
D. Dragonova
University of Sofia, Bulgaria

A20
An Equation of the Crystal Growth Rate in the Presence of Impurities
D. Dragonova
University of Sofia, Bulgaria

A21
Experimental Study for Melting Transition at Interface between Ice Crystal and Glass Substrate
Y. Furukawa,* I. Ishikawa and M. Yamamoto
Hokkaido University, Tohoku University, Japan

A22 - VIDEO PRESENTATION
Real Time, Atomic Scale Observations of Crystal Growth, Step Dynamics, Growth Spirals and Domainal Growth
A.J. Gratz
Lawrence Livermore National Laboratory, USA

A23
Light Scattering During Precipitation of ZnS from a Chemical Reaction
O.N. Mesquita
Universidada Federal de Minas Gerais, Brazil

A24
Coupling Interaction of Couette Flow and Crystal Morphologies in Bridgman Growth
T. Huang,* Y. Yang and Y. Zhou
Northwestern Polytechnical University, China

A25
Studies on Fluid Flow in Czochralski System
K. Sankaranarayanan,* J. Kuman and P. Ramasamy
Anna University, India

A26
Numerical Simulation of Czochralski Growth: Bulk Flow Vs. Thermal-Capillary Models
Q. Xiao* and J. J. Derby
University of Minnesota, USA

A27
On the Effects of Internal Radiation on Convective Flows in High-Temperature Materials Processing Systems
J. J. Derby,* S. Brandown and A. G. Salinger
University of Minnesota, USA

A28
Physical Simulation of Hydrodynamics and Growth of Single Crystals from High Temperature Solutions with Use of Free Convection and ACRT
V. M. Masalov, G. A. Emel'chenko, and V. Nikolov
Institute of Solid State Physics, Russia; Institute of General & Inorganic Chemistry, Bulgaria

A29
Nonlinear Dynamics Near Codimension-Two Singularities in Cellular Growth by Directional Solidification of a Binary Alloy
K. Tsiveriotis and R. A. Brown
Massachusetts Institute of Technology, USA

A30
Calculations of Transient Processes when Pulling Single Crystals with Nonplanar Interface
V. Neeman (Nemenov)
Jerusalem College of Technology, Israel

B31
Crystal Growth, Optical Properties and Ionic Conductivity of $KTiOAsO_4$ Crystals
G. M. Loiacono, D. N. Loiacono* and J. J. Zola
Crystal Associates, Inc., USA

B32
Flux Growth And Properties of TRA Crystals
J.-r. Han, Y. Liu, M. Wang, and D. Nie
Chandong University, China

B33
Growth and Optical Characterization of Large Potassum Titanyl Phosphate Crystals
T. Sasaki, A. Miyamoto, A. Yokotani, and S. Nakai
Osaka University, Japan

B34
Correlation of the Structure of Melts and Crystals of Alkali and Alkali-Earth Borates: The Crystallization Behavior of Barium Metaborate
Yu. K. Voronko, A. V. Gorbachev, V. V. Osiko, A. A. Sobol,* R. S. Feigelson, and R. K. Route
Academy of Sciences, Russia; Stanford University, USA

B35
Study on Growth of Lithium Triborate Crystals
D. Y. Fang, W. R. Zeng, X. Lin, J. G. Wang, Q. L. Zhao, and Q. G. Tan
Fujian Inst. of Research on the Structure of Matter, China

B36
A Study of Strain in $KH_{2(1-x)}D_{2x}PO_4$ (DKDP)
J. J. DeYoreo, B. Woods, C. Ebbers, and S. Mayhugh
Lawrence Livermore National Lab, USA

B37
Viscosity Measurement of Molten $LiNbO_3$ by Oscillation Damping Method
K. Shigematsu, S. Y. Anzai and S. Kimura
Kimura Metamelt Project, Japan

B38
Growth and Characterization of Scandium-Doped $LiNbO_3$
J. K. Yamamoto,* K. Kitamura, N. Iyi, S. Kimura, Y. Furukawa, and M. Sato
Mitsui Mining and Smelting, Japan

B39
Compositional Uniformity in Czochralski Grown $LiTaO_3$ Single Crystals
D. S. Chung,* P. H. Park and Y. S. Kim
RIST, Korea

B40
The Morphology of β-BaB_2O_4
W. Zhong,* H. Hong, Z. Lu, T. Zhang, and S. Hua
Chinese Academy of Sciences, China

POSTER SESSION #2
EXHIBIT HALL
Tuesday 8:00 PM

B41
Growth and Dielectric Study on $KTa_{1-x}Nb_xO_3$
R. Ilangovan,* S. Balakumar, C. Subramanian, and P. Ramasamy
Anna University, India

B42
Growth and Pyroluminescence in Pure and Sm Doped $KNbO_3$ Single Crystals
P. D. Durugkar
Hislop College, India

B43
Apply a Novel Technique to Grow BTO and KTN Crystal
X. Ma,* S. Zhang, W. Hu, Z. Zhao, and X. Zhang
Shanghai Institute of Optics, China

B44
Preparation and Characterization of Lead Zirconate Titanate Thin Films by Sol-gel Processes
F. Leccabue, B. E. Watts, E. Melioli, and D. Carrillo
MASPEC, Italy

B45
Domain and Internal Stress Analysis of $BaTiO_3$ by External Stress
B. W. Lee and K. K. Orr*
Hanyang University, Korea

B46
Studies on Growth Kinetics of $BaTiO_3$ and $Ba_{1-x}Ca_xTiO_3$
S. Balakumar,* R. Ilangovan, C. Subramanian, and P. Ramasamy
Anna University, India

B47
Growth and Habit Modification Studies in $NaClO_3$ Crystals
K. K. Rao* and V. Surender
Kakatiya University

B48
Development of $(KBr\text{-}KCl)(OH^-):(F^{2+})H$ Color Center Laser Crystal Series and Their Spectral Characteristics
C. Xu, C. Huang, J. Qiu, and J. Wu
Hua Qiao University, China

B49
Several Key Problems in the Preparation of $NaCl(OH^-):(F^{2+})H$ Laser Crystal
J. Wu, C. Xu, J. Qiu, and B. Lin
Hua Qiao University, China

B50
Infrared Continuous Wavelength Tunable KCL $(Na^+,OH):(F^{2+})H$ Color Centre Laser Crystal
G. Chen, C. Xu, J. Qiu, M. Huang, and B. Lin
Hua Qiao University, China

B51
Growth And Perfection of Chromium Doped Forsterite
B. Hu,* H. Zhu and P. Deng
Shanghai Institute of Optics, China

B52
Crystal Growth and Optical Properties of $Cr:Mg_2SiO_4$
L. Liu,* Z. Wang, S. Li, and Y. Jiang
Chinese Academy of Sciences, China

B53
Laser Induced Damage in Sapphire and Ti:Sapphire Crystals
F. Gan, Q. Zhang and J. Qiao
Shanghai Inst of Optics & Fine Mechanics, China

B54
New Growth Techniques and Perfection Characterization of Ti:Sapphire Laser Crystal
P. Deng,* G. Qiao, Q. Zhang, B. Yun, Y. Chai, and B. Hu
Shanghai Institute of Optics, China

B55
An X-ray Topographic Examination into The Growth History of Yttrium Aluminium Garnet Grown from High Temperature Solution
K. J. Roberts,* G. ... ell and B. J. Isherwood
University of Strathclyde United Kingdom

B56
Formation of Spiral Shape on Czochralski Grown Dysprosium Garnet Single Crystal
H. Kimura, T. Numazawa, M. Sato, and H. Maeda
National Res. Institute for Metals

B57
Growth of Gadolinium Indium Gallium Garnet (GdInGG) Single Crystal by the Floating Zone Method
M. Kawada, H. Toshima,* Y. Miyazawa, and S. Morita
Namiki Precision Jewel Co. Ltd., Japan

B58
Study On Growth of Bismuth Tellurium Single Crystals
X. Tong, Y. Lu, M. Li, and Q. Sang
Research Inst. of Synthetic Crystals, China

B59
In-situ Observation of the Growth Processes of Oxide and Fluoride Crystals From Melts
J. Chen,* W. Jin and G. Shan
Chinese Academy of Sciences, China

B60
Hydrothermal Growth and Morphology of $Bi_{12}SiO_{20}$ and $Bi_4Ge_3O_{12}$ Single Crystals
A. A. Marjin and L. A. Samoilovich*
All Union Inst. for Syn. of Materials, Russia

C20
Relaxed Buffer Layer Growth using Strained Layers
D. J. Dunstan, P. Kidd,* R. H. Dixon, and L. K. Howard
University of Surrey, United Kingdom

C21
On the Micro-Mechanical Phenomena during Boule Anneal of GaAs
S. Motakef and D. J. Carlson
Massachusetts Institute of Technology, USA

C22
Preparation and Characterization of the Filled Tetrahedral Semiconductor LiZnP Film on InP(111)
K. Kuriyama, Y. Takahashi, and T. Kato
Hosei University, Japan

C23
Numerical Modeling of InP MOCVD with Comparison to Experiment
L. R. Black,* I. O. Clark, E. J. Johnson, J. Kui, and W. A. Jesser
NASA Langley Research Center, USA

C24
Model for MBE and MOVPE Growth on Nonplanar Surface
M. Ohtsuka* and A. Suzuki
Canon, Inc., Japan

C25
Characterization of Undoped InP, Grown in an Inverted-Vertical MOVPE Reactor, using Trimethylindium, Tertiarybutylphosphine and Phosphine
J. D. Parsons, J. Wu, A. K. Chaddha, S.-R. Hahn, H.-S. Chen, C. Deng, S. Wild, and K. Oatis
Oregon Graduate Institute of Sci. & Tech., USA

C26
AB Initio Molecular Orbital Study on the Reaction of TMA With H_2
Y. S. Hiraoka,* M. Mashita, T. Tada, and R. Yoshimura
Toshiba Corporation, Japan

POSTER SESSION #2
EXHIBIT HALL
Tuesday 8:00 PM

C27
Growth of GaAs on Si By Employing AlAs/GaAs Double Amorphous Buffers
W. Y. Uen* and T. Nishinaga
Univeristy of Tokyo, Japan

C28
Reduction of Surface Defects in GaAs Layers Grown by MBE
H. Kawada,* S. Shirayone and K. Takahashi
Hitachi Ltd., Japan

C29
HVPE Growth of InGaAsP Epilayers and their Characterization
D. Arivuoli,* G. Attolini, C. Bocchi, C. Pelosi, and C. Frigeri
MASPEC, Italy

C30
Hydride-VPE Growth of InP and InP:Fe in H_2/N_2 Ambient
R. Gobel
Deutsche Bundespost TELEKOM, Germany

C31
A New Kinetic Model For Vapor Phase Epitaxy of $GaAs_{1-x}P_x$ from the Ga-As-P-H-Cl System
V. N. Mani,* R. Dhanasekaran and P. Ramasamy
Center for Materials for Elec. Tech., India

C32
Numerical Simulation Studies of Concentration Profiles and Growth Rate in InP and GaAs LPE
P. S. Raghavan,* R. Dhanasekeran and P. Ramasamy
Anna University, India

C33
Influence of Solute Convection on InGaSb LPE Layers Grown on Vertically Mounted GaSb Substrate
Y. Hayakawa, K. Asakawa, Y. Torimoto, K. Yamashita, A. Nakayama, and M. Kumagawa
Shizouka University, Japan

C34
Growth of GaInP Thick Layers by the Modified YO-YO Solute Feeding Method
S. Watabe,* K. Tadatomo, T. Sukegawa, and A. Tanaka
Mitsubishi Cable Industries Ltd., Japan

D17
Formation of Secondary Twins in Twins in Thin Films
S. Maruyama
Osaka College, Japan

D27
Studies of Features of Hydride Crystal Growth in Zirconium
D. V. Schur, V. A. Iavrenko, V. B. Wojtowych, and V. M. Adejev
Academy of Sciences, Ukraine

D29
Growth And Properties of Super-length BaF_2 Scintillant Crystal
S. X. Ren, J. Zhang, F. Y. Zhang,* Y, N. Zheng, and F. Z. Li
Beijing Glass Research Institute, China

D30
Growth of Single Crystals of Fast-Ion Conducting Binary and Ternary Copper And Silver Halides for Neutron Scattering
C. Heremans and B. J. Wuensch
Massachusetts Institute of Technology, USA

D31
Study of the HgI_2 Homogeneity Region in the Hg-I System Phase Diagram
H. Hermon, M. Roth, M. Schieber, and J. Shamir
Hebrew University, Israel

D32
Effect of Growth Conditions on the Optical Quality of Mercurous Chloride Crystals
N. B. Singh, M. Gottlieb, J. J. Conroy, R. H. Hopkins, R. Mazelsky, M. E. Glicksman, and W. M. B. Duval
Westinghouse Electric Corporation, USA

D33
Lead Chloride Crystal Growth from Boiling Solutions
S. Veintemillas-Verdaguer, J. Torrent-Burgues, and R. Rodriguez-Clemente
Institut de Ciencia de Materiales, Spain

D34
Single-Crystal Growth of Cuprous Chloride by Flux Method
G. T. K. Fey, D. P. Wright, and J. B. Wagner, Jr.
National Central University, USA

D35
Growth of Sulpho Halides of Antimony and Bismuth in Gel
R. R. Kumar,* G. Raman and F. D. Gnanam
Anna University, India

D36
TEM Study of Phase and Domains in Lanthanum Aluminate (Late News)
Y. Yang
Institute of Physics, Beijing, PR China

D37
The Growth of $DyAlO_3$ Single Crystals by Czochralski Method
H. Sekiwa,* S. Morita and Y. Miyazawa
National Institute for Research, Japan

D38
Studies on the Absorption at 290 nm of BaF_2 Crystals
H. Xiao,* G. Chen, S. Q. Man, S. X. Ren, and J. Q. Zhang
Beijing Glass Research Institute, China

D38
The Growth of $NdAlO_3$ Single Crystals by the Czochralski Method
Y. Miyazawa, H. Toshima and S. Morita
NIRIM, Japan

D39
Growth and Properties of $RAlO_3$ (R=Dy, Ho, Er) single Crystals by the Czochralski Technique
T. Ikeya,* K. Hoshikawa and T. Fukuda
Tohoku University, Japan

D40
Phase Diagram And Crystal Growth of R_2CuO_4
K. Oka, M. J. V. Menken, Z. Tarnawshi, A. A. Menovsky, A. J. M. Windelman, T. Gortenmulder, A. M. Moe, T. S. Han, and H. Unoki
Electrotechnical Laboratory, Japan

D41
Single Crystal Growth of Y-Substituted $NdAlO_3$ by the FZ Method
I. Tanaka, M. Kobashi and H. Kojima
Yamanashi University, Japan

D42
Untwinned and Large Size Single Crystal Growth of YBCO
C. T. Lin,* W. Zhou, W. Y. Liang, E. Schonherr, and H. Bender
Max-Planck-Institute, Germany

D43
On the Flux Growth and Some Properties of Superconducting $YBa_2Cu_3O_{7-x}$ Single Crystals and LPE Films
P. Gornert,* K. Fischer, and C. Dubs
Physikalisch-Technisches Institut, Germany

POSTER SESSION #2
EXHIBIT HALL
Tuesday 8:00 PM

D44
Attenuation of Grain Boundary Effects in Crystalline Superconducting $YBa_2Cu_3O_{7-x}$
R. Cabre, R. Sole, X. Ruiz, M. Aguilo, C. F. Woensdregt, and F. Diaz*
University of Barcelona Tarragona, Spain

D45
Improvement of Superconductivity in YBCO Single Crystals
W. Y. Shui,* P. Bennema, Z. Manna, C. M. Fu, C. Grey,
L. W. M. Schreurs, Q. Xu, P. van der Linden, and Y. Bruynseraede
Nijmegen Universiteit, The Netherlands

D46
Crucible Free Techniques in High Tc Crystal Growth
T. Frieling, J. Kowalewsky, F. Ritter,* and W. Assmus
Johann Wolfgang Goethe University, Germany

D47
High Oxygen Pressure ($P_{O_2} \leq$ 3000 bar) Crystal Growth of Double Chain YBaCuO Phases
J. Karpinski, E. Kaldis, H.-J. Lang, and S. Rusiecki
Eidgenossische Technische Hochschule, Switzerland

D48
Growth of Bulk Single Crystals in 1-2-3 Oxide Superconductors
S. Hayashi, Y. Nishimura, T. Inoue, S. Miyashita, and H. Komatsu
Tohoku University, Japan

D49
Solidification in a Magnetic Field: Application to $YBa_2Cu_3O_7$
R. Tournier
CRTBT/CNRS, France

D50
X-ray Characterization of Laser Ablated Textured $YBa_2Cu_3O_{7-x}$ Thin Films on Zr, Si, MgO and $SrTiO_3$ Substrates
M. Steins, F. Mattheis, R. Gaebel, K. Bente, and H. U. Krebs
Universitat Gottingen, Germany

D51
$YBa_2Cu_3O_{7-\delta}$ Thin Films Grown on Ferroelectric $Bi_4Ti_3O_{12}$ Crystal by R-f Sputtering
M. E. Mendoza-Alvarez, C. Tabares-Munoz, J. G. Mendoza-Alvarez, and O. Alvarez-Fregoso
Universidad Autonoma de Puebla, Mexico

D52
Deposition of $LiNbO_3$ Thin Films on C-axis Oriented Epitaxial $YBa_2Cu_3O_{7-\delta}$ Films by Pulsed Excimer Laser Ablation
B. Ogale,and Nawathey-Dikshit
University of Poona, India

D53
Growth, Characterization and Superconducting Properties of Crystals of the Tl-Ba-Ca-Cu-O System
J. P. Chaminade,* J. C. Frison, P. Dordor, J. C. Grenier, M. Pouchard, J. Etourneau, P. V. Huang, B. Giordanengo, A. Sulpice, and R. Tournier
Universite de Bordeaux I, France

D54
The Surface Morphology, Crystal Habit and Growth Mechanism of $RBa_2Cu_3O_x$(R=Y,Gd,Tm) Single Crystals
H. Wang
CCAST (World Lab), China

SESSION 2A

FREE SURFACE ENERGY AND BURGERS' VECTOR OF THE GROWTH SOURCES ON (101) ADP FACE

A16

P.C. Vekilov, Yu.G. Kuznetsov and A.A. Chernov
Institute of Crystallography, Academy of Sciences of the USSR
Leninskii pr. 59, Moscow 117333, USSR

Michelson interferometry was applied to study dependence of the hillock slope p on the supersaturation σ for various dislocation sources. Supposing triangular form of the critical nucleus, and corresponding specific effective surface energy α of the step riser the same, anisotropy of the kinetic coefficient b and linearity of the step kinetics $v_i = b_i\sigma$ have obtained the formular:

$$\frac{1}{p_1} = \frac{b_1}{b_1\omega} L^* + \frac{b_1}{b_1\omega} \cdot \frac{2\sqrt{3\Omega\alpha}}{kT} B \cdot \frac{1}{\sigma}$$

where ω is the dimensionless frequency of spiral rotation, $b_\perp$ is the component or the Burgers' vector perpendicular to the studied race, Ω is the volume of one effective growth unit, $B = 1/b1 + 1/b_2 + 1/b_3$, $L^* = L_1/b_1 + L_2/b_2 + L_3/b_3$. L_i-linear dimension or the dislocation source (Fig. 1), p_1 is the hillock slope in the sector 1. The "quantization" of the slope for all σ (Fig.1) means the dislocation sources or one and the same strength have the same internal structure. Determining b from dependence v(σ) we have got for three groups of the experimental curves three relations: $b_\perp/\alpha$ = 5.1;3,4 and 1.75 x 10^{-8} cm^3/erg, i.e. they approximately relate as 3:2:1. Since the lowest curve in the fig is linear, we assume that it corresponds to the elementary dislocation, $b_\perp = 5.33 \times 10^{-8}$cm. Then the curve 2 corresponds to double Burgers' vector and the curve 3 - to the triple one. So these relations give us value of α = 29 erg/cm.

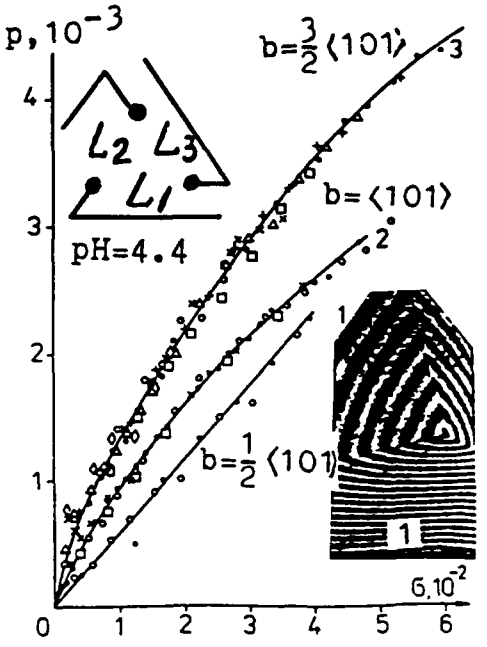

Figure 1. The dependence of the slope of the growth hillock p on the supersaturation σ for sector 1 for all the studied crystals. Right insert: surface interferogram, upper insert: the center of dislocation step source.

THE WANDERING OF STEPS AND THE TERRACE WIDTH DISTRIBUTION ON CLEAN Si (III)

A17

C. Alfonso, J.M. Bermond, J.C. Heyraud and J.J. Metois
CRMC2-CNRS - Case 913 - Campus Luminy
F13288 Marseille Cedex 9 - France

In situ reflection electron microscopy experiments have been done in an ultra high vacuum electron microscope on clean nominal Si(111) surface.

The images were tape recorded, in thermodynamic equilibrium, i.e at temperature high enough (~900°C) to allow step wandering across an average position without evaporation (vapor pressure of Si at 900°C ~ 4×10^{-11}mbar). Two kinds of situation have been analyzed:

-i Isolated step, the fluctuations of which allow an estimation of the step stiffness (roughly 1×10^{-10} J/m).

-ii S ı trains (mean step separation from 20 to 140 nm).

The terrace width distribution has a standard deviation which varies linearly with the mean separation between steps. Over the whole range of step mean separation, the distributions are best fitted by a Gaussian Law. This is ascribed to step interactions decaying as Ax^{-2} (x = normal distance to the step edge). The value of A is determined (A 4.6×10^{-30} J/m).

The result on the crystal equilibrium shape near a (111) facet is discussed.

A18

THE INTERACTION OF PARTICLES WITH AN ADVANCING SOLID-LIQUID INTERFACE IN ALUMINUM BASED COMPOSITES

C. Schvezov and Y. Fasoyinu
UNAM.Posadas.Misiones(Arg) and UBC.Vancouver.BC (Canada)

The interaction of foreign particles with advancing solid-liquid interface has been studied both experimentally and theoretically by many authors during solidification of metallic and non-metallic materials and particles. Recently, there was renewed interest on the subject due to the development of particulate reinforced metals and alloys. Particularly due to the 'segregation' of the particles to interdendritic positions. For planar interface this phenomenon has been usually termed 'pushing' which may arise due to forces developing for short distances between particle and interface. In metal systems and planar interface pushing has not been observed.

In the present investigations directional solidification of aluminum based composites containing alumina and silicon carbide particles has been performed. The solidification interface is normally dendritic and the particles appear in the interdentritic areas. According to the size these particles should have been trapped rather than pushed. In addition small particles are normally trapped by the growing dendrite. These observations suggest that the segregation of particles is due to other mechanism including fluid flow and particle movement. This mechanism is studied on a transparent material (benzoic acid) containing particles which are not pushed by a planar interface. Results of these experiments will be shown and discussed in comparison with the results on metal systems.

A19

CONCENTRATION DEPENDENCIES OF THE DISTRIBUTION COEFFICIENT AT EQUILIBRIUM INCORPORATION

D. Draganova
University of Sofia, Faculty of Chemistry

In earlier papers by the same author it was shown that the well known distribution coefficients K and D depend on the concentration.

$$K = C_{is}/C_{il} \quad (1)$$

is the ratio of the impurity concentration in the solid C_{is} and the mother phase C_{il} at equilibrium.

$$D = x/Y(b - y)/(a - x) \quad (2)$$

where a and b are the initial concentrations of the impurity I and the basic component B, respectively, and x and y - their concentration in the solid and mother phase.

Mostly, the coefficient D depends on the impurity concentration with a maximum in the limits of each mechanism. This type of behavior of D has been observed for all classical types of systems - isomorphic, isodimorphic, and non-isomorphic, a fact that throws a shadow over this classification and over the mixed crystals formation theories based on constant D values.

Working at equilibrium conditions we were able to determine the formation energy of mixed crystals Q_{ss}. We saw that within the limits of one mechanism Q_{ss} changes by three different ways. This means that we have to accept that the energy of formation of solid solution is quanted and the characteristic parameter takes only three values which determine the changes in D. With the first set of energy states D increases, with the second remains constant and with the third falls.

The available experimental data support the above considerations. All this means that it is improper to compare different impurities on the basis of only one concentration c_i. Bearing in mind the different mechanisms and the different energy states such a comparison may only serve for initial suppositions about the influence of the impurities on the crystal properties.

EQUATION OF THE CRYSTAL GROWTH RATE IN THE PRESENCE OF IMPURITIES

A20

D. Draganova
University of Sofia, Faculty of Chemistry

Systematic studies of the processes of incorporation of the ionic impurities into inorganic salts were carried out. This is considered as a beginning of the solution of the problem of the interaction of impurities with the growing crystal in a reversed order - first the final result, equilibrium incorporation was registered, and only then the impurity influence on the growing crystal was studied. Simple crystal matrices such as potassium halogenides were used. The experimental apparatus applied allowed work at optimal stationary conditions. The characteristic curves $R_{100}(c_i)$ and $R_{111}(c_i)$ were taken at

$$c_i = \text{const}, \sigma_i = \text{const}, T = \text{const}, J = \text{const}.$$

Here R_{100} and R_{111} are the linear growth rates of (100) and (111) faces respectively, c_i - the impurity concentration in the intervals 10^{-6}, 10^{-4} - 10^{-1} (the upper c_i value is determined by the double salt formation present in most of the cases), σ_i is the supersaturation, J is the solution flux.

Different mechanisms of impurity incorporation (with some impurities 2, with others -3) were registered for the equilibrium incorporation studies. The curves $R_{100}(c_i)$ and $R_{111}(c_i)$ repeated these results but with some more interesting effects. On the basis of the above results we managed to draw a relatively simple equation for the growth of inorganic salts crystals in the presence of ionic impurities. It has two forms in the two cases: (i) dominating repulsive forces in the absorption layer; and (ii) dominating attractive forces in the absorption layer. It also includes θ_i - the coverage and Φ_{SD} - the thermodynamic potential of the surface diffusion of the impurities.

In the respective paper the equation and the experimental approximations confirming it will be given. For the full description of the crystal growth processes in the presence of impurities one more equation is necessary that is not discussed here.

EXPERIMENTAL STUDY FOR MELTING TRANSITION AT INTERFACE BETWEEN ICE CRYSTAL AND GLASS SUBSTRATE

A21

Y. Furukawa, I. Ishikawa and M. Yamamoto***
Institute of Low Temperature Science, Hokkaido Univ., Sapporo 060, Japan
**Research Institute for Scientific Measurements, Tohoku Univ., Sendai 980, Japan

It has been made clear by both theoretical and experimental studies that an ice crystal surface is covered with the quasi-liquid layer at temperatures just below the melting point (namely, occurrence of surface melting)[1,2]. On the other hand, a phase transition similar to the surface melting can also occur at the interface between ice crystal and substrate. Theoretical considerations have been given for the quasi-liquid layer at the interface between ice and soil particle, concerning to the frost heaving phenomena in the ground[3]. Though Chernov and Yakovlev[4] afforded an evidence for the occurrence of melting transition at the interface between Biphenyl crystal and glass substrate using an ellipsometry, any direct evidence of the melting transition at the ice crystal-substrate interface has not been shown up to the present. The purpose of this work is to obtain the direct evidence of such phase transition at the interface between ice and glass by the method of ellipsometry, and to clarify the structure and physical property of quasi-liquid layer.

A null ellipsometry was operated for the ice-glass interfaces in the walk-in cold room. An ice crystal sample was cut off from the ice single crystal grown from the doubly distilled and deionized water. The ice-glass interface was prepared by the method of refreezing to the triangular glass prism with the apex angle equal to the incidence angle of light.

As a result, a direct evidence of the melting transition at the glass-ice interface was obtained at the temperature range above -1°C. At temperatures below -1°C, the transition layer with mixed properties of ice crystal and glass substrate was detected. Consequently, it is to be emphasized that the threshold temperature of melting transition at the ice-glass interface is below -1°C at least. At the presentation, the structure and physical property of the quasi-liquid layer will be discussed as compared with those of quasi-liquid layer at the ice surface.

1) T. Kuroda and R. Lacmann: *J. Crystal Growth* 56 (1982) 189.
2) Y. Furukawa, M. Yamamoto and T. Kuroda: *J. Crystal Growth* 82 (1987) 655.
3) T. Kuroda: in Ground Freezing, ed. S. Kinoshita and M. Fukuda (Balkema, 1985) 39.
4) A.A. Chernov and V.A. Yakovlev: in Morphology and Growth Units of Crystals, ed. I. Sunagawa (Terra Sci. Pub., Tokyo, 1989) 99.

*Present address: Chichibu Res. Lab., Showa Denko K.K., Chichibu 369-18, Japan.

A22

REAL-TIME, ATOMIC-SCALE OBSERVATIONS OF CRYSTAL GROWTH: STEP DYNAMICS, GROWTH SPIRALS, AND DOMAINAL GROWTH

A.J. Gratz
Lawrence Livermore National Laboratory, Livermore, CA 94550
P.E. Hillner
University of California, Santa Barbara, CA 93106

New techniques using an AFM in fluid cell allow real-time, *in situ* observations of crystal growth at the atomic scale; observations will be presented as movie sequences of growth and dissolution. For calcite in basic solutions, *in situ* observations showed growth was by advance of monomolecular steps; dissolution was by a combination of step retreat and etch pit excavation. However, in contrast to predictions of the classical BCF model, calcite step velocity was independent of step spacing, indicating an unimportant role for surface diffusion. The latter type of behavior requires a *step-site* model for growth and dissolution in which reactions occur only at surface steps. For materials showing step-site kinetics, the surface area is a secondary parameter in determining reaction rate; the critical parameter is step density. On calcite, steps nucleate primarily at screw dislocations which outcrop as spirals which rotate during growth; nucleation was also recorded at topographic protrusions, but never at smooth surface sites. Growth in any region was dominated by local dislocation sites, leading to a domainal growth structure. Examples of poisoned growth will also be presented.

A23

LIGHT SCATTERING DURING PRECIPITATION OF ZnS FROM A CHEMICAL REACTION

M.S. Couto and O.N. Mesquita
Departamento de Física, Instituto de Ciências Exatas
Universidade Federal de Minas Gerais, C.P. 702
Belo Horizonte 30.161, MG Brazil

We study by light scattering the nucleation and aggregation of ZnS crystallites, produced during the chemical reaction between Na_2S and $ZnCl_2$, in aqueous solution.

From dynamic light scattering measurements we determined that the rate of growth of the average aggregate size was exponential on time, in the range of concentrations used, indicating that the mechanism of aggregation was Reaction Limited Cluster-Cluster Aggregation (RLCCA) [1].

From static light scattering measurements we obtained the structure factor of the aggregates and determined their Hausdorff fractal dimension (D_H). We found that $1.9 \leq D_H \leq 2.3$ in partial agreement with the RLCCA aggregation mechanism.

The rate of aggregation was maximum when Zn/S ~ 1, where Zn is the concentration of Zinc and S the concentration of Sulphur, and decreased as the ratio Zn/S becomes increasingly smaller or larger than one. This possibly indicates that the aggregation is controlled by surface charges on the ZnS crystallites and Debye screening by the electrolyte.

1) D.A. Weitz, J.S. Huang, M.Y. Lin and J. Sung, *Phys. Rev. Letters* 54, 1416 (1985).

A24

COUPLING INTERACTION OF COUETTE FLOW AND CRYSTAL MORPHOLOGIES IN BRIDGMAN GROWTH

Tao Huang, Yong Yang and Yaohe Zhou
Dept. of Materials Science and Engineering
Northwestern Polytechnical University, Xi'an, 710072, China

An experimental set-up has been developed recently for Bridgman growth of transparent organic crystals with a layered couette flow perpendicular to the growth direction in front of L/S interface at NPU, Xi'an, in order to study the effects of momentum transport on growth pattern portuberantly. A series of new phenomenon has been presented for the first time, which is focus on momentum transport effects on the evolution of interface pattern wavelength selection and roughness transition.

Extensive experimentation has also been carried out on nonfaceted, faceted and eutectic growth. The results are discussed with the presented computation of the coupling of heat and solute diffusion-convection transport and growth kinetics. These studies clearly underscore the importance of momentum transport on crystal growth in melt.

STUDIES OF FLUID FLOW IN CZOCHRALSKI SYSTEM

A25

K. Sankaranarayanan, J. Kumar and P. Ramasamy
Crystal Growth Centre, Anna University, Madras-600 025, India

Most of the bulk semiconductor single crystals are grown by Czochralski technique because of its technical superiority for growing large size crystals. In recent years much efforts have been devoted to understand the fluid flow behaviour in the melt growth system. In the present study the influence of the rotation rate and the diameter of the crystal and the height of the melt on the fluid visualization technique because of its simplicity and ease of understanding. From Ozoe et al [1] it is noted that the mixed (Natural and Forced) convection can be characterized by a relation between Grashof Number (Gr) and Reynolds number (Re) as Gr/Re^2 and it is independent of the kinematic viscosity. Kobayashi [2] observed that the flow in the crucible mainly depends on the Gr results lead to select silicone oil as the experimental liquid to model the GaAs melt in Czochralski system. Aluminum powder was used as traces to observe the flow pattern. Experiments were carried out for various crystal models having diameter 2.5, 3.75, 5 and 6.25 cm in a 9.75 cm diameter crucible. The modelling crucible was heated by means of three independent zones wound around it. The effect of the rotation rate and diameter of the crystal and height of the melt in the crucible on fluid flow are observed by illuminating the crucible using a slip shaped light beam. The flow patterns for various values of either the Re number or Gr number keeping the other constant are photographed. The observations revealed that the forced convection occupies the upper region of the crucible (i.e.) beneath the crystal when only the crystal is rotated. At higher values of Re number the whole crucible is occupied by forced convection: the flow rises from the bottom of the crucible to the crystal. The critical Re number for different diameter of the crystal and the rotation rate have been determined.

[1] H. Ozoe, K. Toh and T. Inoue, *J. Crystal Growth* 110 (1991) 472.
[2] N. Kobayashi, *J. Crystal Growth* 43 (1978) 357.

NUMERICAL SIMULATION OF CZOCHRALSKI GROWTH: BULK FLOW VERSUS THERMAL-CAPILLARY MODELS

A26

Q. Xiao and J.J. Derby
Department of Chemical Engineering and Materials Science
University of Minnesota, Minneapolis, MN 55455

A computational exercise to compute axisymmetric flows in an idealized model of Czochralski (CZ) crystal growth melts was put forth by Wheeler [1] at the First NATO Workshop on Computer Modelling in Crystal Growth from the Melt. We present results from this bulk-flow model obtained using finite element analysis and contrast them with results obtained from thermal-capillary models which include realistic interfacial geometries and boundary conditions [2,3]. Simulations are performed for small-scale CZ systems with thermophysical properties representative of silicon growth.

Limit points in the steady-state solutions are found with respect to crystal rotation for both models. Although the flow structures obtained for crystal and crucible rotation alone are qualitatively similar, flow intensities are markedly different. Even more dramatic differences are found for flows affected by buoyancy. These results quantify the strong effects of interfacial phenomena in CZ growth systems and illustrate the shortcomings of simple bulk-flow analyses.

[1] A.A. Wheeler, "Four test problems for the numerical simulation of flow in Czochralski crystal growth," *J. Crystal Growth* **102**, 691-695 (1990).
[2] P.A. Sackinger, R.A. Brown and J.J. Derby, "A finite element method for analysis of fluid flow, heat transfer and free interfaces in Czochralski crystal growth," *Inter. J. Numer. Meths. Fluids* 9(4), 453-492 (1989).
[3] J.J. Derby, L.J. Atherton and P.M. Gresho, "An integrated process model for the growth of oxide crystals by the Czochralski method," *J. Crystal Growth* **97**, 792-826 (1989).

A27

ON THE EFFECTS OF INTERNAL RADIATION ON CONVECTIVE FLOWS IN HIGH-TEMPERATURE MATERIALS PROCESSING SYSTEMS

J.J. Derby, S. Brandon and A.G. Salinger
Department of Chemical Engineering and Materials Science
University of Minnesota, Minneapolis, MN 55455

Radiation energy transfer is important in many of the high-temperature processes used to produce modern materials. The impact of radiative energy exchange among *surfaces* is universally recognized in high-temperature systems; however, the effect of *internal* radiation transport within participating solid and liquid phases is generally not well understood.

In this talk, we will address internal radiation heat transfer and convective flows in high-temperature fluid systems which have some degree of transparency to infrared radiation. We specifically analyze a model problem representative of the flow of a semitransparent crystal growth melt and flows encountered in molten glass processing - the Rayleigh-Bénard problem of axisymmetric, buoyancy-driven convection in a vertical cylinder heated from below which contains a fluid which is radiatively participating.

We present a Galerkin finite element method combined with computer-aided bifurcation analysis for the calculation of steady-state, axisymmetric fluid dynamics and heat transfer for these systems [1,2]. The nonlinear coupling of radiative energy transport with conduction and convection leads to interesting and often non-intuitive behavior. Accounting for internal radiation causes imperfections that eliminate the static state and alters the symmetry of the flow states. Flow connectivity is shown to be very different from the classical Rayleigh-Bénard system. We also address the validity of the Rosseland diffusion approximation for optically thick media. The optically-thick approximation is commonly employed for describing heat transfer and accompanying flows in molten glass and crystal growth melts; however, some results obtained using this assumption are shown to differ markedly from those computed using a rigorous analysis of radiative transport.

[1] S. Brandon and J.J. Derby, "Finite element methods for analysis of internal radiative heat transfer and solidification in a finite cylindrical enclosure," *Int. J. Numer. Meth. Heat & Fluid Flow*, submitted (1991).

[2] A.G. Salinger, S. Brandon, R. Aris, and J.J. Derby, "Multiple buoyancy-driven flows of a radiatively-participating fluid," *Proc. Roy. Soc. London*, submitted (1992).

A28

PHYSICAL SIMULATION OF HYDRODYNAMICS AND GROWTH OF SINGLE CRYSTALS FROM HIGH TEMPERATURE SOLUTIONS WITH USE OF FREE CONVECTION AND ACRT

*V.M. Masalov, G.A. Emel'chenko, V. Nikolov**
Institute of Solid State Physics Acad. Sci. USSR,
142432 Chernogolovka, Moscow District, USSR
*Institute of General and Inorganic Chemistry,
Bulgarian Academy of Sciences, 1040 Sofia, Bulgaria

The parameters of free convection in oxide systems have been studied by method of physical simulation. The condition of stationary flow of the melt for the case of the cylindrical crucible was determined in the form:

$$d/D < (4.89\text{-}nD)(1gGr)^{-1.23},$$

where Gr-Grashof criterium, d/D-the relation of crystal diameter to that of a crucible, $n = 0.024\ mm^{-1}$ ($d/D \le 0.7$; $D \le 90mm$; $Pr > 1$).

The dependence of the velocity of liquid motion on the physical and geometric system parameters was obtained.

The conditions of non-stationary flow of liquid under free convection in melts of oxide systems were investigated. The dependence of a period and amplitude of temperature oscillations values on the front of crystallization on the system parameters were determined.

The hydrodynamics and oscillation of temperature in single crystal growth from high-temperature solutions with use of accelerated crucible rotation technique were investigated. The dependence of shape and value of temperature oscillations in flux on the parameters of crucible rotation and temperature gradient were studied.

Single crystals of ferrogarnet and La_2CuO_4 have been grown using the free convection and forced convection (ACRT). The difference between the two types of convection for crystal growth is discussed.

NONLINEAR DYNAMICS NEAR CODIMENSION-TWO SINGULARITIES IN CELLULAR GROWTH BY DIRECTIONAL SOLIDIFICATION OF A BINARY ALLOY

A29

K. Tsiveriotis and R.A. Brown
Department of Chemical Engineering, Massachusetts Institute of Technology

Cambridge, MA 02139 Asymptotic and numerical analysis of cellular growth in directional solidification have revealed a wealth of nonlinear phenomena occurring after the onset of the instability of the planar melt/solid interface. Multiple steady and traveling wave states of the cellular microstructure share tip-splitting of a single cell as the dominant mechanism for changing the number of cells along a solidification front. We show that the tip-splitting phenomenon is a result of quadratic nonlinearities that lead to coupling between the dominant wavelength and the half-length resonant partner. The ubiquity of tip-splitting results because a quadratic term is the dominant nonlinearity near the onset of cellular solidification.

We use weakly nonlinear analysis to unfold the nonlinear dynamics of cellular solidification near these codimension-two bifurcation points. In addition we perform extensive steady and transient computations using a locally refined finite element method combined with a new domain mapping technique that allows the calculation of both shallow and deep solidification cells. As expected, calculations at small interface deformations agree with asymptotics in terms of predicting secondary bifurcations, Hopf points and oscillatory dynamics that can be described solely by interaction of the dominant wavelength and its resonant partner with half the wavelength. In addition, dynamic calculations at higher interface deflections reveal a new strongly nonlinear instability localized at the narrow bottoms of the solidification cells. This instability leads to oscillations of the cell bottom between shallow and deep-drop-shaped formations that are reminiscent of the drop shedding phenomenon observed in experiments. As the growth rate increases more cells appear in a given domain with bottoms oscillating out of phase leading to increasingly complex dynamics through a cascade of period doubling bifurcation. We postulate that large collections of cells are chaotic.

CALCULATIONS OF TRANSIENT PROCESSES WHEN PULLING SINGLE CRYSTALS WITH NONPLANAR INTERFACE

A30

V. Neeman (Nemenov)
Jerusalem College of Technology

The results are presented of mathematical simulation of transient processes occurring when pulling semiconductor and dielectric single crystals from the melt. The mathematical model of growth process is based on the solution of kinetic equations of heat and mass transfer for the case of intensive convection in the melt, the heat transfer serving as a moving force. The model proves most adequate for pulling large-size crystals using Czochralsky and Kyropoulos techniques [1]. The temperature, pulling rate, and crystallization front shape are considered as variables.

Calculation for typical crystallization front shapes and their evolution were made. The paper presents the results of calculations of crystal radius, crystallization rate kinetics and impurity segregation at different relaxation processes. The automatic control by crystal weight and melt level sensors, as well as the effect of heat and other conditions on the stability of growth are also analyzed. Proceeding from the calculation results, the requirements are discussed for the temperature and pulling rate control systems, as well as for the configurations of growth control.

A simplified mathematical model is realized as a dialog PC program that makes it possible, in each particular case, to quantitatively estimate the transient process parameters.

1. G.H. Nalbandyan, V. Nemenov. Transient Regimes in the Growth of Large-diameter Crystals. *Cryst. Res. Technol.* 23, 1988, 4, 577-581.

SESSION 2B

CRYSTAL GROWTH, OPTICAL PROPERTIES AND IONIC CONDUCTIVITY OF $KTiOAsO_4$ CRYSTALS*

B31

G.M. Loiacono, D.N. Loiacono and J.J. Zola
Crystal Associates Inc., 15 Industrial Park, Waldwick, NJ 07463

Crystals of $KTiOAsO_4$ were grown by the high temperature solution method and their optical and ionic conductivity properties evaluated. Large, multidomain crystals (23x28x45mm) were grown in the temperature range 960 to 800°C at rates of 0.5°/day. The band edge and IR cutoff were 370 and 4850nm respectively. A domain structure prevented frequency conversion in as grown crystals. The ionic conductivity at 22° (120KHz) is $1.5x10^{-8}$, $7.3x10^{-9}$ and $1.7x10^{-6}$ S/cm for the [100], [010] and [001] respectively.

FLUX GROWTH AND PROPERTIES OF RTA CRYSTALS

B32

Jianru Han, Yusheng Liu, Min Wang and Dezhen Nie
Institute of Crystal Materials
Shandong University, Jinan Shandong, P.R. China

RTA (formula: $RbTiOAsO_4$) is a new member of KTP crystal family. Recently, we have grown large RTA single crystals by using flux method. In this paper, we discuss the flux growth of RTA crystals and present the primary results obtained from the studies of its basic physical nonlinear optical and ferroelectric properties. The noncongruent melting nature of RTA crystals makes it possible to be grown by hydrothermal or flux techniques. RTA crystals can be grown by using flux method in a process similar to that of growing KTP. The starting materials are H_3AsO_4, TiO_2 and Rb_2CO_3. The mixture was put in platinum crucible and held for 24 hours at about 1000°C. A mixer was used to mix the melt. The crucible was then cooled to the saturation point which was detected by a RTA crystal seed. A good seed was hang in thee melt. Then, the melt was slowly cooled to about 800°C for 6 weeks. A complete crystal has obtained.

RTA crystal is the isomorphic of KTP, it belongs to the orthorhomic mm^2, space group is Pna2. Each unit cell contains 8 formular units. The lattice contances are a=13.2428A, b=10.7642A, c=6.6685A, respectively. The a, b, and c axes are perpendicular to one another. The b axis is the two-fold symmetry axis, whereas a and c are perpendicular to the symmetry planes. The structure of RTA is characterized by the chains of TiO_6 octahedra which are linked at the corners and the chains are separated by AsO_4 tetrahedra. There are two chains in one-unit cell, and the chains change alternately along (011) and (0$\bar{1}$1) directions. The alternation of results in a net-directed polarization and it is the major contribution to the large nonlinear optical coefficients of RTA crystal.

The transmission range of RTA is wider than that of KTP, which extends from 0.138μm to 5.1μm. The near infrared absorption is produced by the radicals of AsO_4 and TiO_6. The refractive indices are measured at several wavelengths in visible bands by using V-prism method. The relations between Na,Nb and Nc are Na<Nc<Nb and (Nc-Na) < (Nb-Nc).

We report the theory of second harmonic generation (SHG) in biaxial crystals. The limitations imposed by birefraction absorption and Gaussian beam on SHG efficiency are discussed in details. A complete theory of Maker fringe in biaxial crystals is introduced, which includes several corrections for making precise determinations of nonlinear coefficients. The experiments were performed using a Nd:YAG Laser and Maker fringes were obtained. In the experiments, KDP crystal was used as a reference sample. By fitting the theoretical overlaps with the experimental date, we obtained the coefficients: d31=3.55d36(KDP), d32=11.71d32(KDP), d33=31.05d36 (KDP), where d31 is smaller than of KTP, whereas d32 and d33 are larger than those of KTP. We also calculate the phase matching curve of RTA, which indicates that RTA crystals are type I phase matchable for 1,064μm SHG. The maximal effective nonlinear coefficient is 3.41d36(KDP). We have investigated the SHG conversion efficiency of RTP and the influences of various fact. The phase matching acceptance angle is 0.5° cm for 1.064μm type I SHG. The appropriate crystal thickness for maximal conversion efficiency is 0.5-1.5cm. The conversion efficiency reaches 42% when the center light intensity of incident Gaussian beam is 200MW/cm for L=0.65cm.

We have also measured the relative dielectric constants, dielectric loss and ac conductivity by using Model 4274A multi-frequency LRC meter. The results show that Ea and Ec are much smaller than Eb. RTA crystals are uniaxial ferroelectrics with spontaneous polarization along b axis. The dielectric anomaly was observed at about 832°C. The phase transition is of displaceable type and the symmetry is probably changed by Pnan to Pan21 phase transition. The result obtained from DTA reveals shows that the transition is a second order it. The conductivity along b axis is large and in a wide range of temperatures αT. This obeys an exponential law with an active energy W=0.736ev, A=3.8 K/ohm-cm, which are the values of ionic conductor. In the case of RTA crystal with large rubidium and arsenic cations, the conductivity is 3 order of magnitude lower than that of KTP. The dielectric loss of RTA is high (tan δ=0.5, f=10KHz at room temperature).

B33

GROWTH AND OPTICAL CHARACTERIZATION OF LARGE POTASSIUM TITANYL PHOSPHATE CRYSTALS

Takatomo Sasaki, Akio Miyamoto, Atsushi Yokotani and Sadao Nakai*
Faculty of Engineering and Institute of Engineering, Osaka University
*Kimura Metamelt Project, ERATO, JRDC

Potassium titanyl phosphate (KTP) crystals are very important optical nonlinear materials. We have succeeded to grow large KTP crystals which were over 90 mm in c-axis. We have investigated the optical inhomogeneities in the crystals. The crystals proved to have different refractive indecies for each growth sectors.

Crystal growth of KTP in the K_6 flux was performed in a platinum crucible with 150 mm diameter and 150 mm in height. The temperature reduction method was used and the saturation temperature of the starting solution was approximately 950°C. The rotation rate was 60 rpm. The weight of a crystal during growth was monitored by an electronic lord cell. It played a very important role to avoid liquid inclusion in a growing crystal. At the initial stage of growth, the temperature was reduced at 3°C/day. The growth rate was slow because the crystal was small and the solution was not enough stirred. After five to six days, the crystal weight suddenly increased and the crystal suffered inclusion. This is because the solution began to be well stirred by size effect of the growing crystal as well that the solution had a large supersaturation. By monitoring the crystal weight and reducing the temperature falling rate, we could obtained a good crystal without inclusion. The dynamics of solution stirring was also investigated by a simulation using silicone oil and dummy crystals with various sizes. The simulation gave the timing of the inclusion occurrence, which agreed well with the experiment.

The grown crystals were cut and polished for investigation of the inhomogeneities of the refractive index in the portion near the seed crystal. Figure shows a transmission interference pattern of a b-cut crystal ($45x12x4^t$ mm^3 in cxaxb axes) by He-Ne laser. We can see the large differences of the refractive indecies between growth sectors. These inhomogeneities in the crystal may be the cause of different data of the nonlinear optical coefficients and the phase matching angles reported by many peoples.

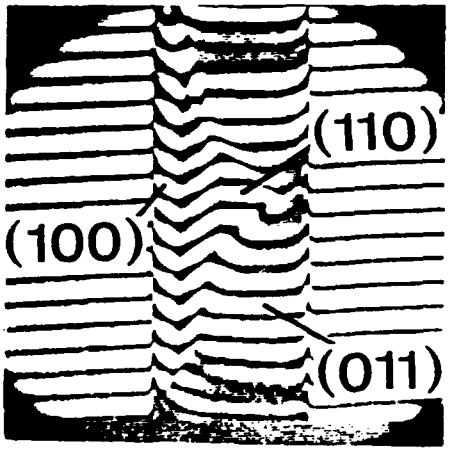

Intereference Pattern by He-Ne Laser

B34

CORRELATION OF THE STRUCTURE OF MELTS AND CRYSTALS OF ALKALI AND ALKALI-EARTH BORATES: THE CRYSTALLIZATIONBEHAVIOR OF BARIUM METABORATE

Yu.K. Voronko, A.V. Gorbachev, V.V. Osiko and A.A. Sohol
General Physics Institute, Russian Academy of Sciences, Moscow, USSR
R.S. Feigelson and R.K. Route
Center for Materials Research, Stanford University, Stanford, CA 94305-4045

The alkali and alkali-earth borates, LiB3O5 and β-BaB_2O_4 have important applications in nonlinear optics. In this investigation, the structure of boron-oxygen groups in borate melts was studied for the first time using a high temperature Raman spectroscopy (HTRS) method. The Raman spectra for different anions made up of $[BO_3]$ groups were identified. These included isolated [BO3] triangles, pyroborate anins $[B_2O_5]$, chain anions $[BO_3]n$ and isolated $[B_3O_6]$-ring metaborate units. This identification was carried out by comparing the Raman spectra of melts with those of crystals having known boron-oxygen structural elements, and also from theoretical calculations using several models of boron-oxygen groups.

$[B_3O_6]$-rings were detected in MBO_2 (M=K,Cs) metaborate melts at temperatures near their melting points. With increasing melt temperature, the rings were found to convert into three-membered $[BO_2]_3$ chains. $[B_3O_6]$-rings were also fund in $NaBO_2$ and BaB_2O_4 melts, but themelts were dominated by three-member and longer chains which were found in increasing numbers at higher temperatures. (In contrast to melts which are formed primarily of these planar rings and chains, borate glasses at low temperature were fund to contain $[BO_4]$ tetrahedral groups. These tetrahedral groups disappeared when the glasses were heated above their meling points.)

Using the HTRS method, the spontaneous crystallization of $[MBO_2]$ (M=Na,Cs) and BaB_2O_4 metaborate melts was investigated "in-situ." It was found that spontaneous crystallization of these phases occurred only when there was a sufficient quantity of $[B_3O_6]$-ring units in the melt. $CsBO_2$ melts, which consist almost entirely of $[B_3O_6]$-rings at the melting temperature, wre found to crystallize spontaneously without significant undercooling. BaB_2O_4 melts, which are cominated by $(BO_2)_n$ chains at the melting point, did not spontaneously crystallize until they had been undercooled by 150°-200°C, where appreciable numbers of $[B_3O_6]$-rings were detected.

B35

STUDY ON GROWTH OF LITHIUM TRIBORATE CRYSTALS

D.Y. Tang, W.R. Zeng, X. Lin, J.G. Wang, Q.L. Zhao and Q.G. Tan
Fujian Institute of Research on the Structure of Matter
Academia Sinica, Fuzhou 350002, P.R. China

Lithium triborate (LBO) is a new and important nonlinear optical crystal. It has already been used to SHG and THG of the high power Nd:YAG Laser. LBO is a compound of incongruent melting point. The method that we can choose is only the more complicated flux growth technique. A broad range of fluxes which contain B_2O_3, PbO, PbF_2 and alkali halides etc. has been therefore attempted in our Lab. in order to grow large high quality LBO crystals. Most of them seem unfavorable to the growth of LBO crystals, and PbO and PbF_2 also have to be excluded from our considerations although these additives can reduce the viscosity of the growth solution and enhance growth rate, since Pb^{2+} ion can easily enter into the crystal lattice and may cause the shatter of crystal thereby. According to our experimental results, an appropriate amount of excessive B_2O_3 seems to be a suitable flux. Our experiments show that there are two crystalline phase LiB_3O_5 and $Li_3B_7O_{12}$ as $Li_2O:B_2O_3$=1:3.5 mol. However, as $Li_2O:B_2O_3$=1:4 mol, obtained crystal is only LiB_3O_5. High optical quality single crystals with dimensions up to 65x65x17 mm^3 have been obtained in this flux system using top-seeded method. We also find that it seems favorable to LBO growth when a small amount LiF adding to the solution.

Other problems, such as crack, parasitic crystals and cover on the surface of growing crystal have also been encountered in our experiments. The crack is more easily happened along [100] or [001] direction. This is caused by the anisotropic character of the thermal expansion. The thermal expansion of LBO crystal has been measured experimentally. The formation of parasitic crystals is related to the solution stability and network structure on the face of the crystal. Parasitic crystals are attached more easily to (110) and (100) faces which network density is higher. These two problems can be solved to some extent by orientational growth. The X-ray powder diffraction pattern and chemical element analysis indicated that the white cover is a compound of $3Li_2O{\cdot}7B_2O_3$, which may weaken the seed strength and also obscure the observation on crystal growth. The possible approaches of forming and overcoming this cover are discussed. Finally, it has been reported that the particular inclusions of the negative-crystal structure in LBO crystals are observed by X-ray projection topograph and light scattering tomograph. The formation of the defects is also due to the compositional supercooling of melt caused by the larger fluctuation of the growth temperature.

B36

A STUDY OF STRAIN IN $KH_{2(1-x)}D_{2x}PO_4$ (DKDP)

J.J. DeYoreo, B. Woods, C. Ebbers and S. Mayhugh
Lawrence Livermore National Laboratory
P.O. Box 808, Livermore, CA 94550

Crystals of $KH_{2(1-x)}D_{2x}PO_4$ are used in a number of optical devices. At Lawrence Livermore National Laboratory advanced designs for the Nova laser system require large aperture, (~32 x 32 cm^2), z-cut plates of highly deuterated DKDP for use in an electro-optic switch. The presence of strain in these crystals generates refractive index variations through the stress-optic effect which result in depolarization losses and phase-front distortion during switch operation. We analyze the combined stress-optic and electro-optic effect in z-cut plates of DKDP and show that while the average shift in refractive index and resulting phase-front distortion are controlled by normal strains in the crystal, the induced birefringence and resulting depolarization losses are determined by the shear strain in the x-y plane. We show that, in both cases, the critical range of stress for practical application is 10^5 to 10^6 Pa which results in a birefringence and wavefront distortion of 14 to 140 nm/cm and 0.08 to 0.80 λ respectively. We also present spatial profiles of the birefringence and phase front distortion measured on 5 x 5 cm^2 to 32 x 32 cm^2 plates of DKDP using polarimetry and interferometry. Our results delineate patterns of strain in the crystals which are correlated with the pyramidal growth habit. They also show that the maximum internal stresses lie within the critical range specified above. We also present the results of high resolution x-ray topography which we have used both to profile the strain in the crystals and to map out variations in lattice parameters. We attempt to relate these variations to spatial inhomogeneities in hydrogen content. Finally, we present thermodynamic and structural arguments which suggest that these variations are caused by changes in hydrogen segregation due to fluctuations in growth parameters and become larger as the overall H content in the solution decreases. These results suggest that the growth of large-sized, low-strain DKDP requires either precise control of growth parameters or very slow growth rates.

VISCOSITY MEASUREMENT OF MOLTEN $LiNbO_3$ BY OSCILLATION DAMPING METHOD

B37

K. Shigematsu, Y. Anzai and S. Kimura
KIMURA METAMELT Project, ERATO, JRDC
Tsukuba Research Consortium, Tokodai 5-9-9, Tsukuba, Ibaraki 300-26, Japan

The viscosity of $LiNbO_3$ was successfully measured by the oscillation damping method which was adapted to the liquid of the viscosity less than 10 mPa s. The melt viscosity of oxide single crystals for industrial use (contains $LiNbO_3$) occupies the region of a few 10 mPa s. This report deals with the modified viscosity measurement technique and the effect of the oxygen atmosphere to this material. We newly designed a sample container which had large size and three-layered structure (Fig. 1). The viscometer (Tokyo Industries Co.) was used for this study (Fig. 2). The sample container and a momentum disk were suspended in a vacuum furnace using a tungsten wire. After supplying needful angular momentum for the container, the attenuation of the oscillation of the container was measured optically using the reflection of laser light. The viscosity was calculated from the attenuation using Roscoe's equation.

The viscosity of MgO doped $LiNbO_3$ of congruent composition is shown in Fig. 3. MgO doping lowers slightly the viscosity. The absolute values were, however, drastically lowered (1/2--1/4) compared with the values previously reported. This drastic decrease could be attributed to non-oxygen atmosphere which was brought about by vacuum pumping and the outside container made of graphite. The $LiNbO_3$ after the measurement indeed changed into black color, which showed the oxygen defects in solidified $LiNbO_3$. We thus conclude that the uniform dispersion of dopant and the uniform liquid structure are realized easily under non-oxygen atmosphere.

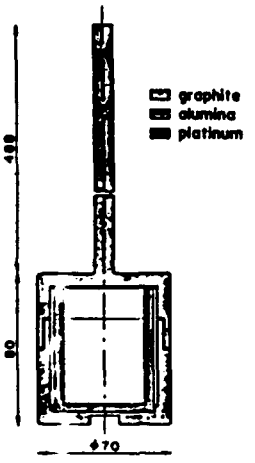

Figure 1. A cross-sectional view of the sample container.

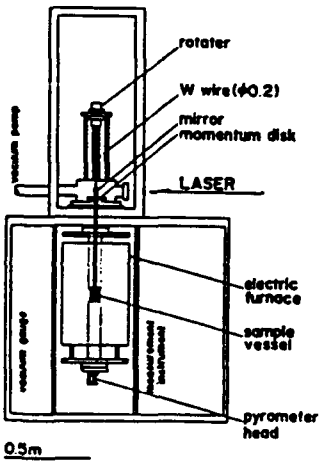

Figure 2. A schematic drawing of the viscometer.

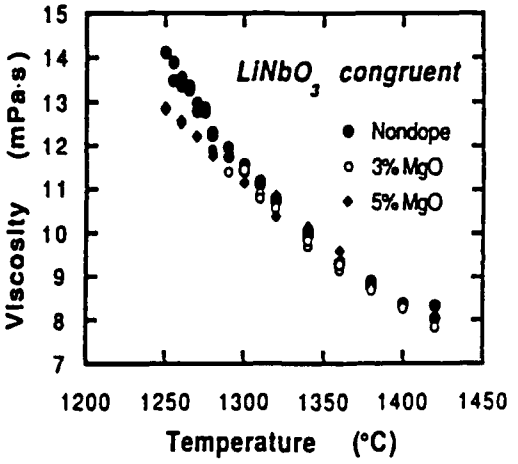

Figure 3. The temperature dependences of the viscosity of $LiNbO_3$ doped MgO.

B38

GROWTH AND CHARACTERIZATION OF SCANDIUM-DOPED $LiNbO_3$

Joyce K. Yamamoto, Kenji Kitamura, Nobuo Iyi and Shigeyuki Kimura*
National Institute for Research in Inorganic Materials, 1-1 Namiki, Tsukuba, Ibaragi, 305 Japan
Yasunori Furukawa and Masazumi Sato
Hitachi Metals, Ltd., 5200 Mikajiri, Kumagaya, Saitama, 360 Japan

The growth of scandium-doped $LiNbO_3$ was achieved using the float zone method to investigate the influence of scandium doping on the optical properties. Scandium was added at a concentration of 1 mole% to the congruent $LiNbO_3$ composition. Growth proceeded from a sintered ceramic feedrod to a c-axis oriented undoped $LiNbO_3$ single crystal seed. The seed and feedrod were rotated at 30 rpm in opposite directions. The melt suspender was approximately in the center of the molten zone, slightly closer to the feedrod. The choice of the size of the holes in the melt suspender was important. Smaller holes did not permit sufficient melt flow through the suspender making growth difficult.

The resulting crystal was clear and transparent. The scandium concentration was estimated to be approximately 0.5 mole%, from a comparison of the lattice parameter and ferroelectric transition temperature results of the grown crystal relative to powder data. Optical absorption measurements revealed that the absorption edge of the $LiNbO_3$:Sc was shifted to 310 nm. This is comparable to the effect of a 5 mole% MgO doped $LiNbO_3$ crystal. Experiments into the optical damage resistance of the $LiNbO_3$:Sc crystal indicate that the resistance level is not reduced relative to the undoped crystal.

These results indicate that the growth of scandium-doped congruent $LiNbO_3$ resulted in good quality crystals. The relatively low scandium addition induced a favorable shift in the absorption edge and did not deleteriously affect the optical damage resistance.

*Present address: Mitsui Mining and Smelting Co. Ltd., 1333-2 Haraichi. Ageo, Saitama, 361 Japan

---

B39

COMPOSITIONAL UNIFORMITY IN CZOCHRALSKI GROWN $LiTaO_3$ SINGLE CRYSTALS

D.S. Chung, B.H. Park and Y.S. Kim
Ceramic Materials Division, Research Institute of Industrial Science & Technology (RIST)
P.O. Box 135, Pohang 790-600, Korea

$LiTaO_3$ single crystals are well known for industrial applications. Much attempts have been made in growing perfect single crystals from incongruent melting compositons such as Li_2O-Ta_2O_5, Li_2O-Nb_2O_5 and SBN. To determine congruent melt composition in Li_2O-Ta_2O_5 system, single crystals were grown in various melt composition. Vertical and Lateral compositional uniformity in the crystals investigated by measuring Curie Temperature (Tc) using Differential Thermal Analysis technique.

B40

THE MORPHOLOGY OF β-BaB_2O_4

Zhong Weizhuo, Hong Huicong, Lu Zhiping, Zhang Tiande and Hua Sukun
Shanghai Institute of Ceramics, Chinese Academy of Science
1295 Ding Xi Road, Shanghai 200050, China

In this paper we have investigated the crystallization habit and the growth defects in the β-BaB_2O_4 crystals grown by the temperature gradient method at the constant temperature from the flux. The positive polar face$(000\bar{1})$ and the negative polar face$(000\bar{1})$ are used as the seeding faces of the seed crystals respectively. The growth faces are positive rhombic faces $R\{10\bar{1}2\}$, negative rhombic faces $r\{01\bar{1}4\}$, rhombohedral faces $S\{11\bar{2}2\}$, hexagonal prism face $s\{11\bar{2}0\}$ and trigonal prism faces $m_1\{10\bar{1}0\}$, $m_2\{01\bar{1}0\}$ and singular faces$\{0001\}$ and $\{000\bar{1}\}$. Among them R and r faces are more developed and the growth forms have a trigonal feature. If the seed crystal has $\{0001\}$ orientation, we find larger R faces and the $\{10\bar{1}0\}$ faces have the distribution of hexagonal symmetry and a kind of shape of long strip. The a $\{11\bar{2}0\}$ faces are smooth and $m_1\{10\bar{1}0\}$, $m_2\{01\bar{1}0\}$faces are small. Below the positive rhombic faces $R\{10\bar{1}2\}$, the growth ridge which is the growth trace of R face and similar to the case of $LiNbO_3$ are found.

The different forms of the crystals grown along different seed orientations are compared and the relative growth rates of different groups of faces are deduced. We have plotted the β-BBO crystal morphology and its stereographic projection. According to the crystal form and the physical properties of the crystal, we reach the conclusion that β-BBO crystal belongs to the point group of C_{3v}-3m, not the point group of C_3-3.

GROWTH AND DIELECTRIC STUDY ON $KTa_{1-x}Nb_xO_3$

B41

R. Ilangovan, S. Balakumar, C. Subramanian and P. Ramasamy
Crystal Growth Centre, Anna University, Madras-25, India

Potassium Tantalate Niobate (KTN) is one of the most interesting members of the ferroelectric solid solution system. KTN crystal will be paraelectric and cubic if $x < 0.39$ while it will be ferroelectric if $x > 0.39$.

Single crystals of Potassium tantalate niobate have been grown by slow cooling technique with composition $x = 0.7$. The starting materials Nb_2O_5, Ta_2O_5 and K_2CO_3 were taken in the 20 CC platinum crucible in the ratio of 40:60 mol%. The charge was melted and then held at the temperature 1210°C for 20 hours to achieve complete homogeneity of the melt. The temperature of the melt was reduced to 1185°C at the rate of 2°C/h. In order to minimize changes in the ratio of tantalum to niobium, the charge was maintained for more than one hour at same temperature. Again the charge was cooled to 1050°C at the rate of 2°C/h. Further it was cooled to 850°C at the rate of 20°C/h and then to room temperature at a faster rate. In the platinum crucible at the top of the frozen melt 12mm x 6mm x 3mm size transparent KTN crystal was obtained [fig. 1]. The grown crystal is easily cleavable as thin platelets. The grown crystal was confirmed by x-ray powder diffractogram and single crystalline nature was checked by Laue pattern. The concentration of niobium and tantalum atoms present in the crystal was analysed by EPMA.

Dielectric constant and tan δ were found over a range of frequency at room temperature [fig. 2]. These measurements were made on small single crystals of a size 5 x 8 x .5mm^3. Large change is dielectric constant and loss tan δ were observed.

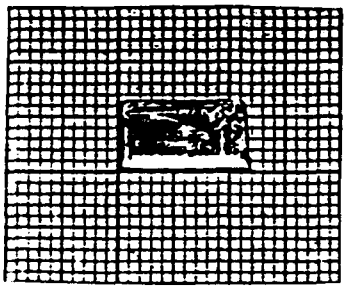

Figure 1.

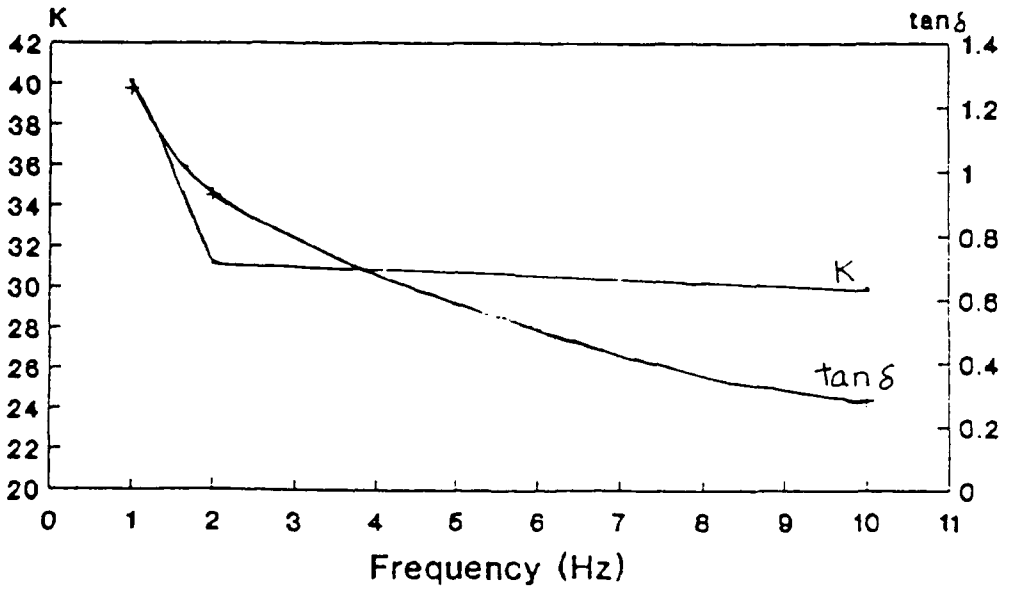

Figure 2.

B42

GROWTH AND PYROLUMINESCENCE IN PURE AND Sm DOPED KNbO3 SINGLE CRYSTALS

P.D. Durugkar
Dept. of Physics, Hislop College, Nagpur, India

Pure and Sm doped KNbO3 were grown by controlled cooling of the melt. For growth K2Co3: Nb2O5 were taken in the molar ratio 1.2:1.0. 1 wt% Sm and 2 wt% Sm were the two doping concentrations for growth of doped KNbO3.

Pyroelectroluminescence (PEL) has been observed in microcrystalline powders of pure & Sm doped KNbO3 single crystals. The glow peak temperatures matches with the Temperatures reported in Pyroelectric study. The role of Sm for enhanced luminescence is under investigation.

B43

APPLY A NOVEL TECHNIQUE TO GROW BTO AND KTN CRYSTAL

Ma Xiaoshan, Zhang Shunxing, Hu Wenge, Zhao Zhiwei and Zhang Xinyu
Shanghai Institute of Optics and Fine Mechanics, PRC
Wang Jiyang and Guan Qengcai
Shandong University, PRC

In this paper, the three thermal zone solute transport flux method (similar to the hydrothermal method in some extent) will be introduced at the first time. The three thermal zones are settled as follows for this technique: the bottom hot zone (C zone) is saturated with Nutrent, the middle zone (B zone) is the hottest zone, in B zone micro-crystal embryos disolve, the top cold zone is supersaturated with solute at which the crystal grows. The solute diffuse from C zone to B zone and transport to A zone by convection. It is well known that convection transport is much quicker than the diffusion process. So change the distance between B and C zones it is very easily to control the total transport rate, and also the crystal growing rate. We apply this technique to grow $BaTiO_3$ and KTN some results are as follows: a) crystals can be grown without descending temperature, b) the pulling can up to 3mm per day and 5mm per day for BTO and KTN respectively, c) the quality of crystals grown by this technique is good though the temperature control equipment is not satisfactory.

B44

PREPARATION AND CHARACTERIZATION OF LEAD ZIRCONATE TITANATE THIN FILMS BY SOL-GEL PROCESSES

F. Leccabue, B.E. Watts, R. Panizzieri, E. Meilioli and D. Carillo
Instituto MASPEC/CNR, Via Chiavari 18/a, 43100 Parma, Italia

Ferroelectrics have recently undergone a renewed interest due to the wide range of properties which can be conveniently exploited in the form of thin films. As pyroelectrics and piezoelectrics they can be integrated into silicon technology and their ferroelectricity can be used at voltages compatible with integrated circuits. Different techniques are being employed to make these films, such as sputtering, laser ablation, however sol-gel methods are a useful and inexpensive route for making films of good quality over large areas.

In this work lead titanate (PT) and lead zirconate titanate (PZT) thin films were made from sols spun onto (100) silicon and sputtered platinum substrates. Two types of heat treatment were used to form the ceramic; a normal heat treatment where the sample is heated and cooled within the furnace and a rapid thermal process where the sample, by moving it in and out of the furnace, is subjected to heating rates of about 100 K/min. The latter method gives specular, crack free films but the stresses induced by the rapid temperature changes led to defects at the substrate interface. Profilometry and electron microscopy confirm the homogeneity of the thickness.

In addition the crystallization mechanism was studied using DTA, TGA, X-ray diffraction and infra-red spectroscopy. The results show that sol-gel techniques crystallize ceramics at low temperatures, compatible with semiconductor technology but the mechanisms of crystallization of bulk and thin film gels differ.

C-V measurements and dielectric hysteresis curves were recorded as a function of heat treatment and also compared for the two different heating methods.

B45

DOMAIN AND INTERNAL STRESS ANALYSIS OF $BaTiO_3$ BY EXTERNAL STRESS

B.W. Lee and K.K. Orr
Department of Inorganic Materials Engineering, College of Engineering
Hanyang University, Seoul 133-791, Korea

Domain configuration and internal stress of $BaTiO_3$ ceramic were investigated by the abrasion and one-dimensional pressure as external stress. The effect of grain size (1 to 40μm) on the dielectric constant and phase transition was also studied.

With the decrease in grain size the transition temperature and the heat of transition decreased, and the x-ray analysis indicated that the tetragonality of fine grained (=1μm) $BaTiO_3$ lowered from 1.01 to 1.009. One-dimensional pressure produced a transient 90° domain switching and induced a resultant tension, and worked differently on the sintered specimen with the grain size variation. The 90° domain switching was observed by the abrasion of sintered surface having all the range of grain size, which switching was closely connected with the plastic deformation and not related to the grain and abrasion media size.

These experimental results show that the internal stress of fine grained $BaTiO_3$ is a compression and the high dielectric constant of this fine grained $BaTiO_3$ is resulted from the 90° domain wall and the internal stress contribution within 90° domains not from the internal stress (tension) by the absence of 90° domains. It is proposed that the decreasing in dielectric constant of the fine grained $BaTiO_3$ with one-dimensional pressure arise from the difficulty of domain wall motion due to the pinning of domain walls by the grain boundary.

B46

STUDIES ON GROWTH KINETICS OF $BaTiO_3$ AND $Ba_{1-x}Ca_xTiO_3$

S. Balakumar, R. Ilangovan, C. Subramanian and P. Ramasamy
Crystal Growth Centre, Anna University, Madras-25, India

Single crystals of $BaTiO_3$ are obtained by spontaneous nucleation technique using KF flux. In this paper we report the growth of cubic crystals of $BaTiO_3$ with soaking period more than 30 hours and growth of Ca substituted $BaTiO_3$ with 4-10 hours soaking period. The growth mechanism was discussed for the both systems.

Usually butterfly twins of $BaTiO_3$ are obtained from the above technique with 4-12 hours soaking period at 1200°C. Only platelets were obtained for above 15-20 hours. Above 24 hours twin formation were reduced and cubic crystals were obtained.

By increasing the soaking period to 30-35 hours we got cubic crystals with Hopper morphology for the first time. The SEM photograph indicated the growth kinetics of such crystals (Fig 1). Since the wall of the crucible was the nucleation site, the crystals grown on them couldn't be separated out easily (Fig. 2). Crystals were reddish colour because of more flux inclusions.

The addition of Calcium as dopant reduced the twin formation. $Ba_{1-x}Ca_xTiO_3$ crystals were grown with different calcium concentration such as x=0.04, 0.08, 0.12, 0.16 and 0.24. For the calcium concentration x=0.16 and above with less soaking period (8-10 hours) we got good transparent reddish colour cubic (5mm x 5mm x 3mm) crystals. The crystals were characterised by DTA, SEM, EPMA and XRD. Dielectric, Hardness and etching studies are also made.

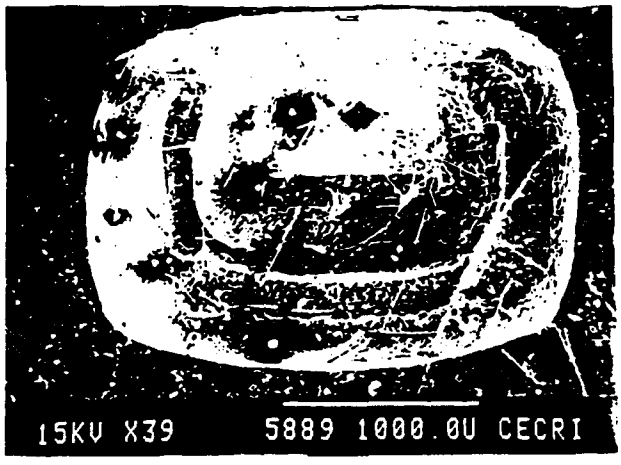

Figure 1

Figure 2

GROWTH AND HABIT MODIFICATION STUDIES IN $NaClO_3$ CRYSTALS

B47

K. Kishsan Rao and V. Surender
Department of Physics, Kakatiya University, Warangal-506 009 India

$NaClO_3$ crystals are optically active and piezoelectric. Hence there is a need for growing crystals of good quality with specific morphology. These crystals grow in cubic form whereas its isomorphous $NaBrO_3$ crystals grow in tetrahedral form. It is known that the habit of $NaClO_3$ is modified in the presence of some impurities. In the present work, a systematic study of effect of presence of borax as impurity on the morphology of $NaClO_3$ crystals is investigated. It has been observed that $NaClO_3$ crystals grow in tetrahedral form when 6% by wt. of borax is present in the solution. For lower concentrations of borax, crystals with different habits are obtained. The faces are identified using X-ray and etching studies. Spectral and microhardness studies on these crystals fail to reveal the presence of borax in the crystals.

As a further study on the role of borax on the habit of $NaClO_3$ crystals, crystals of $NaClO_3$ with (100) faces are placed on the bottom of the jars containing the saturated solution of $NaClO_3$ with different concentrations of borax. The crystals collected in the first phase are called as crop I. The solutions are further allowed to evaporate and subsequently crop II and crop III crystals are collected. It is interesting to note that some crystals with (111) faces are obtained even in the solutions containing lower concentrations of borax. The implications of these studies are discussed. Also the surface features of these crystals are studied.

DEVELOPMENT OF (KBr-KCl)(OH^-):$(F_2^+)_H$ COLOR CENTER LASER CRYSTAL SERIES AND THEIR SPECTRAL CHARACTERISTICS

B48

Xu Chenghuang, Huang Changcang, Qiu Jizhan and Wu Jihuan
Institute of Material Physical Chemistry,
Hua Qiao University, Quanzhou, Fujian, PRC

Among alkali halide crystals, $(F_2^+)_H$ color centre develops rapidly due to its excellent laser activity.[1] However, the limiteness of alternative single host material confines its development and wider application. In this connection, the authors present a (KBr-KCl)(OH^-):$(F_2^+)_H$ color centre laser crystal series,[2] and succeed in preparing them. The report centers on: 1) theoretical basis for selecting complex host system; 2) crystal growth of (KBr-KCl)(OH^-) crystal series and formation of $(F_2^+)_H$ color centers; 3) spectral characteristics of (KBr-KCl) (OH^-): $(F_2^+)_H$ (see Table 1).

The above results indicate that the laser crystal material of complex host color centre are able to regulate and broaden the tunable laser spectrum in very wide wave-length range. For example, (80% KBr-20%KCl) (OH):$(F_2^+)_H$ has an absorption peak regulating from 1.58 μm of KBr(OH^-):$(F_2^+)_H$ (a proper pump can hardly be found) to 1.38 μm (YAG or YAP may be chosen as pump), while it has an emission spectrum as shown in Fig. 1.

The emission spectrum of the complex exceeds that of the addition of single components. Evidently, the study of complex host color centre crystal will open a new field for the study of color centre laser.

Table 1

KCl%	absorption peak of			emission peak of		
(melt)	F band (μm)	$(F_2^+)_H$ I	(μm) II	$(F_2^+)_H$ I	(μm) II	(μm) III
	0.600	1.53	1.58	/	/	/
10	0.590	1.34	1.41	1.75	1.89	2.00
20	0.588	1.30	1.38	1.71	1.82	1.92
45	0.582	1.28	1.28	1.69	1.78	1.90
80	0.570	1.37	1.37	1.67	1.78	1.90
100	0.560	1.45	1.38	/	/	/

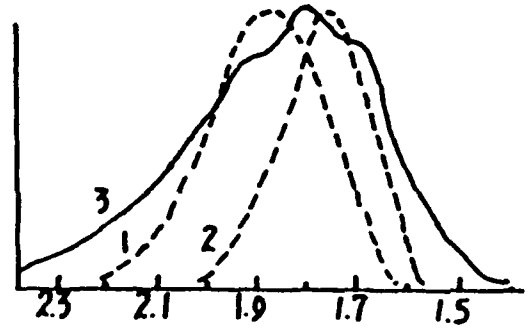

Figure 1. Relation between emission spectrum of $(F_2^+)_H$ and its composition 1) Kbr:(OH^-); 2) KCl: (OH^-); 3) (80% KBr-20% KCl): (OH^-), with wavelength as the ordinate and relative intensity as the abscissa.

1) W. Gellermann, *J. Phys. Chem. Solid*, 52, 1 (1991) 249.
2) Xu Chenghuang, et al, *J. Synth. Crystal*, 20, 3-4 (1991) 378.

B49

SEVERAL KEY PROBLEMS IN THE PREPARATION OF NaCl(OH^-):$(F_2^+)_H$ LASER CRYSTAL

Wu Jihuan, Xi Chenghuang, Qiu Jizhan and Lin Bizhou
Institute of Material Physical Chemistry
Hua Qiao University, Quanzhou, Fujian, PRC

The discovery of HaCl(OH^-):$(F_2^+)_H$ color centre crystal and its laser operation and applications are important progress of color centre crystal research in the recent years. For promoting the output power and the stability of color centre laser, the authors make a study on several key problems in the preparation of NaCl(OH^-):$(F_2^+)_H$ color centre laser: Some satisfactory results are obtained as follows:

1) The formation of $(F_2^+)_H$(color centre in NaCl crystal requires a trace of OH^- in ppm. On the other hand, some other trace impurity ions will affect the formation of $(F_2^+)_H$. These impurity ions as well as OH^- doped inadvertently are rejected by means of recrystallization, RAP method, and growth in tightly sealed vessel. By controlling proper amount of OH^- doping and the condition of crystal growth, a desirable NaCl(OH^-) crystal will surely be grown.

2) The formation of $(F_2^+)_H$ centre has to pass through the processes of coloration, heat treatment and conversion. In each process there occur simultaneously a lot of reaction of defect chemistry. By studying the relations between the state of $(F_2^+)_H$ centre and the conditions of defect chemical reaction in each process of its formation, the authors have ascertained the conditions for preparing a better $(F_2^+)_H$ centre in a higher concentration and purity.

3) In addition to $(F_2^+)_H$ centre, there are also non lasing centres. The effect and influence of them in laser operation are ascertained by laser experiment. On this basis, the authors increase the output power of NaCl(OH^-):$(F_2^+)_H$ by improving the conditions for the formation of color centre and eliminating unfavourable influence of non lasing centres.

1) Wu Jihuan, Xu Chenghuang, et al, *J. Synthetic Crystal*, 20, 34(1991)364.
2) Wu Jihuan, Xu Chenghuang, et al, *J. Hu Qiao University*, 11,3(1990)992.

B50

INFRARED CONTINUOUS WAVELENGTH TUNABLE KCl(Na^+, OH):$(F_2^+)_H$ COLOR CENTRE LASER CRYSTAL

Chen Guangfu, Xu Chenghuang, Qiu Jizhan, Huang Miaoliang and Lin Bizhou
Institute of Material Physical Chemistry
Hua Qiao University, Quanzhou, Fujian, PRC

F_2^+-like type color centre laser is an important object of color centre laser at present.

D. Wandt, et al reported in 1987[1] the obtaining of $(F_2^+)_{AH}$ centre in KCl crystal by O_2^- doping, and pointed out that it is ineffective to obtain $(F_2^+)_H$ or $(F_2^+)_{AH}$ by doping OH^- into KCl host crystal. On the basis of basic physicochemical principle of defect, as well as the analysis and comparison of the similarities and dissimilarities of O_2^- doping and OH^- doping the authors confirm experimentally the possibility of obtaining $(F_2^+)_H$ centre and implement the operation of KCl(Na+,OH^-) $(F_2^+)_{AH}$ color centre laser. The results center on:

1) The KCl(Na^+, OH^-) crystal effectively grown and properly passed through coloration, heat treatment, and conversion in our laboratory reveals its main spectral characteristics in conformity basically to the results from O_2^- doping by D. Wandt, et al. Consequently, the authors cannot agree D. Wandt's opinion on the impossible decomposition of OH^{-+} ion in KCl crystal.

2) Our KCl(Na^+, OH^-) crystal has passed through laser experiment in X-cavity designed by us with 1.34 μm linear pump of YAP laser and 514.5 nm line of Ar^+ laser as auxiliary light. The authors obtain for the first time the $(F_2^+)_{AH}$ color centre laser of that crystal, the laser of which sows a peak wavelength at 1.88 μm.

1) D. Wandt, et al, *Opt. Comm.*, 61(1987) 405.
2) Xu Chenghuang, *J. Hua Qiao Univ.*, 11(1990)209.

B51

GROWTH AND PERFECTION OF CHROMIUM DOPED FORSTERITE

Hu Bing, Zhu Hongbin and Deng Peizhen
Shanghai Institute of Optics and Fine Mechanics, Academia Sinica
P.O. Box 800-216, Shanghai 201800, P.R.China

Chromium doped forsterite, a newly developed phonon-terminated laser crystal with tuning range from 1167 to 1345nm, has drawn much attention in recent years. As a laser host crystal, perfection of the crystal is an important factor to laser performance. To improve the quality of crystal, the efforts in crystal growth and in studies of defects were being made in our laboratory in last three years.

The crystals were grown by CZ method with use of rf-heating and Ir crucible at different atmosphere. The stoichiometric composition of the charge was used for crystal growth at first, and the impurity of Cr in charge was 0.05-0.15wt%. The crystals grown along different orientations exhibit different crystallographic habits. The segregation coefficient of Cr in crystals was measured to be about 0.15. Absorption spectra show that the concentration of Cr^{4+} in the crystals grown in oxiding atmosphere are higher than that grown in nitrogen.

The perfection of the crystal was investigated by means of etching, electron probe, optical microscope and X-ray topography. The typical defects in crystals were inclusions, mosaic structures and dislocations. It was found that inclusions are mainly around the core. The electron probe analysis showed that inclusions were rich in SiO_2. To reveal the distribution and density of the dislocation, a optimum etchant, molten NaOH, was picked out from several etchants, and the polish and etching conditions were developed. Two different types of dislocations were found in the crystal. One is extended along the growth direction and the other is net-work like. The formation of mosaic structure was found to have some relations to both growth direction and pulling rate. Base on the studies of defects, some growth parameters were adjusted with respect to [100] and [001] growth directions. A serial compositions of charge with 0.03-0.15w% excess of MgO over stoichiometry were tried in crystal growth and one of them was adopted in the following experiments. As a result, the inclusions and mosaic structures were successfully reduced and more perfect crystal boules with 25mm in diameter and 80mm in length were obtained.

B52

CRYSTAL GROWTH AND OPTICAL PROPERTIES OF Cr:Mg_2SiO_4

Liu Lin, Wang Zulun, Li Shengjun and Jiang Yandao
Institute of Physics, Chinese Academy of Sciences
100080, Beijing, China

The chromium-doped forsterite crystal (Cr:Mg_2SiO_4) is an attractive tunable laser crystal. Laser action in the range of 1130-1345 nm has already been demonstrated by some authors. In this work the investigation on growth and optical properties of the crystal are reported. The fluorescence spectral shape is sensitive to the oxygen content in growth atmosphere. The ratio of the fluorescence intensity peaked at 920 nm to that peaked at 1120 nm can be controlled by growth atmosphere. The absorption spectra can also be controlled by post-heat treatment. This is favorable to reduce the excited state absorption which is the main problem for the application of the crystal in wide wavelength range.

LASER INDUCED DAMAGE IN SAPPHIRE AND Ti:SAPPHIRE CRYSTALS

B53

Fuxi Gan, Qiang Zhang and Jinwen Qiao
Shanghai Institute of Optics and Fine Mechanics
P.O.Box 800-211, Shanghai 201800, P.R.China

Laser induced damage in crystals can be classified as surface damage and bulk damage. The mechanism of surface damage in optical crystals has been analyzed. The recent experimental results of laser induced damage in sapphire and Ti:sapphire were reported. The new methods of chemical etching and ion polishing for improving the damage threshold have been presented.

The bulk damage in crystals can be raised by defects and intrinsic causes. The laser damage in sapphire and Ti:sapphire crystals caused by different kinds of defects, such as metallic particles, impurity inclusions and dislocations has been presented and analysed.

We have observed the filamental damage by self-focusing of laser beam in sapphire crystals firstly. The influence of laser pulse duration and wavelength on laser damage threshold of sapphire and Ti:sapphire crystals has been reported. On the basis of experimental data the mechanism of intrinsic damage has been analyzed and a new model of intrinsic damage mechanism is proposed.

The nonlinear optical effects in dielectric crystals have been discussed theoretically. A new method for calculating the nonlinear refractive index of optical and laser crystals was proposed. The relationship between laser damage threshold and nonlinear refractive index of a series of optical and laser crystals has been given.

NEW GROWTH TECHNIQUES AND PERFECTION CHARACTERIZATION OF Ti:SAPPHIRE LASER CRYSTAL

B54

Peizhen Deng, Gingwen Qiao, Qiang Zhang, Binfung Yun, Yue Chai and Bing Hu
Shanghai Institute of Optics and Fine Mechanics
P.O. Box 800-211, Shanghai 201800, P.R.China

Ti:Sapphire crystal is one of the most attractive broadband tunable solid state laser materials. In order to meet the demands of current laser systems a variety of growth techniques have been developed. For large diameter and high quality of Ti:sapphire crystals the growth technique and perfection characterization have to be improved.

In this paper we report the new crystal growth techniques, Induction Field Up-shift Method(IFSM) and Temperature Gradient Technology, for Ti:sapphire. Using these methods, it is easy to control the growth parameters and atmosphere. The big crystal boules of 120 mm in diameter and 80 mm in length have been obtained. High laser light conversion efficiency has been performed at different laser pumping conditions, such as $\eta_s > 50\%$, 30% for pulsed and quasi-CW Nd:YAG double frequency laser pumping respectively, $\eta_s > 30\%$ for Cu-vapor laser pumping and $\eta_s > 40\%$ for excimer laser pumping at 499 nm wavelength.

The high structure perfection, optical homogeneity and figure of merit (FOM) value are rather important for high quality Ti:sapphire crystal, but their studies were quite insufficient. We have investigated the defects morphology and distribution of Ti:sapphire crystals by chemical etching and X-ray topography. Recently we obtain clear lattice image of Ti:sapphire crystal by high resolution electron microscope. The dislocation structure and the lattice distortion influenced by impurity atoms are studied, and the computer simulation of crystal structure change is also performed. From the experimental results the crystal quality and growth techniques have been improved too.

B55

AN X-RAY TOPOGRAPHIC EXAMINATION INTO THE GROWTH HISTORY OF YTTRIUM ALUMINUM GARNET GROWN FROM HIGH TEM ERATURE SOLUTION

K.J. Roberts
Department of Pure and Applied Chemistry
University of Strathclyde, 295, Cathedral Street, Glasgow G1 1XL, UK
D. Elwell
Hughes Aircraft Company, 200 Superior Avenue, Newport Beach, CA 92658, USA
B.J. Isherwood
GEC Hirst Res. arch Centre, East Lane, MIDDX HA9 7PP, UK

X-ray topography and some related techniques have been used to probe the growth history of a number of large (≈ 2 x 2 x 1 cm^3) nearly-perfect single crystals of yttrium aluminium garnet crystallised from high temperature solution using a $PbO/PbF_2/B_2O_3$ flux. The 'as-grown' crystals have been found to exhibit well defined {101} and {112} facets and in an examination of a number of crystals the following lattice defects have been routinely observed:

- grown-in dislocations observed at densities in the range 10-100 lines cm^{-2}. Many dislocations were of mixed character and this combined with solvent decoration meant that unambiguous identification of Burgers was rare,
- impurity incorporation of Pt (from crucible material) and Pb (from flux) was observed at the 5000 ppm level. Macroscopic solvent inclusions were also observed and found to predominate in the faster growing {112} growth sectors,
- growth striations, due to growth-induced anisotropy, resulting in a tetragonal distortion along the growth axis associated with a lattice strain of about 5 x 10^{-5}. In the termination facet regions this strain was found to increase to ≈ 5 x 10^{-4}.

The overall perspective of lattice perfection, crystal growth parameters and the resulting growth mechanism will be presented and discussed.

B56

FORMATION OF SPIRAL SHAPE ON CZOCHRALSKI GROWN DYSPROSIUM GARNET SINGLE CRYSTAL

H. Kimura, T. Numazawa, M. Sato and H. Maeda
National Research Institute for Metals, 1-2-1 Sengen
Tsukuba, Ibaraki 305, Japan

A single crystal of Dysprosium garnet is sometimes grown with spiral shape using a conventional Czochralski technique. To investigate an origin of the spiral, we examined the spiral grown single crystal by means of crossed nicols observation, x-ray Laue analysis etc.

Raw materials used are Dy_2O_3 and Ga_2O_3 or Al_2O_3 with 99.99% purity. Single crystals are grown under a conventional growth condition.

Fig. 1 shows a typical spiral grown $Dy_3Ga_5O_{12}$ single crystal. Most crystals are spirally grown counterclockwise from a top view when the crystals are grown under a clockwise rotation, although a clockwise spiral shape crystal is infrequently grown.

According to the X-ray Laue analysis for wafers at several parts of the crystal cut perpendicular to the pulling direction, growth direction is the same as the pulling direction of <111>. The Laue images showing a crystal lattice are rotated around the pulling direction one another. The rotation degree of the Laue image is the same as that of the spiral crystal. An crossed nicols observation of crystal wafers shows a large number of dislocation images in a top part of the crystal, while rare dislocation images from middle to tail part. In these middle to tail parts, we can observe many images based on a stress-birefringence caused by the spiral crystal lattice rotation and by a facet growth.

The cause of spiral shape could be discussed by crystal symmetry.

Figure 1. Spiral shape grown $Dy_3Ga_5O_{12}$ garnet.

B57

GROWTH OF GADOLINIUM INDIUM GALLIUM GARNET (GInGG) SINGLE CRYSTAL BY THE FLOATING ZONE METHOD

M. Kawada, H. Toshima, Y. Miyazawa** and S. Morita***
Nittetsu Mining Co. Ltd.
*Namiki Precision Jewel Co. Ltd.
**National Institute for Research in Inorganic Materials, Science and Technology Agency

1. Introduction. Recently, by using reactive ion beam sputter-deposition process, highly bismuth-substituted films of yttrium iron garnet were synthesized on the GSGG[1] and GLGG[2] substrate for the optical isolator device. The lattice constant of BIG ($Bi_3Fe_5O_{12}$ which is nonexistent at equilibrium form) was estimated as 1.262 nm by extrapolation. The lattice constant of GSGG is 1.256 nm, thus substrate and the films even if it were possible to grow BIG. And the lattice constant of GLGG is around 1.260 nm[3], however, its quality is not good enough for the optical device. We have been looking for better garnet materials than GSGG and GLGG. GInGG ($Gd_3In_2Ga_3O_{12}$ which was yet known) was seemed to be one of the best choice for this purpose.

2. Experiments. GInGG single crystals were grown by the floating zone method. The melting point of GInGG was about 1750 °C. The initial composition which was considered to be appropriate for starting point was $Gd_{3.00}In_{2.00}Ga_{3.00}O_{12}$.

The growth conditions were the following.

pulling rate	1.0 - 4.0 mm/hr
seed and rod rotation rate	30 rpm
atmosphere	air
seed orientation	<111>

In Fig. 1 the photograph of an example of the grown single crystal was shown. The grown crystal has no microcracks and no bubbles inside.

3. Discussion. The lattice constant of GInGG is around 1.266 nm, and GInGG may have the congruent melting point. The GInGG single crystal has no optical absorption at a wavelength between 400 and 2000 nm. We have synthesized the BIG thin films on the GInGG substrate.

Figure 1. As grown single crystal.

1) T. Okuda et al, *J. Magnetic Soc.* Japan 11. Suppl.S1 (1987) 179.
2) T. Takahashi et al, Abstract of The 5th Joint MMM-Intermag Conference, Pittsburgh, 1991, p.343.
3) Y. Miyazawa et al, *J. Crystal Growth* 99 (1990) 854.

B58

STUDY ON GROWTH OF BISMUTH TELLURIUM SINGLE CRYSTALS

Tang Xiaolin, Lu Yong, Li Mingwen and Sang Qunlu
Research Institute of Synthetic Crystals
P.O.Box 733, Beijing 100018, P.R.China

Bismuth Tellurium (Bi TeO), as a net acousto-optic crystal has excellent performance in merit and high frequence response in comparison with commercial materials quartz and TeO. So it will become a AO devices substract in further of wide use.

The influences of Varions growth conditions on Bismuth Tellurium crystal quality were studied. According to the results obtained, we have improved the growth technology. Presently high quality and large size (up to 50x50x25mm) BTO crystal can be grown steadily.

The phase equilibria in the pseudo-binary system Bi O-TeO at 450 C-95 C in open and close crucible were examined by solid-state reaction techniques and x-ray powder diffraction method. According to our experimental results, an appropriate amount of excessive TeO seems to be a available flux for BT0 single crystal growth. TeO is more volatile than Bi O over seven times in air at 910 C-925 C. It is about 0.03g/hcm while TeO :Bi O between 1.3 and 1.1.

Other problems, each as cleavage, parasitic crystals and cover on the surface of growing crystal have also been encountered in our experiments. The cleavage is more easily happened along [100] direction. This is caused by the characteristic of BTO crystal aid thermal expansion. The formation of parasitic crystals is relation to the solution stability and the face network structure of crystal. Moreover, the effects of rotation rate, growth temperature and cooling rate were discussed.

B59

IN-SITU OBSERVATION OF THE GROWTH PROCESSES OF OXIDE AND FLUORIDE CRYSTALS FROM MELTS

Chen Jinyuan, Jin Weiqing and Shan Guoqiang
Shanghai Institute of Ceramics, Chinese Academy of Sciences
Shanghai 200050, China

A high temperature in-situ observation equipment was established to study crystal growth from melt. The highest operating temperature was up to 1400°C and the temperature stability was within ±1°C. In this paper, the growing morphological changes of $Bi_{12}SiO_{20}$ and BaF_2 crystals were observed, and the growth mechanism was also investigated.

By the in-situ observation of the growth of $Bi_{12}SiO_{20}$ crystal, the solid-liquid interface along the direction parallel to (001) face was observed, and the growth rates of $Bi_{12}SiO_{20}$ crystals in the supercooling from 0°C to about 180°C were also studied for (100) and (110) faces. The transition from coincidence with two-dimensional nucleation growth to deviation from this nucleation growth was also obtained by increasing supercooling.

From the experiments of BaF_2 crystal, it was found that unlike most of the oxide crystals, the growth front of BaF_2 crystal was not facetted. In addition, with the increase of supercooling, a planar-to-cellular-to-dendrite morphology transition was also obtained.

B60

HYDROTHERMAL GROWTH AND MORPHOLOGY OF $Bi_{12}SiO_{20}$ AND $Bi_4Ge_3O_{12}$ SINGLE CRYSTALS

A.A. Marjin and L.A. Samoilovich
Research Institute for the Synthesis of Materials, Alexandrov, Russia

$Bi_{12}SiO_{20}$ and $Bi_4Ge_3O_{12}$ crystals (5-10 mm) are synthesized from chemical reagents by hydrothermal method. We've determined physical and chemical parameters of synthesis in isothermal conditions as well as conditions of oriented seed growth by temperature difference method. Because of the synthesis in oversaturated solutions crystals have growth defects: skeleton structure of growth pyramid, zonation, sectoration, gaseous and liquid inclusions. Seed grown crystals have minimum growth defects.

Crystal purity increases in comparison with the initial reagents. The results of spectral analysis show 10 to 100 fold reduction of impurities (Al, Ca, Mn, Fe, Ni, Pb). Due to the effect this method can be used for the synthesis of high purity crystals.

Kinetics of growth shapes has been studied by ball seed crystallization. $Bi_{12}SiO_{20}$ crystals (tritetrahedron class) have the following shapes: cube (100), rhobododecahedron (110), pentagondodechahedron (210) and tetrahedron (111). The ratio of face growth rates is: V_{110} V_{100} V_{210} V_{111}. $Bi_4Ge_3O_{12}$ crystals (hexatetrahedron class) have the following shapes: trigontritetrahedron (211), rhombododecahedron (110), tetrahexahedron (310). The ratio of face growth rates is: $V_{211} < V_{110} < V_{310}$.

SESSION 2C

RELAXED BUFFER LAYER GROWTH USING STRAINED LAYERS

C20

D.J. Dunstan, P. Kidd, R.H. Dixon and L.K. Howard
Strained Layer Structures Research Group
University of Surrey, Guildford, Surrey, GU2 5XH, UK

Lattice-matched epitaxy is restricted to a few systems, typified by AlGaAa/GaAs and InGaAsP/InP. It would be very desirable to be able to chose independently the substrate and the epilayer without regard to lattice constant, in order to be able to grow, for example, GaAs on silicon, or II-VI compound structures in the visible regios of the spectrum on silicon or GaAs substrates. To do this requires a relaxed buffer structure, in which the lattice constant can be changed from that of the substrate to that of the layer while retaining a flat, single crystal free surface with a low density of defects.

Several approaches have been reported in the literature, ranging from simple thick layers to superlattice structures. We have developed a new model of critical thickness and of relaxation above critical thickness. Using this model as a guide, we are developing design principles for relaxed buffer layer structures incorporating strained layers. The results are being applied to buffer layer growth in the InGaAs system, where our objective is the growth of device structures with mismatches of several percent to the GaAs substrate. Experimental results on plastically relaxing layers are in excellent agreement with theory. Optical and structural characterisation of these layers will be reported. We expect our results to be applicable to heteroepitaxy using any combination of the Group IV, III-V and II-VI semiconductors.

ON THE MICRO-MECHANICAL PHENOMENA DURING BOULE ANNEAL OF GaAs

C21

S. Motakef[1] *and D.J. Carlson*[2]
[1]Massachusetts Institute of Technology, Cambridge, MA 02139
[2]MA/COM, 100 Chelmsford St., Lowell, MA 01851

Heat transfer and slip-based creep models are used to analyze experimental observations on plastic deformation, reduction of growth-related residual stresses, and the influence of As precipitates on fracture toughness of GaAs during boule anneal. The discrepancies between the experimental and modelling results are shown to be primarily related to the interaction of point defects with dislocation motion. For example, the state of As precipitates (clusters vs. a fine dispersion) is found to exert an overwhelming influence on the fracture probability of the boule; this interaction is not captured in the presently available micro-mechanical creep model. The strengths and shortcomings of the creep model are discussed, and research needed to enhance our understanding of the thermo-mechanical phenomena during high-temperature processing of GaAs is outlined.

C22

PREPARATION AND CHARACTERIZATION OF THE FILLED TETRAHEDRAL SEMICONDUCTOR LiZnP FILM ON InP(111)

K. Kuriyama, Yukimi Takahashi and Tomoharu Kato
College of Engineering and Research Center of Ion Beam Technology
Hosei University, Koganei, Tokyo 184, Japan

Filled tetrahedral semiconductor LiZnP is viewed as a zinc-blende-like$(ZnP)^-$ lattice filled partially with He-like Li^+ interstitials[1]. This ternary compound is a novel type of direct wide-gap semiconductor with a forbidden gap of 2.04±0.01 eV at room temperature[2], not encountered in any cubic III-V material.

LiZnP films were grown by rapid evaporation onto a InP(III) substrate. The single source method[3] was used for the film preparation. The source material LiZnP, lattice constant a=5.763 Å, was grown by directional solidification[4]. The <111>-oriented InP was used as a substrate material because of a relatively small lattice mismatch (1.76%). The polycrystalline films were obtained by annealing for 30 min at a substrate temperature above 330°C. In particular, the single phase <111>-oriented films were grown by annealing at a substrate temperature ranging from 450 to 520°C after evaporation. A SEM photograph shows triangle patterns with several single crystal domains of 20x20 μm^2 resulting from the three-fold symmetry of <111>-oriented InP substrate. The ratio N_{Zn}/N_P of atomic fractions estimated by Rutherford backscattering analysis exhibited a deficiency of phosphorus. The photoluminescence emission around 710 nm was associated with a phosphorus vacancy-acceptor complex[5].

[1] D. M. Wood, A. Zunger and R. de Groot, *Phys. Rev.* B31 (1985) 2570.
[2] K. Kuriyama and T. Katoh, *Phys. Rev.* B37 (1988) 7140.
[3] K. Kuriyama, N. Mineo and Yukimi Takahashi, *J. Cryst. Growth* 113 (1991) 333.
[4] K. Kuriyama, T. Katoh and N. Mineo, *J. Cryst. Growth* 108 (1991) 37.
[5] K. Kuriyama, N. Mineo and Yukimi Takahashi, *J. Appl. Phys.* 69 (1991) 7812.

C23

NUMERICAL MODELING OF InP MOCVD WITH COMPARISON TO EXPERIMENT

L.R. Black[1*], *I.O. Clark*[1], *E.J. Johnson*[3], *J. Kui*[2*] *and W.A. Jesser*[2]
[1]NASA Langley Research Center, Hampton, VA 23665
[2]Department of Materials Science and Engineering, University of Virginia, Charlottesville, VA 22903
[3]Lockheed Engineering and Sciences Company, Hampton, VA 23666

The results of a numerical model of InP metalorganic chemical vapor deposition (MOCVD) are compared with two experimentally measured quantities: thickness profiles of InP thin films grown on fused-silica substrates and velocity profiles measured by laser velocimetry (LV) in a replica flow channel constructed of optical quality fused-silica with the same dimensions and geometry as that used for the growth experiments. MOCVD of InP is performed in a horizontal reactor using trimethylindium (TMI) and phosphine source materials in a hydrogen carrier gas at pressures of both 1.0 and 0.1 atm. The process is modeled in two and three dimensions using a commercially available fluid dynamics modeling code. Both gas-phase and surface chemical reactions are included in the model. The effect of Soret (thermal) diffusion on the transport of particular chemical species and on the deposition rate is examined. The predicted growth rates are compared with measured growth rates on fused-silica substrates at both operating pressures. Laser velocimetry measurements of the flow field in the replica channel are obtained both at room temperature and with the substrate heated to the growth temperature of 600°C. The LV system uses three color-separated lines of an argon-ion laser to make simultaneous measurements of three orthogonal components of the velocity of the flow field at a specific location in the reactor. The measurement volume is then translated through the reactor to map the flow field. Comparison of the model with the results of the growth and LV experiments is presented.

*University of Virginia Graduate Student

MODEL FOR MBE AND MOVPE GROWTH ON NONPLANAR SURFACE

C24

Mitsuru Ohtsuka and Akira Suzuki
Canon Inc. Research Center, Aisugi, Kanagawa, 243-01, Japan

A model allowing a consistent description of growth morphology formed on nonplanar surfaces by molecular beam epitaxy (MBE) and metalorganic vapor phase epitaxy (MOVPE) is proposed. The elemental processes for admolecules including surface migration, incorporation and desorption are formulated in terms of a continuity equation holding on a growing surface. In MOVPE growth, this equation is coupled with diffusion equation in vapor phase and solved self-consistently for local growth velocity.

On the basis of the model, we have simulated the evolutions of growth morphologies on nonplanar substrates under various growth conditions. Fig. 1 shows a result of MOVPE growth on GaAs(001) substrate where ridges along [1$\bar{1}$0] are periodically formed. The facetting feature is clearly seem: (111) facets develop from both corners of the ridges P, increasing their areas with growth evolution. Also seen is a large difference in the growth velocities at the ridge Q and the trench R, although these surfaces (Q and R) have the same crystal orientation of (001). It is found that this is mainly due to the density distribution of reactant species in vapor phase.

It is also shown that not only the diffusion process in vapor phase but the existence of net surface flow of admolecules significantly affects the formation of growth morphology. At the conference, we will present the results of simulations showing the difference of MBE and MOVPE growth features as well as the influence of various parameters on the growth morphology.

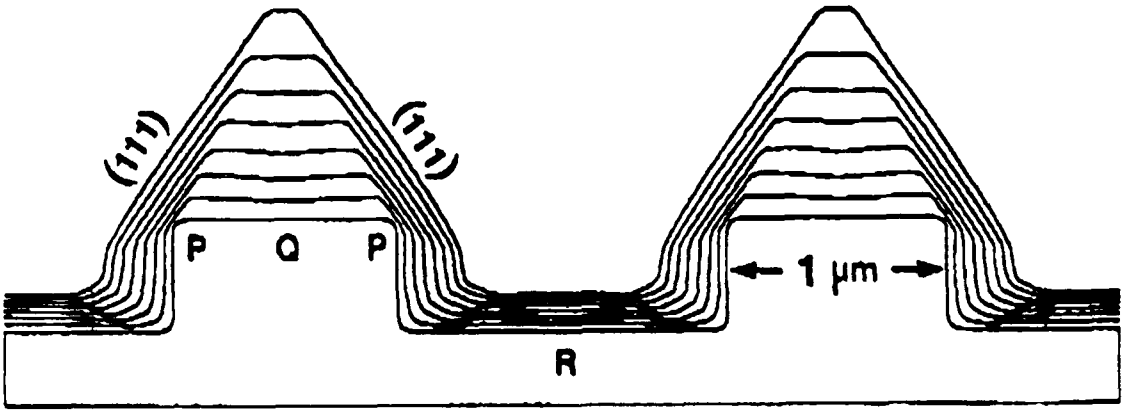

Figure 1. MOVPE growth on GaAs(001) patterened substrate.

CHARACTERIZATION OF UNDOPED InP, GROWN IN AN INVERTED-VERTICAL MOVPE REACTOR, USING TRIMETHYLINDIUM, TERTIARYBUTYLPHOSPHINE AND PHOSPHINE

C25

J.D. Parsons, J. Wu, A.K. Chaddha, S-R. Hahn, H-S. Chen, C. Deng, S. Wild and K. Oatis
Oregon Graduate Institute of Science and Technology
19600 N.W. von Neumann Dr., Beaverton, OR 97006-1999

Undoped InP epilayers with specular surface morphology have been grown at 650°C, at V to III ratios as low as 5 to 1 using PH_3 and TMI and 20 to 1 using TBP and TMI. All InP epilayers grown with TBP exhibit a background n-type carrier concentration of about $4x10^{15}cm^{-3}$. The InP epilayers grown with PH_3 are presently being prepared for van der Pauw measurements, to determine their electrical properties; the results of these measurements will be presented. These epilayers were grown at atmospheric pressure in an inverted-vertical reactor, at a growth rate of 2.1 μms per hour. The morphology and electrical properties of epilayers obtained with TBP and PH_3, at a constant TMI flow rate of 0.5 sccm, will be presented and compared. The morphological results will be correlated with the decomposition properties of the group V sources and the flow characteristics of the inverted-vertical reactor geometry. The electrical results will be correlated with group V source purity and V to III ratios.

C26

AB INITIO MOLECULAR ORBITAL STUDY ON THE REACTION OF TMA WITH H_2

Yoshiko S. Hiraoka, Masao Mashita, Tsukasa Tada and Reiko Yoshimura
Research & Development Center, Toshiba Corporation
1, Komukai Toshiba-cho, Saiwai-ku, Kawasaki 210, Japan

Trimethylaluminum (TMA) is a widely used aluminum source material in metalorganic chemical vapor deposition (MOCVD). The thermal decomposition process of TMA is believed to be radical formation;

$$Al(CH_3)_3 \rightarrow Al(CH_3)_2 + CH_3 \qquad (A)$$

In MOCVD, H_2 is usually used as a carrier gas. One of the authors studied the influences of H_2 on TMA decomposition.[1] It has been shown that the decomposition of TMA is enhanced by increasing the H_2 pressure. This result suggests that the following reaction occurs;

$$Al(CH_3)_3 + H_2 \rightarrow AlH(CH_3)_2 + CH_4 \qquad (B)$$

It is difficult, however, to determine experimentally which reaction of (A) and (B) is easier to occur. From this point of view, we have calculated the dissociation energy and the activation energy of model reactions (A') and (B'), respectively, using the ab initio molecular orbital method.

$$AlH_2CH_3 \rightarrow AlH_2 + CH_3 \qquad (A')$$

$$AlH_2CH_3 + H_2 \rightarrow AlH_3 + CH_4 \qquad (B')$$

In the model reactions, two CH_3 groups are replaced by H atoms.

Fig. 1 shows the relative energies calculated at the MP2/6-31G**//HF/6-31G** level with the zero point vibrational energy correction at HF/6-31G**. The dissociation energy of (A') was 77.1 kcal/mol, while the activation energy of (B') was 34.0 kcal/mol. Therefore, the reaction of TMA with H_2 has been shown to occur rather than the radical decomposition of TMA, if it is under the condition where collisions between TMA and H_2 are sufficiently frequent.

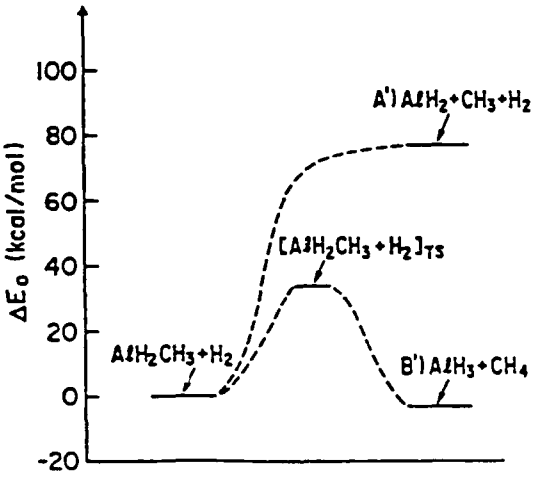

Figure 1. Relative Energies.

1) M. Mashita, Jpn. *J. Appl. Phys.* 29 (1990) 813.

C27

GROWTH OF GaAs ON Si BY EMPLOYING AlAs/GaAs DOUBLE AMORPHOUS BUFFERS

W.Y. Uen and T. Nishinaga
Dept. of Electronic Engineering, The University of Tokyo
7-3-1 Hongo, Bunkyo-Ku, Tokyo 113, Japan

During the past few years a 2-step growth method has been used successfully for obtaining improved quality of GaAs epitaxial layer grown on Si substrate, and has been confirmed to be an effective method for reducing the number of dislocations in this material system. However, the correlation between the crystal qualities of the buffer layer and the epitaxial layer grown directly on the buffer has not been studied in detail, especially when the amorphous buffer(AB) is employed.

In this report, we systematically investigate the influence of buffer layers on the quality of GaAs epitaxially grown on Si(001) substrates. We have successfully grown a high-quality GaAs epitaxial layer on Si by using AlAs/GaAs double AB layers, as compared with the other cases.

The growth was carried out by MBE. As compared with MOCVD, MBE has the large advantage of the capability of preparing the amorphous GaAs and AlAs layers since they require a growth temperature as low as 100°C at which MOCVD can not give the deposition. We grew various buffer layers; not only single AB layer but also single crystalline buffer(CB) layer which was grown at 350°C, and AlAs/GaAs double AB layers (Fig.1(a)) on Si substrate. The thickness of the single buffer layer was kept at 125Å, but the AlAs/GaAs double AB layer consisted of 125Å AlAs and 125Å GaAs, totally 250Å. The AB layers were annealed at an elevated temperature to get single crystal by solid phase epitaxy. On these crystallized and crystalline buffer layers, GaAs was grown epitaxially with the thickness between 1.5 and 3 μm. In some cases, thermal cycles (T.C.) were applied to the sample in order to improve crystal quality. The cycle was usually repeated up to 5 times and the range of temperature oscillation was chosen between 200 and 700°C.

The crystal quality of the epitaxial layer was evaluated by photoluminescence(PL) and KOH etching. The PL intensity was measured for the samples with various buffers, and the result is summarized in Fig.1(b). It is clearly shown that the AlAs/GaAs double AB layers with the thermal cycle gives the highest PL intensity. This is probably because the AlAs covering the GaAs buffer enables us to heat GaAs layer above 800°C without evaporation, which is very much effective to improve the crystal quality of the GaAs buffer. Without this AlAs cap layer, GaAs buffer is easily evaporated at the temperature higher than 700°C. On the other hand, AlAs amorphous and crystalline single buffer layer gave rather poor crystalline quality of GaAs epitaxial layer. This is probably because the strong binding force between Al and Si brings in some unexpected defects during the crystal growth. KOH etching showed the etch pit density (EPD) of GaAs epitaxial layer on AlAs/GaAs double buffers was of the order $3x10^6/cm^2$, while EPD of GaAs with other buffers were higher than $1x10^7/cm^2$.

In summary, 2-step growth with AlAs/GaAs double amorphous buffer may become one of the promising technologies to give high crystal quality of GaAs on Si substrate.

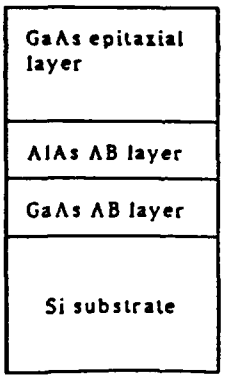

Figure 1(a). Structure of 2-step MBE growth of GaAs-on-Si using AlAs/GaAs double AB layers.

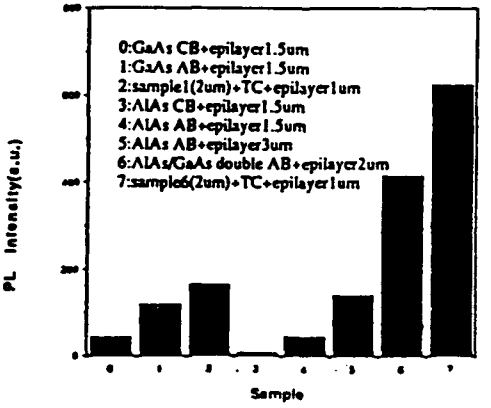

Figure 1(b). PL characterization of GaAs epitaxial layers grown on various buffers.

C28

REDUCTION OF SURFACE DEFECTS IN GaAs LAYERS GROWN BY MBE

H. Kawada, S. Shirayone, K. Takahashi
Mechanical Engineering Research Laboratory,
Hitachi, Ltd., 502 Kandatsu, Tsuchiura-city, Ibaraki-pref., 300 Japan

Elimination of surface defects in the GaAs epitaxial layers becomes the most significant technology for high yield production of GaAs large scale integrated circuits (LSI). In this experiment, some types of defects were reduced by improving growth conditions and structure of effusion cells.

The defects were observed by an defect analysis system. It consists of a Normarski contrast microscope, an image analyzer and a X-Y stage. Figure 1 shows the density of whole defects with varied flux ratio of As/Ga. Ga flux was kept constant for growing GaAs layer in 1 micron/hr. Size of the observed defects is larger than 11 sq. microns, because the smaller defects are difficult to identify their configurations in the following observation. The density is slightly getting lower with decreasing the As/Ga ratio from 7 to 5. But only a specific type of defect were supposed to be decreasing, while the other types of defects were not affected by the As/Ga ratio. Then the defects were observed one by one and classified with its configuration.

Figure 2 shows the density of a specific type of defect with varied As/Ga ratio. This type of defect appeared to be linearly reduced with lowering the As/Ga ratio. Also they can be completely eliminated by adjusting the As/Ga ratio at the lower limit for epitaxial growth. Reduction and elimination of the other types of defects will be reported.

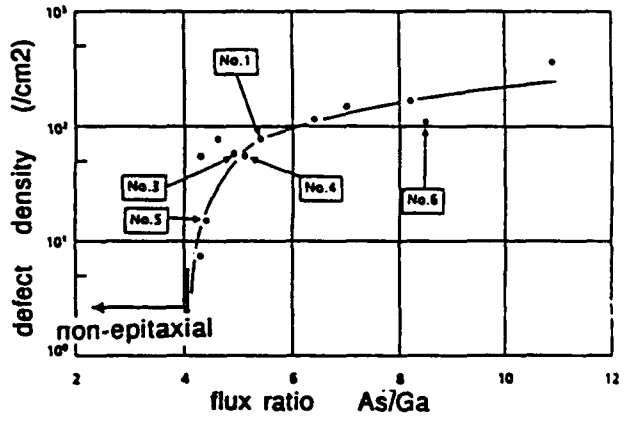

Figure 1. The density of whole defects with varied flux ratio As/Ga.

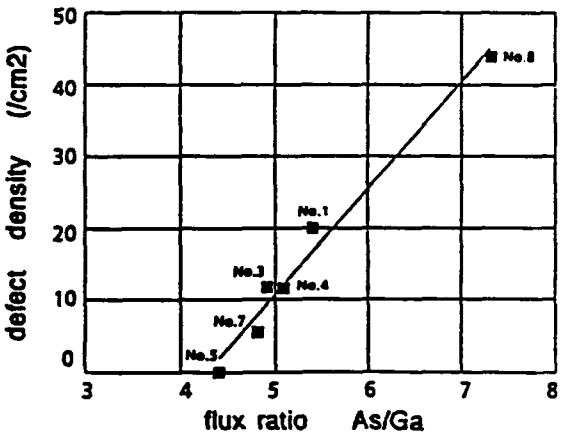

Figure 2. The density of a specific type of defect with varied flux ratio As/Ga.

HVPE GROWTH OF InGaAsP EPILAYERS AND THEIR CHARACTERIZATION

C29

D. Arivuoli, G. Attolini, C. Bocchi, C. Pelosi and C. Frigeri*
Maspec Institute-CNR, Via Chiavari 18/A, I-43100 Parma, Italy
*Crystal Growth Centre, Anna University, Madras-25, India

The development of compound semiconductors and heterojunction devices as important electronic and optoelectronic device technologies has been advanced by the emergence of epitaxial materials exhibiting a high degree of structural perfection. It is known that the input parameters of epitaxial growth are strictly correlated to the quality of grown material and the importance of their role can be inferred if the epitaxial system operate at near-equilibrium conditions.

In this communication we report on the growth conditions and structural characterization of InGaAsP quaternary layers grown on InP substrate. The layers were grown by hydride VPE technique using hydrides (AsH_3 and PH_3) and HCl gaseous source both diluted in hydrogen respectively at 5% and 10%. Taking advantage of the fact that hydride VPE epitaxial technique may be considered operating at near-equilibrium conditions we can assume according to classical thermodynamics laws that the overall deposition process is driven by the chemical potentials of different species in the gaseous and solid phases.

In order to study growth conditions, several parameters (namely deposition temperature, reagent flows and the gas phase stoichiometry) were taken into consideration. Their influence on film properties were studied in order to understand their effect on composition and surface morphology of the epilayers.

The effect of variation of growth temperature and the total hydrogen flow on the structural characteristics of the grown layers were investigated by using High Resolution Diffractometry (HRD), Scanning Electron Microscopy (SEM), Transmission Electron Microscopy (TEM) and Cathodoluminescence; the composition was routinely determined by Electron microprobe. When thick layers were under examination the thermodynamical analysis of growth conditions and the geometrical configuration of the deposition system allowed us to enhance the quality of the layers and to grow with rates unusually low for this technique (700Å in half an hour).

HYDRIDE-VPE GROWTH OF InP AND S.I. InP:Fe IN H_2/N_2 AMBIENT

C30

R. Göbel
Deutsche Bundespost, TELEKOM, D-6100 Darmstadt, FRG

Characteristic growth rates of the epitaxial deposition of InP in atmospheric Hydride-VPE using H_2 as carrier gas are reported in literature to be in the range of 30-60 μ/h. A substantial increase of about 65% could be achieved just by a HCl pre-etch of the reactor's growth zone (not of the sample) a few minutes before growth; thus, growth rates of up to 110 μ/h (not pre-etched 65 μ/h) were achieved without injection of additional free HCl during growth. Detailed experiments are presented and discussed with respect to a better understanding of this pre-etch which improves the efficiency of the input gases and shortens growth time.

It is a typical feature of the Hydride-VPE that injection of free bypass HCl (HCl_{by}) *during* growth reduces the growth rate down to zero, even a polishing etch is possible. Generally an initial increase of the growth rate with the HCl is observed in different laboratories varying from 10 to over 100 %. However, when applying the presented HCl pre-etch process, highest growth rates with good reproducibility are ascertained even at small HCl_{by} flows with no further increase. This is in agreement with model calculations (1). A distinct improvement of the thickness homogeneity with decreasing growth rate by HCl_{by} injection indicates the transition from mass-transport limited to kinetically limited growth.

$FeCl_2$ is used for the growth of s.i. InP as an iron dopant generated by the reaction $Fe + 2HCl \Leftrightarrow FeCl_2 + H_2$. However, $FeCl_2$, the predominant iron chloride compound under the VPE growth conditions, is easily reduced in H_2 ambient. This hinders the source reaction and the Fe transport to the growth zone, as well. For that reason N_2 (with 11% H_2 admixture) was chosen as a carrier gas resulting in high growth rates of 55 μ/h (not pre-etched 35 μ/h), which is to be compared to 110 (65) μ/h in pure H_2. At Fe doping levels between 10^{17} and 10^{19} cm^{-3}, as analysed by SIMS, I-V measurements reveal semi-insulating behaviour with corresponding resistivities ranging from 10^7 up to 10^9 Ω cm. The capability of depositing s.i. InP:Fe at high growth rates together with the good suitability of the Hydride-VPE for selective regrowth over mesa structures are very promising for high speed laser fabrication. This was successfully demonstrated by embedding mushroom-type lasers with s.i. InP:Fe.

(1) H. Jürgensen et al., *J. Crystal Growth* 70 (1984) 123.

C31

A NEW KINETIC MODEL FOR VAPOR EPITAXY OF $GaAs_{1-x}P_x$ FROM THE Ga-As-P-H-Cl SYSTEM

V.N. Mani
Centre for Materials for Electronics Technology
C-92 South Extn. Part II, New Delhi - 110 049, India
R. Dhanasekaran and F. Ramasamy
Crystal Growth Centre, Anna University, Madras - 600 025, India

In this work, we present a model based on thermodynamics, nucleation, and chemical kinetics for the $GaAs_{1-x}P_x$ vapor phase epitaxial growth. Nucleation behaviour has been examined as a function of supercooling and substrate orientation using the classical heterogeneous nucleation theory. The model, which includes an eleven-step reaction mechanism for the deposition of $GaAs_{1-x}P_x$ from the Ga-As-P-H-Cl system. The model predicts surfaced coverage factors of the individual absorbed species and general trends of growth kinetics assuming that the formation of complex molecules at the substrate surface are the rate determining steps, an expression for the deposition rate has been developed[1,2]. The growth rate expression also predicts the effects of deposition temperature and pressure of the gases on the growth rate of the layer. Numerical analysis of our theoretical predictions indicate that gas phase chemical kinetic processes are important in describing $GaAs_{1-x}P_x$ vapor phase epitaxy. The validity of our model has been tested by comparing our results with reported experimental results[3].

The modelling treatment has been extended to other ternary systems like InAsP, GaInP and AlGaAs. The interplay between growth kinetics and compositional control is outlined.

1. V.N. Mani, et al., *Semicond. Sci. Technol.* 2 (1987) 72.
2. V.N. Mani, et al., *J. Crystal Growth* 99 (1990) 333.
3. V.N. Mani, et al., *J. Appl. Phys.* 69 (1991) 1399.

C32

NUMERICAL SIMULATION STUDIES OF CONCENTRATION PROFILES AND GROWTH RATE OF InP AND GaAs LPE

P. Santhana Raghavan, R. Dhanasekeran and P. Ramasamy
Crystal Growth Centre, Anna University, Madras-600 025, India

Epitaxy is especially important for optical devices, because conventional optical devices inevitably utilize epitaxial layers in their active regions. InP, InGaAs and InGaAsP epitaxial layers grown on InP substrates have been widely used in the fabrication of optical devices such as LED's, LD's and photodetectors. For the growth of III-V binary compounds, the composition of the epitaxial layer is not significantly altered by the change in the melt composition as the growth proceeds due to the near stoichiometry of the deposit. But this is not the case for the growth of ternary and quaternary alloys since the segregation coefficients relating the concentrations of various elements in the solid to their concentration in solution may differ from each other. As a consequence the alloy composition may vary significantly depending upon the initial composition of the melt and the growth temperatures. An extensive and reliable method to determine the solute concentration during the growth process is difficult to obtain and hence a mathematical modelling of the growth process of Inp, GaAs based systems by LPE becomes important. In this communication, a diffusive transport model of horizontal multiwell slider method of Liquid Phase Epitaxy of InP from In solution and GaAs from Ga solution is presented. The concentration profiles of solute at different places in front of the growing crystal interface under normal conditions of LPE at successive intervals of time have been simulated using numerical analysis and applying boundary conditions. From the concentration profiles the growth rate has been calculated. Different cooling rates and undercooling have been used in our simulation work and the concentration profile and hence the amount etched or grown are investigated. The estimated growth rates have been compared with the reported experimental values and are in good agreement with our theoretical predictions.

INFLUENCE OF THE SOLUTE CONVECTION ON InGaSb LPE LAYERS GROWN ON VERTICALLY MOUNTED GaSb SUBSTRATES

C33

Y. Hayakawa, K. Asakawa, Y. Torimoto, K. Yamashita, A. Nakayama, and M. Kumagawa
Research Institute of Electronics, Shizuoka University
Johoku 3-5-1, Hamamatsu-shi, Shizuoka 432, Japan

III-V semiconductor crystals with a controlled thickness and a composition ratio are useful for opto-electronic devices. These parameters, however, are affected by the solute convection. In this paper, the influence of thermal convection on morphologies of $In_xGa_{1-x}Sb$ grown crystals was investigated by using a modified liquid phase epitaxial method.

A (111)GaSb substrate was vertically mounted in the In-Ga-Sb source solution. The crystal was grown from 600°C for 4 hours at constant cooling rate. During growth, electric current pulses were introduced across the solution-substrate-solution interfaces at intervals of 30 min, and impurity markers were introduced in the grown layer Intentionally. Grown samples were cut along the growth direction, and their growth morphologies were observed. The shapes of grown layers were nearly trapezoid toward the source solution. The layer thickness of the upper area was larger than that of the lower area.

To explain these experimental results, the convective flow in the source solution was numerically analyzed. By computing equations such as the heat equation, the Navier Stokes and continuity equations with the thermal boundary conditions, the boundary layer thickness was obtained. The growth rate was calculated from the composition gradient in the boundary layer and the growth thickness was obtained by integrating the growth rate with time. This calculated result agreed well with the experimental result. Therefore, the convection in the source solution was found to affect the growth process, especially the growth morphologies.

SESSION 2D

STUDIES OF FEATURES OF HYDRIDE CRYSTAL GROWTH IN ZIRCONIUM

D27

D.V. Schur, V.A. Lavrenko, V.B. Wojtowych and V.M. Adejev
Institute for Problems of Materials Sciences of the Ukrainian
Academy of Sciences, Krzhizhanovskogo Street 3, 252680 Kiev, USSR

A kinetic method is suggested and substantiated to study the mechanism of hydride formation during the isothermal interaction between metal and hydrogen and to evaluate the effect of various factors on the course of this process.

The fine metal foil with 25 μm in thickness is used as a specimen. After recrystallization annealing the metal crystallites have a plane, abutted upon gas phase. Investigation of zirconium foil cross-section fractures, observed by scanning electron microscope, shows that most of grains are arranged transverse to foil and have two boundaries with gas phase at both sides of foil. That is conditioned by metal texturization at rolling.

Thus utilization of polycrystal metal foil allow to study interaction processes between definite faces of metal crystals and gas phase. This is concerned to interaction between metal foil and hydrogen in particular. Great hydrogen mobility and small foil thickness of 25 μm (diffusion zone of 12,5 μm) permit to eliminate influence of diffusion processes on metal-hydrogen interaction. In that case kinetics curves describe processes, proceeding in one separate crystallite.

Elimination of the limiting effect of surface and diffusion processes on the rate of hydride formation using atomic hydrogen and metal foil permits fixing directly from kinetic curves the formational moment of phases and evaluating by means of thermogravimetry the hydrogen content in them. Combined with X-ray phase analysis, the method gives good and reliable results.

Possible and expedient application of this method is shown through an example of zirconium interaction with hydrogen. Interpretation is given for appropriate kinetic effects reflecting peculiarities of structural transformations induced by hydrogen saturation of the metal at different stages of interaction.

STUDIES ON THE ABSORPTION AT 290NM OF BaF_2 CRYSTALS

D28

H. Xiao, G. Chen, S.Q. Man, S.X. Ren and J.Q. Zhang
Beijing Glass Research Institute
Dongdadi 1, Chongwenmenwai, Beijing 100062, P.R. China

Radiation resistance of BaF_2 crystal is the one of most important factors for its using as detector in high energy physics experiments. A lot of experiments showed that the absorption at 290nm of BaF_2 crystal was to disadvantage of its radiation resistance, so this absorption should be removed.

The absorption at 290nm of undoped BaF_2 crystals is similar to that of Ce^{3+}-doped BaF_2 crystals. It is found that there is an absorption at 290nm when the concentration of Ce^{3+}-doped in BaF_2 crystals is lower than 1ppm. The emission spectra of undoped BaF_2 crystals is the same as that of Ce-doped BaF_2 crystals, which there are two peaks at 323nm and 305nm, excited at 290nm. Therefore, there is no doubt that the absorption at 290nm is related to microcontent of Ce^{3+} in BaF_2 crystals.

By controlling the purity of raw materials and improving technics, we grew BaF_2 crystals which had neither absorption at 290nm nor emission peaks at 305nm and 323nm

GROWTH AND PROPERTIES OF SUPER-LENGTH BaF_2 SCINTILLANT CRYSTAL

D29

S.X. Ren, J. Zhang, F.Y. Zhang, Y.N. Zheng and F.Z. Li
Beijing Glass Research Institute, Beijing 100062, China

In order to form the crystal couple of one with the length of 350mm, and the other with the length of 150mm. We have successfully obtained the super-length of 350mm crystals by the use of Bridgman technique. The optical and some scintillant properties were measured. We also find some ways to obtain super-length crystals with high radiation resistance effectively, which include the management of raw material, the process of crystal growth and the high vacuum system.

D30

GROWTH OF SINGLE CRYSTALS OF FAST-ION CONDUCTING BINARY AND TERNARY COPPER AND SILVER HALIDES FOR NEUTRON SCATTERING

Catherine Heremans and Bernhardt I. Wuensch
Massachusetts Institute of Technology, Cambridge, MA, USA

We report the growth of single crystals of copper and silver binary and ternary halides. These materials adopt crystal structures with very simple anion arrangements (BCC, HCP, FCC) in their high temperature fast-ion conducting phases, which make them extremely suitable candidates for investigating the relationship between crystal structure and the property of fast-ion conduction. Neutron diffraction studies constitute a powerful tool for this purpose but require the availability of high quality single crystals several mm^3 in size. Some of these materials have to our knowledge never been synthesized as large single crystals.

We have focused our efforts on the growth of copper mercury iodide, silver mercury iodide, copper iodide and copper bromide by various solution growth techniques at room temperature. These methods include growth by evaporation and vapor dilution of solutions using solvents such as acetonitrile and halogen acids. Other methods that have proven successful use a gel as medium for decomplexation and exchange reactions.

Single crystals of copper mercury iodide (space group $I\bar{4}2m$) have been grown for the first time. The crystals of this material adopt different habits depending on the growth technique. Some of them grow in the shape of small tetrahedra of 0.5mm edge with very nicely defined (112) facets. Others grow as fragile needles of much lower quality.

We have also successfully grown silver mercury iodide crystals (space group $I\bar{4}$) of much larger dimensions than previously reported. The largest crystals have the shape of (001) platelets or long triangular prisms with volumes up to $2mm^3$. Neutron diffraction studies of this material have until now been precluded by the non-availability of crystals of sufficient size.

Copper iodide, which presents two high temperature fast-ion conducting phases, has been obtained by various techniques. The most promising method at room temperature yields crystals of high quality and large sizes reaching volumes of several mm^3. We have also obtained much larger dendritic crystals of lower quality as well as small tetrahedra.

Finally, we have synthesized copper bromide crystals that are large enough for a proper neutron diffraction study.

D31

STUDY OF THE HgI_2 HOMOGENEITY REGION IN THE Hg-I SYSTEM PHASE DIAGRAM

H. Hermon[a], M. Roth[a], M Schieber[a] and J. Shamir[b]
[a]Graduate School of Applied Science and Technology
[b]Department of Inorganic and Analytical Chemistry
The Hebrew University of Jerusalem, Jerusalem 91904, Israel

The near stoichiometric region of HgI_2 has been studied for updating the phase diagram of the iodine - mercury system.

The stoichiometric evaluation has been performed using Raman spectroscopy to determine the Hg excess as Hg_2I_2. Photometric analysis has been employed for determination of the iodine excess. The sensitivity of the methods enable us to determine minute amounts of either mercury or iodine excess at a level of few ppm.

HgI_2 crystals doped by either mercury or iodine excess were grown from the vapor phase at temperatures ranged from 58 to 200°C and the results were used to complement the near-stoichiometric region of the HgI_2 phase diagram. It has been found that the maximum amount of Hg_2I_2 dissolved in the HgI_2 crystal occurs at 120°C (720 ppm) but is reduced at higher temperatures (to 100 ppm at 180°C) due to thermal decomposition of Hg_2I_2. The iodine maximum solubility in the α-HgI_2 crystal was found to be 140 ppm (at about 100°C), whereas in the β-HgI_2I it is 210 ppm at 150°C and is reduced to 90 ppm at 200°C.

The effect of deviations from stoichiometry on the electronic properties of HgI_2 is also discussed.

EFFECT OF GROWTH CONDITIONS ON THE OPTICAL QUALITY OF MERCUROUS CHLORIDE CRYSTALS

D32

N.B. Singh, M. Gottlieb, J.J. Conroy, R.B. Hopkins and R. Mazelsky
Westinghouse Science and Technology Center, Pittsburgh, PA 15235
M.E. Glicksman
Materials Science and Engineering Department, R.P.I. Troy, NY 12180
Walter M.B. Duval
NASA Lewis Research Center, Cleveland, OH 44135

Mercorous halides (I) are extremely attractive compounds for acousto-optic compounds because of their large birefringence, wide range of transparency and large acousto-optic figure of merit. However, the unavailability of optical quality single crystals has limited the commercialization of the devices made from this material. We have carried out a detailed study to examine the effect of growth conditions on the bulk homogeneity of crystals. The crystal growth velocity exhibits a strong crystal anisotropy and depends on the orientation. Acousto-optic Tunable Filters (AOTF) and Bragg Cells (BC) were fabricated and tested from [110] oriented boules and shored very exciting results.

Authors are grateful to Ms. Debbie Todd for preparing the subject matter and to NASA Headquarters, MSAD, Code SN, for the financial support.

LEAD CHLORIDE CRYSTAL GROWTH FROM BOILING SOLUTIONS

D33

S. Veintemillas-Verdaguer, J. Torrent-Burgues and R. Rodriguez-Clemente
Institut de Ciencia dels Materials de Barcelona. C.S.I.C.
Campus de la UAB. 08193 Cerdanyola. SPAIN

Lead chloride single crystals can be grown from boiling water solutions using KNO_3 as a mineralizer. Crystals of 1mm size produced by gel-growth technique were used as seeds. The solubility of $PbCl_2$ increases almost linearly with the molality of KNO_3, being 0.628 m in a 7m KNO_3 aqueous solutions at 105.4 C and pH=2.6, this increase is related with the decrease of the activity coefficient of lead chloride in these solutions.

In the first experiments, the supersaturation was attained by solvent extraction, but due to the simultaneous changes in the concentration of the KNO_3 mineralizer during the extraction, the growth rate was irregular and defective crystals were obtained. The experimental set-up was, thus, modified and a transport technique was added to the system in order to feed continuously the boiling reactor with fresh lead chloride solution. The growth of the crystals takes place at constant concentration of KNO_3 in these new conditions. With this experimental modification, clear and isometric $PbCl_2$ crystals of up to 1cm size were obtained in three weeks. The observed morphology is close to that calculated by Woensdregt and Hartmann [1].

[1] Woensdregt, C.F. and Hartmann, P., *J. Crystal Growth*, 87 (1988) 561-566.

D34

SINGLE-CRYSTAL GROWTH OF CUPROUS CHLORIDE BY FLUX METHOD

*G.T.K. Fey**
Department of Chemical Engineering
National Central University, Chung-Li, Taiwan 32054
D.P. Wright and J.B. Wagner Jr.
Center for Solid State Science
Arizona State University, Tempe, Arizona 85287-1704

This paper reports our recent studies on single-crystal growth of cuprous chloride by the Bridgman method in $SrCl_2$ flux. Anhydrous strontium chloride was selected as the flux solvent to reduce the temperature of CuCl solidification below both its normal melting point (420°C) and the zinc blende-wurtzite phase transition temperature (408°C).

The cuprous chloride powder (98% purity) received from J.T. Baker was gray, rather than bright white. Hence, it contained impurities such as cupric chloride, cupric oxide, metallic sulfate, and hydrates of copper and iron. These impurities may produce color centers, decrease light transmission and hinder single-crystal growth. Therefore, it was necessary to remove as many of the impurities as possible in order to obtain an optical or electrochemical grade single crystal of CuCl. The preparation consisted of three separate stages: (1) purification of CuCl by chemical separation, (2) further purification by sublimation of the purified CuCl, and (3) crystal growth of the sublimed CuCl, with $SrCl_2$ flux, using a modified Bridgman method in a vertical shunt furnace (2" i.d. x 24" long).

Visual inspection of the vessel and sample, after they were removed from the furnace, revealed a white solid which was bright white at the tip and became progressively darker towards the top of the melt. When light was transmitted through the tip of the white solid, small sections within the bulk appeared translucent or almost clear. It is hoped that these areas are single crystal domains.

Above the top of the sample, a very thin layer of black residue was affixed to the walls of the vessel. This residue resembled that which was observed in the sublimation vessels after purification of the CuCl by sublimation. The above is consistent with the proposed mechanism by which $SrCl_2$ and impurities in the melt are excluded from the growing CuCl crystal and accumulate at the top of the sample. The initial temperature of the tip was about 480°C and the descent rate of the vessel was near 1 mm/hr during a ten day period. Solidification began between 408°C and 344°C.

D35

GROWTH OF SULPHO HALIDES OF ANTIMONY AND BISMUTH IN GEL

R. Roop Kumar, G. Raman and F.D. Gnanam
Alagappa College of Technology, Anna University, Madras - 600 025, India

Among the ternary chalcogenides of the group $A^{V} B^{VI} C^{VII}$ compounds (where A = Sb, Bi, As; B = S, Se, Te and C = I, Br, Cl, F), Antimony and Bismuth Sulpho Halides have drawn much attention because of their optical, photo conducting and ferroelectric properties. These displacive-type of ferroelectric semiconducting crystals are grown mainly by high temperature techniques. The present work describes the growth conditions of SbSBr, SbSCl, SbSF, BiSI and BiSCl crystals in Sodium silicate gel under ambient temperature. The reactants used for the growth of these crystals are Antimony Trioxide. Bismuth Trioxide, Bismuth Triiodide, Bismuth Trichloride, KF, KI, Thiourea, Di-hydrogen sulphide and acids like HCl, HBr, H_2SO_4 and HI. The effects due to the change of concentration of the reactants, density of the gel solution, introduction of neutral gel and seeding are also investigated and discussed. Single crystals of SbSBr of size 7mm, SbSCl of size 5mm and SbSF of size 2mm are grown in a period of 15 days. Black platelets of BiSI of size nearly 5mm with high shining surface was obtained in 30 days. Needles of BiSI crystals of length 7mm was also obtained by Hybrid method. To control spontaneous nucleation at the interface of the gel medium for the growth of BiSI. Neutral gels of different heights ranging from 1 to 5 cm were taken over the set gel. Good single platelets of dimension 7-9 mm were obtained in 30-40 days when the height of the neutral set was 4.0 cm. Reddish crystals of BiSCl of size 5 mm were obtained in St. tubes. To improve the size of BiSCl crystals, modified -u-tube apparatus has been adopted and crystals of size up to 10 mm with controlled nucleation was obtained. The grown crystals were confirmed by x-ray diffraction studies.

D36

TEM STUDY OF PHASE AND DOMAIN IN LANTHNUM ALUMINATE

*Y. Yang, Y.C. Chang, C.Y. Yang, Y.Q. Zhou and K.K. Fung**
Institute of Physics, Chinese Academy of Sciences
P.O. Box 603, Beijing 100080, P.R. China
*Also Beijing Laboratory of Electron Microscopy, Chinese Academy of Sciences
P.O. Box 2749 Beijing 100080, P.R. China

Lanthanum Aluminate ($LaAlO_3$) single crystal as a substrate for high T_c superconducting film has attracted attention recently. The crystallographic properties and structural phase transitions in this material have been a subject of detailed study for quite some time. The space group determined by X-ray diffraction has been reported to be $R\bar{3}c$. A systematical study by Transmission Electron Microscopy (TEM) using Convergent-beam Electron Diffraction (CBED) found that the structure of $LaAlO_3$ is cubic, with lattice parameter twice that of its high temperature perovskite phase and space group $Fm\bar{3}c$. The coexistence of lower symmetry monoclinic phase and cubic phase have also been observed. The previously reported $R\bar{3}c$ space group is probably due to the coexistence of the cubic phase and lower symmetry phase in the same crystal. The domain structure in the cubic and lower symmetry monoclinic phase have also been observed.

D37

THE GROWTH OF $DyAlO_3$ SINGLE CRYSTALS BY CZOCHRALSKI METHOD

H.Sekiwa[1], S.Morita[2] and Y. Miyazawa[3]
[1]Nippon Mektron, Ltd.
[2]Mitsubishi Heavy Industries, Ltd.
[3]National Institute for Research in Inorganic Materials
1-1 Namiki Tsukuba-shi Ibaraki, Japan

1. Introduction. Rare earth aluminate single crystals may be used as substrates for the high Tc super-conductors. We were able to grow the dysprosium aluminate(DAO) single crystals by Czochralski (Cz) method. The relation between the crystal qualities and the seed rotation, cooling rate, and crystal growth furnace design have been examined.

2. Experiments. DAO single crystals were grown by Czochralski method. The iridium crucible whose size was 50mmϕ x 50mmh x 1.5mmt was used for RF heating. The initial melt was composed of 99.99% Dy_2O_3 and 99.999% $Al2O_3$ mixed in a stoichiometric ratio. The crystal was grown on a <001> axis at a pulling rate of 2mm/h and seed rotation rate of 2rpm.

3. Discussion. The radiation emitted by DAO melt was absorbed by the growing crystal, which causes low temperature gradient near the growing interface. Therefore, DAO single crystals must be grown under a large temperature gradient and low seed rotation rate in order to avoid cell growth and to control the diameter of crystals.

It was evident some phase transitions existed below melting point, so it was necessary to cool very fast after growth to avoid cracking. In Fig 1. the photograph of an example the grown DAO single crystal was shown.

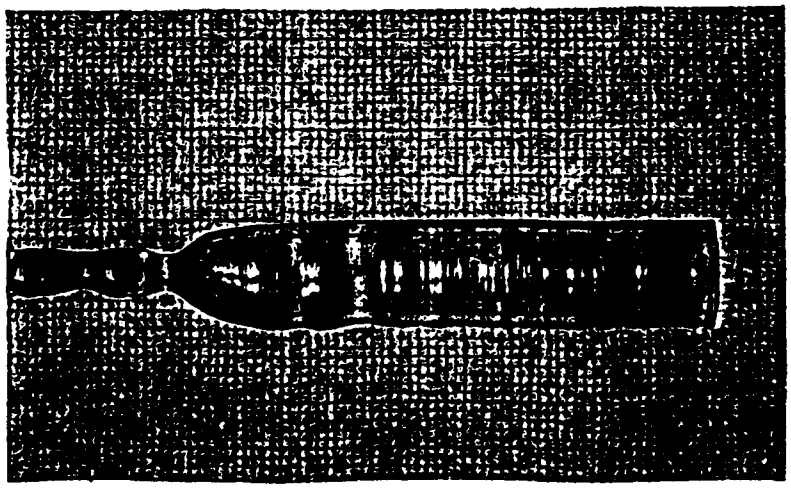

Figure 1. As grown DAO single crystal.

D38

THE GROWTH OF $NdAlO_3$ SINGLE CRYSTALS BY CZOCHRALSKI METHOD

*Yasuto Miyazawa, Hiroaki Toshima and Syouji Morita**
National Institute for Research in Inorganic Materials
1-1 Namiki Tsukuba-shi Ibaraki, Japan
*Mitsubishi Heavy Industries, Ltd.

1. Introduction. Perovskite-like rare-earth aluminate crystals, such as $LaAlO_3$, $YAlO_3$ have been considered to be suitable as substrate for high Tc oxide superconductor film. We have been searching other perovskite-like rare-earth aluminate. We chose $NdAlO_3$ as an example and tried to grow the single crystals by Czochralski method.

2. Experiments. $NdAlO_3$ single crystals were grown by conventional Czochralski method. The Iridium crucible whose size was 47 mmϕ x 48.5 mmh x 1.5 mmt was used for RF heating. The initial melt composition was strictly stoichiometric. Better than 4N quality of Nd_2O_3 and Al_2O_3 powders were used to make melt.

The growth conditions were the following.

pulling rate	2.0 mm/hr - 4.0 mm/hr
seed rotation rate	20 - 40 rpm
atmosphere	N2 (1 atm, 1.5 liter/min)

In Fig. 1 the photograph of an example of the grown single crystal was shown. No cracks and no bubbles were observed.

3. Discussion. The melting point of $NdAlO_3$ was estimated to be about 2080°C, which was much lower than reported value. The wafer cut from the crystal was observed by polarizing microscope. The twin boundaries were observed everywhere in the crystal. It may be concluded that it is very difficult to avoid twin formation.

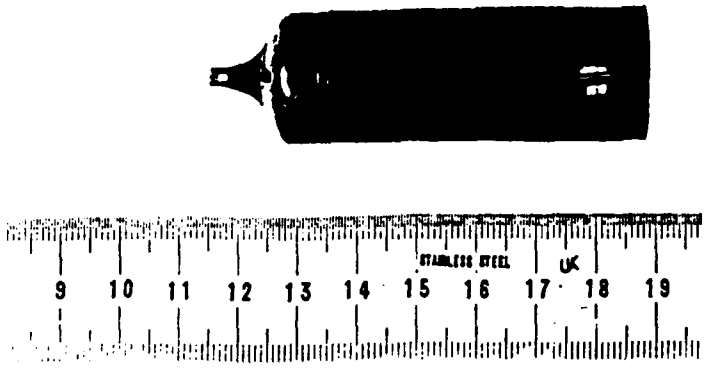

Figure 1. As grown $NdAlO_3$ single crystal.

GROWTH AND PROPERTIES OF $RAlO_3$ (R= Dy, Ho, Er) SINGLE CRYSTALS BY THE CZOCHRALSKI TECHNIQUE

D39

T. Ikeya, K. Hoshikawa and T Fukuda
Institute for Materials Research, Tohoku Univ.
2-1-1, Katahira, Aoba-ku, Sendai 980, Japan

Single crystals of rare-earth complex oxides are promising optical and magnetic materials. In the garnets, such as GGG, YAG and DyAG etc., a large number of studies on bulk crystal growth and properties for applications were published. On the other hand, in the series of perovskite-like compounds, there are no works except $YAlO_3$ on large size crystal grown from the melt, although a few reports on solution grown crystals. In this paper, we report on growth and properties of rare-earth ortho-aluminates ($RAlO_3$) single crystals, where R = Dy, Ho, Er. Characteristics features in growth processes and conditions for high quality crystal growth are discussed.

In order to investigate the growth and properties of $RAlO_3$, we used the Czochralski technique. Iridium crucible was utilized for containing melt and RF-heating in Ar gas flow. As the growth condition, crystal pulling rate was 5 mm/hr and rotation rate was 5~20 rpm, pulling direction was along c-axis. Crystals with 10~20 mm diameter and 30~60 mm length were obtained.

In $DyAlO_3$ single crystal growth, there are many difficulties. Typical $DyAlO_3$ crystal has twisted shape and a large number of cracks. Crack-free transparent $DyAlO_3$ crystals could be grown in very limited condition. Even in such cases, many twinning-planes parallel to (110) or (110) were observed. Whereas, in the case of $HoAlO_3$ and $ErAlO_3$, crystals were easily grown without twisting, crack and twinning, as shown in Fig. 1.

The as-grown crystals of $DyAlO_3$, $HoAlO_3$, and $ErAlO_3$ were colored yellow, brown, and pink, respectively. Absorption spectra were measured in the range of about 200 to 1100 nm. As can be seen in Fig. 2, in the spectrum of $DyAlO_3$, several strong peaks were observed in infrared region. And other physical properties, such as thermal conductivity and magnetic susceptibility, etc., were measured. In addition, material properties of $Ce:HoAlO_3$ and $Ce:ErAlO_3$ will also be reported.

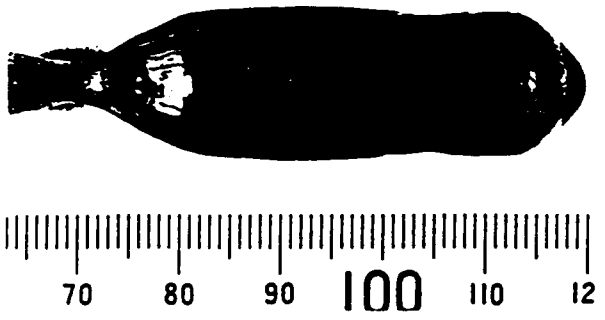

Figure 1. $HoAlO_3$ single crystal.

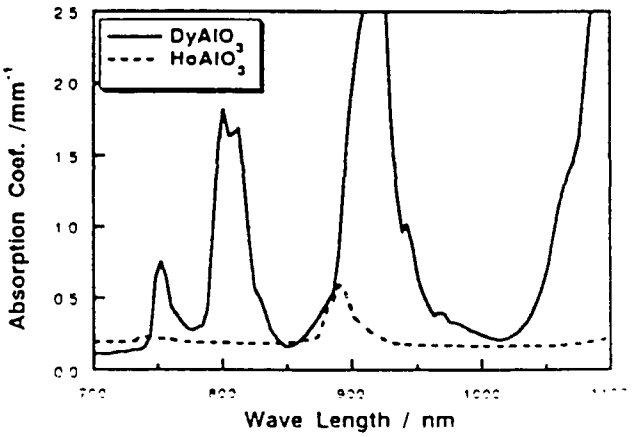

Figure 2. Absorption spectra of $RAlO_3$.

D40

PHASE DIAGRAM AND CRYSTAL GROWTH OF R_2CuO_4

K. Oka[1,2], *M.J.V. Menkena*[1], *Z. Tarnawski*[1], *A.A. Menovsky*[1], *A.J.M. Winkelman*[1], *T. Gortenmulder*[3], *A.M. Moe*[2], *T.S.Han*[2], *and H.Unoki*[2]

[1]Van der Waals-Zeemann Laboratorium Universiteit van Amsterdam
Valcknierstraat 65, 1018-XE Amsterdam, The Netherlands
[2]Electrotechnical Laboratory, Tsukuba, Ibaraki, 305 Japan
[3]Kamerlingh Onnes Laboratorium, Leiden Universiteit, 2300-RA Leiden, The Netherlands

Phase diagrams of La_2O_3-CuO system, Nd_2O_3-CuO system, $Nd_{1.85}Ce_{0.15}O_3$-CuO system and $La_{0.8}Sm_{1.0}Sr_{0.2}$-CuO system have been prepared to find crystal-growth conditions of R_2CuO_4 compounds. Differential thermal analyses of R_2CuO_4(R=La,Pr,Nd,Sm,Eu,Gd) systems have suggested the equivalent aspect of liquidus lines in each phase diagram. The concentration width of the liquidus line increases with increasing ionic radii of R^{+3} atoms (Fig. 1).

We have tried to grow single crystals of R_2CuO_4 systems by travelling-solvent floating zone and top-seeded solution growth methods, based on the phase diagrams.

Solution of R_2CuO_4 system caused much difficulty, e.g. evaporation of CuO melt, climbing of the melt along crucible wall and sucking up of the melt zone into polycrystalline feed rod.

A stable crystal growing by TSFZ method has been achieved by use of rapidly-crystallized feed rod in place of polycrystalline rod. To use the rapidly-crystallized material as the feed rod has advantages in keeping the homogeneous composition and decreasing the penetrate of solvent. So that the feed rod is not broken by solvent, though the growth speed is very slow, and the molten zone is kept for a long time.

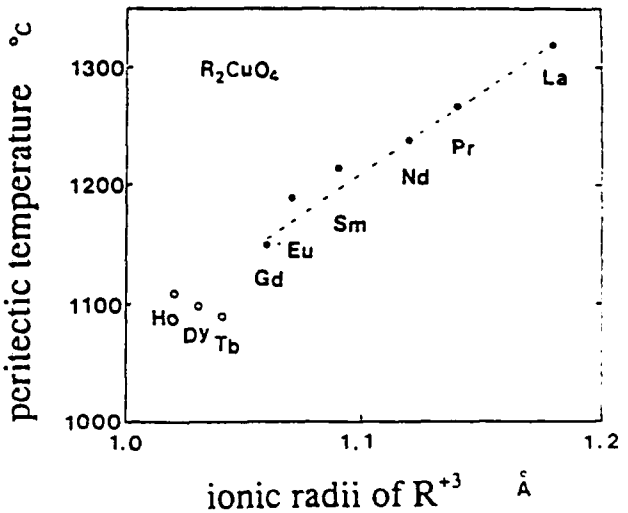

Figure 1

SINGLE CRYSTAL GROWTH OF Y-SUBSTITUTED $NdAlO_3$ BY THE FZ METHOD

D41

Isao Tanaka, Muneyoshi Kobashi and Hironao Kojima
Institute of Inorganic Synthesis, Faculty of Engineering,
Yamanashi University, Miyamae 7, Kofu, Yamanashi 400, Japan

$NdAlO_3$ crystals are used as the substrates for epitaxial growth of thin films of high-T_c oxide superconductors. However, the crystals of $NdAlO_3$ are twin crystals, so that it is problem that the twining lowers the orientation of the thin films. If $NdAlO_3$ is stabilized from the rombohedral phase to the cubic phase by substitution of a metal atom for Nd in $NdAlO_3$, twining would be removed in its crystals.

Fig. 1 shows the lattice parameters of sintered $Nd_{1-x}Y_xAlO_3$ by XRD. The lattice parameters of $a_H/\sqrt{2}$ and $C_H/2\sqrt{3}$ are equal to each other above 20 at%Y. Therefore, it was found that $NdAlO_3$ is stabilized from the rombohedral phase to the cubic phase by substitution above 20 at%Y for Nd in $NdAlO_3$.

The single crystals of undoped $NdAlO_3$ were grown easily by the FZ method using an infrared heating furnace. In the case of crystal growth of Y-substituted $NdAlO_3$ ($Nd_{1-x}Y_xAlO_3$), however, the molten zone was unstable during growth. Fig. 2 shows an as-grown crystal of $Nd_{1-x}Y_xAlO_3$. The as-grown crystal, about 5 mm in diameter and 50 mm in length, had some cracks as well as many gas bubbles. The Y concentration of the grown crystals was lower than that of the feeds, so that it seems that the distribution coefficient of Y into $NdAlO_3$ is smaller than unity. Consequently, the crystal growth of $Nd_{1-x}Y_xAlO_3$ has been investigating by the TSFZ method with using the solvent Y-richer than the feeds right now. We will discuss also the results of the crystal growth by the TSFZ method at this conference.

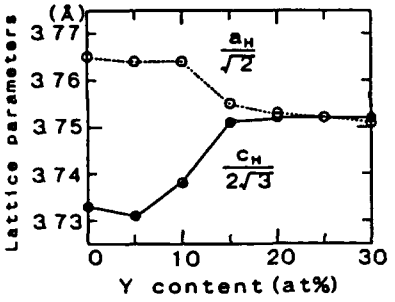

Figure 1. Lattice parameters of $Nd_{1-x}Y_xAlO_3$.

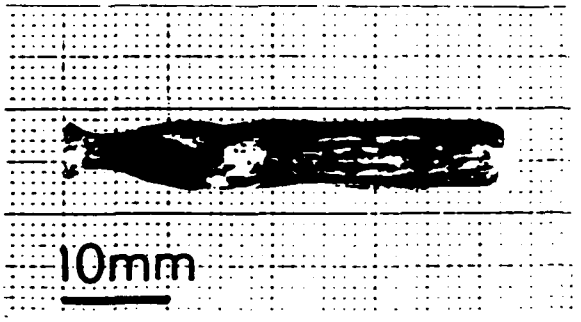

Figure 2. As-grown crystal of $Nd_{1-x}Y_xAlO_3$.

UNTWINED AND LARGE SIZE SINGLE CRYSTAL GROWTH OF YBCO

D42

C.T. Lin, W. Zhou and W.Y. Liang
IRC in Superconductivity, University of Cambridge
Cambridge CB3 OHE, UK
E. Schönherr and H. Bender
Max-Planck-Institute für Festkörporfortschung
Heisenbergstrsse I, 7000 Stuttgart 80, F. R. Germany

Large Size (up to 5 x 4 x 1.5 mm^3) single crystals of $YBa_2Cu_3Cu_{7-x}$ with perfect orthorhombic morphology were successfully grown from extra rich CuO flux in large alumina crucible. The crystals could be isolated from a CuO remaining flux by placing the crucible up side down with a Pt wire at 960°C. The number of nucleation centers could be reduced using a smooth inner wall crucible and a temperature oscillation method. By a treatment of thermomechanical technique, the twin domains in the crystals were readily removed and a single untwined domain was obtained. The conditions used were 10^7 N/m^2, 450°C and flowing oxygen. The structural characterization of both twin- and single-domain crystals was performed by high resolution electron microscopy. We also report the magnetic properties of the single crystals.

D43

ON THE FLUX GROWTH AND SOME PROPERTIES OF SUPERCONDUCTING $YBa_2Cu_3O_{7-x}$ SINGLE CRYSTALS AND LPE FILMS

P. Gönert, K. Fischer and C. Dubs
Institut für Physikalische
Hochtechnologie e.V., Helmholtzweg 4, O-6900 Jena, Germany

DTA/TG investigations were carried out in order to select suitable conditions for the flux growth of (i) pure and doped $YBa_2Cu_3O_{7-x}$ single crystals and of (ii) epitaxial films. The influence of oxygen partial pressure on the crystallization of the 123 phase has been studied carefully. Although reduced oxygen partial pressure results in lower crystallization and eutectic temperatures, till now the most single crystals with lateral dimensions (crystallographic ab-plane) of some mm and thicknesses of typical 50 - 150 µm and all LPE films were grown under normal air conditions.

Except twin boundaries the platelet $YBa_2Cu_3O_{7-x}$ crystals are relatively perfect. After annealing in oxygen a $T_c \approx 92$ K and a transition range of $\Delta T \approx 0.1$ K were measured by means of ac.susceptibility technique. The strongly anisotropic critical current densities j_c are $j_c ab \approx 10^4$ A/cm^2 ($\vec{B}$ parallel c) and $j_c c \approx 5 \times 10^2$ A/cm^2 ($\vec{B} \perp$ c) determined with a vibrating sample and a torque magnetometer at temperature T = 77 K and induction B = 1 T.

For the liquid phase epitaxy experiments the "LPE dipping technique" was applied. $YBa_2Cu_3O_{7-x}$ films were grown on $NdGaO_3$ and $LaGaO_3$ substrates as proved by optical polarization microscopy, scanning electron microscopy, microprobe measurements; by X-ray diffraction, and magnetic measurements. Partly the films show twin patterns without additional oxygen loading. The physical properties of the films will be compared with those of single crystals and discussed in terms of the preparation conditions.

All correspondence to: Prof. Dr. P. Görnert, IPHT Jena, Helmholtzweg 4, O-6900 Jena, Germany.

D44

ATTENUATION OF GRAIN BOUNDARY EFFECTS IN CRYSTALLINE SUPERCONDUCTING $YBa_2Cu_3O_7$

R. Cabré, R. Solé, X. Ruiz, M. Aguiló, C.F. Woendregt and F. Díaz*
Laboratory and Crystallography, University of Barcelona at Tarragona
*Institute of Sciences, Faculty of Geochemistry, Section of Crystallography, Utrecht, the Netherlands

After the discovery of high-T_c superconductors copper oxides, such as YBa_2Cu3_{7-x}, many efforts have been made to obtain high critical current densities in polycrystalline aggregates. This may be achieved by the preferred orientation of the high T_c copper oxide grains in such a way that the high-J_c directions are aligned in the direction of the current travel. The process of thermal texturation seems to be effective in order to produce such an orientation. In the present study the results of the thermal texturation of polycrystalline materials and the formation of oriented grains will be presented.

First polycrystalline $YBa_2Cu_3O_{7-x}$ has been synthesized by heating during 16 hours at 930°C the stoichiometric mixture of its constituent oxids in the presence of an excess of oxygen. After grinding the thus obtained crystalline powder this process has been repeated two times more. Rectangular shaped bars (dimensions 30x10x6 mm) have been produced by the process of dry pressing, i.e filling of a closed rectangular die with the polycrystalline $YBa_2Cu_3O_{7-x}$ powder and subsequentially pressing at 500 MPa with a plunger.

This sample is heated in a two-zone vertical tubular furnace in such a way that there exists a gradient parallel to its vertical bar axis of 27°C/cm. First the sample is heated during 2.5 minutes at 1070°C and subsequently cooled down slowly (6°C/hr), and oxygenized at T<900°C (see fig. 1). At the highest temperature the sample is partly melted. This melt will percolate downwards and react with the lower levels of the sample. At the highest level, which was submitted to the highest temperatures, the bar is fully recrystallized and clearly textured, showing $YBa_2Cu_3O_{7-x}$ crystals, of which the largest elongation is about 3-4 mm. X-ray analysis of the bar shows that besides $YBa_2Cu_3O_{7-x}$ also $BaCuO_2$ is present.

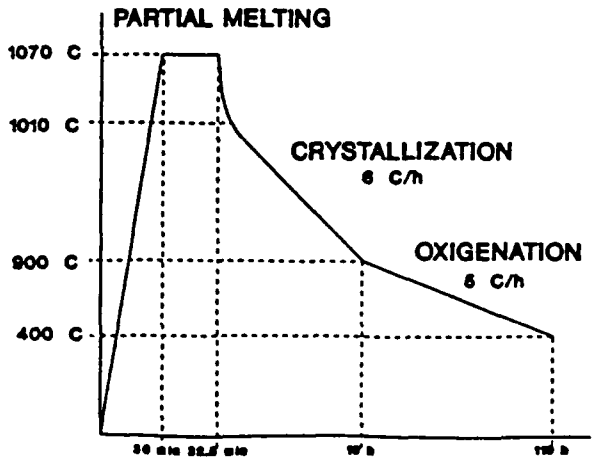

Figure 1.

D45

IMPROVEMENT OF SUPERCONDUCTIVITY IN YBCO SINGLE CRYSTALS

Wang Yao Shui, P. Bennema, Zheng Manna, C.M. Fu, C. Grey, L.W.M. Schreurs, Q. Xu**, P. van der Linden and Y. Bruynseraede***
Research Institute for Materials, University of Nijmegen
Toernooiveld, 6525 ED Nijmegen, The Netherlands
*Fujian Institute of Research of the Structure of Matter, Fuzhou 350002, China
**Physics Departments, University of Leuven, B-3030 Leuven, Belgium

An effective procedure for the improvement of superconductivity in the YBCO compound by increasing the oxygen content in the crystals is proposed, which uses the strong oxidizer Barium peroxide (BaO_2) in place of $BaCO_3$ and self-flux for preparing the crystals. Oxygen evolution experiments are used to show the differences of oxygen content in the as-grown crystals. The total amount of evolved oxygen from samples prepared using BaO_2 was considerably higher, implying that BaO_2 may provide more oxygen to the crystals. Magnetization measurements indicate that, by using BaO_2, the superconducting transition temperature of the as-grown crystals is several degrees higher and the crystal quality was much better, than when $BaCO_3$ is used. BaO_2 may also be involved in a partial oxidation of Cu(II) into Cu(III). The mixed-valence of copper is necessary for superconductivity. Some new procedures, for instance, the double crucibles method and the liquid flow technique, which were developed in the university of Nijmegen for the crystal growth are also reported.

D46

CRUCIBLE FREE TECHNIQUES IN HIGH T_c CRYSTAL GROWTH

T. Frieling, J. Kowalewsky, F. Ritter, W. Assmus
J.W. Goethe-University, Physikalisches Institut
Robert Mayer Strasse 2-4, D-6000 Frankfurt/Main, Germany

The growth of high quality YBCO (123-Phase) single crystals from a BaO/CuO-flux with several mm length in all dimensions is difficult. The strong anisotropy of the maximum growth rate and the incongruent melting behaviour requires a low growth rate, on the other side there is a lack of suitable crucible materials. All crucibles are attacked by the BaO/CuO-flux which makes a high growth rate necessary. The solution of this problem are crucible free or quasi crucible free methods.

We report on two different crucible free techniques. In the first a block of an YBCO/flux mixture which never melts completely is placed on a ZrO_2-plate. The mixture is heated up to the melting temperature of the flux. Here a grain growth mechanism is responsible for crystal growth.

The second technique which we present is a combination of the pedestal method and THM. A pressed and densified pellet of YBCO is used as crucible for the saturated BaO/CuO-flux. As seed we use a cooled YBCO single crystal grown by the first technique. Stirring by accelerated crucible rotation (ACRT) increases the achievable growth rate.

Both methods are discussed in detail.

D47

HIGH OXYGEN PRESSURE $Po_2 \leq 3000$bar) CRYSTAL GROWTH OF DOUBLE CHAIN YBaCuO

J. Karpinski, E. Kaldis, H.-J. Lang and S. Rusiecki
Laboratorium für Festkörperphysik ETH 8093-Zurich

In order to grow single crystals of the 247 and 124 double chain YBaCuO phases, a high oxygen pressure atmosphere is necessary. Direct melting of 124 samples under high oxygen pressure shows that at $Po_2 \leq 3000$bar 124 melts incongruently and decomposes to 211 and 023 phases. Therefore, in order to decrease the melting temperature and avoid peritectic decomposition use of flux is necessary. The oxygen pressure has been varied for different experiments from 59 to 2800bar. The composition, number and size of crystals depend on the various experimental parameters, Po_2, T_{max},time, cooling rate, composition of the flux. The flux used for crystal growth contains $BaCuO_2$, and CuO in addition to the YBaCuO phase. This changes the phase equilibrium of the system [1,2]. However, the crystals grow at higher temperature and higher pressure much faster, than under normal pressure. Therefore, instead of the weeks necessary for obtaining milimeter size crystals of the 123 phase at Po_2=1bar, 12-24 hour are enough to grow 124 crystals under pressure. As a result of many crystal growth experiments we have obtained hundreds of crystals under various oxygen pressures from 50 to 2800 bar. The maximum size of the crystals is 7-8 mm length and 1.5 mm width, the average length 1-0.8 mm and width 0.5 mm. The morfology of the growth interface has been investigated by STM and SEM [1,2]. It is atomically flat with step height equal to the lattice constants. Based on the STM and SEM results a discussion of the growth mechanism will be given. The depletion zone near the step edges is seen directly for the first time. Appreciable evidence for a mixed VLS growth mechanism is existing.

1. E. Kaldis, J. Karpinski, S. Rusiecki, Proceedings "Toshiba Inter. School of Superconductivity," *Kryoto*, July 1991.
2. J. Karpinski, E. Kaldis, K. Conder, S. Rusiecki, E. Jilek, Proceedings of Fall MRS Meeting Boston Dec. 91.

GROWTH OF BULK SINGLE CRYSTALS IN 1-2-3 OXIDE SUPERCONDUCTORS

D48

S. Hayashi, Y. Nishimura, T. Inoue, S. Miyashita and H. Komatsu
Institute for Materials Research, Tohoku University, Sendai 980, Japan

Bulk single crystals of $RBa_2Cu_3O_{7-\delta}$ (R=Eu, Gd and Nd) were grown from a Ba and Cu-rich flux in MgO crucibles, by slow cooling at a rate of 2°C/h. Single crystals were about 5x5x5 mm3 in average size and of parallelepiped with edges parallel to the direction of <100>, separated from the solidified matrix by melting at 950°C (fig. 1). ICP analysis shows that the ratio of cations was close to 1:2:3 and traces of Mg from MgO crucibles were detected in the bulk single crystals. Crystal surface morphology was observed under an optical microscope to analyse the growth mechanism of the bulk single crystals. As a result of annealing in oxygen gas flow, many fine twins were introduced in the crystals. All of the single crystals showed a superconducting behavior in electrical measurements, however, the Tc-values (mid-point) were scattered in the range of 60°80 K. Resistance anisotropy along the c-axis was measured about 40 times as large as that in the c-plane as shown in fig. 2. To control the twin boundaries, an annealing treatment under a stress was applied for the crystals with multi-domain structures.

Details are described for the growth conditions, crystal characterization and growth mechanism of the bulk single crystals.

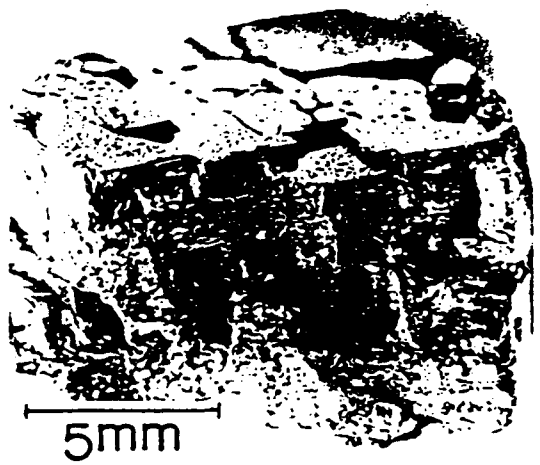

Figure 1. The bulk single crystal (max. size) of $NdBa_2Cu_3O_{7-\delta}$.

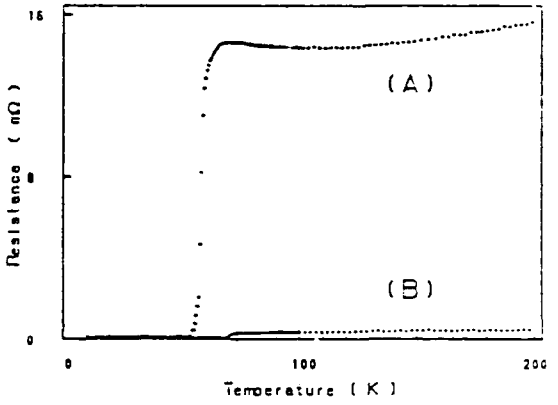

Figure 2. Temperature vs. resistance of the parallel (A) and perpendicular (B) to c-axis for $EuBa_2Cu_3O_{7-\delta}$.

D49

SOLIDIFICATION IN A MAGNETIC FIELD: APPLICATION TO $YBa_2Cu_3O_7$

R. Tournier
CRTBT/CNRS Grenoble France

High inhomogeneous magnetic fields can levitate paramagnetic substances and even diamagnetic organic materials. In the second case, levitation can be stable without crucible. A magnetic force can also be used to enhance or to suppress buoyancy-driven convection in a normal paramagnetic fluid which has a susceptibility varying with temperature, the sign of the effect depending of the relative orientation of magnetic fields and temperature gradients. Crystal growth from liquids submitted to a magnetic force in which the natural convection is damped can be monitored.

In addition, texturing of anisotropic magnetic material such as $YBa_2Cu_3O_{7-\delta}$ can be produced by solidification in a magnetic field. High transport d.c. currents larger than 11000 A/cm2 have been measured in H-7 tesias at 77 K for $H \perp I$ in the (ab) plane.

Nature (1991), 340, 470, 349, 6312, 354, 134.

D50

X-RAY CHARACTERISATION OF LASER ABLATED TEXTURED $YBa_2Cu_3O_{7-x}$ THIN-FILMS ON Zr, Si, MgO AND $SrTiO_3$ SUBSTRATES

M. Steins, F. Mattheis, R. Gaebel, K. Bente and H.-U. Krebs**
Mineralogisch-Kristallographisches Institut
*Institut für Metallphysik, University of Göttingen, Germany

The studied thin-films of $YBa_2Cu_3O_{7-x}$ were produced by pulsed laser ablation. The superconducting properties of these films are highly correlated with their orientation and texture. The texture- and orientation-measurements were done on a four-circle diffractometer and on a special thin-film diffractometer in guinier-geometry, using x-rays. With both instruments it is possible to get information in the growth direction as well as in the film plane.

The best properties ($T_c \approx 91K$, $j_c(77K) > 3 \cdot 10^6 A/mm^2$) were obtained on single-crystal substrates with lattice-constants near to the a/b lattice constants of $YBa_2Cu_3O_{7-x}$. By using $SrTiO_3$ as substrate, $YBa_2Cu_3O_{7-x}$ grows epitaxially with very good texture in the c-direction and in the a/b-plane. The crystallinity allows "Quasi-Single-Crystal Structure-Refinements" with x-ray reflection data. The results show the crystal-structure of the film to be in agreement with refinements based on single-crystal data. On MgO, the films grow epitaxially too, but the texture is not as good as on $SrTiO_3$, due to the larger lattice mismatch in MgO. The disadvantage of these both substrates are their small available sizes, high costs and deficiency of plasticity.

Silicon single-crystal substrates are much cheaper and available in sizes up to 20 cm in diameter, but silicon atoms diffuse into the film, which reduces T_c to about 84K. Additionally, only c-axis textured films on Si were synthesized with an FWHM of nearly 15°. In the a/b-plane no orientation was observed.

With respect to the price and the plasticity and to reduce the diffusion between substrate and film, Zr-sheets were used as substrates for $YBa_2Cu_3O_{7-x}$-films. During the deposition process, the sheets oxidize to a depth of 5µm to a high textured black crust of ZrO_2 (Baddelyite). The films are c-axis textured with a FWHM of 12° and show a preferred orientation in the a/b-plane. This orientation of the thin film is strongly correlated with the texture of the precursing ZrO_2. Different surface treatments of the Zr-sheet reveal different texture qualities. Polishing of the Zr-sheets before the film deposition produces much better oriented films in c-axis direction (FWHM = 3°), but the orientation in the film plane is not improved by this method. Chemical polishing by reaction in Se-atmosphere results in smoothed Zr-surfaces, but the quality of texture decreases in all directions in comparison with untreated substrates.

The influence of the orientation, the structure and the surface of substrates on the superconducting properties will be discussed.

$YBa_2Cu_3O_{7-\delta}$ THIN FILMS GROWN ON FERROELECTRIC $Bi4Ti_3O_{12}$ CRYSTAL BY r.f. SPUTTERING

D51

M.E. Mendoza-Alvarez, C. Tabares-Muñnoz*, J.G. Mendoza-Alvarez** and O. Alvarez-Fregoso****
*Inst. of Physics, UAP;
**Physics Dept.- CINVESTAV/IPN
***IIM-UNAM, MEXICO

$Bi_4Ti_3O_{12}$ is a displacive ferroelectric layered oxide formed by Bi_2O_2 layers and stacks of perovskite-like layers along the [001] axis. Bismuth titanate single crystals were grown using the spontaneous nucleation technique at high temperature [1]. The crystals obtained present a lamellar habit with a mica-like aspect, they are transparent with a clear yellow color. These bismuth titanate crystals were used as substrates to grow $YBa_2Cu_3O_{7-\delta}$ thin films by the r.f. sputtering technique changing the substrate temperature in the range 50-200°C. As a target a ceramic superconductor was used [2]. Optical microscopy examination shows a good film uniformity; the average thickness was around 800Å. X-ray powder diffraction patterns show the typical reflections for $YBa_2Cu_3O_{7-\delta}$ at $2\Theta = 32.88°$ and 38.54°, corresponding to the (013) (110) (103) and (014) (005) (104) planes respectively [3]. Structural properties and the possible superconductivity phase in these films will be discussed.

[1] F.S. Galasso in Inorganic Syntheses. Ed. J.K. Ruff [Mc Graw-Hill, New York 1973] Vol. XIV.
[2] C. Tabares-Muñoz, v. Pacheco-Espejel, M. Sosa-Rivadeneyra M.E. Mendoza-Alvarez, Superficies y Vacío 2, 69 (1990).
[3] P.K. Gallagher, H.M. O'Bryan, S.A. Sunshine & D.W. Murphy, *Mater. Mater. Res. Bull*, 22, 7(1987).

DEPOSITION OF $LiNbO_3$ THIN FILMS ON C-AXIS ORIENTED EPITAXIAL $Y_1Ba_2Cu_3O_{7-\delta}$ FILM BY PULSED EXCIMER LASER ABLATION

D52

S.B. Ogale and Rashmi Nawathey-Dikshit
Center for Advanced Studies in Materials Science and Solid State Physics
Department of Physics, University of Poona, Pune 411 007, India

Deposition of stoichiometric and epitaxial films of $LiNbO_3$ on different substrates is considered an important problem due to the well known importance of $LiNbO_3$ material in optoelectronics. Integration of $LiNbO_3$ with the new oxide based high T_c superconductors is considered even more important due to the immense device possibilities offered by such a material combination. In this work, Pulsed Excimer Laser ablation is used to deposit $LiNbO_3$ thin films on epitaxial c-axis oriented $Y_1Ba_2Cu_3O_{7-\delta}$ films grown on (001) Y-stabilised ZrO_2 substrates by laser ablation. The laser is operated at the wavelength of 248 nm and the laser energy density is held fixed at 2 J/cm^2. The effects of the nature and the partial pressure of the ambient and the substrate temperature on the quality of the grown film are examined by using the X-ray diffraction, Scanning Electron Microscopy, Rutherford BackScattering and spectroscopic ellipsometry techniques. Initial parameter optimisation studies for achieving the desired stoichiometry have been performed by depositing the $LiNbO_3$ films on (001) Silicon substrates and the corresponding results have been used as guidelines for realisation of high quality films on the $Y_1Ba_2Cu_3O_{7-\delta}$ surface. It is shown that depositions in vacuum or in pure oxygen atmosphere lead to Lithium deficient films and that the correct stoichiometry can be attained only if the deposition is carried out in a mixture of O_2 and Ar. The optimum partial pressures of O_2 and Ar are found to be 100 and 400 mTorr respectively. The films deposited under these conditions are found to be dense with a dielectric constant in the range between 2.2 to 2.3 over the entire visible spectrum. It is suggested that inclusion of inert gas controls the kinetics of the reactive radicals impinging on the surface of the growing film via modifications of the properties of the laser generated plasma and thereby the reactive sputtering during film formation. The substrate temperature variation over a range between 400°C and 700°C is also shown to influence the film growth significantly. The systematics of these data will be presented and the issues of the dependence of film texture and degree of epitaxy on the growth conditions will be analysed.

D53

GROWTH, CHARACTERIZATION AND SUPERCONDUCTING PROPERTIES OF CRYSTALS OF THE Tl-Ba-Ca-Cu-O SYSTEM

J.P. Chaminade, J.C. Frison, P. Dordor, J.C. Grenier, M. Pouchard and J. Etourneau
Laboratoire de Chimie du Solide du CNRS, 351, course de la
Libération, 33405 Talence Cedex, France
Pham V. Huong
Laboratoire de Spectroscopie Moléculaire et Cristalline (URA 124, CNRS)
351, cours de la Libération, 33405 Talence Cedex, France
B. Giordanengo, A. Sulpice and R. Tournier
Centre de Recherches sur les Très Basses Températures CNRS
BP 166 X, 38042 Grenoble, France

Plate-like crystals of mm size have been grown in the Tl-Ba-Ca-Cu-O system using $BaCuO_2$-CuO rich melts containing Tl_2O_3 and CaO oxides. They have been classified from their lattice parameters as belonging to different families having 1212, 1223, 2201, 2212 and 2223 ideal stoechiometry.

Several chemical and physical characterizations have been done by means of x-ray and microprobe analysis, optical and electronic microscopies, micro-raman spectroscopy, resistivity and magnetic measurements. On the basis of these results, some characteristic features of the system can be related:

- presence in the same batch of single crystals and polycrystals (syntactic intergrowth crystals),
- variation of lattice parameters and chemical composition within a same ideal family and consequently on the superconducting transition. For example "2201" crystals show Tc varying from 19K to 104K.
- preferential departure of one TlO chain layer in "2212" by thermal treatment,
- strong anisotropy as demonstrated by a large $\frac{Hc1 // \vec{c}}{Hc1 // \vec{ab}}$ ratio of about 1000 deduced from the fist magnetization curve of a "2212" crystal.
- improvement of the superconducting property by oxygen or argon annealing depending of the initial state of the crystals.

D54

THE SURFACE MORPHOLOGY, CRYSTAL HABIT AND GROWTH MECHANISM OF $RBa_2Cu_3O_x$ (R=Y, Gd, Tm) SINGLE CRYSTALS

Hong Wang
CCAST (World Laboratory), P.O. Box 8730, Beijing 100080
Mail address: Institute of Crystal Materials, Shandong University, Jinan 250100, P.R. China
Shuxia Shan
Experimental Centre, Shandong University, Jinan 250100, P.R. China
Zhuo Wang
ICM, Shandong University, Jinan 250100, P.R. China
Xiaonong Shen
Physics Department, Yantai University, Yantai

The surface morphology and crystal habit of high Tc superconducting single crystals $RBa_2Cu_3O_x$ (R=Y, Gd, Tm) have been investigated by scanning electron microscopy. The crystal growth process and growth mechanism were discussed. It is found that the well developed $RBa_2Cu_3O_x$ (R=Y, Gd, Tm) crystals have a plate-like form with square corners, while the developing crystals have more faces, e.g. (110), (111), (011) faces, these faces will gradually disappear along with the crystal growing up. The crystal growth mechanism is two-dimensional nucleation, layer by layer growth process on smooth surface of crystal grown in Pt crucible, but for crystals grown in Al_2O_3 crucible there are many spiral island in (100)/(010) surfaces, this indicates the spiral growth mechanism. The anisotropy of surface growth rate is observed and the ratio of width versus thickness of crystals depends on growth condition. This result is similar to the prediction of PBC theory. The relation between defects and the critical current Jc of single crystal and sputtered film of $YBa_2Cu_3O_x$ was also discussed.


POSTER SESSION
NUMBER 3
THURSDAY
3:15 PM
EXHIBIT HALL

POSTER SESSION #3
EXHIBIT HALL
Thursday 3:15 PM

A31
Numerical Application of TIC Float Zone Growth
Y. T. Chan* and H. L. Grubin
Scientific Research Associates, Inc., USA

A32
Influence of Some Parameters on Interface Shape During Temperature Gradient Technique (TGT)
P. Pan* and G. Liu
Shanghai Institute of Ceramics, China

A33
Radiation-Conductive Heat Transfer in Optical Crystals
Yu. Lingart
Crystal Growth & Equipment (CGE), Czechoslovakia

A34
Ordered Structure in Non-Axisymmetric Flow of Molten Silicon Convection
K. Kakimoto,* M. Watanabe, M. Eguchi, and T. Hibiya
NEC Corporation, Japan

A35
Experimental Investigation of The Effect of Thermosolutal Convection On Crystal Growth
B. J. Lee, M. S. Kang and Z. H. Lee*
KAIST, Korea

A36
Computations of the Temperature Distribution in Crystals Grown by the Vertical Bridgman Method
K. Grasza
Polish Academy of Sciences, Poland

A37
Observation of Crystal-Melt Interface Shape in Simulated Czochralski Method with Model Fluid
A. Hirata, M. Tachibana,* Y. Okano, and T. Fukuda
Waseda University, Tohoku University, Japan

A38
Visualization of Low Prandtl Number Convection in Czochralski Melts
U. Krzyminski and A. G. Ostrogorsky*
Technical University Munich, Germany; Columbia University, USA

A39
Computer Simulation of a Furnace for High-Purity Czochralski Grown Ge Crystals
T. A. Cherepanova,* A. F. Spivak, A. V. Gusev, O. V. Potapov, and V. A. Gava
Center for Microelectronics, Latvia; Institute of High-Purity Materials, Russia

A40
Integrated Heat Transfer Analysis for Complete Vertical Bridgman Crystal Growth Systems
D. E. Bornside and R. A. Brown
Massachusetts Institute of Technology, USA

A41
Transport Phenomena in Metallic Solutions with Special Regard to Thermal Diffusion
T. Boech* and A. N. Danilewsky
Humboldt-University of Berlin, Albert-Ludwigs-University of Freiburg, Germany

A42
Baroclinic Flow Instability in the Rotating Silicon Melt
M. Watanabe,* M. Eguchi, K. Kakimoto, Y. Baros, and T. Hibiya
NEC Corporation, Japan

A43
Morphological Instability in Epitaxially-Strained Dislocation-Free Solid Films
B. J. Spencer,* P. W. Voorhees and S. H. Davis
Northwestern University, USA

A44
Nucleation-Limited Aggregation in Crystal Growth
N.-b. Ming, M. Wang,* and R.-W. Peng
Nanjing University, China

A45
Estimation of Diffusion Coefficients and a Plausible Identification of Species from One Dimensional Liesegang Ring Formations in Multicomponent Systems
G. Varghese, M. A. Ittyachen* and C. Joseph
Mahatma Gandhi University, India

B61
Growth of Bubble Free BSO and BGO Crystals-Fluid Flow Analysis
D. Krishnamurthy,* R. Gopalakrishnan, D. Arivuoli, and P. Ramasamy
Anna University, India

B62
Habit And Defects of Bismuth Silicon Oxide Crystal (BSO)
W. Zhong, H. Luo, Z. Lu, and T. Zhao
Chinese Academy of Sciences, China

B63
Etch Morphology of Bismuth Silicate (BSO) Crystal
W. Zhong, H. Luo, Z. Lu, and T. Zhao
Chinese Academy of Sciences, China

B64
Computer Simulation of the Growth of BSO with Elliptic Adaptive Grid Procedure
G. S. Liaw,* Y. M. Zheng and L. C. Chou
Alabama Agr & Mech University, USA

B65
Impurity Induced Photochromic Behavior in $Bi_{12}SiO_{20}$:Mn, Cr Crystals
L.-Y. Xu, J.-c. Liu, B.-y. Shu, and B. Xiao
Shanghai Institute of Ceramics, China

B66
Crystal Growth of Compounds in the $MgO\text{-}Nb_2O_5$ Binary System
E. Bruck,* R. K. Route and R. S. Feigelson
Stanford University, USA

B67
$Bi_6Te_2Mo_2O_{21}$ - A New Synthetic Crystal and Its Physical Properties
M. Deng
Chinese Academy of Sciences, China

B68
Mechanical Behavior of Flux Grown $LaBO_3$,$RFeO_3$,(R=Y,Dy & YB) Crystals
A. Jain, K. K. Bamzai, U. Raina, S. Beigh, P. N. Kotru,* and B. M. Wanklyn
University of Jammu, India

B69
Effects of ZrO_2 And Sc_2O_3 Addition on FZ-Growth of Rutile Single Crystals
M. Higuchi* and K. Kodaira
Hokkaido University, Japan

B70
The Growth of Al_2O_3 Single Crystals by Czochralski Method
S. Morita,* H. Sekiwa, H. Toshima, and Y. Miyazawa
National Institute for Research, Japan

POSTER SESSION #3
EXHIBIT HALL
Thursday 3:15 PM

B71
Deposition of Epitaxial Cu_2O Films on (100) MgO by Laser Ablation and their Processing using Ion Beams
S. B. Ogale, P. G. Bilurkar,* N. Parikh, B. Patnaik, and D. D. Sharma
University of Poona, India

B72
Etching Characteristics of (110) and (001) Faces of Flux-Grown $ErFeO_3$ Single Crystals
K. K. Sharma, A. K. Razdan, P. N. Kotru,* and B. M. Wanklyn
University of Jammu, India

B73
Studies On (0001) Cleavages, Etchings and Microhardness of Flux Grown M-Type Hexaferrites
U. Raina,* S. Bhat, P. N. Kotru, and F. Licci
University of Jammu, India

B74
Flux Growth of Bulk Single Crystals of Pure and Substituted $BaFe_{12}O_{19}$ using Solvents of The Na_2O-B_2O_3 System
R. Varadinov, V. Nikolov, and P. Peshev*
Bulgarian Academy of Sciences, Bulgaria

B75
Optimization of Monolitic ZnSe Fabrication by Chemical Vapour Deposition
T. A. Cherepanova,* A. F. Spivak, E. M. Gavrishchuk, and I. A. Korshunov
Latvian Academy of Sciences, Latvia

B76
Characterization of ZnTe Epitaxial Films Grown by MOVPE
N. Lovergine, A. M. Mancini, D. Manno, and L. Vasanelli
Universita' di Lecce, Italy

B77
Direct Observation of Point-Defect-Assisted Growth of Bulk ZnSe
K. Terashima,* T. Hayashi and E. Tokizaki
Kimura Metamelt Project, Japan

B78
Control of Microtwins in MOCVD of CdTe on Sapphire
H. L. Glass,* M. L. Buehnerkemper, D. L. Varnum, and T. P. Weismuller
Rockwell International, USA

B79
The Growth of Cubic, Single Phase, Single Crystal $Cd_{0.6}Mn_{0.4}Te$ By The Vertical Gradient Freeze (VGF) Method
M. Azoulay,* R. Weingarten, H. Schacham, and H. Feldstein
Israel Atomic Energy Commission, Israel

B80
Segregation Engineering during Crystal Growth by the Travelling Heater Method
P. Gille,* R. U. Bloedner and N. Puhlmann
Humboldt University of Berlin, Germany

B81
The Correlation Between Supercooling and Overheating in Associated Semiconductor Melts During Unseeded Bridgman Growth
M. Muhlberg,* P. Rudolph, M. Laasch, and E. Treser
Humboldt University of Berlin, Germany

B82
Determination of Phase Equilibrium Data in the Hg-Cd-Te System from LPE Experiments
T. Boeck* and K. Jacobs
Humboldt-University of Berlin, Germany

B83
Variation of Surface Morphology with Precursors Supply Ratio in MOVPE CdTe Layers
T. Ferid,* M. Ekawa, K. Yasuda, A. Tanaka, and M. Saji
Nagoya Institute of Technology, Japan

B84
Growth and Characterization of Some I-III-VI Compound Semiconductors
K. Balakrishnan,* B. Vengatesan and P. Ramasamy
Anna University, India

B85
Crystal Growth of $AgGaS_2$ by the Bridgman-Stockbarger-Technique Using Shaped Crucibles
E. Treser,* E. Post and V. Kramer
Albert-Ludwigs University Freiburg, Germany

B86
Growth and Characterization of CdS Films Deposited on $CdInGaS_4$ by Evaporation Method
S. Ando, S. Endo, H. Nakanishi, T. Irie, and T. Toyoda
Science University of Tokyo, Japan

B87
Growth of ZnTe by Physical Vapor Transport and Traveling Heater Method
C.-H. Su,* M. P. Volz, D. C. Gillies, F. R. Szofran, S. L. Lehoczky, and M. Dudley
NASA, USA

B88
High Pressure Bridgman Growth of ZnTe And ZnSe
F. P. Doty* and J. F. Butler
Aurora Technologies Corporation, USA

B89
Growth And Characterization of ZnSe for Low Temperature Calorimetry Applications
F. Allegretti,* A. Carrara and S. Pizzini
University of Milan, Italy

B90
Transport Rate And Epitaxial Growth of $Hg_{1-x}Zn_xTe$ by Chemical Vapor Transport In A Closed Ampoule
Y.-G. Sha,* C.-H. Su, S. L. Lehoczky, and F. R. Szofran
NASA, USA

C35
Improvement of High Brightness AlGaAs/GaAs DH Red LED under Optimized Growth Condition
B. T. You, J. Y. Kao, J. R. Deng, J. S. Shea, Y. S. Chang, C. Y. Juan, and T. P. Chen
Industrial Technology Res. Institute, China

C36
A Mass Production Method for High Brightness 655 nm AlGaAs Double Heterostructure Red LED
J. S. Shea, J. Y. Kao, B. T. You, J. R. Deng, Y. S. Chang, C. Y. Juan, and T. P. Chen
Industrial Tech. Research Institute, China

C37
Lattice Compensation Effect in GaAs n^+-n^- Junctions using Liquid Phase Epitaxy
T. Kamiya, A. Tomita, M. Kimura, A. Tanaka, and T. Sukegawa*
Shizuoka University, Japan

C38
In-Situ Observation of Morphological Change on LPE Grown Surface in Semiconductor
Y. Inatomi and K. Kuribayashi
The Inst. of Space & Astro Science, Japan

C39
Defect Formation in Semiconductor Layers during Epitaxial Growth
B. Steiner, W. Tseng, J. Comas, U. Laor, and R. C. Dobbyn
NIST, USA

POSTER SESSION #3
EXHIBIT HALL
Thursday 3:15 PM

C40
Growth Kinetics of Vapor Grown SiC
T. Kaneko
Science University of Tokyo, Japan

C41
Epitaxial Growth of Cubic SiC by Hot Filament CVD
Y. Hirabayashi, S. Karasawa and K. Kobayashi
Institute of Industrial Research, Japan

C42
A Thermodynamical Approach to Tetramethylsilane (TMS) Pyrolysis, Application to SiC Coatings Obtained by LPCVD
S. Veintemillas-Verdaguer, A. Figueras-Daga,* and R. Rodriguez-Clemente
Institut de Ciencia de Materiales, Spain

C43
An Experimental Study of the Effects of Temperature, Fluid Flow, and Gas Precursors in Epitaxial Growth of SiC Thin Films on Si Substrates
B. Bahavar, M. I. Chaudhry and R. J. McCluskey
Clarkson University, USA

C44
Growth of Secondary Particles of SiC Polyhedra
Y. Ando and H. Iwanaga
Meijo University, Japan

C45
MOCVD SiC Layers Morphology and Textures Dependence on Thickness and Total Pressure
J. Santiso,* A. Figueras, R. Rodriguez-Clemente, B. Armas, C. Combescure, A. Mazel, Y. Kihn, and J. Sevely
Institut de Ciencia de Materiales, Spain

C46
Crystal Growth of Epitaxial CVD Diamond using C-13 Isotope and Characterization of Dislocation by Raman Spectroscopy
S. Karasawa,* M. Mitsuhashi, S. Ohya, K. Kobayashi, T. Watanabe, and F. Togashi
Industrial Research Institute, Japan

C47
High Quality Thick Diamond Films by Biased Hot Filament CVD
L. Hou, P. Yang, X. Pu, Z. Xuan, L. Qi, and G. Hu
R.I.S.C., China

C48
Ion Beam Deposition of Amorphous Films of Cubic And Hexagonal Diamond
V. E. Mashchenko, V. M. Puzikov, A. V. Semenov, and D. I. Zosim
Academy of Sciences Ukraine

C49
Synthesis And Morphology of CVD Diamond on Ta and TaC Film
F. Togashi,* K. Kobayashi, M. Mitsuhashi, S. Karasawa, S. Ohya, and T. Watanabe
Science University of Tokyo, Japan

C49
The Growth of Thick GaN Film on Sapphire Substrate by using ZnO Buffer Layer
T. Detchprohm, H. Amano, K. Hiramatsu,* and I. Akasaki
Nagoya University, Japan

C50
Growth of Single Crystalline GaN on Si Substrate using AlN as an Intermediate Layer
T. Takeuchi, A. Watanabe, K. Hirosawa*, H. Amano, K. Hiramatsu, and I. Akasaki
Nagoya University, Japan

C51
Growth of SiC and SiC-AlN Solid Solution by Container-Free Liquid Phase Epitaxy
V. A. Dmitriev* and A. E. Cherenkov
Howard University, USA

D55
Phase Analysis of Bi-Ca-Sr-Cu-O Superconducting Films at Different Growth Temperatures from KCl Supercooled Solutions
K. K. Raina, S. Narayanan and R. K. Pandey
Texas A&M University, USA

D56
Growth of Bi-Sr-Ca-Cu-O (Tc=85K) Single Crystals by the Traveling Solvent Method
K. Shigematsu, T. Satoh, Y. Nishimura, S. Hayashi, and H. Kamatsu
Iwate University, Republic of China

D57
Growth and Characterization of $Bi_2(Sr,Ca)2CuO_x$ Single Crystals
Y. Huang, W. J. Wen and M. K. Wu
National Tsing Hua University

D58
Improved Thermogravimetric Analysis and Crystal Growth of Bi-Sr-Ca-Cu-O
B. Wanklyn, E. Dieguez,* C. Chen, Y. Hu, D. Smith, F. Wondre, and P. A. J. de Groot
University Autonoma de Madrid, Spain

D59
Growth of $Bi_2Sr_2CaCu_2O_8$ by Immersed Heater Floating Zone Melting Technique
P. Murugakoothan,* R. Jayavel, C. R. V. Rao, C. Subramanian, and P. Ramasamy
Anna University, India

D60
Crystallization Process and Physical Properties of $Bi_2Sr_2CaCu_2O_{8+x}$
V. G. Bessergenev, A. A. Kamarzin, O. Bonfigt, R. Kubiak, H. Somnitz, K. Westerholt, and H. Bach
Ruhr-Universitat Bochum, Germany

D61
Surface Coarsening on High Tc Superconducting Single Crystals
Y. S. Wang, J. P. van der Eerden, P. Bennema, C. Grey, L. W. M. Schreurs, J. Wnuk, and P. van der Linden
University of Nijmegen, The Netherlands

D62
Preparation and Superconductivity of $Ba_{1-x}K_xBiO_3$ Single Crystals
J. Z. Liu,* W. D. Mosley, P. Klavins, L. Zhang, M. D. Lan, T. J. Goodwin, Y. X. Jia, and R. N. Shelton
University of California, USA

D63
Crystal Growth and Characterization of Superconductors in the Ba-K-Bi-O System
P. D. Han,* L. Chang and D. A. Payne
University of Illinois, USA

D64
Growth of Large Pure Doped and Co-doped La_2CuO_4 Single Crystals
A. Cassanho, B. Keimer and M. Greven,
Massachusetts Institute of Technology, USA

D65
Crystal Growth Analysis in Magnetically Oriented Melt Grown $DyBa_2Cu_3O_7$ Sintered Pellets
R. Cloots, A. Rulmont, C. Hannay, P. A. Godelaine, H. W. Vanderschueren, P. Regnier, and M. Ausloos
University of Liege, Belgium

POSTER SESSION #3
EXHIBIT HALL
Thursday 3:15 PM

D66
Growth of $CaLnBaCu_3O_{7-\delta}$ (Ln=La,Pr&Nd) Single Crystals by Flux Technique
C. R. V. Rao, P. Murugakoothan, R. Jayavel, C. Subramanian, and P. Ramasamy
Anna University, India

D67
Some Considerations on the Equilibrium Phase Diagram of the Y_2O_3-BaO-Cuo System
E. Cruceanu
Institute of Physics, Bucharest, Romania

D68
The Surgeon and Crystal Growth
Y. M. F. Marickar,* S. Sindhu, R. K. Vathsala, H. K. Moorthy, N. Elizabeth, and S. V. Roshni
Medical College Hospital, India

D69
Is it Possible to Grow the Urinary Stone in the Test Tube?
R. K. Vathsala, Y. M. F. Marickar,* C. Arvindakshan, S. Sindhu, T. G. Dhanalakshmik and H. K. Moorthy
Medical College Hospital, India

D70
Habit Modification and Inhibition of Crystallization of Fatty Acids by Some Surfactants
P. B. V. Prasad
SR Lab for Studies on Crystal Phenomena, India

D71
Growth Processes of Cholesteral Monohydrate and Gallstones in Silica Gel
T. Abraham and M. A. Ittyachen
Mahatma Gandhi University, India

D72
Extreme Decrease of the Dislocation Density of Al Crystals Grown from the Melt under Pressure
V.O. Esin*, A.S. Krivonosova and I.J. Sattibaev
Institute of Metal Physics, Russia

D73
Crystallographic Study of Calcium Oxalate Monohydrate Crystals Grown in Silica Gel Medium
A. Salim, S. Sindhu, Y. M. F. Marickar,* N. Elizabeth, and N. Subbanna
Medical College Hospital, India

D74
Growth of Pure and Doped Crystals of Strontium Tartrate and their Fourier Transform IR Studies
F. J. Rethinam,* T. J. Bhoopathy, S. Ramasamy, and P. Ramasamy
Anna University, India

D75
Spherulitic Crystal Growth of Pure (Y,Sm) and Mixed $Y_{1-x}:Sm_x$ Rare Earth Tartrates in Silica Gels
A. Jain, A. K. Razdan and P. N. Kotru
University of Jammu, India

D76
In-Situ Observation of Unidirectional Solidification in Transparent Organic Alloy
T. Higashino, Y. Inatomi, and K. Kuribasyashi
The Inst. of Space & Astro Science, Japan

D77
Growth of Caprolactam from the Melt and Solutions Part I: Theoretical Calculations
R. M. Geertman, E. P. G. van den Berg and P. Bennema
University of Nijmegen, The Netherlands

D78
Growth of Caprolactam from the Melt and Solutions Part II:Experimental Observations
E. P. G. van den Berg, R. M. Geertman, and P. Bennema
University of Nijmegen, The Netherlands

D79
Scanning Tunneling Microscopy Studies on Odd and Even n-paraffin Molecules Absorbed on Graphite
M. da Silva Couto, X.-Y. Liu, H. Meekes, and P. Bennema
University of Nijmegen, The Netherlands

D80
Relations Between Solubility and Stability of Urea in Various Solvents and Solvnet Mixtures
L. Cheng
Res. Institute of Synthetic Crystals, China

D81
The Crystallization of Highly Perfect Metal-Free Phthalocyanine Powders for 'AB-initio" Structure Solution by Diffraction Methods
P. G. Fagan,* K. J. Roberts and R. Docherty
University of Strathclyde, U.K.

D82
The NASA Center for the Development of Commercial Crystal Growth in Space
W. R. Wilcox
Clarkson University, USA

D83
Process Feasibility, Crystallization Kinetics and Habit Study of Potassium Chloride Using Ammonia as a Diluent
D. Jagadesh,* M. R. Chivate, N. S. Tavare, and S. Rohani
Hindustan Petroleum Corp., India

D84
Light Scattering Kinetics Study of Cyclopropane Hydrate Growth
J. P. Monfort* and A. Nzihou
Inst. National Polytechique de Toulouse, France

D85
Predictions with Unifac of Liquid-Solid Phase Diagrams: Application to Water-Sucrose-Glucose, Water-Sucrose-Fructose and Water-Xylose-Mannose
N. Gabas* and C. Laguerie
National Polytechnique Institute, France

SESSION 3A

NUMERICAL APPLICATION OF TiC FLOAT ZONE GROWTH

A31

Y.T. Chan and H.L. Grubin
Scientific Research Associates, Inc., 50 Nye Road, Glastonbury, CT

The present work applies numerical results to construct a knowledge data base which when accessed by a digital controller can be used for automation control of the inductive-heated TiC float zone growth. The numerical method determines the fluid and heat transports together with the induced AC electric current and the shapes of the melt-solid interfaces and molten zone free surface. In these calculations, the heating intensity and profile due to RF induction depend on the coil geometry, AC voltage and location of the molten zone free surface and is modeled through an integral equation based on the Biot-Savart law for the electromagnetic field. The molten zone free surface shape which determines the magnetic coupling of the heating distribution is calculated with a balance of the hydrostatic pressure, surface tensional force and the electromagnetic force. At present, the primary control parameters are the RF AC voltage and the translating speed of the crystal rod. The digital controller which provides feed-forward control of the primary growth parameters on process-time-scales consists of a PC, control software, DAS board and various motor and heater controllers. A "look-up table" data base was constructed using the above numerical models for the primary control parameters vs. several thermophysical constants. Results from a typical run will be presented.

INFLUENCE OF SOME PARAMETERS ON INTERFACE SHAPE DURING TEMPERATURE GRADIENT TECHNIQUE (TGT)

A32

Pan Peicong and Liu Guangzhao
Shanghai Institute of Ceramics, Academia Sinica
Home Address: Room 103, 306 Ta Cheng Road, Jia Ding County, Shanghai, 201800, P.R.China

Both analytical method and finite element numerical technique were applied to study of relationship between some parameters and interface shape during Temperature Gradient Technique (TGT). These parameters mainly included: the instantaneous cooling rate, longitudinal temperature distribution in the side of crucible and conductivity of crucible.

Our calculation shows that the instantaneous cooling rate (dT/dt) causes the interface to become increasingly concave. Dimensionless numble $D_e = R^2 2\rho C C_o/[K(T_h T_c)]$ is defined to express the extent that the interface become more concave arised from instantaneous cooling rate. Physical meaning of the term $[K(T_h T_c)D_e]/R^2$ is revealed to be heat source. It is the sensible heat carried by instantaneous cooling rate that caused the increasingly change of temperature field in ampoule. Dimensionless parametre D_e representing a ratio of heat carried by instantaneous cooling rate to heat conduction corresponds to $P_e = v\rho cR/k$ in B-S method.

Longitudinal temperature distribution expressed by $T_f(z)$ in the side of crucible in TGT powerfully influenced convexity of interface. By means of zero setting for convexity of isothermal it is convenient to determined the convexity distribution along crucible axis by the sign and absolute value of $\partial^2 T_f(z)/\partial z^2$. The function $T_f(z)$ can be obtained through taking measure of the temperature in out side crucible by thermocouple.

The influence of the crucible conductivity on the interface shape and position has also been studied. Longitudinal temperature gradient in growth region decreases sharply when heat conductivity of crucible become large than that of crystal. On the contrary, it keeps constant approximately if heat conductivity of crucible become smaller than crystal. The effect of crucible heat conductivity can be neglected when heat transfer coefficient between crucible side and environment remains large enough. It was emphasized that heat conductivity of crucible can be adjusted by heat treatment.

A33

RADIATION - CONDUCTIVE HEAT TRANSFER IN OPTICAL CRYSTALS

Der Yu.Lingart
Crystal Growth and Equipment - "CGE"

This article presents the results of theoretical and experimental researchs of the radiation - conductive heat transfer while growing optical crystals.

A phenomen of nonmonotone and inversion of a stationary temperature field (T-field) was founded out in optical 2-layered and double-phase system by the help of mathematical modelling. That is case when the optical materials temperature grows up from hot boundary to cool boundary.

Table shows the dependences of maximal by optical thickness (τ) amplitudes of the T-field inversion in double-layer system with a distance boundaries from the refructive index ($N = 0.01$, $X_e = 0.5$; $T = 1000$ K; $T_x = 100$ K).

B	1.01	1.05	1.1	1.2	1.33	1.5	1.75	2.0
A_t,K	15.5	35.7	42.2	41.4	35.0	27.55	19.6	14.4
τ_{max}	0.03	0.05	0.07	0.08	0.09	0.1	0.1	0.11

This phenomen experimental researches were done by the help of special IP-pirometer for sapphire crystals.

A34

ORDERED STRUCTURE IN NON-AXISYMMETRIC FLOW OF MOLTEN SILICON CONVECTION

Koichi Kakimoto, Masahito Watanabe, Minoru Eguchi and Taketoshi Hibiya
Fundamental Research Laboratories, NEC Corporation
31, Miyukigaoka, Tsukuba 305, Japan

Flow regime of molten silicon during CZ crystal growth has been recognized as turbulent. This judgment has been done from the fixed view point outside a crucible. However, Watanabe et al. observed molten silicon flow by an X-ray radiography method and found a three-dimensionally ordered structure through analyzing particle paths from the rotating view point: view point on the crucible [1]. The observed structure was characterized as "Baroclinic instability flow." In order to reproduce the structure and temperature field in the melt, three-dimensional numerical simulation was performed, where assumption of axisymmetric flow was relaxed.

Figures 1a and 1b show experimentally observed and calculated particle paths from the rotating view point. We can recognize a vortex indicated by closed arrows. A large wavy flow indicated by an open arrow was also observed in numerically calculated result (Fig. 1b). The origin of the wavy flow is identical to that of a jet stream on the rotating earth. It was also found that temperature field is modulated along the azimuthal direction because the vortex affected heat transfer coefficient in the azimuthal direction. Consequently, a crystal rotating at different rate from that of vortex feels oscillating temperature field.

[1] M. Watanabe et al., "Baroclinic Flow Instability in the Rotating Silicon Melt," ICCG10.

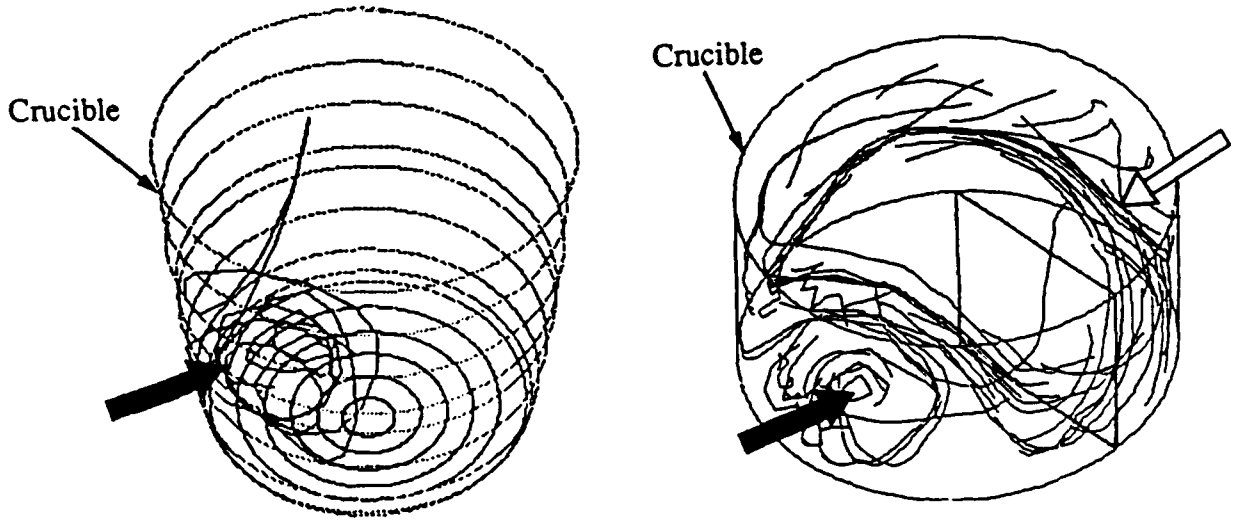

Figure 1. Particle paths from the rotating viewpoint on the crucible: (a) experimentally obtained and (b) numerically calculated.

EXPERIMENTAL INVESTIGATION OF THE EFFECT OF THERMOSOLUTAL CONVECTION ON CRYSTAL GROWTH

A35

B.J. Lee, M.S. Kang and Z.H. Lee
KAIST, Dept. of Materials Sci. and Eng., Taejon, Korea

There have been some theoretical and computational papers on the thermosolutal convection and convective instabilities during unidirectional solidification of binary alloys. But little experimental results are known on the actual effect of the thermosolutal convection on the crystal growth.

In this work, experiments are carried out to test the existence of thermosolutal convection and its effect on the solute distribution in the solid. Binary alloys (Al-Mg, Pb-Sn, In-Sb) were solidified unidirectionally upward and the temperature variations in the melt ahead of solidification front were measured by DTA. Solidification interface was revealed by quenching method and the solute distribution in the solid was analyzed by SIMS.

COMPUTATIONS OF THE TEMPERATUARE DISTRIBUTION IN CRYSTALS GROWN BY THE VERTICAL BRIDGMAN METHOD

A36

Krzysztof Grasza
Institute of Physics, Polish Academy of Sciences
Al.Lotnikow 32/46, PL 02-668 Warsaw, Poland

The temperatuare field was calculated for the vertical Bridgman method of crystal growth. Physical bases of the model and computer analyses of the shape of the solid-liquid interface are presented. Trajectories of the temperature of several points on the load-ampoule border are experimentally measured and computed. The dependence of the heat transfer mechanism on temperature and ratio of furnace-ampoule diameters is discussed. The effect of pulling velocity on temperature field is shown. More details on the special effects of the ampoule end on heat transfer are presented [1].

Comparison of theoretical and experimental results shows lack of noticeable convection in the liquid when crystallization is performed in the direction opposite to acceleration of gravity, and strong convection which makes the effective thermal conductivity of the liquid greater than that without convection in the opposite case. The analysis of the nature of the convective flow is performed on the basis of the theoretical model [2].

1. K. Grasza and U. Zuzga-Grasza, *J. Crystal Growth*, November 1991 (accepted for publication).
2. K. Grasza and A. Jedrzejczak, *J. Crystal Growth* 110 (1991) 867.

A37

OBSERVATION OF CRYSTAL-MELT INTERFACE SHAPE IN SIMULATED CZOCHRALSKI METHOD WITH MODEL FLUID

A. Hirata and M. Tachibana
Department of Chemical Engineering, Waseda University
3-4-1 Ohkubo, Shinjuku-ku, Tokyo 169, Japan
Y. Okano and T. Fukuda
Institute for Materials Research, Tohoku University
2-1-1 Katahira, Aoba-ku, Sendai 980, Japan

In this study, the convective phenomena in melt and crystal-melt interface shape were observed in simulated CZ method with model fluid and the effect of convective phenomena in melt on crystal-melt interface shape was discussed.

Liquid and solid of $C_{20}H_{42}$(m.p.= 37-38°C) were used for model fluid and dummy crystal in simulated CZ method. In order to observe the convective phenomena in the melt, fine aluminum powders were used as tracer material and slit light was applied.

When spontaneous convections were dominant in the melt at the low crystal rotation rate, the melt flowed upward along the crucible wall to the melt surface where melt turned downward to the bottom of crucible and crystal-melt interface shape became convex toward the melt. Increasing the crystal rotation rate, the forced convection became dominant in the melt and the melt flowed in opposite direction to the spontaneous convection and the crystal-melt interface shape became concave toward the melt. The crystal rotation rate at the point where the crystal-melt interface became flat was defined as critical crystal rotation rate. The authors have previously studied the effect of convective phenomena on critical crystal rotation rate theoretically and proposed the method of evaluating whether the Marangoni convection or natural convection is dominant in the melt[1]. According to this method, it can be suggested that the Marangoni convection is dominant in the melt in our experiment. This means that in order to control the crystal-melt interface shape during growth of single crystal, it is necessary to take into account the Marangoni convection as well as the natural convection.

[1] Y. Okano et al., *J. Chem. Eng.* Japan 22(1989)389.

A38

VISUALIZATION OF LOW PRANDTL NUMBER CONVECTION IN CZOCHRALSKI MELTS*

U. Krzyminski
Technical University Münich, 8000 Münich, Germany
A.G. Ostrogorsky
Columbia University, New York, N.Y. 10027, USA

An experimental method that enables visualization of natural convection semiconductor melts is presented; heat transfer by thermal radiation and volumetric heating is used to increase the effective conductivity of transparent fluids. As a result, the high Prandtl number of transparent fluids is effectively lowered to a desired value. Volumetric heating thickens the thin boundary layers of transparent fluids, yielding buoyancy forces and pumping, similar to flow conditions in semiconductor melts.

An experiment has been built to model the flow in semiconductor Czochralski melts. Molten salts, which are transparent to infrared radiation, were used as working fluids. The best results were obtained utilizing a mixture of Sodium Chloride and Calcium Chloride at 900 K. A tubular resistance heater provided realistic boundary conditions on the salt melts. The special design of the experimental apparatus permitted a full side view to the melt. Flow visualization was realized using streak photography.

Asymmetric unsteady flow patterns were observed in the melt. As was expected, the crystal and crucible counter-rotation substantially improved the symmetry of the flow in the melt.

*Supported by National Science Foundation, Grant Number MSM 8808115.

A39

COMPUTER SIMULATION OF A FURNACE FOR HIGH-PURITY CZOCHRALSKI GROWN Ge CRYSTALS

T.A. Cherepanova, A.F. Spivak, A.V. Gusev, O.V. Potapov* and V.A. Gava**
Centre of Microelectronics, Latvian Academy of Sciences
19 Turgenev Street, Riga, Latvian Republic
*Institute of High-Purity Materials, Russian Academy of Science
49 Tropinina Street, Nizhnij-Novgorod, Russian Republic

High-purity germanium with the controlled dislocation density and high spatial uniformity is a requirement for the ionizing-radiation detectors. The aim of the present paper is to determine the influence of process parameters including heating power, pulling rate, etc., on the thermoelastic stresses and dislocation maps.

Computer simulation of the global furnace model has been carried out taking into account the geometry and spectral radiation-transparence properties of quartz thermal shields. Conductive, radiation and convective heat transfers in the melt and ambient gas are considered. Hf heating by a graphite heater is described by assigning the heater power input taken from experiment, namely, by its distribution along the crucible walls. Temperatures on the cuter surface of the quartz chamber and the furnace dome are also given by the experiment. The effective numerical method proposed here allows to realize the computer simulation of the global model on IBM PC AT. The temperature distribution in the melt and crystal, forced and natural convection in the melt are calculated for different values of melt depth, crystal and crucible rotation rates, crystal length and ambient gas discharge. The influence of growth conditions on the dislocation density and uniformity of dislocation distribution is analyzed theoretically, as well as by X-ray topography and selective chemical etching. Computer simulation results are consistent with the experimental data.

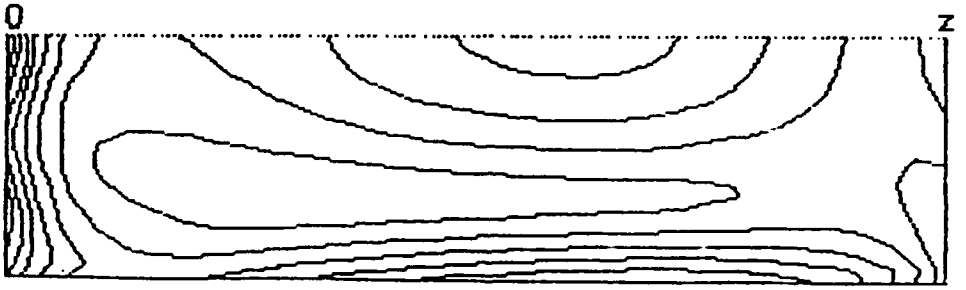

Isoline of the von Mieses stress invariant. The line z=0 coincides with the interface.

A40

INTEGRATED HEAT TRANSFER ANALYSIS FOR COMPLETE VERTICAL BRIDGMAN CRYSTAL GROWTH SYSTEMS

David E. Bornside and Robert A. Brown
Department of Chemical Engineering
Massachusetts Institute of Technology, Cambridge, MA 02139

A quasi-steady-state, integrated system model describing high temperature heat transfer and solidification in vertical Bridgman crystal growth is solved by the finite-element/Newton method. The numerical analysis couples the calculation of the temperature field in all phases, the determination of the melt/crystal free-boundary, and the power inputs to the resistance heaters needed to maintain thermocouples at set-point values. The analysis includes conductive heat transfer in the melt, crystal, boat, ampoule, pedestal, heater and the surrounding insulation, latent heat release at the melt/crystal free boundary and diffuse-gray radiation, which couples the heat transfer between surfaces through the view factors. Finite element approximations are used to reduce the entire problem to a coupled set of nonlinear algebraic equations, which are solved simultaneously by Newton's method with the Jacobian matrix computed by a combination of closed form expressions and finite difference approximations. Quadratic convergence of the Newton iteration is demonstrated. The von Mises stress throughout the crystal is computed from the calculated position of the melt/crystal free boundary and temperature field. The model is demonstrated by a series of calculations for a prototype vertical Bridgman system that shows the sensitivity of the location of the melt/crystal free boundary and of the von Mises stress in a GaAs crystal on the ampoule position and growth rate.

A41

TRANSPORT PHENOMENA IN METALLIC SOLUTIONS WITH SPECIAL REGARD TO THERMAL DIFFUSION

T. Boeck[1] *and A.N. Danilewsky*[2]
[1]Institut für Kristallographie und Materialforschung
Humboldt-Universität zu Berlin, Invalidenstr. 110, 0-1040 Berlin, Fed. Rep. of Germany
[2]Kristallographisches Institut, Albert-Ludwigs-Universität
Freiburg, Hebelstr. 25, W-7800 Freiburg, Fed. Rep. of Germany

THM crystal growth experiments under microgravity (μg) which are designed for basic studies of interface kinetics offer in parallel the possibility to investigate different modes of material transport in the solution zone. In contrast to studies on earth, diffusional processes become more relevant than the influence of thermal and solutal convection. In addition to ordinary diffusion, the cross effect of thermal diffusion (Soret phenomenon) resulting from an interaction between the thermodynamic fluxes of heat and matter in a mixture of two or more components will have an important influence on mass transport in the solution zone and on the morphological stability of the growing interface, if steep temperature gradients exist. A promising approach is to compare transport rates of matter under μg- as well as 1g-conditions. This has been performed for the growth of the III-V-compounds InP, GaAs and GaSb from In and Ga solutions, respectively.

The transport rates can be experimentally determined from time markers set by lamp pulses in mirror heating facilities. From calculations taking thermal diffusion into account the following results are to be expected for the μg-case: (i) a strong reduction of growth rate for In-P, (ii) no remarkable influence in case of Ga-As and (iii) a higher growth rate for Ga-Sb. For the growth system InP-In an enrichment of the solvent In caused by the Soret phenomenon can be assumed at the two zone boundaries leading to a destabilizing effect for the morphology of the growth face.

A42

BAROCLINIC FLOW INSTABILITY IN THE ROTATING SILICON MELT

Masahito Watanabe, Minoru Eguchi, Koichi Kakimoto, Yann Baros and Taketoshi Hibiya*
Fundamental Research Laboratories, NEC Corporation
34 Miyukigaoka, Tsukuba 305, Japan

The flow in the silicon melt during CZ crystal growth originally contains flow instability, because thermal convection due to temperature gradient in the melt and forced convection due to crucible rotation coexist in the melt[1]. The flow instability should generate a temperature oscillation which is an origin of striation in grown crystals. So that, it is necessary to remove the flow instability in order to obtain more homogeneous silicon crystals. From this requirement, we must clearly understand the origin of flow instability.

In the present study, the origin of flow instability has been clarified through three-dimensional flow visualization using the double-beam X-ray radiography system[2]. Experiments were carried out for various conditions of temperature gradient and crucible rotation rate. It was found that flow mode changed from axisymmetric to non-axisymmetric at a specific crucible rotation rate. Particle path of non-axisymmetric flow seems to be random from fixed view point as shown fig. 1(a). However, it was found that the particle paths from the rotating view point show a vortex structure as shown fig. 1(b). This vortex structure means that the sloping convection due to the Baroclinic instability exists in the silicon melt. Consequently, the origin of flow instability in the silicon melt during CZ crystal growth is attributed to the Baroclinic instability.

[1] K. Kakimoto et al., *J. Crystal Growth* 102(1990)16.
[2] M. Watanabe et al., ASME '91 Winter Meeting Proceedings.

*On leave from ISEP, Paris.

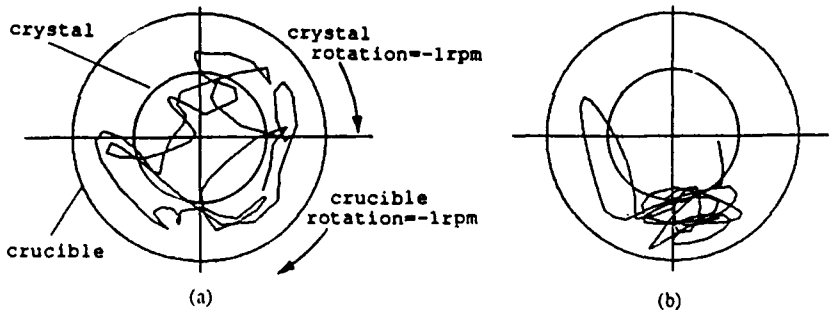

Figure 1. Top view of a particle path: (a) from fixed viewpoint and (b) from rotating viewpoint.

MORPHOLOGICAL INSTABILITY IN EPITAXIALLY-STRAINED DISLOCATION-FREE SOLID FILMS

A43

B.J. Spencer, P.W. Voorhees and S.H. Davis
Northwestern University

We give the first analysis of the morphological instability of a growing epitaxially-strained dislocation-free solid film. We derive an evolution equation for the film surface based on the transport mechanisms of vapor deposition and surface diffusion due to a stress-dependent chemical potential. From a linear stability analysis we find an instability that is driven by the misfit strain. We also find that the instability is suppressed by elastically-stiff substrates, low temperatures and large deposition rates. The instability described contains many features associated with the onset of the "island instability." We determine the nonlinear evolution of this instability and present comparisons with observed island morphologies.

NUCLEATION-LIMITED AGGREGATION IN CRYSTAL GROWTH

A44

Nai-ben Ming, Mu Wang and Ru-Wen Peng
National Laboratory of Solid State Microstructures and Department of Physics
Nanjing University, Nanjing 210008, People's Republic of China

In-situ observation technique is employed to study the fractal growth in a thin isothermal aqueous-solution film of $Ba(NO_3)_2$. The micromorphology and microstructure, as well as the growing process of the fractals have been investigated. The experiments indicate that the fractals is the aggregate of small crystals and is formed by random successive nucleation. Nucleation-limited aggregation (NLA) model is proposed to describe the fractal growth in our system. The NLA process need not obey the Laplace equation, and the sticking probility onto the fractals branches does not equal to the gradient of solute concentration in front of the growing interface. Therefore the NLA process is different from the diffusion-limited aggregation (DLA). A Monte-Carlo simulation using NLA model is also argued and compared with the DLA clusters.

ESTIMATION OF DIFFUSION COEFFICIENTS AND A PLAUSIBLE IDENTIFICATION OF SPECIES FROM ONE DIMENSIONAL LIESEGANG RING FORMATIONS IN MULTICOMPONENT SYSTEMS

A45

George Varghese M., Ittyachen and Cyriac Joseph
School of Pure & Applied Physics
Mahatma Gandhi University, Kottayam, Kerala 686 631 India

Diffusion is the spontaneous equalization of concentration of molecular ions or colloidal particles in a system as a result of their chaotic motion. Using a simple mathematical model Kirov dealt with the diffusion controlled growth in a qualitative way and calculated the diffusion coefficient from the ring system formed due to the counter diffusion of two reacting substances in a media. Making use of the theory of one dimensional Liesegang ring phenomena Shirohara could estimate the diffusion coefficient of the ions inside a gel column. All the work reported until now was in double component system where one component is allowed to diffuse through a gel medium having impregnated with the counter acting component and their subsequent crystallization whereever the nucleation conditions are satisfied.

In this study, we have examined the phenomenon of Liesegang ring formation in multicomponent outer electrolyte systems and we have extended the theories for estimating the diffusion coefficients. Depending on the diffusion coefficients priority of forming different species of crystals may be predicted. In a mixed system of reactants separate systems of rings consisting of each species are expected. If the diffusion coefficients are identical mixed complexes results. The detailed experiments were conducted using lanthanum nitrate and copper nitrate as outer electrolytes and oxalic acid ions, the incorporated component of the gel medium. As expected different ring systems were observed. In all cases the time law and space law are found to be obeyed. Dependence of diffusion rates on the pH of the medium and the concentration of the reactants were also studied and compared with the theoretical results.

SESSION 3B

B61

GROWTH OF BUBBLE FREE BSO AND BGO CRYSTALS-FLUID FLOW ANALYSIS

D.Krishnamurthy, R. Gopalakrishnan, D. Arivuoli and P. Ramasamy
Crystal Growth Centre, Anna University, Madras-25, India

Single crystals of $Bi_{12}SiO_{20}$ and $Bi_{12}GeO_{20}$ have wide applications extending from transient holography to image processing. Bubble free BSO and BGO crystals of 15 mm diameter and 40 mm length were grown using Pt crucibles. Crystals grown with rotation rate of 5-15 rpm were found to have gas bubbles, but between 15-35 rpm the growth became very difficult and no crystals were obtained. Good quality crystals with no bubbles were obtained in the region 35-45 rpm. Further increase resulted in cracks. The diameter was maintained at 15 mm and growth rate at 3mm/hr. We correlated this growth sequence with the fluid flow simulated by Whiffin[1] and attribute the existence of the middle danger rotation rate to the coexistence of both free and forced convection which makes the flow not conducive for crystal growth.

By applying the equation of bubble nucleation[2] to the BSO melt it is determined that when the concentration of the dissolved gas in the liquid adjacent to the growing crystal exceeds a pressure of 55 Atm., bubbles get nucleated inside the melt. According to Miyazawa[3] when forced convection is made dominant in the melt, bubbles will not get incorporated into the crystals. But according to Yinchun Hou[4] the bubbles nucleate at the bottom and when forced convection becomes dominant, they will get trapped in the crystal.

In our case bubble free crystals are obtained only when a rotation rate higher than the middle danger rotation rate is employed. This corresponds to forced convection dominant flow because as the rotation rate is increased forced convection increases. Thus we substantiate the validity of Miyazawa's theory and predict that when a rotation rate corresponding to forced convection dominant flow is employed, bubble free crystals can be grown. The fact that those crystals do not have bubbles is verified using optical microscope.

The stoichiometry of the grown crystals was verified by EPMA and the results obtained will also be discussed.

[1] P.A.C. Whiffin, T.M. Burton and J.C. Brice, *J. Cryst. Growth*, 32 (1976) 205.
[2] W.R. Wilcox and Vincent H.S. Kuo, *J. Cryst. Growth*, 19 (1973) 221.
[3] S. Miyazawa, *J. Cryst. Growth*, 49 (1986) 515.
[4] Yin Chun Hou, in Recent Trends in Crystal Growth, Ed. P. Ramasamy Vol. 2 (1991) p.329.

B62

HABIT AND DEFECTS OF BISMUTH SILICON OXIDE CRYSTAL (BSO)

Zhong Weizhuo, Luo Haosu, Lu Zhiping and Zhao Tiande
Shanghai Institute of Ceramics, Chinese Academy of Science
1295 Dig Xi Road, 200050, China

The morphology of Bi_2SiO_{20} (BSO) crystal grown by Czochraski technique under different growth conditions is reported in detail in this paper. The growth appearances of all faces and the influence of growth conditions such as seed orientation, temperature field and rotation rate on morphology are systematically analyzed on the basis of the morphological importance of all faces and of the variation of specific surface energy with temperature by applying the generalized principle of minimum surface energy.

The crystal defects have been identified by X-ray topography. Main defects are planar defects.

B63

ETCH MORPHOLOGY OF BISMUTH SILICATE (BSO) CRYSTAL

Zhong Weizhuo, Luo Haosu, Lu Zhiping Zhaotiande
Shanghai Institue of Ceramics, Chinese Academy of Science
1295 Ding Xi Road, Shanghai 200050, China

The etch morphology of Bismuth Sicicate ($Bi_{12}SiO_{20}$) crystals grown by Czochralski method was investigated and characteristics of the etch figures and etch rates of {100}, {110}, {211}, {11·} faces were compared. The etch morphology was explained by applying the PBC theory of Hartman and Perdok. Based on characteristics of the etch figures, it is convenient to orientate the crystal, to determine the relative position of the etch faces and the direction of the polar axis.

COMPUTER SIMULATION OF THE GROWTH OF BSO WITH ELLIPTIC ADAPTIVE GRID PROCEDURE

B64

G.S. Liaw, Y.M. Zheng and L.C. Chou
Alabama A&M University, Normal, Alabama 35762, USA

A comprehensive numerical modeling of the Czochralski Crystal growth system has been performed for the growth of Bismuth Silicon Oxide (BSO). A pressure-based numerical algorithm in conjunction with an elliptic adaptive arid procedure is employed to obtain the simultaneous solutions of the melt flow field and the global melt/solid temperature distribution. Both the thermal buoyancy and the surface tension effects due to conduction, convection and radiation heat transfer are included. The free surface effect is treated by coupling the Young-Laplace equation at a fixed contac: angle with the interface of melt/solid. The melt flow is assumed laminar and incompressible. The computations show that the developed numerical scheme is efficient and robust. The comparison of the computed interface shape and the experimentally grown crystal interface shape are in reasonable agreement.

IMPURITY INDUCED PHOTOCHRONIC BEHAVIOR IN $Bi_{12}SiO_{20}$:Mn, Cr CRYSTALS

B65

Xu Liang-ying, Liu Jian-chang, Shu Bi-yun and Xiao Bing
Shanghai Institute of Ceramics, Academia Sinica

The pure $Bi_{12}SiO_{20}$ and $Bi_{12}SiO_{20}$:0.05wt.%MnO_2, 0.02wt.%Cr_2O_3 (BSO:Mn,Cr) crystals were grown along the A-axis by the Czochralski technique using resistance heated platinum crucibles. Electron spin resonance spectre indicate that acceptable charge states of the centers after illumination are Mn^{5+} and Cr^{4+}, and the g-factors of centers are 2.0009 and 1.9616, respectively. Observed BSO:Mn before illumination, the absorption band between 410-750nm which overlaps the absorption edge is due to $^3A_1$--$^3T_2$, $^3T_1$ transition of Mn^{5+} ions, and Mn^{5+} and Mn^{4+}+ are simultaneously present in the crystal. Absorption due to Mn^{5+}+ will increase after illumination. The photochromic effect of BSO:Cr is explained in terms of a Cr^{5+}-Cr^{4+} charge transfer process. An ESR band appears at g-2.0109 with peak width of 75G at RT in pure BSO crystal powder, and this band is attributed to an intrinsic trapped hole center.

CRYSTAL GROWTH OF COMPOUNDS IN THE MgO-Nb_2O_5 BINARY SYSTEM

B66

E. Brück, R.K. Route and R.S. Feigelson
Center for Materials Research, Stanford, CA 94305-4045

In the system MgO-Nb_2O_5, four compounds are known to exist.[1] $MgNb2O_6$ is congruently melting at 1570°C while the compounds (Mg,Nb)$O_{2.42}$,$Mg_5Nb_4O_{15}$ and $Mg_4Nb_2O_9$ decompose peritectically at 1445°, 1580° and 1730°C, respectively. We have grown small crystals of all four compounds by the laser-heated pedestal growth (LHPG) method. The Nb_2O_5-rich compounds showed some tendency to partial reduction of Nb^{+5} even when grown in an O_2 atmosphere, resulting in a bluish-black color of the as-grown crystals. In contrast to this, the MgO-rich compounds were colorless, even though they were grown at higher temperatures. Additionally, we report on basic optical properties (luminescence, optical absorption) of the four compounds.

[1] R. Grühn and H. Schäfer, *J. Less-Common Met.*, 10(2), 152 (1966).

$Bi_6Te_2Mo_2O_{21}$ - A NEW SYNTHETIC CRYSTAL AND ITS PHYSICAL PROPERTIES*

B67

Deng Mengxiang
Institute of Geochemistry, Chinese Academia Sinica
Guiyang, Guizhou 550002 P.R. China

Single crystal of $Bi_6Te_2Mo_2O_{21}$ attaining 2 x 2 x 5 mm^3 were synthesized by the fusion method, and physical properties were investigated. This is a new phase found in nature, and given a new mineral name. Chillumite. The crystal belongs to the orthorhombic system and D^6_2-C_{222} space group with lattice parameters a=5.602 Å, b=5.553 Å, and c=22.816 Å according to the CAD4SDP results. The other physical properties, such as DTA analyze, refractive indexes, reflectivity and IR spectrum of the crystal are also given, and has a potential applicability for acoustic-optical and light-reflective material.

*This project was financially supported by the Natural Science Foundation China.

B68

MECHANICAL BEHAVIOUR OF FLUX GROWN $LABO_3$, $RFeO_3$, (R = Y,Dy & Yb) CRYSTALS

Anima Jain, E.Y. Bamzai, Urvashi Raina, Shafqat Beigh, P.N. Kotru and B.M. Wanklyn
Dept. of Physics, Univ. of Jammu, Jammu, J & K State, India
*Dept. of Physics, Clarendon Laboratory, Univ. of Oxford, Oxford 3PU1

Mechanical behaviour of flux grown $LaBO_3$, and rare earth orthoferrites $RfeO_3$, (R = Y,Dy, & Yb) are studied using identation induced harness testing by employing Vicker's microhardness tester. Mechanical behaviour of (100) and (110) faces of $LaBO_3$ crystals, (001) and (110) faces of $RFeO_3$ crystals are described and discussed. The Vicker's microhardness value (H_v) for different planes is given in Table 1. The variation of H_v with load (10 - 100g) is non-linear irrespective of the planes considered and is not in accordance with the Kick's law. The results are explained on the basis of Hay's and Kendall's law. Anisotropic behaviour of Vicker's hardness is shown by taking measurements in different orientations of crystals. Whether the planes are (100), (110) of $LaBO_3$ or (001), (110) of $RFeO_3$, the variation is periodic, the maxima and minima repeating every 30° change in orientation, Fracture toughness and Brittle index are also calculated and are given in Table 1.

Table 1

Planes	Crystals	H_v (Kg/mm^2)	K_c (MNm$^{-3/2}$)	B_2 (μm$^{-1/2}$)
(100)	$LaBO_3$	808.0468	1.6302	4.3163
(110)	$LaBO_3$	850.2504	1.3355	5.2774
(001)	$YFEO_3$	1027.12	0.5975	1.8757
(110)	$YFEO_3$	1235.08	0.1912	2.195
(001)	$DyFeO_3$	884.474	0.2775	3.5658
(110)	$DyFeO_3$	939.055	0.2443	4.1045
(001)	$YbFeO_3$	1188.8	0.1464	2.4092
(110)	$YbFeO_3$	1083.9	0.2004	5.4725

Note: These values are taken as the average of values at loads ranging from 10-100g.

EFFECTS OF ZrO_2 AND Sc_2O_3 ADDITION ON FZ-GROWTH OF RUTILE SINGLE CRYSTALS

B69

Mikio Higuchi and Kohei Kodaira
Department of Applied Chemistry, Faculty of Engineering
Hokkaido University, Sapporo 060, Japan

Rutile (TiO_2) single crystals are an important material for polarizing devices because of large refractive indices and large birefringence. We have already reported on the growth of rutile single crystals by the floating zone (FZ) method [1]. The formation of low-angle grain boundaries was effectively suppressed under a relatively low oxygen partial pressure up to 10^{-2}. The oxygen partial pressure, however, led the reduction of the grown crystal, which became black and opaque. The essential color of rutile, i.e. pale yellow, can be restored by a long-term annealing at 800°C in air. In this study, we have successfully grown grain-boundary-free and transparent rutile single crystals by adding small amount of ZrO_2 and Sc_2O_3.

Fig. 1 shows polarizing microphotographs of cross sections of rutile crystals grown in oxygen atmosphere. The crystal added with 0.5 mol% ZrO_2 (a) involves no low-angle grain boundaries even at peripheral region, while many grain boundaries are observed in the pure TiO_2 crystal (b). The migration and rearrangement of dislocations are responsible to the formation of low-angle grain boundaries. The addition of ZrO_2 was effective to restrict the migration of the dislocations, which is so-called solution hardening, and the formation of low-angle grain boundaries was consequently suppressed. However, the grain-boundary-free crystal added with ZrO_2 still showed black color owing to the reduction at high temperatures.

The addition of Sc_2O_3 was effective to grow a transparent rutile crystal as shown in fig. 2. If Sc^{3+} substitutes Ti^{4+} site, oxygen vacancies inevitably occurs for the electrical charge compensation. Oxide ions would easily diffuse through the vacancies as the grown crystal cooled, so that the transparent and pale yellow rutile single crystal was obtained. The formation of low-angle grain boundaries was not completely suppressed by the addition of Sc_2O_3, but simultaneous addition of ZrO_2 was again effective to reduce the number of low-angle grain boundaries.

[1] M. Higuchi et al. J. Crystal Growth 112 (1991) 354.

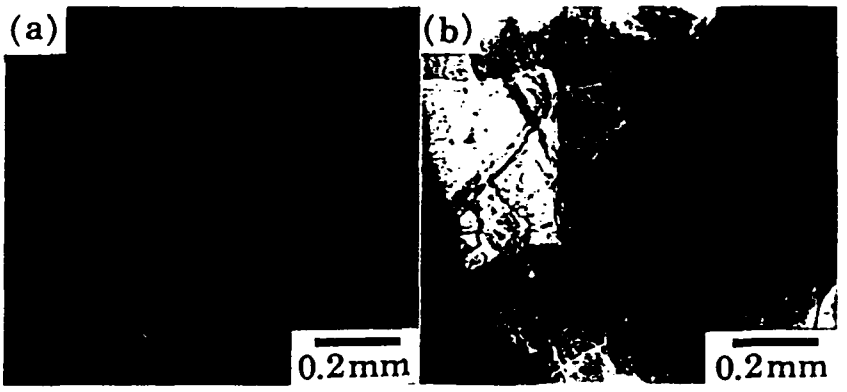

Figure 1. Polarizing microphotographs of FZ-grown rutile crystals. (a) added with ZrO_2, (b) pure TiO_2.

rutile

Figure 2. Cross section of the as-grown rutile single crystal added with Sc_2O_3.

B70

THE GROWTH OF Al_2O_3 SINGLE CRYSTALS BY CZOCHRALSKI METHOD

S. Morita[1], *H. Sekiwa*[2], *H. Toshima*[3] *and Y. Miyazawa*[3]
[1]Mitsubishi Heavy Industries, Ltd.
[2]Nippon Mektron, Ltd.
[3]National Institute for Research in Inorganic Materials
1-1 Namiki Tsukuba-shi Ibaraki, Japan

Bubbles in Al_2O_3 single crystals become serious problems for optical applications such as laser hosts or optical windows. Therefore, it is important to understand the formation mechanism of bubbles in order to grow crystals of good optical qualities.

In this study, the effects of growth parameters of Czochralski method, especially atmosphere and dopant concentration were investigated. And the temperature distributions were measured in order to optimize the growth conditions.

As a result, the effects of atmosphere on the formation of bubbles were very small in the case of pure Al_2O_3 single crystals. On the contrary, in the case of $Ti:Al_2O_3$, many bubbles were observed in the whole crystals grown under N_2+1.5%O_2 atmosphere. But, $Ti:Al_2O_3$ grown under N_2+20%H_2 atmosphere and low pulling rates had good optical qualities without any bubbles, as shown in Fig. 1. Although the temperature distributions were almost the same for both atmospheres, the temperature fluctuations and the flow patterns of melt surface strongly depended on atmospheres. And, the segregation coefficients of Ti under N_2+20%H_2 atmosphere were larger than under N_2+1.5%O_2 atmosphere.

These experimental results show that the formation of bubbles in $Ti:Al_2O_3$ are caused by constitutional supercooling. It may be concluded that the lower pulling rates and thin boundary layer conditions are desirable in order to avoid the formation of bubbles.

Figure 1. $Ti:Al_2O_3$ single crystal grown under N_2+20%H_2 atmosphere.

B71

DEPOSITION OF EPITAXIAL Cu_2O FILMS ON (100) MgO BY LASER ABLATION AND THEIR PROCESSING USING ION BEAMS

S.B. Ogale and P.G. Bilurkar
Center for Advanced Studies in Materials Science and Solid State Physics
Department of Physics, University of Poona, Pune 411 007, India.
Nalin Parikh and B. Patnaik
Department of Physics and Astronomy, University of North Carolina, Chapel Hill, NC 27599
D.D. Sharma
Indian Institute of Sciences, Bangalore, India

Epitaxial thin films of Cu_2O have been deposited on (100) oriented MgO substrates by pulsed excimer laser ablation technique. Chemical polishing of the substrates by etching them in hot phosphoric acid prior to film deposition is found to be a critical step in realising epitaxy. A KrF excimer laser operating at 248 nm wavelength was used for ablation. The depositions were carried out at a laser energy density of 2 J/cm^2 and the pulse repetition rate of 5 Hz. The substrate temperature was held at 700°C and the oxygen partial pressure during deposition and cooling was 10^{-3} Torr. The epitaxial nature of the deposited films was established via x-ray diffraction (XRD) and Rutherford BackScattering (RBS) channeling measurements. The epitaxial films thus obtained were then subjected to ion bombardment for studies of damage formation and solid phase regrowth. Implantations were carried out using 100 KeV Ar^+ and N_2+ ions over a dose range between 5 x 10^{14} and 10^{17} ions/cm^2. The implanted samples were subjected to annealing treatments at different temperatures and oxygen partial pressures chosen on the basis of the Cu-O phase diagram and the regrowth behaviour was examined using the XRD and RBS techniques. In the case of N_2+ implanted samples the issues of compound formation were also studied. In this context the technique of X-ray photoelectron spectroscopy was employed. The as-grown, implanted and annealed samples were also subjected to resistivity vs. temperature measurements in view of the importance of the Cu-O system in the context of the phenomenon of high temperature superconductivity.

ETCHING CHARACTERISTICS OF {110} AND {001} FACES OF FLUX-GROWN $ErFeO_3$ SINGLE CRYSTALS

B72

K.K. Sharma, Ashok K. Razdan and P.N. Kotru
Department of Physics, University of Jammu, Jammu Tawi 180 001, India
B.M. Wanklyn
Department of Physics, Clarendon Laboratory, University of Oxford, Oxford OX1 3PU [ENGLAND]

Etch patterns of ((110)) and ((001)) faces of flux-grown single crystals of $ErFeO_3$ are formed by H_3PO_4, and H_3PO_4 in combination of HNO. Etching processes of these crystals in phosphoric acid were conducted at various temperatures, ranging from 150 to 250°C. Point-bottomed pits exist at all stages of successive etching, and originate at the sites of dislocations. The morphology of etch pits on ((001)) face changes with the increase of etchant temperatures. The point-bottomed pits at 150°C are well defined as compared to those of appearing at higher temperatures. Etching kinetics including vertical and lateral dissolutions at different temperatures, and effect of composition of the etchant are studied. The activation energy and the Arrhenius factor for both vertical as well as lateral etch rates are presented.

STUDIES ON (0001) CLEAVAGES ETCHING AND MICROHARDNESS OF FLUX GROWN M-TYPE HEXAFERRITES

B73

*Urvashi Raina, Sushma Bhat, P.N. Kotru and F. Licci**
Dept. of Physics, University of Jammu, J&K, India
*Intituto MASPEC-CNR, Parma, Italy

Studies on the fractography of flux grown pure and doped M-type hexaferrites ($SrFe_{12}O_{19}$ and $SrGa_xIn_yFe_{12-(x+y)}O_{19}$; where x = 5,7,9 and y = 0.8,1.3,1.0) were carried out. It is observed that the pure hexaferrites show far mare perfect (0001) cleavages in comparison with those of substituted ones. Through experiments on successive etching and etching of matched cleavages, it is shown that H_3PO_4 at 120°C and 37% HCl at 100°C are dislocation etchants for these crystals. The morphology of etch pits is dependent on the composition of the hexaferrite. The substituted hexaferrites develop circular beaked etch pits whereas the pure $SrFe_{12}O_{19}$ exhibits hexagonal etch pits on (0001) planes. Preferential etching along grain boundaries and impurity striations are observed. Etching also reveals inter-penetrating type of twinning in crystals. It is shown that the twinned structures penetrate deep into the body of the crystal. Evidence indicating inclined, stepped and bending dislocations in pure hexaferrites is offered. Microhardness measurements on (0001) planes show vickers microhardness value to be around 900 kg/mm^2. This value is strongly dependent on load showing decrease till 80gm and thereafter, achieves saturation. An attempt is made to explain the results.

FLUX GROWTH OF BULK SINGLE CRYSTALS OF PURE AND SUBSTITUTED $BaFe_{12}O_{19}$ USING SOLVENTS OF THE Na_2O-$B_2O_3$3 SYSTEM

B74

R. Varadinov, V. Nikolov and P. Peshev
Institute of General and Inorganic Chemistry
Bulgarian Academy of Sciences, 1113 Sofia, Bulgaria

Single crystals of hexaferrites with a magnetoplumbite structure such as $BaFe_{12}O_{19}$ are applied in different microwave devices. In order to adjust the magnetic characteristics of barium hexaferrite to the specific requirements with respect to these devices, the Ba^{2+} and/or Fe^{3+} ions in the $BaFe_{12}O_{19}$ lattice are partially replaced by other metal ions (e.g. Pb^{2+}, Ga^{3+}, Al^{3+}, etc.).

Two new solvents of the Na_2O-B_2O_3 system (1) are used in the work and single crystals of pure barium hexaferrite and $BaFe_{12}O_{19}$ in which part of the metal ions are replaced by Pb^{2+} or Ga^{3+}, Al^{3+} and Mn^{2+} + Ti^{4+}, respectively, are grown from high-temperature, solutions in these solvents using the slow cooling technique and a rotating $BaFe_{12}O_{19}$ seed immersed in the solution. The single crystals obtained have a diameter of up to 20 mm and a length of up to 8 mm.

The effect of various technological parameters (cooling rate, character of temperature field, solvent composition and ratio between the components of the solute) on the growth rate, habit, chemical homogeneity and distribution of the substituent ions in the crystals is studied. The saturation magnetization and the Curie temperature of the single crystals with different composition are determined.

On the basis of the results obtained, suitable conditions of crystal growth with the compositions investigated are found.

1. R. Varadinov, V. Nikolov, P. Peshev, I. Mitov and Kh. Neykov, *J.Crystal Growth* 110 (1991) 763.

B75

OPTIMIZATION OF MONOLITHIC ZnSe FABRICATION BY CHEMICAL VAPOUR DEPOSITION

T.A. Cherepanova, A.F. Spivak, E.M. Gavrishchuk and I.A. Korshunov*
Centre of Microelectronics, Latvian Academy of Sciences,
19 Turgenev Street, Riga, Latvian Republic
*Institute of High-Purity Materials, Russian Academy of Science,
49 Tropinina Street, Nizhnij-Novgorod, Russian Republic

Computer simulation has been carried out for the gas patterns and ZnSe deposition in the CVD reactors at subatmospheric pressure. We consider nucleation in the gas phase and deposition at the reactor tube surface in the Zn-H_2Se-Ar system. As controlling process parameters we use the geometry and the surface temperature profile of reactor tube as well as the discharge, molar fractions of reactive components and temperature of inlet gases.

We discuss the influence of CVD process parameters on the gas flow patterns and the deposition rate profiles over the deposition area and inlet gas injectors. It is shown that the ratio of the H_2Se-Ar discharge through the central nozzle and Ar discharge through the narrow slot around that nozzle determines the existence of gas flow vortices near the reactor inlet. The influence of the Zn-Ar discharge through a ring injector surrounding the central one on the flow patterns is relatively low. We present the range of ratios where such vortices do not exist. The process parameters are determined which allow to minimize the clogging of nozzles due to the deposition at the injector tube. Computational results are compared with the experimental data on visualization of gas flow with TiO_2-fume.

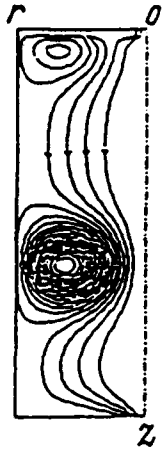

Figure 1. Stream lines for the gas flow in the axisymmetrical non-isothermal reactor.

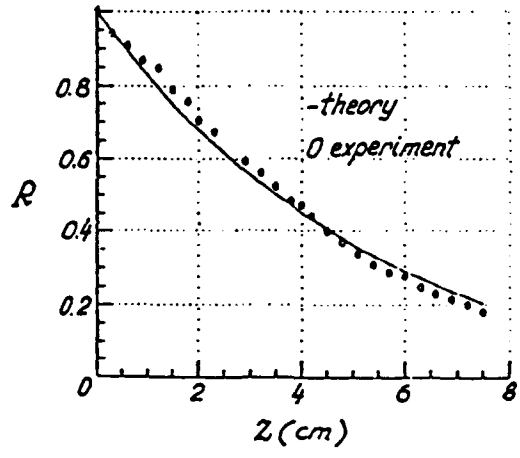

Figure 2. Non-dimensional ZnSe deposition rate along the reactor wall.

CHARACTERIZATION OF ZnTe EPITAXIAL FILMS GROWN BY MOVPE

B76

N. Lovergine, A.M. Mancini, D. Manno, L. Vasanelli
Dipartimento di Scienza dei Materiali
Universita' di Lecce, Italy

The morphology and the structure of ZnTe layers, deposited on GaAs substrates by metalorganic vapor phase epitaxy (MOVPE), have been characterized in detail by x-ray diffraction, reflection electron microscopy (REM) and reflection high energy electron diffraction (RHEED).

The layers have been grown from di-methyl zinc and di-isopropyl telluride using a temperature of 350°C in a atmospheric pression reactor.

The measured growth rate was about 0.5 nm s^{-1}.

The x-ray diffractions indicate that the heterostructure epitaxial relationship is (001)ZnTe//(001)GaAs. The RHEED observations show a azimuthal orientation of [011]ZnTe//[011] GaAs lattices according to x-ray data.

Scanning Electron Microscopy shows surfaces undulations with transverse size of about 1 μm. The REM observations allow us to image these undulations and perform height measurements. The undulation height, in the best samples, ranges between 2.5 and 6.0 nm.

Both structural and morphological characterizations confirmed that ZnTe/GaAs samples have a very good quality.

OBSERVATION OF POINT-DEFECT-ASSISTED GROWTH OF BULK ZnSe

B77

K. Terashima, T. Hayashi and E. Tokizaki
Kimura Metamelt Project, ERATO JRDC
Tsukuba Research Consortium, Tokodai 5-9-9,Tsukuba, Ibaraki 300-26, Japan

Over the past two decades, crystal growth technique for ZnSe single crystals have attracted much attention for their application as a substrate in blue light emitting devices. Many papers reported on the growth techniques for ZnSe crystals [1,2]. However, numerous twins and heavy impurity contamination occurred in boules obtained by these techniques [3]. Recently, an improved solid phase growth technique was developed for ZnSe single crystals using nonstoichiometric annealing, i.e. ,a grain grew from 10 μm to 10 mm in diameter by annealing a polycrystalline aggregate under a selenium atmosphere for two weeks, whereas a grain grew up to 2 mm by annealing under a zinc atmosphere [4].

A cluster of atoms in a crystal grown under a selenium atmosphere has a tendency to move easily during TEM observation with a focused electron beam [5]. This tendency causes the anomalous grain growth under a selenium atmosphere. To identify the defect structures closely related to the observed grain growth, point defects in bulk ZnSe were subsequently investigated using positron annihilation technique [6]. It has been found that the selenium interstitial type defects were dominantly observed in the crystals grown under a selenium ambient. This result suggests that the selenium interstitial type defects enhance the atomic migration in the crystal and assist the recrystallization by dislocation climb.

In order to observe the actual growing state, we have developed a transparent growing furnace with a tele-microscope. We studied the anomalous grain growth in situ, as a function of a selenium pressure and growth temperature. This paper reports the results of direct observation of anomalous grain growth. The absolute growth rate and the existence of the quasi-liquid layer at the grain boundaries will be discussed in terms of the direct observation system.

[1] I. Kikuma and M. Furukosi, Japan. *J. Appl. Phys.* 24(1985)L941.
[2] S. Fujita, H. Mimoto, H. Takebe and T. Noguchi, *J. Crystal Growth* 47(1979)326.
[3] K. Terashima and M. Takena, *J. Crystal Growth* 110(1991)623.
[4] K. Terashima, M. Kawachi and M. Takena, *J. Crystal Growth* 102(1990)387.
[5] K. Terashima, M. Kawachi and M. Takena, *J. Crystal Growth* 104(1990)467.
[6] K. Terashima et. al. to be published.

B78

CONTROL OF MICROTWINS IN MOCVD OF CdTe ON SAPPHIRE

H. L. Glass, M. L. Buehnerkemper, D. L. Varnum and T. P. Weismuller
Electro-Optical Center, Rockwell International Corporation
Anaheim, California 92803, USA

Sapphire wafers with an epitaxial buffer layer of CdTe serve as large, rugged substrates for epitaxial deposition of HgCdTe infrared detector materials. One concern with CdTe is the ready formation of twins which are difficult to remove and can degrade device performance. In the case of epitaxial CdTe, twinning usually takes the form of microtwins. When c-plane sapphire is used as the substrate, a high concentration of microtwins occurs near the interface. We have found that, by suitable choice of MOCVD conditions, the microtwin content diminishes rapidly with distance from the interface. Extremely low microtwin content can be obtained a few micrometers away from the interface. As measured by X-ray diffreaction, microtwin content close to or below the detection limit of 0.002 volume percent is achieved routinly on large wafers in a production environment. For rapid inspection, low microtwin content is verified by an optical scattering technique which supplements the more time consuming X-ray diffraction methods.

We will describe the procedures used to minimize microtwin content in CdTe deposited on 2-inch and 3-inch diameter c-plane sapphire in a conventional, vertical MOCVD reactor using dimethyl precursors of Cd and Te. In addition, a producible method for removing microtwins will be reported.

B79

THE GROWTH OF CUBIC, SINGLE PHASE, SINGLE CRYSTAL $Cd_{0.6}Mn_{0.4}Te$ BY THE VERTICAL GRADIENT FREEZE (VGF) METHOD

M. Azoulay, R. Weingarten, H. Schacham and H. Feldstein
Soreq Nuclear research Center, Yavne 70600, Israel

CdMnTe is a semi-magnetic, semi-conductor with promising properties. It can be applied for both magneto optic devices and substrates for the epitaxial growth of HgCdTe layers[1]. However, the growth of CdMnTe single crystal faces some difficulties due to phase transition in the solid state at high temperature, just after solidification. To overcome this problem it has been suggested to grow the crystal by the THM method[2], or to grow the crystal from the melt at high axial thermal gradient near the interface[3].

In this paper we present for the first time, the growth of cubic, single phase, $Cd_xMn_{1-x}Te$ single crystal by the vertical gradient freeze technique under a very low axial thermal gradient in the melt (3°C/cm) and high Manganese content (X ≈ 40%). The solidification stage is characterized by a rapid cooling of the crystal through the phase transition temperature region followed by annealing at about 800°C. The crystal exhibits a very high crystalline perfection as measured by the Double Crystal X-Ray Rocking Curves with a FWHM of 30 arcseconds and low optical losses of about 1 dB/mm between 650 nm and 800 nm with λ-cutoff at 630 nm. Further magneto optical properties are currently examined for a possible application in devices.

1. W. Giriat and J.K. Furdyna, In "Semiconductors and semimetals" vol. 25, Willardson & Beer, Academic press, Inc. (1988).
2. R. Triboulet, A. Heurtel and J. Rioux, *J. Cryst. Growth* 101. (1990) 131.
3. M. Katsuda, K. Hosoe and M. Nakaseko, *Sumitono Elec. Tech. Rev.* (1990) 84.

SEGREGATION ENGINEERING DURING CRYSTAL GROWTH BY THE TRAVELLING HEATER METHOD

B80

P. Gille, R. U. Bloedner and N. Puhlmann
Humboldt University of Berlin, Department of Physics, Institut for Crystallography and Materials Science, Invalidenstraße 110, O-1040 Berlin, Germany

The travelling heater method (THM) has been successfully applied to crystal growth of mixed crystals especially in the II-VI and III-V semiconductor systems. Regarding THM as a continuous liquid-phase epitaxy, it is these steady-state conditions which cause the main advantage of growing crystals being homogeneous with respect to the mole fraction of the alloy or to the doping concentration.

Like with other methods of crystal growth from solution, in THM the equilibrium temperature can be chosen in a wide range. Usually the growth temperature as well as the other parameters are held as constant as possible to result in homogeneous crystals [1]. Nevertheless, for purposes of basic research sometimes there is a special need for crystals with a well-defined long-range variation of the alloy composition.

The paper gives a simple mathematical description of the influence of temperature variation during THM growth on the composition of the resulting crystal. Use is made of mass balance equation, axial temperature distribution and thermodynamical equilibrium feed data. Starting with a macroscopically homogeneous feed ingot, this procedure is a tool to grow a cylindrical mixed crystal having alternatively an increasing, a constant or a decreasing alloy composition along the axial direction.

Experimental results of the axial distribution of mole fractions will be given for some II-VI semiconductor systems ($Hg_{1-x}Cd_xTe$, $Hg_{1-x}Zn_xTe$, $Cd_{1-x}Zn_xTe$). But, complete theoretical description needs exact knowledge of the ternary solid-liquid phase relations which are only available for the $Hg_{1-x}Cd_xTe$ system, up to now.

[1] P. Gille et al., A new approach to crystal growth of $Hg_{1-x}Cd_xTe$ by THM, *J. Crystal Growth*, in press.

THE CORRELATION BETWEEN SUPERCOOLING AND OVERHEATING IN ASSOCIATED SEMICONDUCTOR MELTS DURING UNSEEDED BRIDGMAN GROWTH

B81

*M. Mühlberg, P. Rudolph, M. Laasch and E. Treser**
Humboldt University of Berlin, Department of Physics, Institute for Crystallography and Materials Science, Invalidenstraße 110, O-1040 Berlin, Germany
*University of Freiburg, Institute for Crystallography
Hebelstraße 25, W-7800 Freiburg, Germany

The renewed attention to the Bridgman method includes more and more semiconducting compounds. Depending on the substance, the use of a seed crystal is quite difficult. Therefore, a unseeded growth procedure is mainly carried out and attention has to be focused on the nucleation process.

In associated melts (II-VI and IV-VI compounds) it is assumed to exist a correlation between the actual temperature of the melt T_L before the growth beginning (overheating over the melting point $\Delta T_{oh} = T_L - T_M$; T_M - melting point) and the supercooling in the tip region ($\Delta T_{sc} = T_M - T_S$, T_S - temperature of the crystallisation beginning). The supercooling measured in the tip region is a function of overheating, degree of deviation from the stoichiometric composition as well as the holding time. Additionally, these results will be compared with DTA measurements.

In the case of CdTe, the use of a stoichiometric melt composition demands an overheating of more than 10 K in order to destroy any Cd-Te associates in the liquid phase. The step-like increasing in the stoichiometric case (see Fig.) shows that a reduced supercooling effect can be realized by only a slight overheating regime. Melt compositions with a Te excess give rise always to a considerable supercooling. The Te excess is assumed to dissolve the Cd-Te associates. Further consequences on the crystalline quality and the anomalous segregation behaviour will be discussed.

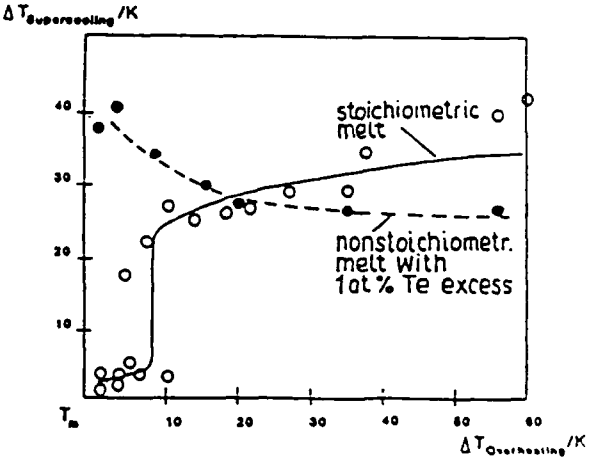

B82

DETERMINATION OF PHASE EQUILIBRIUM DATA IN THE Hg-Cd-Te SYSTEM FROM LPE EXPERIMENTS

T. Boeck and K. Jacobs
Institut für Kristallographie und Materialforschung
Humboldt-Universität zu Berlin Invalidenstr. 110,
O-1040 Berlin, Fed. Rep. of Germany

The mixed crystal composition of $Hg_{1-x}Cd_xTe$ layers grown by liquid phase epitaxy (LPE) from Te-rich solutions depends very sensitively on the composition of the liquid phase. Data from the literature are only rather crude or show intolerable differences.

For this reason liquidus temperatures ($450°C < T_L < 480°C$) and the corresponding mixed crystal compositions ($0.2 < x < 0.4$) have been determined experimentally as a function of various melt compositions. The data have been obtained ex situ from special experiments as well as in situ from LPE experiments. At the same time expressions for liquidus temperatures and materials constants have been derived from common equations describing the LPE growth kinetics. The materials constants appearing in these equations have been determined from LPE growth runs performed in the step-cooling mode. Good lateral and vertical homogeneity in composition as well as reproducibility of thickness, composition and good surface morphology can only be achieved after optimizing the homogenization procedure. The only reliable method is a mechanical stirring of the melt solution. A criterion is given characterizing the perfectness of source melt homogenization. The analysis of the experimentally determined correlations between layer thicknesses, growth time and deposition temperatures confirms the ex situ determined liquidus temperatures. Linear extrapolation of the x values to the liquidus temperatures allows the determination of the equilibrium mixed crystal composition. Second order polynomials for liquidus temperatures and solid compositions, respectively, have been derived from the experiments.

B83

VARIATION OF SURFACE MORPHOLOGY WITH PRECURSORS SUPPLY RATIO IN MOVPE CdTe LAYERS

Touati Ferid, Mitsuru Ekawa, Kazuhito Yasuda, Akikazu Tanaka and Manabu Saji*
Nagoya Institute of Technology, Nagoya, Japan
*Sumitomo Metal Mining, Tokyo, Japan

The Te/Cd ratio at the growth surface is an essential factor which characterizes the MOVPE CdTe growth. This ratio is notably important for extrinsic p- and n-type doping. As a measure of the ratio, the supply precursors ratio is commonly employed. However, since the growth is generally performed near the pyrolysis temperature of the precursors, the ratio at the surface is expected to change from one growth system to another, even for same supply conditions. This is because the transport processes during growth and the heating up manner of the precursors are strongly altered by the effect of the reactor configurations differences.

In this paper, the variation of the surface morphology of (100) CdTe layers with the supply precursors ratio varied in a wide range, was deliberately studied. Different morphology features were reproducibly obtained for different ratios. These features were highly correlated with the growth characteristics and the optimal extrinsic doping conditions. Thus, the comparison of the surface morphologies can be used as an effective way to correct the individual growth conditions for the above effect. The CdTe layers were grown on (100) GaAs around 400°C using dimethylcadmium (DMCd) and diethyltelluride (DETe). The DETe/DMCd supply ratio was varied in the range from 0.1 to 6. Layers grown at DETe/DMCd ratios in the 0.1-1 range exhibited pyramidal hillocks. The size of the hillocks decreased by increasing the ratio up to unity. In this region, efficient As-doping could be achieved. For the DETe/DMCd ratio between 1 and 2, the surfaces showed mirror-like specular morphologies. The layers grown in this region showed PL spectra with sharp (A^oX) emission line without deep level emission. This indicates that high quality layers were grown at these ratios. In the DETe/DMCd ratio range of 0.1-2, the growth rate increased with the DETe flow which indicates that the growth mechanism is dominated by Te coverage rate. For ratios exceeding 2, the surfaces showed ellipse-like pits, elongated towards the n. The size and the density of the pits increased for increased ratio. In this region, the growth rate was not dependent on the DETe flow but on the DMCd flow.

B84

GROWTH AND CHARACTERIZATION OF SOME I-III-VI_2 COMPOUND SEMICONDUCTORS

K. Balakrishnan, B. Vengatesan and P. Ramasamy
Crystal Growth Centre, Anna University, Madras 600 025, India

Ternary and pseudo ternary $A^{I}B^{III}X^{VI}$ compounds are attracting attention from fundamental point of view as a third generation of semiconducting materials after elemental and binary systems. In the present investigation, single crystals of some ternary chalcopyrite semiconductors such as $CuInS_2$, $CuInSe_2$, $CuInTe_2$, $CuGaS_2$, $AgGaS_2$ and pseudo ternary compounds, CuInSSe, AgGaSSe, CuGaSSe and AgInSSe have been grown by chemical vapour transport technique (by adopting oscillating temperature profile) using iodine as the transporting agent. Attempts are being made to grow these crystals using $TeCl_4$ as the transporting agent and the efficiencies of these two transporting agents have been studied. The growth details are tabulated in the table below:

Crystallization behaviour of the grown crystals was investigated by taking x-ray powder diffractograms using CuKα radiation and the lattice parameters have been calculated. XPS and chemical analyses have been carried out in order to confirm the stoichiometry of the crystals. The hardness, anisotropy of hardness and creeping in some of the grown crystals are explained in terms of bond energies. Energy gaps of the crystals have been determined by optical method.

Crystal	Source Temperature T_s (°C)	Growth Temperature T_d (°C)	Transporting agent	Size (mm^3)
$CuInS_2$	830	800	I_2	7 x 3 x 1
$CuInSe_2$	809	770	I_2	5 x 3 x 2
$CuInTe_2$	710	670	I_2 & $TeCl_4$	3 x 1 x 1
$CuGaS_2$	840	750	I_2	3 x 1 x 1
$AgGaS_2$	930	891	I_2	3 x 2 x 1
$CuInSS_e$	950	900	I_2	3 x 2 x 1
AgGaSSe	934	852	I_2	4 x 2 x 2
CuGaSSE	980	940	I_2	3 x 2 x 1
AgInSSE	976	932	I_2	4 x 2 x 1

B85

CRYSTAL GROWTH OF $AgGaS_2$ BY THE BRIDGMAN-STOCKBARGER-TECHNIQUE USING SHAPED CRUCIBLE

E. Treser, E. Post and V. Krämer
Kristallographisches Institut der Universität, Hebelstraße 25
D W-7800 Freiburg, Federal Republic of Germany

The I-III-VI_2 compound $AgGaS_2$ crystallizes with the chalcopyrite structure type ($I\bar{4}2d$). High nonlinear susceptibility, a wide area of transparency in the infrared region (0.6 - 13 μm), and the possibility of phase matching are interesting properties for nonlinear optical applications.

Careful engineering to overcome problems caused by anomalous thermal expansion along the c-axis has enabled the successful crystal growth of $AgGaS_2$ bulk material by the vertical Bridgman-Stockbarger-technique using growth ampoules with circular cross-sections.

For specific device applications $AgGaS_2$ crystals has to be cut at various angles to their optic axis. Therefore these investigations should answer the question whether crystals with controlled crystallographic orientation could be grown in square cross-section ampoules (Feigelson & Route, 1990).

Melt growth was performed by self-seeding as well as with seeds oriented with their [001] direction parallel to the ampoule axis. Both procedures yielded single crystals up to 40 mm lengths. In comparison to previous publications they show a relatively high transparency in the visible due to the feed material received from earlier crystal growth experiments. Compositional variations in growth direction could not be determined. Additional heat treatment by annealing the $AgGaS_2$ crystals at 900°C for 21 days in the presence of an Ag_2S atmosphere led to visually clear crystals.

Lamellar twinning is not frequently observed in crystals grown by self-seeding. It seems that lamellar twinning in the tip has the possibility of "running out" of the crystal, if crystal growth is enforced in square cross-section ampoules. The seeded $AgGaS_2$ crystals were always free of twins.

R.S. Feigelson & R.K. Route, *J. Cryst. Growth* 104 (1990) 789-792.

B86

GROWTH AND CHARACTERIZATION OF CdS FILMS DEPOSITED ON $CdInGaS_4$ BY EVAPORATION METHOD

Shizutoshi Ando, Saburo Endo, Hisayuki Nakanishi and Taizo Irie
Department of Electrical Engineering, Faculty of Engineering
Science University of Tokyo, Shinjuku-ku, Tokyo 162, JAPAN
Taro Toyoda
University of Electro-Communications, Choufu-shi, Tokyo 182, Japan

The II-VI compound CdS is well known to show a green photoluminescence at liquid nitrogen temperature (77K). Recently we have found a new material Cd_3InGaS_6 which shows very intense green photoluminescence at 77K. We suggested from the results of crystal structure analysis that Cd_3InGaS_6 is a laminated material composed of CdS and $CdInGaS_4$[1]. We prepared the samples of CdS/$CdInGaS_4$ by vapor deposition of CdS on $CdInGaS_4$ single crystal and observed very intense green photoluminescence at 77K[2]. Then, we suggested that the intense green emission is edge emission in CdS enhanced by the laminated $CdInGaS_4$[3].

In this work, we prepared the samples of CdS/$CdInGaS_4$ by evaporation of CdS films on $CdInGaS_4$ single crystals. The evaporated CdS films on $CdInGaS_4$ were annealed for 5 hours in N_2 gas at various temperatures. The samples of CdS/$CdInGaS_4$ were characterized by X-ray diffraction, photo luminescence and scanning electron microscope (SEM).

Figure 1 shows the photoluminescence spectrum at 77K of CdS/$CdInGaS_4$ produced by evaporation of CdS film on $CdInGaS_4$ single crystal and subsequent annealing at 600°C. For comparison, the photoluminescence spectrum of CdS film evaporated and annealed at 600°C on glass substrate is also shown in the figure. It can he seen that the green emission of CdS/$CdInGaS_4$ is much stronger than that of CdS/glass. It can be concluded that the edge emission in CdS can be enhanced by laminated $CdInGaS_4$.

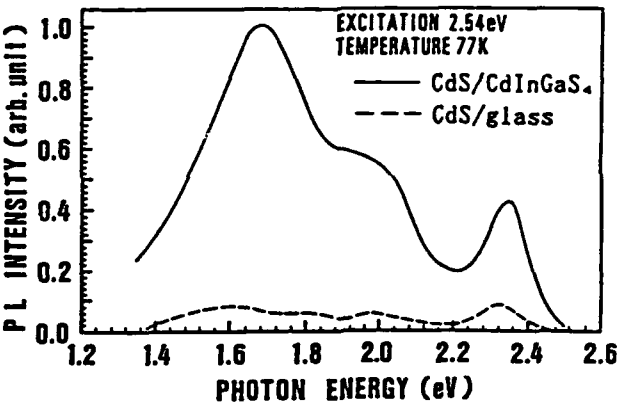

Figure 1. Photoluminescence spectra of CdS/$CdInGaS_4$ and CdS/glass.

[1] H. Matsushita, S. Nomura, S. Ando, S. Endo, T. Irie: *Jpn. J. Appl. Phys.* 29 (1990) L872.
[2] S. Ando, S. Endo, H. Nakanishi, T. Irie: *Jpn. J. Appl. Phys.* 30 (1991) 2540.
[3] S. Ando, T. Okada, S. Endo, T. Irie, T. Miya, H. Nakanishi: *J. Cryst. Growth* (1991) (to be published).

B87

GROWTH OF ZnTe BY PHYSICAL VAPOR TRANSPORT AND TRAVELING HEATER METHOD

Ching-Hua Su, M.P. Volz, D.C. Gillies, F.R.Szofran and S.L. Lehoczky*
Space Science Laboratory, NASA/Marshall Space Flight Center
M. Dudley
State University of New York at Stony Brook

ZnTe crystals were grown by the following two methods:

(1) Physical vapor transport – a growth process for the physical vapor transport in closed ampoules were developed. With the technique applied in the heat treatment of the starting materials and the temperature profiles provided by a horizontal three-zone translational furnace, large crystals of ZnTe have been grown successfully at lower temperatures than previously used.

(2) Traveling heater method (THM) – ZnTe crystals were grown by THM in a vertical three-zone translational furnace in Te-rich solution at about 900°C.

The crystals were examined by X-ray (Laue) diffraction, synchrotron radiation, optical and scanning electron microscopy to study the growth orientation and the crystalline structural perfection. The crystals were also characterized by low temperature infrared (IR) absorption as well as Hall measurements. Several distinct peaks were observed in the IR absorption spectra at 4.2 K for THM samples and they were identified to be Cu^{2+}. Similar measurements on vapor grown ZnTe showed featureless absorption spectra.

*Universities Space Research Association

B88

HIGH PRESSURE BRIDGMAN GROWTH OF ZnTe AND ZnSe

F.P. Doty and J.F. Butler
Aurora Technologies Corporation, 7408 Trade Street, San Diego, CA 92121-2410

Compounds which decompose into volatile constituents below their melting points pose problems for crystal growth from the melt. The high pressure Bridgman (HPB) method is a relatively uncomplicated approach suited to growth of such materials. Design features of the HPB apparatus and its advantages in the growth of materials such as the wide bandgap II-VI compounds are discussed.

ZnTe and ZnSe crystals were grown from the melt by the HPB method. Boules of up to 10 cm in diameter and 4 Kg mass have been grown, yielding grains up to 6 cm. Properties reported include etch-pit densities (EPD), double-crystal rocking curves (DCRC), low temperature photoluminescence (PL) and resistivity.

With carefully purified starting materials, HPB yields high quality ZnTe crystals, as evidenced by PL spectra remarkable for their line sharpness and absence of the deep level bands associated with oxygen and native defects. The crystals exhibited EPD in the low-10^3 to low-10^4 cm^{-2} range and DCRC full widths at half maximum of less than 20 arc-seconds.

Commercial powdered ZnSe was used as the starting material for the ZnSe crystals. Characteristics of the resulting material are presented.

B89

GROWTH AND CHARACTERIZATION OF ZnSe FOR LOW TEMPERATURE CALORIMETRY APPLICATIONS

F. Allegretti, A. Carrara and S. Pizzini*
Physical Chemistry Department, University of Milan
*Consorzio Milano Ricerche, 15, via Emanueli, 20126 Milano Italy

Zinc selenide, already used in electroluminescent and photoconductive devices, is also a potentially good candidate for a variety of applications in optoelectronics (lasers, light emitting diodes), as material for IR optics and as a detector for low temperature thermal phonons and for double beta decay events. For most of these applications, high structural quality and low impurity content is a fundamental prerequisite.

As we were mainly interested in the application for low temperature calorimetry and for laser host matrices, we have grown ZnSe single crystals using the PVD technique, with the aim of determining the critical growth parameters. So far, the nature and the purity of the starting material, the prepurification conditions, the inert gas pressure inside the silica ampoule and the growth conditions were considered in correlation to the growth results. The microstructure of the crystals was investigated in detail, by chemical etching and direct observation of etch pits by optical and SEM microscopy. Additionally, photoluminescence spectra were used as a criterion for electrically active impurity detection.

B90

TRANSPORT RATE AND EPITAXIAL GROWTH OF $Hg_{1-x}Zn_xTe$ BY CHEMICAL VAPOR TRANSPORT IN A CLOSED AMPOULE

Yi-Gao Sha, C.-H. Su**, S. L. Lehoczky and F. R. Szofran*
Space Science Laboratory
NASA Marshall Space Flight Center, Huntsville, Alabama 35812

The transport properties of $Hg_{1-x}Zn_xTe$-iodine system are investigated for the first time both theoretically and experimentally. The thermochemical properties of the system are considered and the partial pressures of all vapor species calculated according to the possible chemical reactions involved. Mass flux equations of vapor species are solved simultaneously using numerical methods. The transport rate and the composition of the grown crystals are predicted. The experimental results are compared with the theoretical calculations.

Epitaxial layers of $Hg_{1-x}Zn_xTe$ are grown on the lattice matched CdZnTe substrates employing the chemical vapor transport technique. Different growth temperatures and various partial pressures of HgI_2 as a transport agent are used while the source materials have a fixed composition. The grown epitaxial layers are characterized by optical microscopy and SEM for the surface morphology, by chemical etching for the structural defects, and by EDX measurements for the compositional analysis. The effects of the growth temperature and HgI_2 pressure on the grown epitaxial layers are discussed.

*Science and Technology Corporation.
**Universities Space Research Association.

SESSION 3C

C34

GROWTH OF GaInP THICK LAYERS BY THE MODIFIED YO-YO SOLUTE FEEDING METHOD

S. Watabe, K. Tadatomo, T. Sukegawa and A. Tanaka**
Central Research Laboratory, Mitsubishi Cable Industries,
4-3 Ikejiri, Itami, Hyogo 664, Japan
*Research Institute of Electronics, Shizuoka University,
3-5-1 Johoku, Hamamatsu 432, Japan

A new process for the yo-yo solute feeding method has been proposed to grow a thick GaInP alloy layer with constant composition.

In the yo-yo method, the temperature of a sandwich system consisting of a substrate (upper) growth solution (middle) and a source material (lower) is modulated. This leads to the spatial modulation of the solute distribution in the growth solution, and enhances the upward transport of the solute due to the difference in specific gravity between solute and solvent. Repetition of this process allows sequential growth of layer by layer as far as the source material exists, resulting in a very thick layer growth.

For the growth of GaInP alloy, GaP wafers can be used for the source material. In this case, Ga and P to be incorporated in the grown alloy are fed from the GaP source material, and In from the In-Ga-P solution. Therefore, if the average temperature is held constant, the liquidus composition (or alloy composition) changes during the yo-yo process. This problem is serious in case the growing alloy of which composition is in the range of $x<0.9$. To maintain an alloy composition uniform, the average temperature should be lowered based on the In-Ga-P ternary phase diagram.

In the experiments, a GaAsP VPE layer was used as the substrate lattice-matching to $Ga_{0.68}In_{0.32}P$. The solution was prepared by saturating indium with InP and GaP to grow the alloy at 800°C. The sandwich system of GaAsP substrate/Ga-In-P solution/GaP source was loaded in a carbon vessel placed in H_2 gas ambience. Molten B_2O_3 was used to suppress the phosphorus vapor escaping from the vessel. The temperature was raised to 800°C and held for 2h. Then, the yo-yo cycles with the amplitude of 25°C were repeated. In each cycle, the average temperature was lowered by 5°C. With 3 cycles only, the growth thickness of about 70 μm was obtained. EPMA and PL measurements revealed that the grown layer had high quality. By removing the substrate from the alloy layer, a self-sustained GaInP allow substrate was fabricated. The thickness of the alloy layer can be increased by increasing modified yo-yo cycles.

C35

IMPROVEMENT OF HIGH BRIGHTNESS AlGaAs/GaAs DH RED LED UNDER OPTIMIZED GROWTH CONDITION

B.T. You, J.Y. Kao, J.R. Deng, J.S. Shea, Y.S. Chang, C.Y. Juan and T.P. Chen
Materials Research Laboratories, Industrial Technology Research Institute
Chutung, Hsinchu, 31015, Taiwan, Republic of China

The high brightness AlGaAs red light emitting diodes (LEDs) with a double heterostructure (DH) grown on a GaAs substrate by liquid phase epitaxy (LPE) have been produced with efficiencies significantly higher than other visible red LEDs. These high brightness AlGsAs red LEDs now are widely used in applications such as outdoor displays and high mounted third brake light. In these work we conduct a detailed study to improve the brightness of the AlGaAs DH red LEDs. The influence of growth conditions on AlAs mole fraction in the epitaxial layer as well as the epitaxial layer thickness are investigated by photoluminence double crystal x-ray and optical microscope. It is shown that uniform AlAs mole fraction of the active layer can be obtained by optimized growth conditions, i.e. optimized cooling rate and initial supercooling. Also the luminous intensity of the AlGaAs DH red LEDs grown by LPE is increased by increasing the growth temperature in the growth temperature range of 800-900°C under optimized the carrier concentration of the epitaxial layers. The typical luminous intensity of the DH AlGaAs red LEDs operated at 20 mA is about 15 mcd grown under optimized conditions and have very good reproducibility and reliability. The highest luminous intensity of the unencapsulated LEDs is about 20 mcd.

C36

A MASS PRODUCTION METHOD FOR HIGH BRIGHTNESS 655nm AlGaAs DOUBLE HETEROSTRUCTURE RED LED

J.S. Shea, J.Y. Kao, B.T. You, J.R. Deng, Y.S. Chang, C.Y. Juan and T.P. Chen
Materials Research Laboratories, Industrial Technology Research Institute
Chutung, Hsinchu, 31015, Taiwan Republic of China

A novel graphite boat which enables the growth of multi-layer AlGaAs/GaAs double heterostructure (DH) by liquid phase epitaxy (LPE) on 2 pieces of 40 mm ϕ substrates per growth run was developed. The graphite boat is a 3 tier design. Three melt reservoirs located in the upper tier are separated from. the slider by a shutter. The shutter has an opening which allows the melt to be transferred from the melt reservoir to the slider. The slider, which is 1 cm thick, has an elliptical opening that is large enough to cover 2 pieces of 40 mm ϕ substrates. With this kind of design, the graphite boat allows a sequential selection and dropping of the melts at desired intervals of time, and the two-phase liquid epitaxy can be used. Preliminary experiments on 655 nm AlGaAs DH red LEDs grown by this novel graphite boat showed very good uniformity and reproducibility. These results promise a mass productive and economical liquid phase epitaxy system for preparing 655 nm AlGaAs/GaAs DH structure.

C37

LATTICE COMPENSATION EFFECT IN GaAs n^+-n^- JUNCTIONS USING LIQUID PHASE EPITAXY

T. Kamiya, A. Tomita, M. Kimura, A. Tanaka and T. Sukegawa
Research Institute of Electronics, Shizuoka University
Johoku 3-5-1, Hamamatsu 432, Japan

Fabrication of GaAs power devices requires n^+-n^-(p^-) or p^+-n^-(p^-) junctions with abrupt transition regions. However, wafer bending is serious problem. This phenomenon is attributed to the difference in lattice constant between the substrate and the grown layers. The discrepancy of lattice constant is affected by the size and concentration of impurity atoms. As reported before [1], we could grow p^+ layer on n^- GaAs substrate under lattice matching condition using Ge as a dopant. The purpose of this paper is to present the lattice compensation effect in n^+-n^- junction using LPE growth of GaAs. Our technique is based on simultaneous doping of Te and Si.

In the case of Si-doped layer, the lattice constant is smaller than that of the intrinsic GaAs because covalent radius of Si (1.17Å) is smaller than the average value of GaAs (1.22Å). On the contrary, that of Te-doped layer is larger because of its larger radius (1.32Å). Therefore the lattice constant of the epitaxial layer can be fitted to that of the low-impurity substrate by simultaneous doping of Te and Si. All the epitaxial growth reported in this paper was performed using Ga as a solvent. The epitaxial layers were grown on (100) oriented, n^- GaAs substrate ($1x10^7$ kΩ-cm) by ramp cooling from 800°C to 799°C. In this condition, layers of approximate 5 μm thickness are reproducibly obtained. The lattice constants were measured by Bond's method and high resolution 5-crystal X-ray Diffractometer (5CXRD). 5CXRD rocking curves have been recorded using a computer controlled goniometer having an angular resolution of 0.1 arc sec; the CuKα_1 radiation, the (004) symmetric reflection and a 4-crystal (Ge) monochromator have been used.

The layers under lattice matching conditions were confirmed to reveal n-type conduction. Using this effect, we can prepare thick n^+($\sim 10^{18}$cm^{-3})-n^-($\sim 10^{12}$cm^{-3}) junction under lattice matching condition for the fabrication of GaAs power devices. Detailed relation between lattice matching condition and carrier concentration will be discussed.

[1] T. Sukegawa, M. Suzuki, M. Kimura, T. Kamiya, A. Tomita and A. Tanaka, Proceedings of Symposium on Materials and Devices for Power Electronics - MADEP, Firenze, ITALY, September 1991, 019-024.

C38

IN SITU OBSERVATION OF MORPHOLOGICAL CHANGE ON LPE GROWN SURFACE IN SEMICONDUCTOR

Y. Inatomi and K. Kuribayashi
The Institute of Space and Astronautical Science
Yoshino-dai, Sagamihara, Kanagawa 229, Japan

On the surface of crystals grown epitaxially in the liquid phase (LPE) macrosteps are frequently observed. Macrosteps vary with the growth conditions of LPE growth process morphologically and induce the segregation of dopant atoms. Many investigators have studied the characteristics of macrosteps, their morphologies and their relationships with dopant distribution. However, the dynamics of formation, migration and coalescence of macrosteps have not been revealed precisely and the quantitative relation between the segregation of dopant atoms and the atomic step velocities have been still in veil. In order to obtain precise understanding of the phenomenon, it is necessary to get the quantitative relation between growth condition and surface morphological change. Danilewsky et al. [1] reported that growth rate and temperature gradient can be regarded as the disappearance condition for macrosteps in case of travelling heater method (THM). The influence of the growth rate and temperature gradient upon the surface morphology during LPE growth process have been studied by means of the real-time observation setup.

Semiconductors with rather large bandgap are transparent to infrared radiation. For instance, the critical wavelength corresponded to the bandgap are 873 nm for GaAs and 549 nm for GaP, respectively. Authors, based on the transparent properties of semiconductors for infrared radiation, observed the morphological changes of the solid-liquid interface and measured the growth rate during LPE growth process in GaP with the infrared microscope with the interferometer directly [2].

Figure 1 shows the comparison between the theoretical growth rate and the experimental one in GaP. The theoretical curve is indicated by a bold line. The experimental data are plotted by closed and opened circles. As easily understood from this figure, the measured data does not obey the theoretical prediction. The reason for the discrepancy of the experimental values from the theoretical ones should be attributed to other factors, for instance, convection. Figure 2 is an example of the bright field image of macrosteps which appeared on a facet in GaP during growth process. The growth method was stepcooling and the temperature gradient in the liquid was parallel to and negative along the direction of the gravity vector. On the other hand, it was shown that the positive temperature gradient in the liquid tends to suppress the appearance of macrosteps.

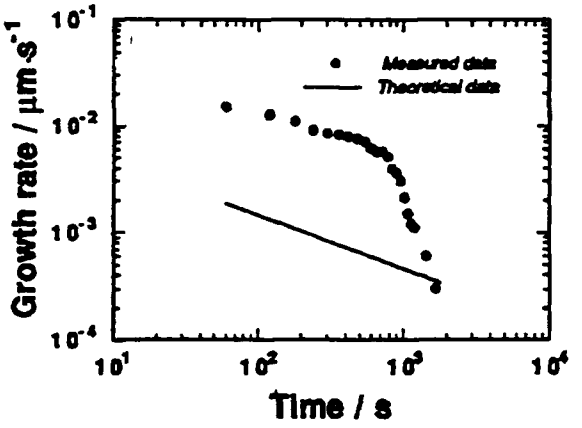

Figure 1. Comparison between theoretical values and experimental ones for growth on condition of ΔT = 10 K at 1073 K.

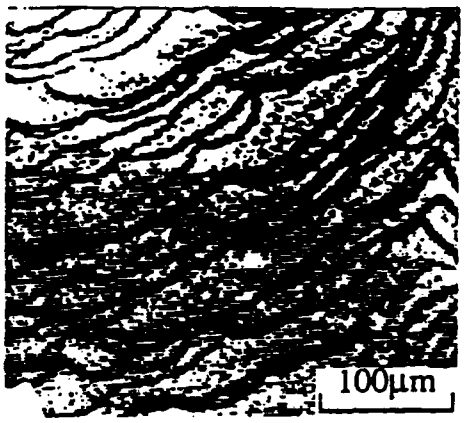

Figure 2. The typical example for the bright field image during growth process.

[1] A.N. Danilewsky, K.W. Benz, T. Nishinaga, *Journal of Crystal Growth* 99 (1990) 1281.
[2] Y. Inatomi and K. Kuribayashi, *Journal of Crystal Growth* 114 (1991) 380.

C39

DEFECT FORMATION IN SEMICONDUCTOR LAYERS DURING EPITAXIAL GROWTH

Bruce Steiner, Wen Tseng, James Comas, Uri Laor, and Ronald C. Dobbyn
National Institute of Standards and Technology
Krishna Rajan
Rensselaer Polytechnic Institute

High resolution monochromatic synchrotron radiation diffraction images of five epitaxial heterojunctions of various II, III, IV, V, and VI materials portray a range of irregularities. The differences observed suggest fundamental factors in the formation of defects in these layered systems. The systems observed include: 1) a germanium/silicon superlattice on a silicon substrate; 2) an MBE-grown gallium arsenide HEMT structure on gallium arsenide substrate; 3) a mercury cadmium telluride grid on a layer of cadmium telluride, on a gallium arsenide buffer layer, on a silicon substrate; 4) another gallium arsenide HEMT structure on an indium phosphide substrate; and 5) an indium gallium arsenide superlattice on an iron-doped indium phosphide substrate.

Residual lattice mismatch is reflected in each system by the warping of the substrate after layer deposition. Nevertheless, lattice orientation is maintained in all five of these systems. In two of them, the germanium/silicon superlattice on silicon and the HEMT structure on a gallium arsenide substrate, no arrays of dislocations associated with the layering are observed. A set of pure edge dislocations is found in the system with the grid structure. Denser sets of linear defects of a mixed nature are found in the other two systems.

The observations suggest that the formation of extensive arrays of dislocations during uniform one micrometer layer deposition depends on the simultaneous fulfillment of two criteria. The first of these is the formation of a distinct new layer mismatched with the substrate by several tenths of a percent. The second is the presence of local irregularities in the substrate. If either of these criteria is not fulfilled, the formation of dislocations appears to be inhibited. However this inhibition may be overridden by localized residual stress.

GROWTH KINETICS OF VAPOR GROWN SiC

C40

Tsutomu Kaneko
Department of Applied Physics, The Science University of Tokyo
Kagurazaka, Shinjuku-ku, Tokyo-162

According to equilibrium gas kinetics, the reported experimental data of vapor grown SiC are compared with the theoretical prediction. The Arrhenius plot of the growth rates reveals simply the formulated growth mechanisms for many cases. The criteria is based on considerations of the rate-determining conditions and of the impinging molecular flux in equilibrium as we reported[1].

We have calculated the concentration of the transport limiting species and then transport rates from the HK (Hertz-Knudsen) equation. The calculated values are shown in Figures as a solid line, the reported data as solid circles and the fitted formulation as a dashed line.

The data of von Muench et al[2] for β-SiC CVD are rearranged in Fig. 1 where the temperature of the DDS bubbler is 12°C and the substrate is two carbon rods of 6 mm in diameter and 150 mm in length. The difference between the experimental growth rates and calculated values is smaller at higher temperatures and it is formulated as a surface-kinetics-limited process[1] as follows,

$$G_{hk} = \frac{M_s}{\rho} J = \frac{M_s}{\rho} \frac{P_{eq}}{\sqrt{2\pi M_s RT}}$$

$G = \alpha G_{hk}$,

$\alpha = A \exp(-E_d/RT)$.

The activation energy is 16 kcal/mol. Our experiment for β-SiC CVD[3] indicates similar temperature dependence of the growth rates and gives the energy of 23 kcal/mol.

The data of Bootsma et al[4] for SiC whisker can be compared with the equilibrium vapor pressure of SiO since the growth chamber includes SiO_2. The process is formulated by the temperature-independent sticking coefficient and HK equation. It is found in Fig. 2 that the sticking coefficient is 0.01.

The data of Vodakov et al[5] for epitaxial β-SiC can be compared with the equilibrium vapor pressure of SiC[6]. The sublimation process has the small gap in Sandwich method and the sticking coefficient of 0.22 (ΔT=2°C), as shown in Fig. 3.

These considerations are simple and useful for vapor growth kinetics. Other cases of vapor grown SiC are also discussed on the session.

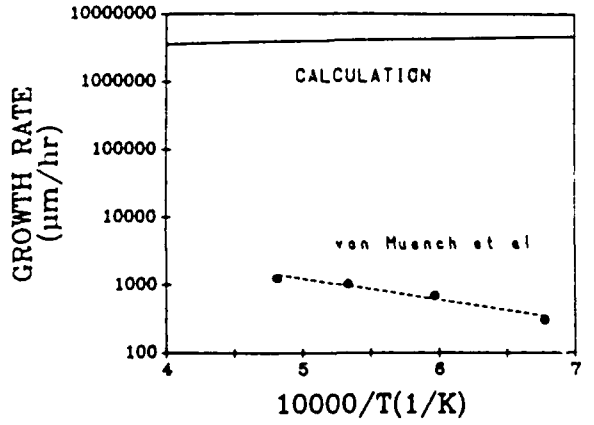

Figure 1

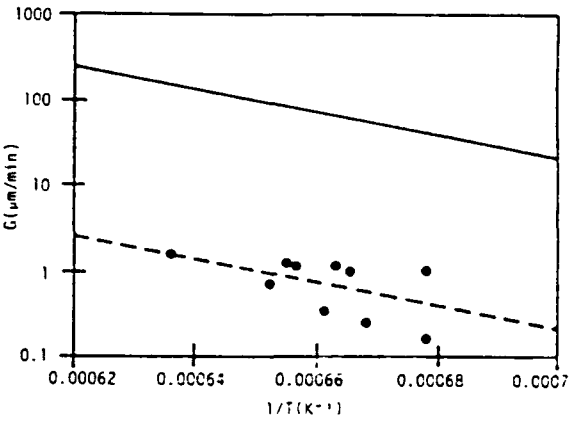

Figure 2

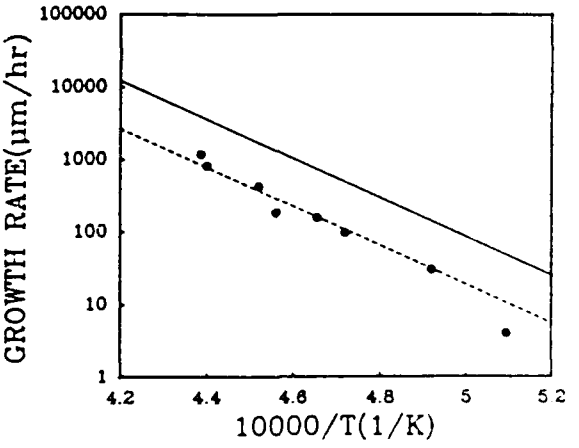

Figure 3

[1] T. Kaneko, *J. Crystal Growth* 69 (1984) 1.
[2] W. von Muench and E. Pettenpaul, *J. Elecrochem. Soc.* 125 (1978), 294.
[3] T. Kaneko T. Okuno and H. Yumoto, *J. Crystal Growth* 91 (1988) 599.
[4] G.A. Bootsma, W.F. Knippenberg and G. Verspui, *J. Crystal Growth* 11 (1971) 997.
[5] Yu. Vodakov, E.N. Mokhov, M.G. Ramm and A.D. Roenkov, *Kristall u. Technik* 14 (1979) 729.
[6] G.V. Samsonov and I.M. Vinitskii, "Refractory Compounds (Handbook)" (Metallugia Pub., Moscow, 1976).

C41

EPITAXIAL GROWTH OF CUBIC SIC BY HOT FILAMENT CVD

Yasuo Hirabayashi, Shiro Karasawa and Ken Kobayashi
Industrial Research Institute of Kanagawa Prefecture
13 Showa-machi, Kanazawa-ku, Yokohama 236, Japan

Heteroepitaxial growth techniques of cubic SiC films on Si substrates require high temperatures, such as 1400°C in chemical vapor deposition. Low temperature epitaxy of cubic SiC would be quite useful for electronic device applications. In this study, epitaxial layers of cubic SiC films were grown onto (111)Si substrates at relatively low temperature of 1100°C by hot filament chemical vapor deposition. The reactant gases were SiH_4 and C_2H_2 or SiH_4 and C_3H_8 systems which were diluted in H_2.

In this experiment, the temperature of the filament, which was measured by an optical pyrometer, was about 1800-2000°C. The substrate temperature could be varied and maintained by appropriate control of the holder heater. Total gas pressure was 1 Torr. The mixture gas was introduced above the filament. We have experimented the influence of carbonization condition on crystallinity of SiC growth film. The carbonization was carried out by introducing acetylene and hydrogen mixture. The temperature of carbonization was increased from 700°C (named the beginning temperature T) and was held at 1100°C for 2 minutes (named holding time t). After the carbonization, silane gas was additionally introduced. A RHEED pattern showed the SiC film epitaxially grew but had a twin. When t was changed from 2 to 10 minutes, the RHEED pattern showed polycrystalline SiC. When T was changed from 700 to 400°C and t was 2 minutes, the RHEED pattern showed diffuse spots of SiC. Without carbonization process, the non-oriented polycrystal SiC layer grew.

When propane gas, instead of acetylene gas, was introduced at the optimum carbonization condition of T=700°C and t=2 minutes, the film epitaxially grew and had a twin. This suggests that propane as well as acetylene was decomposed by hot filament and similar precursors were produced, which played an important role in growth process.

In conclusion, carbonization process effectively affected the epitaxial SiC growth in hot filament CVD. The carbonization was controlled by the holding time and the beginning temperature.

C42

A THERMODYNAMICAL APPROACH TO TETRAMETHYLSILANE (TMS) PYROLYSIS, APPLICATION TO SIC COATINGS OBTAINED BY LPCVD

S. Veintemillas-Verdaguer, A. Figueras-Dagá and R. Rodriguez-Clemente
Institut de Ciencia dels Materials de Barcelona. C.S.I.C.
Campus de la UAB. 08193 Cerdanyola, Spain

Tetramethylsilane is one of the usual organometallic precursors in the CVD of SiC films. However, little is known about the chemical reactions involved in the process. The thermal decomposition of TMS in the presence or absence of H_2 carrier gas, has been thermodynamically model led considering the components detected in the exhaust gas and some others that theoretically could be present: C, Si, H_2, mononuclear silanes and organosilanes, methane, ethane, ethene, acetylene and SiC gas. Taking into account only gaseous equilibria, partial pressures of all components, including gaseous SiC, were calculated. Comparing these results with the vapour pressure of solid Sic in such conditions, an estimation of the supersaturation acting in the crystallization process is obtained.

These calculations provide some light in the interpretation of the dependence of the SiC deposition rate on hydrogen partial pressures and the nature of the obtained films. The plot of such dependence presents three well defined zones. Each of them presents a differentiated morphology.

AN EXPERIMENTAL STUDY OF THE EFFECTS OF TEMPERATURE, FLUID FLOW, AND GAS PRECURSORS IN EPITAXIAL GROWTH OF SiC THIN FILMS ON Si SUBSTRATES

C43

B. Bahavar, M.I. Chaudhry and R.J. McCluskey
Center for Advanced Materials Processing, Clarkson University, Potsdam, NY 13699

In this paper we describe an experimental study of the effects of temperature, susceptor slope, natural convection, and the different chemistry of C_3H_8 and CH_4 as carbon sources on the growth rate, crystal quality, and uniformity of SiC thin films in horizontal epitaxial reactor.

All experiments were carried out at atmospheric pressure. Epitaxial silicon carbide films have been produced on Si (100) substrates using the H_2 - C_3H_8 - SiH_4 system. Influence of natural convection was greater at steeper susceptor slopes, at larger free height (gap between substrate and reactor wall), and at lower temperatures. Growth rate uniformity and growth quality issues are also discussed in this paper. It is shown that the useable film area is increased by reducing substrate slope from 10 degrees to 6 degrees. It is also shown that smaller free height, corresponding to lower natural convection, results in both higher quality and greater useable area. We have also found a critical free height value below which the natural convection is "turned off" and growth rate uniformity is greatly enhanced. This is attributed to the absence of recirculation flows in the reactor.

Among possible carbon gases, methane is the purest commercially available hydrocarbon source, but methane has not been commonly used for growth of silicon carbide due to its low chemical reactivity. Our study demonstrates the feasibility of achieving high SiC growth rates while using a carbon source that is predominantly methane. We have established that silicon carbide films grown at 1350°C in a CVD reactor using a methane to propane mole ratio of thirty results in quality single crystalline films at similar growth rates and lower carrier concentrations than films grown with propane as the only carbon source.

The main tools used to characterize the grown films are x-ray and electron diffraction, optical microscopy, surface profilometry, Hall measurements, and thickness measurements.

GROWTH OF SECONDARY PARTICLES ON SiC POLYHEDRA

C44

*Yoshinori Ando and Hiroshi Iwanaga**
Department of Physics, Meijo University, Nagoya 468, Japan
*Faculty of Liberal Arts, Nagasaki University, Nagasaki 852, Japan

The study of growth morphology of SiC is very interesting, because SiC is polar crystal and has no center of symmetry. In the previous SEM observation [1] we found that secondary particles grow epitaxially on one type of the polar surfaces of b-SiC during sintering of ultrafine powder of SiC prepared by gas evaporation technique [2]. The necessary conditions for such secondary particle growth were inclusion of a large amount of free-Si in raw ultrafine SiC powder and addition of boron as the sintering agent.

In the present study we show another example of SEM image of SiC polyhedron including twins as seen in fig. 1. The polyhedron was obtained by sintering [3] of ultrafine SiC powder including 35% free-Si with the aid of 1% boron. The raw powder was primarily sintered at the temperature 1450°C in vacuum and secondly at 1960°C in Ar 140Torr. The shape of the polyhedron is a truncated octahedron with two rotational twines shown by arrow T' and T''. Remarkable growth of the secondary particles can be observed on A-surfaces, and very few growth on B-surfaces, which correspond to $\{111\}_{Si}$ and $\{111\}_{C}$ surfaces, respectively. Intermediate grain growth is seen on C-surfaces which is {110}. The crystal structure of the secondary particles was confirmed to be β-SiC by using TEM.

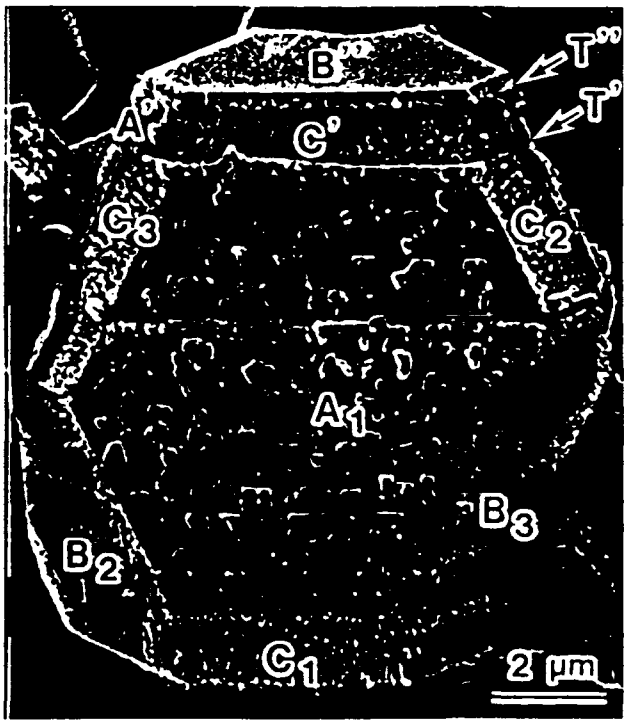

Figure 1. SEM image of SiC polyhedron with secondary particles.

[1] Y. Ando and N. Iwanaga, 1CVGE-7 (Nagoya, 1991) 16aA10.
[2] Y. Ando and M. Ohkohchi, *J. Cryst. Growth* 60 (1982) 147.
[3] Y. Ando and M. Ohkohchi, *Jpn. J. Appl. Phys.* 29 (1990) 2429.

C45

MOCVD SiC LAYERS MORPHOLOGY AND TEXTURE DEPENDENCE ON THICKNESS AND TOTAL PRESSURE

J. Santiso, A. Figueras*, R. Rodriguez-Clemente*, B. Armas**, C. Combescure**, A. Mazel***, Y. Kihn*** and J. Sevely****

*ICMAB-CSIC, Campus UAB, 08193 Bellaterra, Barcelona, Spain

**IMP-CNRS, BP 5, F6652O Font Romeu, France

***CEMES-LOE, CNRS, 29 rue J. Marvig, BP 4347, 31055 Toulouse, Cedex, France

SiC layers have been deposited on non-polished graphite substrates by the LP-MOCVD technique using tetramethylsilane as precursor gas and H_2 as carrier gas. The morphological and structural characteristics of the deposited layers have been studied as a function of the film thickness and the influence of the total pressure in the reaction chamber.

Rocking curves performed on the most intense X-ray reflections allowed us to analyse the crystalline planes distribution as a function of the tilt angle. The morphological characterisation was carried out by SEN and the microstructural characterisation by TEM and electron diffraction.

It has been observed that in the initial stages of the layer growth, the SiC crystallites were randomly oriented showing a powder-like x-ray diffraction pattern. Above a critical layer thickness, depending on the total pressure, we observe well crystallized and preferentially layers produced by a geometrical selection of crystal growth orientations.

C46

CRYSTAL GROWTH OF EPITAXIAL CVD DIAMOND USING C13 CHARACTERIZATION OF DISLOCATION BY RAMAN SPECTRUM

*Shiro Karasawa, Masahiko Mitsuhashi, Seishiro Ohya, Ken Kobayashi, Takeshi Watanabe and Fumitaka Togashi**

Industrial Research Institute of Kanagawa Prefecture,

3173 Showa-machi, Kanazawa-ku, Yokohama 236, Japan

*Science University of Tokyo

1-3 Kagurazaka, Shinjuku-ku, Tokyo 162, Japan

Artificial synthesized diamond using C13 isotope is expected to have potential in a higher thermal conductivity than that of natural diamond. The thermal conductivity depends on the crystallinity. The purpose of this research is to improve the crystallinity of epitaxial CVD diamond using C13 isotope. Dislocation is one of the most important problems in characterizing the crystallinity. Dislocations make strain field in crystal and create geometrical scattering of phonon and decrease the phonon lifetime. The full width at half-maximum (FWHM) of Raman spectrum is determined by the inverse of the phonon lifetime.

The edge dislocation was observed as etch pits on epitaxial CVD diamond thin films using C13 isotope. The FWHM of Raman spectra correlated with etch pit density through dislocations. When the etch pit density was decreased, the smallest ratio of FWHM at the first order Raman line of C13 to C12 was obtained to be 1.23.

Epitaxial diamond thin films were grown on the (100) planes of synthesized type Ib and IIb diamond substrates by the electron-assisted chemical vapor deposition method. The methane reactant gas consisted of C13 was used and was diluted at 1% by hydrogen gas. The epitaxy was confirmed by reflection high-energy electron diffraction streak patterns. The surface morphology was observed by optical microscopy. The three kinds of etch pits were observed. One was etch pits with an apex, which corresponds to an edge dislocation. Another was etch pits with a flatbottom. The others were etch grooves. The Raman spectrum of epitaxial thin films was separated from that of the diamond substrates. The correlation between spectra of C13 and C12 will be discussed, related to the dislocations in thin films and substrates.

C47

HIGH QUALITY THICK DIAMOND FILMS BY DC-BIASED HOT FILAMENT CVD

Hou Li, Yang Peichun, Pu Xin, Xuan Zhenwu, Qi Lichang and Hu Guangya

R.I.S.C., P. 0. Box 733, Beijing 100018 China

In this paper, the apparatus and the experimental conditions for diamond films over 200 μm in thickness are reported. In terms of results of the experiments growth rate of diamond film can be increased with DC bias current. Raman spectrums on cross section of thick diamond films shows that diamond films quality will be improved with increasing of the thickness. Also observation on the interface between diamond grains discovered that gas source containing oxygen will efficiently decrease the IR absorption.

C48

ION BEAM DEPOSITION OF AMORPHOUS FILMS OF CUBIC AND HEXAGONAL DIAMOND

V.E. Mashchenko
Institute for Steel and Alloys, MOSCOW, USSR
V.M. Puzikov, A.V. Semenov and D.I. Zosim
Institute for Single Crystals, Kharkov, Ukraine

Hydrogen-free amorphous diamond file containing up to 90 + 95% sp^{-3} - phase were prepared by ion-beam deposition method. Structural studies and the analysis of maxima of electron absorption near tile edge of optical absorption showed that the films had two sp^{-3}-phases, corresponding to cubic and hexagonal diamond.

The results of the study of the deposition conditions for sp^{-3} monophase amorphous films are described in the present paper. The ratio between cubic and hexagonal phases in the deposition process was found to depend essentially on the ion energy, ion current density, temperature of the substrate. The amorphous films of cubic and hexagonal *diamond with a phase content of up to 90%* were obtained.

The spectra (N1, N2) of diamond film optical density are shown in figure. The films, 800 and 700 Å thick, were deposited on KCl single crystals. The spectra of 1 have maxima at 7.10 eV and 5.45 + 5.50 eV ($E_0\alpha$) which correspond to the direct ($\Gamma_{25} - \Gamma_{15}$) and indirect ($\Gamma_{25} - \Delta_x$) transitions in the cubic phase. In the spectra 2 the maximum at 5.95 eV ($E_0\beta$) corresponds to the intrinsic transition in a partially ordered hexagonal diamond. Electrical, IR optical and other properties of amorphous films of cubic and hexagonal diamond did not differ in the limits of measurement errors.

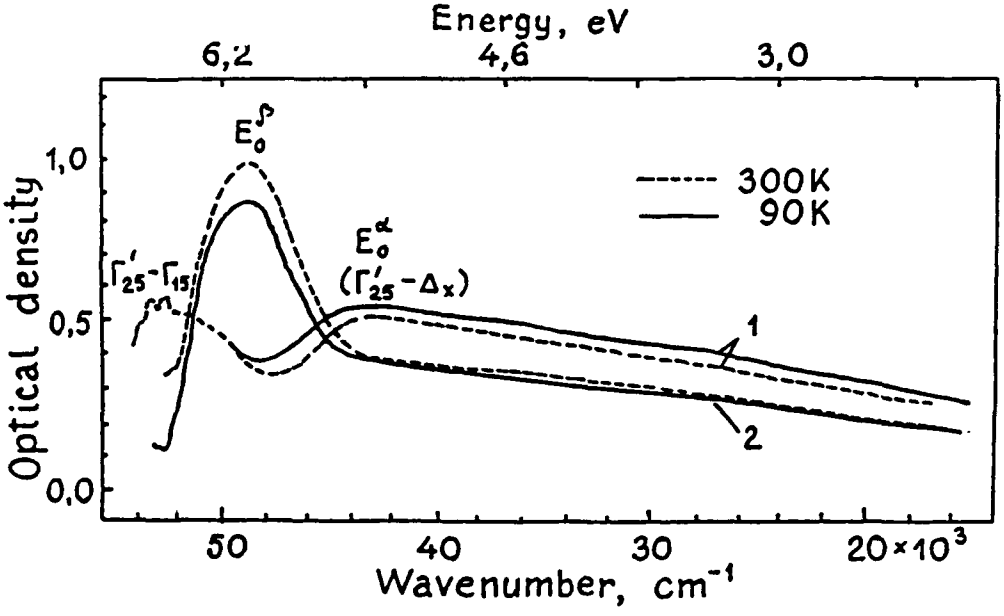

C49

SYNTHESIS AND MORPHOLOGY OF CVD DIAMOND ON Ta AND TaC FILM

Fumitaka Tagashi, Ken Kobayashi, Masahiko Mitsuhashi*, Shiro Karasawa*, Seishiro Ohya* and Takeshi Watanabe**
Science University of Tokyo
1-3 Kagurazaka, Shinjuku-ku, Tokyo 162, Japan
*Industrial Research Institute of Kanagawa Prefecture
3173 Showa-machi, Kanazawa-ku, Yokohama 236, Japan

The chemical vapor deposition method for synthesis of diamond has been developed by many investigator. In synthesis of CVD diamond, the diffusion of carbon into the substrate and the thickness of carbide layer affect the nucleation and subsequent growth of crystalline diamond.

The purpose of this study is observing the differences of nucleation, subsequent growth and morphology of synthesized diamond. For this purpose, tantalum, silicon and tantalum-carbide thin films deposited on Si(111) wafer were used for substrate. Because the diffusion of carbon into tantalum is about 105 times larger than silicon at 1000°C. The synthetic diamond was deposited on these substrates using an electron-assisted chemical vapor deposition method (EACVD). The reactant gas was 1% CH4 diluted in H_2 and the pressure was 30 Torr. Tantalum carbide i.e. TaC were readily synthesized by evaporation of Ta on the Si substrate in the presence of 1% CH_4/H_2 in vacuum 5 Torr.

The nucleation density of diamond deposited on TaC/Si substrate was greater than that deposited on Si substrate and the growth morphology differed among them. In the scratched Si and TaC/Si substrates, the nucleation density of diamond deposited on these were about $10^8/cm^2$. On the other hand, in the not scratched Si and TaC/Si substrates, these were about $10^3/cm^2$ and $10^5/cm^2$, respectively. The shape of diamond on scratched Si substrate was dominant (111) plane, but the shape of diamond on the scratched TaC/Si substrate was dominant (100) planes. On the other hand, the shape of diamond on not scratched Si, TaC/Si substrates were dominant cube-octahedral particles and mirror ball shaped, respectively. The growth rate of diamond nucleation deposited on the TaC/Si substrate was 5 times greater in the direction of diameter than deposited on Si substrate. Diamond film deposited on not scratched Ta substrate peeled off, but the diamond film deposited on scratched TaC substrate did not peel off. Nucleation density and surface morphology of diamond deposited on scratched and not scratched TaC/Ta substrates were same as deposited on TaC/Si substrates.

C50

THE GROWTH OF THICK GaN FILM ON SAPPHIRE SUBSTRATE BY USING ZnO BUFFER LAYER

T. Detchprohm, H. Amano, K. Hiramatsu and I. Akasaki
Department of Electronics Engineering, Nagoya University
Furo-cho, Chikusa-ku, Nagoya 464-01, Japan

GaN is a promising material for optical devices in blue and UV regions. Growing a large scale "bulk" single crystal of GaN is very difficult, because of the high dissociation pressure of nitrogen gas at the growth temperature. Therefore, the preparation of GaN single crystal is mainly based on hetero-epitaxial growth using sapphire substrate. By hydride vapor phase epitaxy (HVPE) method, it is easy to grow a hundred micra thick GaN layer with high growth rate. But, the reproducibility of growing GaN single crystal was fairly poor.

Here we have used an ~100 nm thick ZnO layer, sputtered on a sapphire substrate, for preparation of GaN film by HVPE method. ZnO plays an important role which can be explained as follows: Firstly, its physical properties such as crystal structure, lattice constant and molecular mass, are almost similar to those of GaN. Therefore, its sputtered layer could be able to be used as buffer layer with high possibility. Secondly, ZnO can be eliminated by aqua regia, and hence it is possible to separate a GaN single film from the sapphire substrate by etching ZnO.

In this work, we have found that the reproducibility of growing GaN single crystal is greatly improved by using ZnO buffer layer. We have also succeeded in preparation of hundreds micra thick "bulk" single crystal of GaN for the first time. Moreover, the growth of GaN has been achieved not only on C-oriented sapphire substrate but also on A-oriented sapphire substrate by using ZnO buffer layer. And the ZnO buffer layers reveal strong C-orientation on both type of sapphire substrate. This implies that C-oriented ZnO buffer layer is necessary for growing GaN single crystal.

C51

GROWTH OF SINGLE CRYSTALLINE GaN ON Si SUBSTRATE USING AlN AS AN INTERMEDIATE LAYER

Tetsuya Takeuchi, Atsushi Watanabe, Kouji Hirosawa, Hiroshi Amano, Kazumasa Hiramatsu and Isamu Akasaki*
Department of Electronics, School of Engineering, Nagoya University,
Furo-cho, Chikusa-ku, Nagoya 464-01, Japan
*Corporate R&D Lab, Pioneer Electronic Corp., Saitama 350-02, Japan

GaN has attracted much attention as a candidate for fabrication of optoelectric devices in the blue and near UV regions, because it has a direct band gap of 3.39 eV at RT. For the growth of single crystalline GaN films, heteroepitaxy is inevitable. Si wafer is thought to be one of the most promising substrates for heteroepitaxy because it has fine merits: high quality, large size and low cost. However it is difficult to grow single crystalline GaN on bare Si because of the large lattice mismatch (17%) and/or the large difference in the thermal expansion coefficient between GaN and Si. Previously, we have proposed to use an intermediate layer for the growth of GaN on Si[1]. AlN could be grown on Si[2] and lattice mismatch between GaN and AlN is 2.5%. Therefore AlN is thought to he a candidate as an intermediate layer. In this paper we reported the successful growth of high quality single crystalline GaN on Si using AlN as an intermediate layer.

Growth of AlN and GaN was carried out in horizontal type MOVPE reactor. Before growth of GaN, AlN layer was grown on (111)Si at 1250°C. GaN film was grown at 1050°C on Si covered with AlN intermediate layer. The RHEED patterns of GaN films are shown in Fig 1(a) and (b). Strong streaks and Kikuchi lines are clearly observed for the first time, which indicates that high quality single crystalline GaN films can be grown on Si.

[1] T. Takeuchi, H. Amano, K. Hiramatsu and I. Akasaki; Proc. 7th ICVGE, to be published
[2] M. Morita, I. Isogai, N. Shimizu, K. Tsubouchi and N. Mikoshiba; Jpn. J. Appl. Phys. 20 (1981) L173

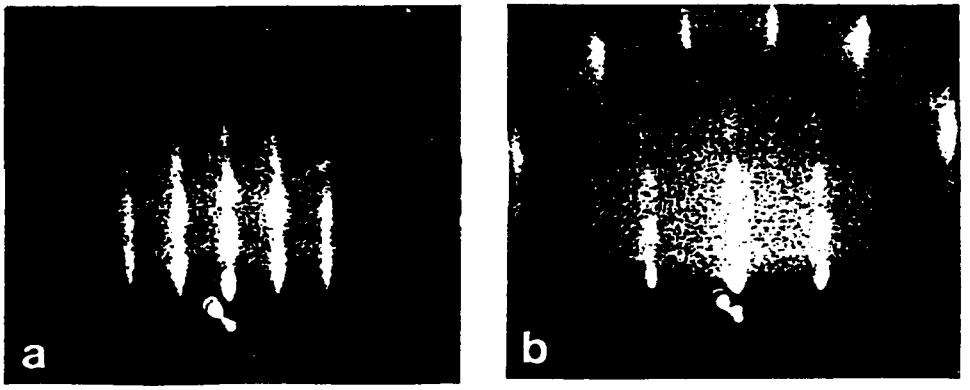

Figure 1. RHEED patterns of GaN film grown on Si using AlN intermediate layer. The azimuths of the electron beam are parallel to (a)[10$\bar{1}$0]GaN and (b)[11$\bar{2}$0]GaN.

C52

GROWTH OF SiC AND SiC-AlN SOLID SOLUTION BY CONTAINER-FREE LIQUID PHASE EPITAXY

V.A. Dmitriev and A.E. Cherenkov*
A.F. Ioffe Institute, St. Petersburg, USSR
*Materials Science Research Center of Excellence
School of Engineering, Howard University, Washington, DC, USA

Container-free liquid phase epitaxial technology[1] has been used to grow silicon carbide, $(SiC)_{1-x}$-$(AlN)_x$ alloy layers and multilayers pn structures from the silicon melt on 6H-SiC substrates. In this method, the melt does not come into contact with the container but is suspended in an electromagnetic field. The dependence of the growth rate on growth conditions will be presented.

For 6H-SiC layers, the growth temperature was varied from 1440°C to 1700°C. Growth rate may be controlled from 0.02 to 3 μm/min. The layers with the thickness less than 0.1 μm have been grown. If dopant (Al or N) is introduced into the melt, the growth rate will be a few times higher than for undoped layers. For nitrogen doped layers, the N_d-N_a concentration was controlled from $8x10^{15}$ cm^{-3} to 10^{19} cm^{-3}. The growth of 6H-SiC doped with Ga (acceptor in SiC) and oxygen (donor in SiC) has been studied. Ga distribution coefficient was estimated at 10^{-5} 10^{-5}.

For the first time, heteroepitaxial growth of 3C-SiC on 6H-SiC substrates from the liquid phase has been studied. Surface morphology and crystallinity of the 3C layers have been investigated. The characteristics of red LED made on p6H-n3C heterojunction will be presented.

$(SiC)_{1-x}(AlN)_x$ layers and pn structures have been grown at 1400-1500°C. The maximum AlN concentration was 10 mol.%. Dependence of composition and conductivity on growth conditions will be discussed.

1. Dmitriev, V.A. et al. *Sov. Tech. Phys. Lett.* **11**(2), p.98, 1985.

SESSION 3D

PHASE ANALYSIS OF Bi-Ca-Sr-Cu-O SUPERCONDUCTING FILMS AT DIFFERENT GROWTH TEMPERATURES FROM KC1 SUPERCOOLED SOLUTIONS*

D55

Kanwal. K. Raina, S. Narayanan and R.K. Pandey
Center for Electronic Materials, Electrical Engineering Department
Texas A&M University, College Station, TX 77843-3128, USA

Films of Bi-Ca-Sr-Cu-O superconductor have been grown from KC1 solutions in the range of 890-830°C at different growth temperature regimes by LPE process. Twin free single crystal substrates of $NdGaO_3$ with (001) orientation are used for growing these films. The temperature range of 850-830°C is found to be the most favorable region for the formation of 2122 phase of BCSCO. Above 850°C, formation of 2122 phase is highly suppressed with the separation of $Bi_2CaSr_2Cu_2O_{8+x}$ into 2021. Calcium Copper oxide ($CaCu_2O_3$ and Ca_2CuO_3) and Copper Strontium oxide. X-ray powder diffraction, SEM, EDAX and RBS are used to identify different phases and subphases of BCSCO films. The results obtained from these techniques are described and discussed. The onset of transition for the 2122 phase films is observed at 90 K and the zero resistance is reached at 83 K.

*This work is supported by grants from NASA's Microgravity Programme and NASA's Center for Space Power, a division of Texas Engineering Experiment Station (TEES).

GROWTH OF Bi-Sr-Ca-Cu-O (Tc=85K) SINGLE CRYSTALS BY THE TRAVELING SOLVENT METHOD

D56

K. Shigematsu, T. Satoh, Y. Nishimura, S. Hayashi* and H. Komatsu**
Faculty of Education, Iwate University, Morioka 020, Japan
*Institute for Materials Research, Tohoku University, Sendai 980, Japan

Bi-Sr-Ca-Cu-O (85K phase) single crystals of 3 x 5 x 1.8mm^3 were successfully grown from Bi rich solvent by a modified traveling solvent technique using an MgO crucible coated by CuO. Two kinds of rods (diameter 10mm, height 20mm) were prepared by quenching the liquids of raw materials at 1000°C. The composition of a feeding rod was rich in $Bi(BiO_{1.5}$:SrO:CaO:CuO = 33:24:18:25 in at.%). The other rod was stoichiometric composition of $Bi_2Sr_2CaCu_2O_y$, which was settled on the bottom of the crucible. The feeding rod was set upon the stoichiometric rod, and we started heating the upper part of the rod via crucible wall at 1100°C in an optical image furnace. The length of the molten zone was about 10mm. The crucible was moved upward at the rate of 0.15mm/h. After traveling the molten zone whole through the crucible, the solidified ingot was slowly cooled down to the room temperature. By sectioning the ingot along the crucible axis, we found a few large single crystals (3 x 5 x 1.8mm^3 in size) in the upper part of the ingot (Fig. 1) The other part was composed of aggregated small crystals. The composition of the ingot was analyzed by EDX. It showed that the most of the ingot was $Bi_2Sr_2CaCu_2O_y$ except the bottom part which was rich in Bi. The superconducting behavior of the single crystals thus grown were shown in Fig. 2.

Figure 1. Single crystals bounded by cleavages

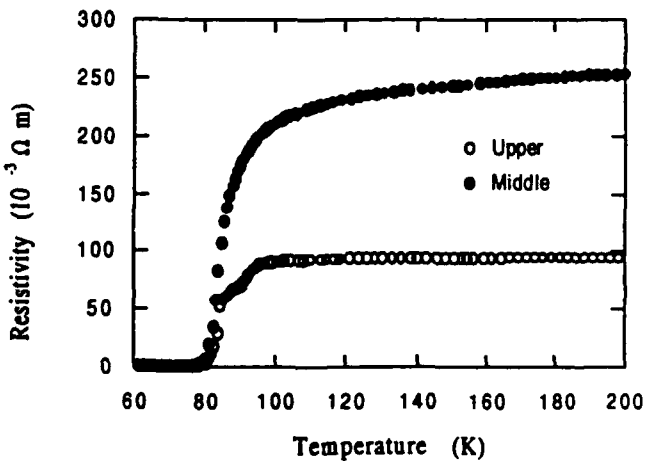

Figure 2. Temperature dependences of resistivity of single crystals.

D57

GROWTH AND CHARACTERIZATION OF $BI_2(SR,CA)_2CUO_x$ SINGLE CRYSTALS

Y. Huang, V.J. Wen and M.K. Wu
Materials Science Center, National Tsing Hua Univ., Hsinchu 30043, Taiwan, R.O.C.

Single crystals of superconducting $Bi_{2+x}(Sr_{1-y}Ca_y)_{2-x}CuO_{6+}\delta$ (2201) phase have been grown from Cu-rich flux in alumina crucibles. The crystals grew with a micaceous habit, and were separated from the solidified flux by cleavage. Crystals were annealed under various conditions to separate the effects of oxygen nonstoichiometry and cation nonstoichiometry on the superconducting properties. The effects of the substitution of Ca for Sr on T_c were systematically studied. The Bi-2201 phase exhibit relatively large T_c variations: 4 to 26K. XRD and EPMA analyses were performed on crystals annealed under various conditions. The superconducting phase shows alkaline-earth deficient/Bi excess compared to ideal 2201 composition. The changes of the lattice parameters of these crystals at various stages were carefully examined. The cation changes, particularly Sr, is correlated with the resulting changes in c-axis length and T_c.

D58

IMPROVED THERMOGRAVIMETRIC ANALYSIS AND CRYSTAL GROWTH OF Bi-Sr-Ca-Cu-O

B. Wanklyn, E. Diéguez, Chen Changkang, Hu Yongle, D. Smith and F. Wondre*
Clarendon Lab., University of Oxford, Parks Road, Oxford, UK
P.A.J. de Groot
Physics Department, Southampton University, Southampton, UK

Superconducting crystals of Bi-Sr-Ca-Cu-O with or without Pb or Y dopant have been grown in the platinum or alumina crucibles from KCl or self-flux. The improved thermogravimetric analysis (ITGA) enables to measure the crystallisation temperature from the growth system and then to grow the crystals by introducing a Pt wire as a nucleation centre or by top-seeding. In the end of crystal growth, the crystals could easily be separated from the flux. Differential thermal analysis (DTA) may be useful to obtain some information for designing the temperature program. The crystals of Bi-Sr-Ca-Cu-O, Bi(Pb)-Sr-Ca-Cu-O and Bi-Sr-Ca(Y)-Cu-O were identified by X-ray diffraction technique and electron probe microanalysis (EPMA) as 2212 phase with two Cu-O layer structure. The as-grown crystals are superconducting with transition temperature of 80 K.

*Visiting scholar from Department of Applied Physics, Autonoma University, Madrid, Spain.

D59

GROWTH OF $Bi_2Sr_2CaCu_2O_8$ BY IMMERSED HEATER FLOATING ZONE MELTING TECHNIQUE

P. Murugakoothan, R. Jayavel, C.R. Venkateswara Rao, C. Subramanian and P. Ramasamy
Crystal Growth Centre, Anna University, Madras - 25, India

Immersed Heater Floating Zone Melting (IHFZM) Method was used to grow textured $Bi_2Sr_2CaCu_2O_8$. IHFZM process has several additional advantages over conventional Floating Zone Melting (FZM). The following procedure was adopted to prepare the polycrystalline rods of $Bi_2Sr_2CaCu_2O_8$ from 3N' pure Bi_2O_3, $SrCO_3$, $CaCO_3$ and CuO. The appropriate amounts of starting materials were taken and mixed in triple distilled water. The resulting mixer was dried and calcined at 800°C for 24 hours. The samples were again milled in isopropyl alcohol. The homogenized slurry was again dried and calcined at 800°C for 48 hours. The black bulk sample was then crushed in an agate mortar and sieved to get uniform particle size. The well reacted black powder was then mixed with acetone and charged into the steel die to prepare the ceramic rods. The prepared rods were sintered at 790°C in flowing oxygen for 2 hours. The crystal growth apparatus is a home made immersed heater type floating zone furnace. A platinum strip was used as the resistive immersed heater. The seed crystal was prepared from a crystalline boule obtained by zone melting the polycrystalline rod. During growth process, the heater was maintained just above the melting point of the polycrystalline rod. The melting point of the polycrystalline sample was measured by DTA. The pulling and rotation rates were optimized as 1 mm/hr and 20 rpm respectively. The optical microscopic pictures of the cleaved surface shows highly textured morphology. Powder X-ray diffraction confirms the orthorhombicity. The composition of the grown crystal boule is found to be close to 2212. The crystal boule was cut into rectangular bars both parallel and perpendicular to the growth axis and then polished using silicon carbide papers. The resistivity measurements were made on both the samples and the T_c is found to be 83.5 K. The resistivity of these samples shows anisotropic behaviour with the factor of 2. The results and the effect of annealing will be discussed in detail.

CRYSTALLIZATION PROCESS AND PHYSICAL PROPERTIES OF $Bi_2Sr_2CaCu_2O_{8+x}$

D60

V.G. Bessergenev, A.A. Kamarzin*, O. Bonfigt, R. Kubiak, H. Somnitz, K. Westerholt and H. Bach*
Institut für Experimentalphysik, Ruhr-Universität, D-4630 Bochum, FRG
*Institute of Inorganic Chemistry, Lavrenteva Ave. 3, 630090 Novosibirsk, USSR

To improve the crystal quality and size of the high T_c superconductor $Bi_2Sr_2CaCu_2O_{8+x}$ the process of solidification has been studied near the melting point in air. The crystal structure formed from the melt depends on the oxygen concentration. After quenching first a non-superconducting crystal structure solidifies with a higher oxygen deficiency. During annealing it transforms into the usual quasi tetragonal structure.

Therefore, we have grown single crystals by a modified Bridgman-Stockbarger technique with a slow lowering rate. After about 10 days we got single crystals which then were annealed in an Ar/O_2-atmosphere. They showed a supermodulation in the Laue pattern. We measured the physical properties of these crystals, for instance the pressure dependence of the superconducting transition temperature and of the lower critical field $H_{C1}(T)$. The magnetic susceptibility showed even an anisotropy in the a- and b-axis.

This work was financially supported by 'Deutscher Akademischer Austauschdienst (DAAD)' and 'Deutsche Forschungsgemeinschaft (DFG)'.

SURFACE COARSENING ON HIGH Tc SUPERCONDUCTING SINGLE CRYSTALS

D61

Wang Yao Shui, J.P. van der Earden, P. Bennema, C. Grey, L.W.M. Schreurs, J. Wnuk** and P. van der Linden*
Research Institute for Materials, University of Nijmegen,
Toernooiveld, 6525 ED Nijmegen, The Netherlands
*Thermodynamica Debye Institute, University of Utrecht,
Sorbonnelaan 16, 3584 CA Utrecht, The Netherlands
**Institute for Low Temperature and Structure Research,
Polish Academy of Science, Wroclaw, Poland

Surface coarsening on high Tc superconducting single crystals is proposed to be due to the effect of impurity adsorption on the collective motion of growth steps. Growth spiral hillocks, twins, microinclusions could be explained by a model for impurity adsorption. Surface contamination by flux and crucible materials, especially alumina crucible evidently effect the crystal quality and surface morphology. The use of ZrO_2 crucible lead to considerable improvement of the quality and the size of the Pb,Bi,Sr,Ca,Cu,O superconducting single crystals.

Differential interference contrast microscopy (DICM) and scanning tunnelling microscopy (STM) were used for the surface phenomena observations. It is shown that crystals surface coarsening strongly correlates with the superconductivity.

PREPARATION AND SUPERCONDUCTIVITY OF $Ba_{1-x}K_xBiO_3$ SINGLE CRYSTALS*

D62

J.Z. Liu, W.D. Mosley, P. Klavins, L. Zhang, M.D. Lan, T.J. Goodwin, Y.X. Jia and R.N. Shelton
University of California, Davis, CA 95616

Single crystals of $Ba_{1-x}K_xBiO_3$ with various x values were grown by a modified electrochemical method[1]. A mixture of $Ba(OH)_2\ 8H_2O$ and Bi_2O_3 were dissolved into a melted solution of KOH, which was kept in a 100 ml Pt crucible. Two electrodes, a Bi rod as reference and Pt wire as anode, were inserted into solution. The Pt crucible was taken as cathode. (The distance between these two electrodes can be adjusted.) The growth temperature is about 200-220°C and the relative voltage between the Bi rod and Pt wire can be changed from 0.6 V to 0.8 V depending on the distance of the two electrodes. By adjusting the compositions of the raw materials, millimeter-size superconducting crystals with different T_c were obtained. The growth conditions will be given in detail. Results from magnetic and resistive measurements are also given.

1. Michael L. Norton, et al. Mat. Res. Bull., 24, 1391 (1989).
*Research supported by the U.S. DOE under contract No. W-7405-ENG-48 to Lawrence Livermore National Laboratory and by the NSF under grant No. DMR-90-21029.

D63

CRYSTAL GROWTH AND CHARACTERIZATION OF SUPERCONDUCTORS IN THE Ba-K-Bi-O SYSTEM

P.D. Han, L. Chang, and D.A. Payne
Department of Materials Science and Engineering,
Science Technology Center for Superconductivity, and
Materials Research Laboratory, University of Illinois at Urbana-Champaign, Urbana, IL 61801 USA

Single crystals of $Ba_{1-x}K_xBiO_3$ (x~0.38) with a zero resistance T_c~32K, a Jc~$2x10^6$ A/cm^2 and a Meissner fraction~35% were grown by an anode electrolytic technique from a potassium hydroxide solution containing BaO and Bi_2O_3. Cubic crystals mm in size with a blue color were characterized by optical microscopy, SEM, TEM and x-ray diffraction. Data are reported for the superconductive parameters as determined by magnetic and resistive measurements.

We present results for the growth parameters, as a function of starting composition, electro-overpotential, current density, temperature, seed rotation rate and post-treatments (annealing in oxygen at different pressures, potassium diffusion in KOH, etc.).

Crystal growth mechanisms are discussed in the context of observable morphological features, such as dislocations, low angle boundaries, voids, and inhomogeneities in potassium content. Data are discussed with respect to the effect of structure/defect relations on superconducting properties.

D64

GROWTH OF LARGE PURE, DOPED AND CO-DOPED La_2CuO_4 SINGLE CRYSTALS

A. Cassanho, B. Keimer and M. Greven
Center for Materials Science and Engineering
Massachusetts Institute of Technology, Cambridge, MA 02139

Pure, singly Sr, Ba, Ce, Zn, Nd doped and Sr, Nd co-doped La_2CuO_4 single crystals have been grown by the top-seeded solution growth technique, utilizing a Pt crucible to contain the melt. All crystals were pulled with a rate of 0.1 mm/hr. We have done experiments using high, low and very low thermal gradients at the growth interface. High gradients have produced crack-free crystals with shiny faces and highly anisotropic transport properties. The crystal size is usually about 0.5 cm^3. Crystals grown in very low gradients, can reach volumes up to 3 cm^3 but have cracks due to flux inclusions. Tc for Sr-doped crystals grown in high gradients is depressed in comparison to crystals with the same composition grown in very low gradients. Crystals could be grown along the (001) and (100) directions in low as well as large thermal gradients. In large thermal gradients, the crystals grew basically in the same way for both directions and reached the same dimensions. For very low thermal gradients, however, crystals grown along the (001) direction were longer than crystals grown along the (100) direction. In the first case, the crystal bottom is very flat and parallel to the melt surface. In the second case, there are two facets on the bottom of the crystal at an angle with the surface of the melt and the crystal loses contact with the melt after a while. Crystals could not be grown longer than 5 mm for this direction. Doping, in the growth conditions used, made it easier to get large size single crystals, especially when the dopants were Zn and Ce ions.

Work supported by NSF contract No. DMR90-22933.

D65

CRYSTAL GROWTH ANALYSIS IN MAGNETICALLY ORIENTED MELT GROWN $DyBa_2Cu_3O_7$ SINTERED PELLETS

R. Cloots and A. Rulmont
S.U.P.R.A.S., Institut de Chimie B6, Université de Liège, B4000 Liège, Belgium
C. Hannay, P.A. Godelaine and H.W. Vanderschueren
S.U.P.R.A.S., Institut d'Electricité Montèfiour B28, Universite de Liège, B4000 Liège, Belgium
P. Règnier
S.R.M.P., CEREM, CEN Saclay, F91191 Gif sur Yvette, France
M. Ausloos
S.U.P.R.A.S., Institut de Physique B5, Université de Liège, B4000 Liège, Belgium

Interesting and surprising features have been found in the synthesis of $DyBa_2Cu_3O_{7-x}$ superconducting ceramics under a magnetic field at high temperature. Different runs have been made under various magnetic fields, temperature range, heating and cooling rates, and oven geometries. Strips and rods have been grown. Temperatures encompass 940-1040°C. Terrace-like substructures are seen and are oriented with respect to the field.

Rayleigh-Bénard-like patterns are "frozen in" upon solidification. Textured material is thus grown. A little discussion of these observations is presented in terms of an Eden model with geometrical screening effect upon growth rate.

This work is part of a Brite-Euram research project (BE-3015-89) with CEREM (CEN-Saclay) and MSED (University of Liverpool).

GROWTH OF $CaLnBaCu_3O_{7-\delta}$ (Ln=La, Pr & Nd) SINGLE CRYSTALS BY FLUX TECHNIQUE

D66

C.R. Venkateswara Rao, P. Murugakoothan, R. Jayavel, C. Subramanian and P. Ramasamy
Crystal Growth Centre, Anna University, Madras 600 025, India

$CaLaBaCu_3O_{7-\delta}$ is a tetragonal superconductor related to '123' structure. This is a layered type perovskite with copper in mixed valency. It shows superconducting transition above liquid nitrogen boiling point. Presumably, Ca occupies the La-site and La the Ba-site due to ionic size matching. This is an interesting system wherein it exhibits high T_c with tetragonality. This is amenable to rich chemical substitution at the rare-earth site. Its effect on Tc is well established. Synthesis of single crystals is of immense use over the polycrystalline counterparts, to understand the phenomenon as well as to the material applications.

Single crystals of $CaLnBaCu_3O_7.\delta$ (Ln=La,Pr & Nd) were grown by flux technique using BaO-CuO eutectic mixture as the flux. Incongruent melting of this material makes flux growth to be the choice. 28 mol% BaO - 72 mol% CuO flux is found to be the suitable flux for growing bigger size single crystals. Starting compounds are high pure Ln2O3 (Ln=La Pr & Nd) $CaCO_3$, $BaCO_3$ and CuO. Presynthesised compounds were taken with flux in platinum crucibles. The mixture is heated up to 1030°C, kept there for 12 hours to make the fluxed melt homogeneous. Then slowly cooled at a rate of 2°C/hour up to 800°C, and fast cooled to room temperature.

Black shining platelet crystals embedded in the flux are usually obtained. X-ray diffraction studies on these crystals show that the compounds are formed. Further characterization results will be discussed.

SOME CONSIDERATIONS ON THE EQUILIBRIUM PHASE DIAGRAM OF THE Y_2O_3-BaO-CuO SYSTEM*

D67

Eugen Cruceanu
Institute of Physics & Technology of Materials, Bucharest, Romania

The pseudo-ternary Y_2O_3-BaO-CuO phase diagram and especially its isobaric $YBa_2Cu_3O_B$-$BaCuO_x$ section is very important not only for the optimization of the synthesis and properties, but also for the single crystal growth processes. In view of various factors (e.g. enhanced wetting and creeping of the melts, crucible corrosion, slow equilibration reactions), the published phase diagram data are spread.

On the basis of our crystal growth experiments and the published information we discuss in the present work a tentative $YBa_2Cu_3O_B$-$BaCuO_x$ isobaric section through the pseudo-ternary Y_2O_3-BaO-CuO phase diagram. In addition, conclusions are reported on the growth conditions as well on the characterization of the single crystals.

*This work was performed in Institut für Festkörperforschung Jülich-Germany and was supported by A. von Humboldt Foundation, Germany.

THE SURGEON AND CRYSTAL GROWTH

D68

Y.M. Fazil Marickar, S. Sindhu, R.K. Vathsala, H. Krishna Moorthy, Neena Elizabeth and Sapna V. Roshni
Department of Surgery, Medical College Hospital, Trivandrum 695 011, S. India

INTRODUCTION: The involvement of the surgeon in the field of crystal growth has been very minimal. We have tried to grow the biological crystals in the laboratory in as much of simulated biological environment as possible with regard to the body temperature, the pH of the biological environment and the chemical constitution available inside the body.

MATERIALS AND METHODS: Crystal growth in silica gel medium was utilised. The single diffusion technique was attempted in Hane's tubes and double diffusion technique in 'U' tubes. Calcium oxalate monohydrate, calcium oxalate dihydrate, brushite, apatite, octocalcium phosphate, struvite, newberyite, uric acid and cholesterol were grown using different nucleating solutions, one being incorporated in the gel and the other added to the top of the gel. Purity of the crystals was identified by X-ray diffraction and infra red analysis. The morphology was studied by macroscopic, light microscopic and SEM studies.

OBSERVATION: Single diffusion technique was fast in producing crystals compared to the double diffusion technique. The crystals grown proved to be chemically pure and similar in composition to the crystals naturally occurring in the human body. The similarities and variations, between the crystals formed *in vivo* and those formed in the lab will be compared.

CONCLUSION: It is possible to grow biological crystals in the silica gel medium. The characteristics of these crystals are similar to those seen *in vivo*. The responsibility of the surgeon in preventing stone formation in the body by studying the crystal growth pattern is stressed in this context.

D69

IS IT POSSIBLE TO GROW THE URINARY STONE IN THE TEST TUBE?

R.K. Vathsala, Y.M. Fazil Marickar, C. Aravindakshan, S. Sindhu, T.G. Dhanalakshmi and H. Krishna Moorthy
Department of Surgery, Medical College Hospital, Trivandrum 695 011, S. India

INTRODUCTION: In this study we have attempted the *in vitro* growth of mixtures of oxalate, phosphate and uric acid crystals in silica gel medium in order to simulate the *in vivo* situation.

MATERIALS AND METHODS: Hane's tubes were used for growing the crystals using modifications of the conventional silica gel medium. Sodium metasilicate of 1.03 density was prepared. The following combinations of reagents were added in the gel or to the top solution. 1) calcium chloride + ortho phosphoric acid 2) calcium chloride + magnesium acetate 3) calcium chloride + ammonium dihydrogen orthophosphate 4) calcium chloride + uric acid 5) oxalic acid + ortho phosphoric acid 6) oxalic acid + ammonium dihydrogen orthophosphate 7) oxalic acid + magnesium acetate 8) oxalic acid + uric acid 9) calcium chloride + ortho phosphoric acid + magnesium acetate 10) ortho phosphoric acid + magnesium acetate + ammonium dihydrogen orthophosphate 11) magnesium acetate + ammonium dihydrogen orthophosphate + uric acid 12) calcium chloride + magnesium acetate + ammonium dihydrogen orthophosphate + uric acid 13) calcium chloride + ortho phosphoric acid + magnesium acetate + ammonium dihydrogen orthophosphate 14) calcium chloride + ortho phosphoric acid + magnesium acetate + ammonium dihydrogen orthophosphate and 15) calcium chloride + oxalic acid + ammonium dihydrogen orthophosphate + uric acid. The crystal growth patterns were analysed.

OBSERVATIONS AND DISCUSSION: Combined crystal patterns appeared fast in the gel medium in the following combinations as numbered above - 12, 13, 4, 14, 3 and 9 in that order. The rate of growth varied depending upon the combination of reagents used.

D70

HABIT MODIFICATION AND INHIBITION OF CRYSTALLIZATION OF FATTY ACIDS BY SOME SURFACTANTS

P.B.V. Prasad
SR Laboratory for Studies on Crystallization Phenomena
P.O. Box 23, Hanumakonda - 506 001, India

The inhibiting influence of certain surfactants on the crystallization of linear chain saturated fatty acids with carbon number 10, 12, 14, 16, 18 and 20 have been studied, based on the measurements of intensity of the scattered light by the continuously stirred solutions at different temperatures. The inhibition efficiency of the surfactants in the 3° to 40°C range is evaluated.

Insitu studies were made on the habit modification of fatty acid crystals. SEM observations have also been made on the precipitates. The results will be discussed in terms of the molecular interactions.

D71

GROWTH PROCESSES OF CHOLESTEROL MONOHYDRATE AND GALLSTONES IN SILICA GEL

Thomas Abraham and M.A. Ittyachen
School of Pure and Applied Physics
Mahatma Gandhi University, Kottayam, Kerala 686 631 India

Cholesterol, which is universally distributed in animal tissues, is both a vital and lethal sterol. It plays a key structural and functional role in cell membranes, serum lipoproteins, and in the mixed micelles of bile. Cholesterol monohydrate constitutes the major component of most gallstones.

In this paper we present the growth of cholesterol monohydrate crystals in silica gel in the presence and absence of calcium and oxalate as additives. Addition of substances to a saturated solution reduces the solubility and helps to create the crystallization condition. Ethanol water mixture saturated with cholesterol has been used to reduce the solubility of cholesterol which was initially dissolved in the gel. Fibrous crystals of cholesterol monohydrate was seen in the gel by one week, at the same time needle cholesterol crystals of 1-2 cm length was seen in the upper solution. Addition of oxalic acid along with the acetic acid resulted in the growth of platelets of cholesterol monohydrate crystals of 3-4 cm length and 1 cm width.

The same procedure was repeated with the bile salt solution along with calcium ions in the gel medium. We got spherulite growth of cholesterol monohydrate crystals of size 1-2 mm, with the same morphology of the human gallstone. The crystals were characterized using the usual investigating probes. It became clear that the spherulite crystals are composed of multiple plate single crystals of cholesterol monohydrates with well defined c-planes and are arranged radially. Initial nucleation of calcium oxalate crystalline embryo acts as a nucleus for the collection of cholesterol monohydrates as in the case of human gall bladder stones. It is also noticed that platy cholesterol monohydrate crystals easily join together at the c-planes due to the presence of oxalate ions.

EXTREME DECREASE OF THE DISLOCATION DENSITY OF Al CRYSTALS GROWN FROM THE MELT UNDER THE PRESSURE

D72

V.O. Esin, A.S. Krivonosova and I.J. Satibaev
Metal Physics Institute, Ural Department of Academy of Sciences, Ekaterinburg, Russia

X-ray diffraction topography, etch figure method and mass-spectrum analysis were used to investigate the dislocation structure and impurity of single crystals of aluminum grown from the melt by Bridgman method with <100>, <111> and <210> orientations with the rate range from 1 to 15 mm/min by various low gas pressures in the crystallize chamber.

It has been shown that the dependence of the dislocation density and impurity of single crystals on the low pressures is extremely large. There are optimal pressures values depended on the growth rate and the crystallographic orientation of the solid-liquid interface, when the dislocation density decreases greatly (by one or two orders). Efficiency of the refinement by this pressure increases by a factors of 8-10. The results obtained are in principle new and are not explained on the basis of the known concepts.

Theoretical analysis of experimental results allow us to assume the following influence mechanism of low pressures. At the neighbourhood of solid-liquid interface accumulation of free superfluous volume distinguished at phase transformation takes place, because of relaxation rate of free volume is final. In this case dilatation in the neighbourhood of interface may attain the top value and atomic transition across interface becomes zero energy barrier. The solid-liquid interface is in supermobility state [1].

[1] V.O. Esin. Supermobility of solid-liquid interface. Abstracts of Seventh All-Union Conference on Crystal Growth. Moscow, 1988, v.2, p.43.

CRYSTALLOGRAPHIC STUDY OF CALCIUM OXALATE MONOHYDRATE CRYSTALS GROWN IN SILICA GEL MEDIUM

D73

A. Salim, S. Sindhu, Y.M. Fazil Marickar, Neena Elizabeth and N. Subbanna
Department of Surgery, Medical College, Trivandrum and
Department of Material Science, Indian Institute of Science, Bangalore

INTRODUCTION: *In vitro* techniques for growing biological crystals have successfUlly fabricated crystals of structure similar to those seen in the biological environment. In this study, use of X-ray crystallography to ascertain the purity of calcium oxalate monohydrate crystals grown *in vitro* in silica gel medium is evaluated.

MATERIALS & METHODS: Calcium oxalate monohydrate crystals were grown *in vitro* in modification of the conventional silica gel medium. The crystals that grew in the test tubes in 30 days were washed and powdered and sprinkled on a glass slide at uniform coating and introduced into the X-ray powder diffractometer PW 1140/90 Philips model. The graphics were recorded and the 'd' values obtained were compared with the standard values.

OBSERVATIONS: The calculated 'd' values were 5.9, 2.96 & 1.97. The standard 'd' values are 5.9, 2.98 & 1.95. There was a slight deviation of 'd' values from the standard values. This may be due to the ions present in water. The 'd' values obtained corresponded to those of oxalate monohydrate. This confirms the tetragonal structure of the calcium oxalate monohydrate crystal.

CONCLUSIONS: Crystallographic study shows that the calcium oxalate monohydrate crystals grown in silica gel medium *in vitro* art pure crystals demonstrating the pattern described for the pure crystals. Fabrication of such pure crystals will aid further study of the effect of various environmental factors on various physical properties of the crystals grown.

D74

GROWTH OF PURE AND DOPED CRYSTALS OF STRONTIUM TARTRATE AND THEIR FOURIER TRANSFORM IR STUDIES

F. Jesu Rethinam, T.J. Bhoopathy, S. Ramasamy and P. Ramasamy***
Department of Nuclear Physics, Madras. 25, India
*Department of Physics, Pachiyappa's College, Madras.30, India
**Crystal Growth Centre, Anna University, Madras.25, India

Crystals of strontium tartrate have been grown in silica gel medium by single diffusion method in pure form and with Chromium, Iron, Cobalt, Nickel, Copper, Cadmium and Tin as dopants. Growth kinetic studies have been undertaken to estimate the optimum growth conditions of these crystals. Chlorides of the dopants have been used with varying concentrations. Investigations under concentration programming of the growth have led to crystals of well defined faces and considerable change in size. Crystals grown with certain dopants exhibit deep colours. However, for some of the dopants, the relative transparency seems to increase compared to that of the pure crystals. Some special morphological modifications like triangular-single-pyramidal, needle shaped, wedge shaped, dendritic and double-pyramidal growth have been observed. In the solution-gel interface transparent and colourless crystals resembling herring-bone structure are invariably seen with their bulk size normally more than the crystals grown within the gel.

The Fourier Transform Infrared Spectra of these crystals have been recorded on a Bruker IFS 85 FTIR Spectrometer using KBr pellet techniques. The vibrational modes for C-OH, C-C and G-H groups have been assigned. The shift or modification observed far the vibrational modes of carboxyl and hydroxyl group frequencies indicates the effect of the dopants.

D75

SPHERULITIC CRYSTAL GROWTH OF PURE (Y,Sm) AND MIXED Y_{1-x}: Sm_x RARE EARTH TARTRATES IN SILICA GELS

Anima Jain, Ashok K. Razdan and P.N. Kotru
Dept. of Physics, University of Jammu, J & K India

Pure and mixed rare earth tartrate crystals of Y & Sm crystallize as spherulites in the system $R(NO_3)_3$-Na_2SiO_3-$C_4H_6O_6$ using single and double diffusion techniques. An attempt has been made to understand the mechanism of crystallization of spherulites by studying their morphologies, using optical and scanning electron microscopy. The spherulites exhibit different types of formations under different conditions of growth. The fibrous structure of the spherulites and their cleaved sections are described and discussed. The formation of spherulitic morphology is explained to be as a result of crystal fibres diverging radially from multiple nuclei dispersed within a small volume at the centre of the spherulites as shown in Figs. 1 & 2. The observations strongly support this explanation and thus reject the commonly accepted possibility of spherulitic morphology to be only due to divergence of crystal fibres from a single nuclei.

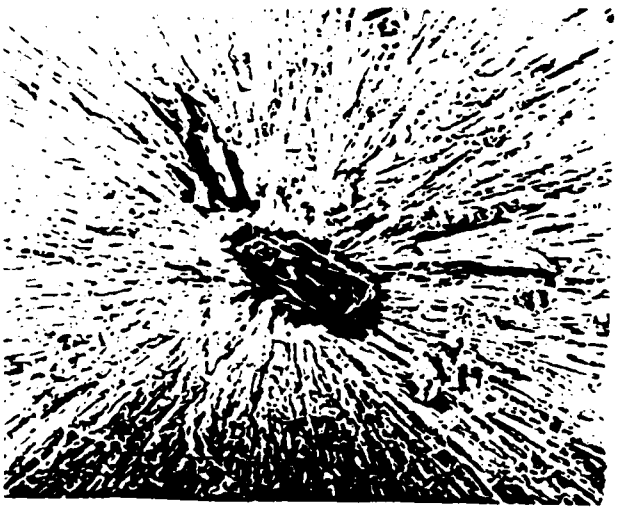

Figure 1. Cleaved section of yttrium tartrate spherulite.

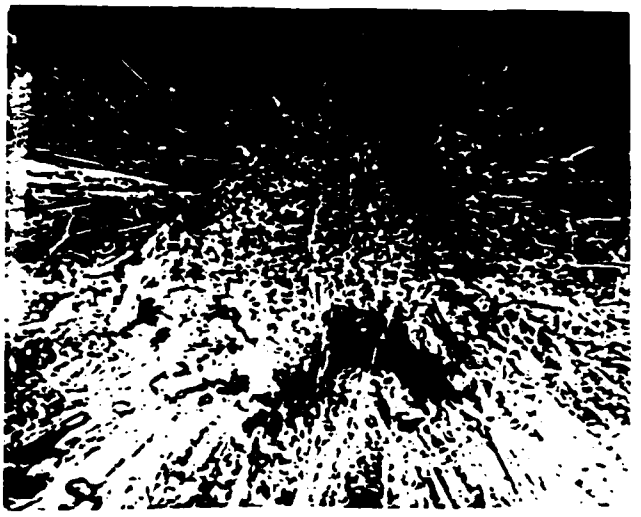

Figure 2. Cleaved section of samarium tartrate spherulite.

IN SITU OBSERVATION OF UNIDIRECTIONAL SOLIDIFICATION IN TRANSPARENT ORGANIC ALLOY

D76

Terumichi Higashino, Yuko Inatomi and Kazuhiko Kuribayashi
The Institute of Space and Astronautical Science
3-1-1 Yoshino-dai, Sagamihara, Kanagawa 229, Japan

Solidification process of metal and semiconductor from melt usually has the problems such as segregation of impurity and instability of surface morphology. These phenomena are not favorable for making high quality crystals. It is difficult to compare the measured data with the calculated ones based on the morphological instability theories because of difficulty of measuring temperature and concentration distributions in liquid phase precisely. In this study, in situ observation of unidirectional solidification for transparent organic alloys, for example succinonitrile with acetone and t-butyl alcohol with salol, were performed. Succinonitrile and t-butyl alcohol were used to be the simulation material for metallic and semiconductor solidification, respectively.

Specimens were contained in a quartz glass cell, having two Peltier heating and cooling units. The temperature gradient in the solidification cell was parallel to and positive along the direction of the gravity vector to suppress natural convection. These alloys were unidirectionally solidified at the constant cooling rates under certain temperature gradients. The Machzehnder microscopic interferometer was used to visualize the concentration profile in the liquid as well as the solidification rate, therefore the influence of supersaturation, temperature and concentration gradients were evaluated precisely.

The result of the solidification rate as a function of time in succinonitorile-6.5mol%acetone alloy is shown in Fig. 1, which implies that the transportation process of solute atom in liquid phase was not only by diffusion. Typical example of the finite interference fringe pattern during growth process is shown in Fig. 2, which is taken in the same alloy. Displacement of fringe pattern near the solid-liquid interface particularly shows the built-up of the boundary layer of solute diffusion. The surface morphological instability of anisotropic material will be also discussed.

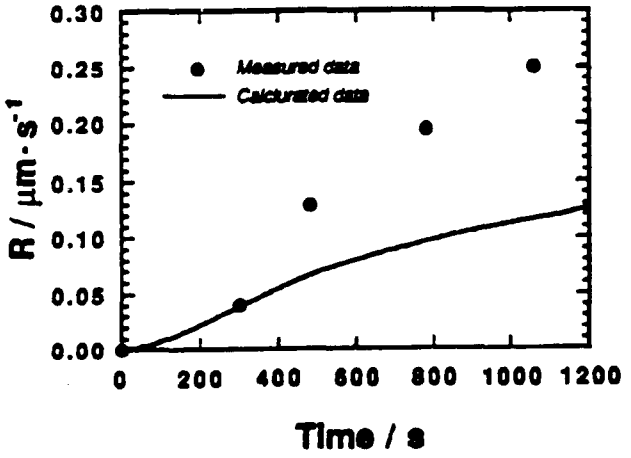

Figure 1. The calculated growth rate based on the diffusion controlling model. The measured values are plotted by close circles. R_c = 0.10 K/min, C_0 = 6.5 mol% acetone.

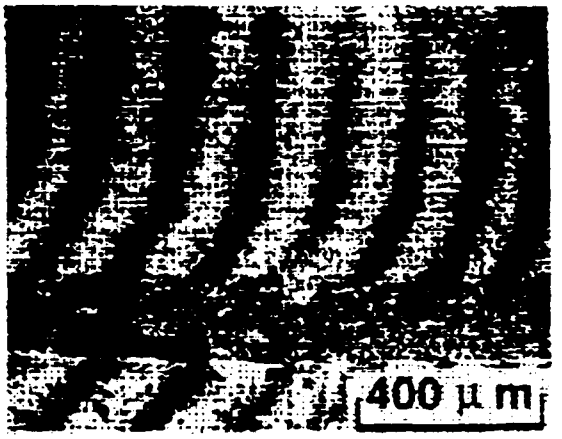

Figure 2. The typical examples of the interference fringe pattern during growth process on the same condition in figure 1 (t = 1000 s).

D77

GROWTH OF CAPROLACTAM FROM THE MELT AND SOLUTIONS PART II: EXPERIMENTAL OBSERVATIONS

E.P.G. van den Berg, R.M. Geertman and P. Bennema
Laboratory of Solid State Chemistry, University of Nijmegen
The Netherlands

Caprolactam ($C_6H_{11}NO$, CAP) is an important intermediate on the nylon-6 route. For a high quality polymer very pure CAP is needed. A possible method to achieve this purity is crystallization. However, despite the fact that CAP is commercially produced on a very large scale little is known about its crystallization behaviour. For application of crystallization on an industrial scale it is necessary to know more about the morphology of CAP and the mechanism of separation by crystallization of CAP from its main contaminants, water and cyclohexanone.

The experimental part of the research focuses on the system caprolactam-cyclohexanone. The efficiency of separation and the blocking of the different faces of CAP are investigated with the following methods:

- measurement of undercooling vs. growth rate curves of CAP in uniformly undercooled melts with different cyclohexanone content,
- measurement of undercooling vs. growth rate curves of CAP in melts with different cyclohexanone content and radial temperature gradients and
- determination of the variation of the cyclohexanone concentration in single Bridgeman grown CAP crystals.

The undercooling vs. growth rate curves indicate that cyclohexanone has an influence on the growth rate of CAP and that it differs upon the face of the CAP crystal involved. These measurements will be repeated with a cell with a radial temperature gradient to see whether new faces develop under influence of such gradients and varying cyclohexanone concentration. The concentration profile in the Bridgeman grown crystals indicate that the BPS law for the concentration profile of impurities holds very well.

D78

GROWTH OF CAPROLACTAM FROM THE MELT AND SOLUTIONS PART I: THEORETICAL CALCULATIONS

R.M. Geertman, E.P.G. van den Berg and P. Bennema
Laboratory of Solid State Chemistry, University of Nijmegen
The Netherlands

Caprolactam ($C_6H_{11}NO$.CAP) is an important intermediate on the nylon-6 route. For a high quality polymer very pure CAP is needed. A possible method to achieve this purity is crystallization. However, despite the fact that CAP is commercially produced on a very large scale little is known about its crystallization behaviour. For application of crystallization on an industrial scale it is necessary to know more about the morphology of CAP and the mechanism of separation by crystallization of CAP from its main contaminants, water and cyclohexanone.

The morphology of CAP was predicted by a PBC analysis.' The analysis consisted of two parts: an analysis for the case that CAP was growing with monomers and for the case that CAP was growing with dimers. The results of this analysis were compared with the morphology of CAP crystals grown from the melt and fifteen different solvents, giving a quite good agreement and showing that CAP has a strong tendency to grow with dimers. The only exception is CAP grown from a solution in water, in which case the {200} and {110} faces are blocked by water-CAP complexes. Further experiments where the rate of growth of the crystals was varied made it possible to explain the way in which water interacts with the different faces of CAP.

Another approach was chosen to understand the interaction of cyclohexanone with the different faces of the CAP crystal. The interaction energy of a cyclohexanone molecule with the different faces of CAP and the energy of a molecule cyclohexanone in the CAP crystal was calculated. From these data a qualitative prediction of the equilibrium concentration can be made. This can ' compared with the results described in part II.

SCANNING TUNNELING MICROSCOPY STUDIES ON ODD AND EVEN n-PARAFFIN MOLECULES ADSORBED ON GRAPHITE

D79

M. da Silva Couto, Xiang-Yang Liu, H. Meekes and P. Bennema
Laboratory of Solid State Chemistry University of Nijmegen
The Netherlands

Because the phenomena of surface melting seems to play an important role in the growth of at least the n-alkanes, we decided to study the ordering and orientation of the molecules at the surfaces of the paraffines.

To this purpose both odd and even numbered paraffines are interesting because they have different interactions in the solid and also a different structure. In order to be able to use scanning tunneling microscopy (STM) as an experimental tool, our first approach was to adsorb thin layers of the alkanes on graphite as the latter material is well suited for surface topological studies with STM, offering atomic resolution easily. A second reason for using graphite is that the distance between two next nearest neighbours within a paraffin molecule is the same as the lattice constant of the graphite.

The first experiments showed that for n-$C_{23}H_{48}$ the molecules are well-aligned, parallel to the surface, though this ordering is confined to limited areas. The distance between the is almost the same as that in bulk paraffin. The thickness and quality of the adsorbed layer depends on the solvents used and the way in which the solutions are applied to the surface. Thus, this system offers a model for the {110} faces of the corresponding paraffin.

For the even paraffines n-$C_{16}H_{34}$ showed either no ordering or possibly an ordering with molecules perpendicular to the surface, making the resolution extremely low. Given these early results, we investigated the ordering of the different types of paraffines in more detail and tried to bring the results in connention with the growth properties of paraffin crystals.

RELATIONS BETWEEN SOLUBILITY AND STABILITY OF UREA IN VARIOUS SOLVENTS AND SOLVENT MIXTURES

D80

Lisen Cheng
Research Institute of Synthetic Crystals,
P.O. Box 733, Beijing, 100018, P.R. China
Zhangshou Gao and Minhua Jiang
Institute of Crystal Materials Shandong University,
Jinan, 250100, P.R. China

Solubility and supersaturation intervals (or stability) of urea in various solvents and solvent mixtures were measured by laser diffraction method and dilatometric technique respectively. Following results have been obtained from our experiments:

(1) Supersaturation intervals of urea in alcohol solutions shrink with the increase of size of the alcohol molecules, and they also shrink with the decrease of its solubility.

(2) In alcohol mixtures or in alcohol-water mixtures, supersaturation intervals of urea shrink with the increase of its solubility.

(3) In methanol-formamide mixtures, supersaturation intervals of urea enlarge with the increase of its solubility.

From above results, no regular relations between stability and solubility of urea in the solvents and solvent mixtures mentioned above were found, but this irregularity can be explained by the solvent-solute and solvent-solvent interactions in solutions.

D81

THE CRYSTALLISATION OF HIGHLY PERFECT METAL-FREE PHTHALOCYANINE POWDERS FOR 'AB-INITIO' STRUCTURE SOLUTION BY DIFFRACTION METHODS

*P.G. Fagan and K.J. Roberts**
Department of Pure and Applied Chemistry, University of Strathclyde,
Glasgow, G1 1XL, UK
R. Docherty
ICI Specialities Research Centre, Blackley, Manchester, M9 3DA, U.K.
*Also at SERC Laboratory, Daresbury, Warrington, WA4 4AD, U.K.

The solution of molecular structure by X-ray diffraction usually requires the production of good quality single crystals which for many important industrial materials eg dyes and pigments, can be very problematic. Where single crystals are unavailable 'ab-initio' powder methods can be used, but as these also require the production of good quality crystalline powders there has been a growing awareness of the importance of optimising crystallisation processes for the preparation of such materials.

The phthalocyanines are used extensively in the paint and dyestuffs industries. Due to structural polymorphism they exhibit a structural dependence with respect to colour, which demands a better understanding of its molecular structure in order that the crystal properties can be controlled in production. Single crystal growth has been-demonstrated for metal bound polymorphs such as Copper (II) Phthalocyanine and thus structures solved. However the growth of the metal free polymorphs is hampered by an insolubility in most common solvents expected for pigments. Commercial crystallisation gives rise to poor quality deformed crystals which are inadequate for structural studies.

In this paper we present a crystallisation route to the preparation of high quality powders of metal free phthalocyanines together with a discussion of the role of crystallisation conditions on polymorph formation.

D82

THE NASA CENTER FOR THE DEVELOPMENT OF COMMERCIAL CRYSTAL GROWTH IN SPACE

William R. Wilcox
Clarkson University, Potsdam, NY 13699-5700, USA

The Center for Crystal Growth in Space is managed by Clarkson University. It is one of seventeen centers for the commercial development of space (CCDS's) funded by the Office of Commercial Programs at NASA Headquarters. The Director is William R. Wilcox and the Deputy Director is Brian Hoekstra. An industrial Board of Directors sets policy and budgets. Board members contribute cash and support relevant activities within their companies. Current Board members are Grumman, Boeing, Westinghouse, Rockwell and Teledyne-Brown. The annual budget is approximately $1.5 million. Of this, approximately 14% is for management expenses and 7% is for R&D at Clarkson University. The remaining 79% of the budget is for R&D elsewhere, flight hardware acquisition, and payload integration. Below are described briefly the R&D projects.

The R&D effort at **Clarkson University** itself is devoted to directional solidification of cadmium telluride. Activities include development of coatings and linings to reduce wetting and sticking, eddy current measurement of solid-liquid interface shape, development of an inexpensive flight furnace, modelling of radiant heat transfer in the growth apparatus and stress in the crystals, determination of the influence of in-situ and post-growth annealing, and measurement of the mechanical properties of CdTe at temperatures approaching the melting point. Flight experiments are planned for COMET and Spacehab.

Professor Heribert Wiedemeier at **Rensselaer Polytechnic Institute** developed techniques for vapor growth of CdTe at rates and diameters approaching those used for directional solidification, but at lower temperatures and precisely controlled.

PROCESS FEASIBILITY, CRYSTALLIZATION KINETICS AND HABIT STUDY OF POTASSIUM CHLORIDE USING AMMONIA AS A DILUENT

D83

D. Jagadesh, M.R. Chivate, N.S. Tavare and S. Rohani
31/602, H.P. Nagar (East), Mahul Road, Chembur, Bombay 400074, India

India has no really good source of Potassium salts which are good fertilizers and also an important industrial raw material. Sea-bitterns can be a good source. Manufacture of Potassium Chloride from bitterns by crystallization is however, a very complex and energy intensive process.

In this study it was demonstrated that Potassium Chloride can be crystallized from treated Sea-bitterns containing chlorides of potassium,sodium and calcium by ammoniation by two different methods. Four important variables viz ammonia concentration, temperature, addition of salt like ammonium chloride and concentration of feed by evaporation were varied. In crystallization with ammoniation of feed solution at 25°C practically no enrichment of potassium chloride over up to 50% ammonia concentration in mother liquor was realized. When the feed solution was first cooled to 0° followed by ammoniation up to about 40% wt ammonia concentration, reasonable purity of potassium crystals was obtained. The addition of ammonium chloride (up to 5% wt) to feed solution has improved both purity and yield of potassium crystals Alternatively the feed solution was concentrated before ammoniation by evaporating water and concentrated solution amniated to about 35% wt ammonia concentration in mother liquor at 25°C. This method also resulted in reasonable purity and yield of potassium crystals. Both these routes employing ammoniation step deserve further detailed study to arrive at optimal conditions for any commercial application.

A process simulation technique was developed for the production of potassium chloride from its aqueous solutions by using ammonia as a diluent in batch crystallizer. A series of experiments was performed in a Draft Tube Baffled Crystallizer over range of experimental conditions varying process variables such as Ammonia concentration, ammonia gas flow rate and stirrer speed.

The calculated time variations of ammonia and potassium chloride concentrations in the solution phase and population density curves determined from simulation algorithm were compared with experimentally observed profiles. The agreement between these is not entirely consistent, but is line with previous studies.

The cubic crystal habit of potassium chloride did not change when crystallized in the ammoniation process even in the presence of other chlorides. Some twinning was observed especially at low speeds of agitation. Addition of ammonium chloride modified the morphology from cubes to platelets. Percentage of agglomerates in product crystals from treated bitterns was generally smaller than that from nearly saturated potassium chloride solution.

LIGHT SCATTERING KINETICS STUDY OF CYCLOPROPANE HYDRATE GROWTH

D84

J.P. Monfort and A. Nzihou
Laboratoire de Génie Chimique, URA CNRS 192, 31078 Toulouse, France

Gas hydrates, as well as cyclopropane hydrate, which are water clathrates of small gas molecules can be formed when light hydrocarbons and/or some other light gases and water are in contact. These inclusion compounds are well known as plugging solid crystals in flowlines and in process equipment in the gas arid oil industry. After a long time period dedicated to the thermodynamics studies on water gas hydrates equilibria in order to develop improved methods to combat hydrate formation, recent studies come to consider kinetic phenomena during the crystallization of gas hydrates.

In this paper we describe an experimental set-up using a laser diffraction particle sizer to evaluate tile kinetic parameters which control the crystals growth in the cyclopropane-water system. In addition to this technique we use the more classical measurement of gas consumption during gas hydrate formation.

The experimental arrangement is constituted of a thermostated continuous stirred reactor, glass made of 1 l capacity, the operating pressures and temperatures are respectively 200-500 kPa and 278-288 K. Both gas and liquid flows are recirculated, the hydrate slurry is transported through a pressure cell where it is analyzed by a laser granulometer. Gas consumption is measured by a mass flowmeter; all experimental parameters are monitored on a micro-computer.

The experimental set-up has been tested by studying the influence of the subcooling and of the initial state of the aqueous solution on the induction time for the following hydratation reaction:

$$5.75\ H_2O\ (l) + C_3H_6\ (g) \rightarrow C_3H_6,\ 5.75\ H_2O\ (s)$$

The main parameters to be considered in the kinetics studies are:

- degree of subcooling
- pressure and temperature
- degree of mixing

Preliminary results have shown the effects of the degree of subcooling and temperature on the crystal size distributions and are discussed in this paper. Reaction rates based on gas consumption values versus time are presented; we present the advantages and limitations of the granulometer technique applied to gas hydrate crystal size distribution measurement.

D85

PREDICTIONS WITH UNIFAC OF LIQUID-SOLID PHASE DIAGRAMS: APPLICATION TO WATER-SUCROSE-GLUCOSE, WATER-SUCROSE-FRUCTOSE AND WATER-XYLOSE-MANNOSE

N. Gabas and C. Laguerie
LGC (URA CNRS 192), ENSIGC, chemin de la Loge, F-31078 Toulouse Cedex, France

The knowledge of liquid-solid phase diagrams is obviously fundamental in understanding crystallization processes of common sugars such as sucrose, glucose and fructose. Moreover, increased interest in recovery crystalline added-value monosaccharides such as xylose and mannose has revealed a need for solid-liquid equilibrium data of mixtures containing such biological molecules. Despite this necessity, relatively few data are available in literature for multicomponent sugar mixtures. This is probably due to difficulties to analyse very concentrate and very viscous sugar solutions.

The present investigation undertakes to apply UNIFAC model to predict isothermal liquid-solid equilibria in three ternary sugar systems: water - sucrose - D-glucose, water - sucrose - D-fructose and water - D-xylose - D-mannose and to compare the results with experimental data.

According to thermodynamic considerations, calculation of solubility requires the knowledge of component activity coefficients as a function of liquid phase composition from a suitable thermodynamic model. UNIFAC group contribution method is precisely able to predict liquid phase activity coefficients of non-electrolytes. Its application needs to fragment molecules into independent functional groups and to know physical and interaction group parameters, most of them are found in the data base. Because of the "proximity effects" existing in a saccharide molecule, it seems unconceivable to break up the cyclic skeleton of such a molecule. So three new groups representing the cyclic structures of glucose (G), fructose (F) and xylose (X) are created. These groups permit to model monosaccharides like mannose composed of X, OH and CH_2, disaccharides like sucrose made of G, F and -O- or more complex polysaccharides containing these basic rings. The interaction parameters between X, OH, H_2O and CH_2 on one hand and G, F, -O-, H_2O and OH on the other hand have been calculated from solubility data at different temperatures of binary sugar systems involved in the mixtures.

Then, the computed phase equilibrium compositions have been compared with experimental ones. For water-sucrose-glucose at 70°C, the agreement is very good: the greater difference between calculated and measured weight percentages of sucrose, observed in the invariant point region, is less than 3% For water-sucrose-fructose at 70°C, there is a large discrepancy between experimental and calculated solubilities only in the region saturated with the two sugars: the model predicts greater sucrose solubility and smaller fructose solubility than the data. For water-xylose-mannose at 25°C the predictions with UNIFAC are satisfactory: the averaged difference is less than 3.5 wt for xylose and 2.5 wt % for mannose. So this attempt proves successful. A similar technique could be easily extended in calculation of more complex multicomponent sugar systems experienced industrially.


POSTER SESSION
NUMBER 4
THURSDAY
3:15 PM
EXHIBIT HALL

POSTER SESSION #4
EXHIBIT HALL
Thursday 3:15 PM

A46
A New Cluster-Cluster Aggregation Model for the Sol-gel Transition of SiO_2
M. Kudoh,* X. Hu, K. Ohno, and Y. Kawazoe
Tohoku University, Japan

A47
Experimental Observation of Morphological Instabilities in Crystal Growth from Vapors
R.-F. Xiao* and F. Rosenberger
University of Alabama in Huntsville, USA

A48
Growth-Related Morphology of Porous Inorganic Salts
S. Halasz, S. Farkas and K. Kincses
Hungarian Academy of Sciences, Hungary

A49
Periodic Morphology Transitions between the Dendrite and the Dense-Branching Morphology in Electrodeposition
M. Wang* and N.-b. Ming
Nanjing University, China

A50
Uniformly Valid Asymptotic Solutions of Dendrite Growth from Melt with Convection Motion
J. J. Xu
McGill University, Canada

A51
Growth of Ammonium Nitrate (II) Dendrites
C. A. van Driel,* G. M. van Rosmalen, and T. T. Tjioe
Delft University of Technology, DSM Research, The Netherlands

A52
Kinetic Effects on Dendrite Growth
Y. Saito and T. Sakiyama
Keio University, Japan

A53
In-situ Observation of Growth Morphologies in Systems with High Melting Temperature
W. Schmidbauer, T. Wilke and W. Assmus*
Johann Wolfgang Goethe University, Germany

A54
Noise Reduction Effect on the Pattern Formation in the Electrochemical Deposition System
M. Wang* and N.-b. Ming
Nanjing University, China

A55
Impurity Induced Change of the Crystal Habit
D. Dragonova
University of Sofia, Bulgaria

A56
Structure of Tetrapod-like ZnO Crystals
M. Fujii,* H. Iwanaga, S. Takeuchi, and M. Ichihara
Nagasaki Institute of Applied Science, Nagasaki University, University of Tokyo, Japan

A57
Modelling the Morphology of Molecular Crystals in the Presence of Blocking Tailor-Made Additives
G. Clydesdale and K. J. Roberts*
University of Strathclyde, Glasgow, United Kingdom

A58
Alkaloid Ephedrine And A Dichlorine Substituted Chiral Cyclic Phosphoric F-Face Analysis and Structural Morphology of the Diastereomeric Salt of the Alkaloid Ephedrine and a Dichlorine Substituted Chiral Cyclic Phosphoric Acid
C. S. Strom* and F. J. J. Leusen
University of Utrecht, University of Nijmegen, The Netherlands

A59
Morphology of Rose Quartz Base Surface
I. B. Makhina, A. A. Mar'in, V. E. Khadzi
All Union Institute For Synthesis of Materials, Russia

A61
Segregation and Distributions of Dopings along the Crystals Length
A. Ya. Gubenko
The Institute of Electronic Machine-building, Russia

A62
The Effect of the Melt Structural State on the Stability of the Growing Surface
A. Ya. Gubenko
The Institute of Electronic Machine-building, Russia

B91
Mechanical Properties of CdTe at Temperatures Approaching the Melting Point
R. Balasubramanian and W. R. Wilcox
Clarkson University, USA

B92
Eddy Current Diagnostics of the Directional Solidification of Cadmium Telluride
G. J. Rosen and F. M. Carlson
Clarkson University, USA

B93
Macro And Micro Defects in CdTe, Related to the Thermal Gradients Near The Interface
M. Roth and M. Azoulay
Israel Atomic Energy Commission, Israel

B94
The Growth of (Cd,Zn)Te Mixed Crystals from the Vapour Phase
W. Sang, K. Durose, J. E. Lewis, and A. W. Brinkman
University of Durham, United Kingdom

B95
Melt Dynamics in Directional Solidification of PbSnTe
K. Grasza and A. Jedrzejczak
Polish Academy of Sciences, Poland

B96
Crystal Growth of Chalcopyrite Semiconductor $CuInSe_2$ by the Method of Horizontal Bridgman with Two Temperature Zones
H. Matsushita, S. Endo, H. Nakanishi, and T. Irie
Science University of Tokyo, Japan

B97
Bridgman Growth of $CuInSe_2$ Free of Adhesion to Ampoule
C.H. Champness
McGill University, Canada

B98
Study of Microstructural Characteristics of $CuGaSe_2$ Polycrystalline Thin Films
B. Mansour, M. A. Epwagry and S. A. Abdel-Hady
Helwan University, Egypt

B99
Near-Infrared Absorption in $ZnGeP_2$
P. G. Schunemann,* T. M. Pollak, M. C. Ohmer, and P. J. Drevinsky
Lockheed Sanders, Inc., USA

B101
Growth and Characterization of the Layered Structure Compounds InTe and GaTe
D.N. Bose
Indian Institute of Technology, India

POSTER SESSION #4
EXHIBIT HALL
Thursday 3:15 PM

B102
Electrocrystallisation by a Periodic Pulse Technique
S. M. Babu, R. Dhanasekaran and P. Ramasamy
Anna University, India

B103
Pressure Dependence of Prototype Structures of Metastable Niobium Oxides
K. Obara
Kagoshima University, Japan

B104
Measurement of Physical Properties of Lithium Borate Melt
Y. Anzai and S. Kimura
Kimura Metamelt Project, Japan

B105
Crystal Growth And Properties of $Ag_{7-x}TaSe_{6-x}(0<x<1)$
H. Wada and A. Sato
National Institute for Research, Japan

B105
$RAlO_3$:Ce(R=Y,Gd,La) Monocrystals - Fast Acting Scintillators
S. Smirnova, A. G. Davydchenko, M. V. Korzhik, and A. A. Fyodorovich
All Union Inst. for Syn. of Materials, Russia

B106
Growth and Characterization of $Li_2B_4O_7$ Single Crystals Grown by Novel Bridgman Techniques using Graphite Container
T. Katsumata, H. Konoura, A. Konno, K. Takei, M. Shinohara, K. Kano, and K. Takahashi
Toyo University, Japan

B107
Crystal Growth and Characterization of LBO ($Li_2B_4O_7$) Crystal by Bridgman Method
M. Ishii, S. Nakikawa, T. Ryouh, and I. Yamaga
Shonan Institute of Technology, Japan

B108
Solvents for the Growth of $BaFe_{12-(x+y)}Co_xSn_yO_{19}$ Bulk Crystals from HTS
X. Ruiz, V. Nikolov, F. Sandiumenge, R. Sole, R. Cabre, M. Aguilo, and F. Diaz*
University of Barcelona Tarragona, Spain

B109
The Growth Mechanism of the New Modified Method for $Mn_{1-d}Zn_dFe_2O_4$ Single Crystal
J. W. Chung, J. Y. Uhm* and K. K. Orr
Hanyang University, Korea

B110
Fast Solid State Growth of Large Hexaferrite Crystals
P. David* and C. Maillault
C.E.A.-D.A.M., France

B111
Flux Growth of Single Crystals of $(Nd_{1-x-y}Ce_xSr_y)_2CuO_{4-z}$ Containing Varying Amounts of Sr
A. J. S. Chowdhury,* B. M. Wanklyn, and F. R. Wondre
University of Oxford, U.K.

B112
Crystal Growth and Photoelectrical Study of Copper Tungstate
S. K. Arora* And T. Mathew
Sardar Patel University, India

B113
Studies on the Morphology of Inclusions in Flux-Grown Ruby
X. Wang, L. Fu, W. Liu and M. Qin
Research Inst of Synthetic Crystals, China

B114
Micromorphological Studies on Some Flux Grown $RCrO_3$ (R=Y,La,Gd,Yb) Single Crsytals by Optical and Scanning Electron Microscopy
A. K. Razdan,* B. M. Wanklyn and P. N. Kotru
University of Jammu, India

B115
Molecular Dynamics Study on the Structure of BaB_2O_4 Liquid Just After Melting
H. Ogawa
Kimura Metamelt Project, Japan

B116
Preparation of β-BaB_2O_4 Using a Zone Melting Technique
T. Katsumata
Toyo University, Japan

B117
Crystallization of Supercooled BaB_2O_4 Melts
A. Yokotani and S. Kimura
Kimura Metamelt Project, Japan

B118
Impurity Striation and its Evolution in the Process of Growth and Annealing of Corundum Single Crystals
E. R. Dobrovinskaya, L. A. Litvinov, and V. V. Pishchik
Academy of Sciences, Russia

B119
Evolution of Dislocation and Grain Boundary Structure at Growth and Thermal-Mechanical Loading of Corundum Single Crystals
E. R. Dobrovinskaya, L. A. Litvinov, and V. V. Pishchik
Academy of Sciences, Russia

B120
Growth and Properties of Needle-Shaped Crystals of Borate Aluminium
E.G. Yarotskaya,* V. P. Golenko, M. E. Andreev, E. V. Polyanski, V. A. Vanyshev, and V. G. Yarotski
All Union Inst for Syn of Materials, Russia

B121
Scintillator Crystals ZnSe(Te) - A Novel Material for Detectors of Ionizing Radiation
V.D. Ryzhikov
Institute for Single Crystals, Ukraine

B122
Isovalent Doping and Radiation Stability of $A^{II}B^{VI}$ Scintillation Crystals
V.D. Ryzhikov
Institute for Single Crystals, Ukraine

B123
Characteristic Features of the $ZnSe_{1-x}Te_x$ Solid Phase Synthesis
V.D. Ryzhikov
Institute for Single Crystals, Ukraine

B124
In Situ UHV REM Observations of Epitaxial Growth on the Semiconductor Surfaces
A.V. Latyshev
Institute of Semiconductor Physics, Russia

B125
Growth and Properties of Cerium and Praseodymium Doped Gadolinium Orthosilicate Single Crystals
V. A. Voloshin, M. B. Kosmyna, B. I. Minkov, M. V. Korzhik, V. I. Moroz, and A. A. Fedorov
Academy of Sciences, Ukraine

C53
Estimation of the Optimal Conditions for the Crystal Growth from the Vapour Phase with No Contact Between Crystal and Ampoule Wall
K. Grasza
Polish Academy of Sciences, Poland

POSTER SESSION #4
EXHIBIT HALL
Thursday 3:15 PM

C54
A Historical View on the Bridgman Method
M. Mohlberg* and M. Pfeiffer
Humboldt University of Berlin, Germany

C55
Temperature Monitoring on Bridgman Crystal Growth Process
S. Yan, Y. Chai, S. Wang, F. Wang, S. Ying, and H. Zhu
Shanghai Institute of Optics, China

C56
A New Technique for Measuring the Heat Transfer Between an Ampoule and Furnace
W. Rosch,* W. Debnam, A. Fripp, G. Woodell, and T. K. Pendergrass
NASA Langley Research Center, USA

C57
Application of Productivity Function in Closed Tube Chemical Vapour Transport
K. Balakrishnan,* B. Vengatesan and P. Ramasamy
Anna University, India

C58
Gravitation and Thermal Effects in Chemical Vapor Deposition
I. O. Clark, L. R. Black, E. J. Johnson, P. V. Hyer, P. W. Culotta, W. K. Gerdes, W. A. Jesser, and J. Kui
NASA Langley Research Center, USA

C59
Development of Computational Holographic Interferometry for Observation And Control of Vapor Deposition Processes
P. R. Griffin and S. Motakef*
Massachusetts Institute of Technology, USA

C60
Developments in Flux Growth
S. K. Arora
Sardar Patel University, India

C61
A Macintosh Based System with Automatic Diameter Control for Czochralski Crystal Growth
M. R. Singelenberg, R. A. Manente, C. L. Melcher, C. A. Peterson, J. S. Schweitzer, and F. J. Bruni
Schlumberger-Doll Research, USA

C62
Study of Directional Crystallization Process in a Cold Container with Direct Radio-Frequency Heating
V. V. Osiko,* D. L. Penyaz and N. P. Khaneev
Academy of Sciences, Russia

C63
The Single Crystal Growth of Sapphire Tube by EFG Process and the Study on the Defects of The Crystal
J. H. Lee and K. K. Orr
Hanyang University, Korea

C64
MHOI: Multidirectional Holographic Interferometer for Crystal Growth Experiments in Space
L. Gatti, F. Solitro, F. Bedarida, and G. A. Dall'Aglio
Alenia Spazio S.p.A., Italy

C65
Block Structures in Sapphire Crystals Produced by Stepanov Technique
S. V. Artyomov, V. S. Papkov, and V. F. Perov
NPO "Elma", Russia

C66
Aspects Referring to the Control of Crystal Growth Process by Electrically Modifying the Interface Tension
Z. Schiett, S. Balint, A.M. Balint, I. Jadaneaut, M. Serbanescu and V. Vanca
Universitatea din Timisoara, Romania

C67
Method of Coaxial Crystal Growth from Melt
E. R. Dobrovinskaya, L. A. Litvinov, and V. V. Pishchik
Academy of Sciences, Ukraine

C68
Heterophase Equilibria Investigation Method
A.A. Gamazov and A.A. Gamazov, Jr.
"Invect" Company, Russia

C69
The Obtaining of Semiconductor Crystals
A.A. Gamazov
"Invect" Company, Russia

D66
Solution Convection Effects on the Growth of Hen-Egg White Lysozyme
S. Liu, W. Xiao, T. Huang, and Y. Zhou
Northwestern Polytechnical University, China

D67
Problems in Growing Uric Acid Crystals
C. Aravindakshan, Y. M. F. Marickar,* T. G. Dhanalakshmi, N. Sylaja, S. Sindhu, H. K. Moorthy, and S. V. Roshni
Medical College Hospital, India

D68
Growth and Characterization of Some Urinary Crystals
T. Irusan, D. Arivuoli* and P. Ramasamy
Anna University, India

D69
Effect of Environment on Cholestral Crystal Growth in Vitro
E. A. Salim, Y. M. F. Marickar,* N. Sylaja, C. Aravindakshan, and N. Kalkura
Medical College Hospital, India

D90
Doping in Urinary Oxalate Crystal Growth - an SEM Study
S. Sindhu, Y. M. F. Marickar,* C. Arvindakshan, N. Elizabeth, and P. Koshy
Medical College Hospital, India

D91
Crystallization of Uric Acid
S. N. Kalkura, V. K. Vaidyan, M. Kanakavel, and P. Ramasamy
Anna University, India

D92
Dielectric Studies of Gel Grown Neodymium Molybdate Crystals
S. Bhat,* P. N. Kotru and R. P. Tandon
University of Jammu, India

D93
Absolute Control of Nucleation in the Gel Growth of Crystals by GNGT
G. Sivanesan
RSG College, India

D94
Characterization of Gypsum ($CaSO_4.2H_2O$) Twins by X-ray Topography
C. Rinaudo* and M. Franchini-Angela
Universita degli Studi di Torino, Italy

D95
The Influence of Additives on the Growth of Potassium Chloride and L-Alanine
R. Lacmann and W. Schroder
Institute fur Physiklische u., Germany

D96
Growth of $LiClO_4$ Crystal and In-Situ Observation
W. C. Chen and A. Y. Xie
Chinese Academy of Sciences, China

POSTER SESSION #4
EXHIBIT HALL
Thursday 3:15 PM

D97
Crystal Morphology of Brushite, $CaHPO_4{:}2H_2O$
F. Abbona,* F. Christensson, M. A. Franchini-Angela, and H. E. Lundager Madsen
Universita della Calabria, Italy

D98
Growth and Crystal Structure of $LiCuO_2$
K. Imai,* M. Koike and H. Takei
The University of Tokyo, Japan

D99
Automatic Facility for Crystal Growth from Solution Microgravity Experiments
M. J. Krasinski,* P. Kidula and M. Idzikowski
Technical University, Institute of Physics, Poland

D100
Very Large Melting Point Depression of Water in Silica
J. C. van Miltenburg and J. P. van der Eerden
University of Utrecht, The Netherlands

D101
Oriented Growth of Silica Molecular Sieve Crystals as Supported Films
J.C. Jansen and G.M. van Rosmalen
Delft University of Technology, The Netherlands

D102
Application of an Automated Crystallization Cell to Studies of The Nucleation Kinetics of Ionic Systems
P. Meenan and K. J. Roberts
University of Strathclyde, United Kingdom

D103
The Role of Solvent in the Nucleation and Growth of Normal Alkanes in the Homologous Series from $C_{16}H_{36}$ to $C_{28}H_{58}$
A. R. Gerson, K. J. Roberts, J. N. Sherwood, and A. Taggart*
University of Strathclyde, United Kingdom

D104
Synchrotron Radiation Studies of the Phase Transformations within Oleic Acid
S. R. Craig,* Y. Hayashi, K. J. Roberts and J. N. Sherwood
University of Strathclyde, United Kingdom

D105
Growth and Characterization of Triglycine Sulph-Phosphate Mixed Crystals
G. Ravi,* S. Anbukumar and P. Ramasamy
Anna University, India

D106
Radiation Effects in Ge-doped Crystalline Quartz
H. Bahadar
National Physics Laboratory, India

D107
Thin Film Growth Behavior of $YBa_2Cu_3O_7$ in Sequential Deposition with High Purity Ozone Gas
T. Shimizu
Electrochemical Lab, Japan

D108
Non-destructive Analysis of Oxygen Distribution in A Cu(1) Plane of an Orthorhombic $YBa_2Cu_3O_7$ using EXAFS Spectroscopy
H. Kajiyama
Advanced Research Labs, Japan

D109
Microscopic Studies of YBCO Crystals
A. Drake, M. Rand, M. Alndow, and J.S. Abell
University of Birmingham, UK

SESSION 4A

A46

A NEW CLUSTER-CLUSTER AGGREGATION MODEL FOR THE SOL-GEL TRANSITION OF SiO_2

M. Kudoh, X. Hu, K.Ohno and Y. Kawazoe
Institute for Materials Research, Tohoku University
2-1-1 Katahira, Aoba-ku, Sendai 980, Japan

Recently, fractal pattern formation has attracted considerable interest in solid state physics. In order to understand detailed formation processes, cluster-cluster aggregation models have been successfully applied to various physical systems involving colloid aggregates. The so-called sol-gel transition has also been investigated applying these modes. One typical example in this category is SiO_2 glass. Its detailed transforming process and properties are investigated experimentally.[1] In this paper we propose a new model for the cluster-cluster aggregation of SiO_2 system, and study its fractal structure by computer simulation.

The number of OR units in $Si(OR)_4$ replaced by OR units is related to the amount of doped water. Since polymers are formed via these OHs, the fractal dimension of the polymers depend on the mole ratio of added water. As a simple model we take seven kinds of basic monomers [Fig. 1]. The hands of the monomers represent the OHs and monomers grow into a polymer if the hands are linked with each other. The mole ratio of added water corresponds to the percentage of the cross monomer. With the different time scales of chemical reactions in mind we presume that the formation of polymer is a diffusion limited aggregation. Namely diffusing monomers meet to each other and aggregate into clusters and clusters diffuse with diffusion constants proportional to the inverse square-root of masses and aggregate into polymers.

To investigate the behavior of this system, we have performed intensive computer simulations. For simplicity, the simulation has been carried out in two dimensional schematics. The results are shown in Fig. 2, in which, the fractal dimension seems to be almost independent of the percentage of the cross monomer. However, it is expected that there is a crossover from the fractal dimension of self-avoiding walks to the cluster-cluster aggregation at a very small percentage of the cross monomer. We suppose this theoretical crossover corresponds to the experimental observation of the change of the fractal dimension of the glasses. We are currently investigating simulations in three dimensions to obtain more direct correspondence between theoretical predictions and experimental results.

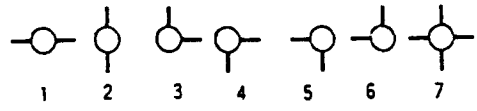

Figure 1. Monomer model

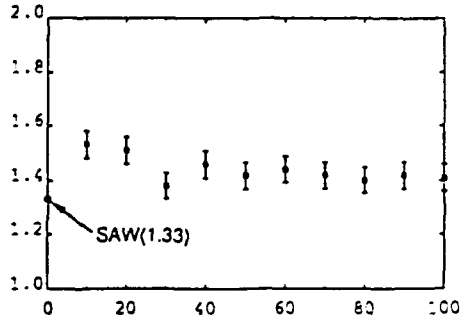

Figure 2. Fractal dimensions vs percentages of cross monomer.

[1] M. Mikami: Master Thesis, Tohoku University, 1990.
[2] P. Meakin: in *Phase Transitions and Critical Phenomena*, edited by C. Domb and J.L. Lebowitz 12(Academic Press, 1988).

A47

EXPERIMENTAL OBSERVATION OF MORPHOLOGICAL INSTABILITIES IN CRYSTAL GROWTH FROM VAPORS*

Rong-Fu Xiao and Franz Rosenberger
Center for Microgravity and Materials Research
University of Alabama in Huntsville, Huntsville, Alabama 35899, USA

We have investigated surface morphologies of CBr_4 and I_2 crystals during vapor growth with high resolution microscopy and image processing under closely controlled supersaturation and inert gas pressure conditions. We found that the high temperature (fcc) phase of CBr_4 is morphologically considerably less stable than the low-temperature (monoclinic) phase. The morphological stability depends not only on temperature and supersaturation, but also sensitively on the total pressure in the vapor. With increasing inert gas pressure, crystals with initially smooth surface first exhibit cellular and then dendritic morphologies. We have found that dendrites with six-fold (snow-flake-like) symmetry appear only at pressures close to one atmosphere.

These dendrites bear morphological similarity with those found in melt and solution experiments. However, the destabilizing transport mechanism appears to be more complex than the bulk diffusion that causes instabilities in growth from liquid phases. It appears that surface diffusion on the supporting substrate plays also an important role. This is evident from a rapid decrease in the growth rates of mutually approaching dendritic tips. The surface-diffusion induced morphological instability is particularly pronounced in the growth of faceted I_2 crystals. There we found that the instability starts from shallow steps at the face center. This is followed by step bunching at the cusps of macrosteps and finally, by the formation of river-valley-like patterns. Some of these observations will be interpreted in terms of results of our earlier Monte Carlo simulations.

This work has been supported by NASA's Microgravity Science and Applications Division through grant NAG1-972, and by the State of Alabama through the Center for Microgravity and Materials Research at the University of Alabama in Huntsville.

A48

ON THE MORPHOLOGICAL AND CHEMICAL STABILITY OF VITAMIN C CRYSTALS

S. Halász and B. Bodor
Research Institute for Technical Chemistry of the Hungarian
Academy of Sciences, H-8201 Veszprém, P.O. Box 125, Hungary

Vitamin C (L-ascorbic acid) has got an enormous industrial utilization. In this year nearly one thousand papers have been published among which only a few crystallization studies can be found, although stability problems are often mentioned.

The unit cell of ascorbic acid crystal contains four small molecules in a relatively well packed arrangement which would allow us to grow good quality crystals. In spite of this fact we concluded that the strong secondary nucleation is responsible for the usual low quality of the industrial products.

For the semi-batch cooling crystallization of vitamin C a special mixing program is recommended (first ultrasonic-, and then hydrodynamic agitation) in order to save the uniformity of the firstly appeared nuclei and to obtain more isometric habit, homogeneous CSD and better chemical stability.

Data of X-ray analysis will also be given.

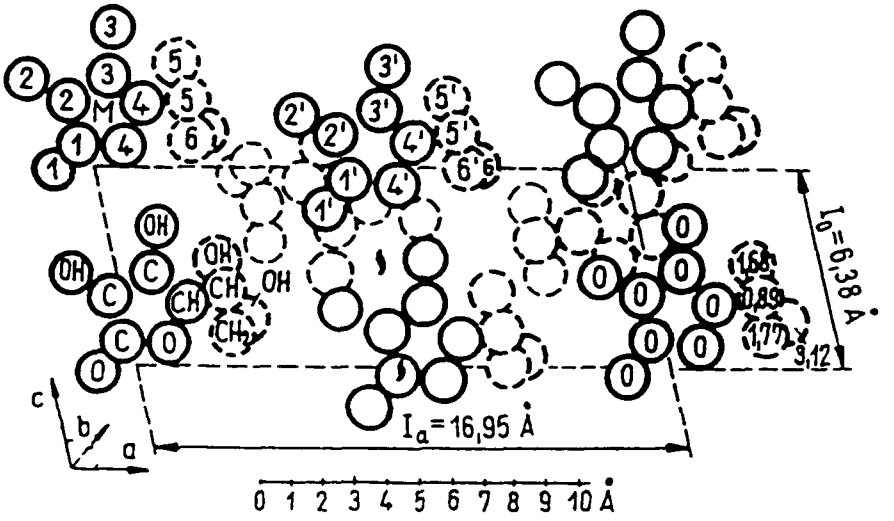

The unit cell characteristics of ascorbic acid.

PERIODIC MORPHOLOGY TRANSITIONS BETWEEN THE DENDRITE AND THE DENSE-BRANCHING MORPHOLOGY IN ELECTRODEPOSITION

A49

Mu Wang and Nai-ben Ming
National Laboratory of Solid State Microstructures and Department of Physics
Nanjing University, Nanjing 210008, People's Republic of China

Periodic morphology transitions between dendrite and dense branching morphology DBM is investigated using *in-situ* observation method in electrochemical deposition system of $FeSO_4/H_2O$. The experimental results show that the dendritic pattern and the DBM may coexist and may transfer from one kind of pattern to another. Morphology transition process and the growth rate of the deposit during the process, as well as the concentration field near the growing interface have been studied. The periodic morphology transition is possibly caused by the influence of impurities on the anisotropy of the growing interface, and hence on the interfacial growth dynamics. A possible selection role in pattern formation is discussed.

UNIFORMLY VALID ASYMPTOTIC SOLUTIONS OF DENDRITE GROWTH FROM MELT WITH CONVECTION MOTION

A50

Prof. J.J. Xu
McGill University

This work deals with the effect of convection motion in melt on dendritic growth. In the present paper, we consider steady growth with zero surface tension. Assuming the Prandtl number *Pr*, based on the tip velocity and the thermal length is large, we are able to obtain a uniformly valid asymptotic solution to the steady state in the whole growth region.

GROWTH OF AMMONIUM NITRATE (II) DENDRITES

A51

C.A. van Driel, G.M. van Rosmalen* and T.T. Tjioe***
*Faculty of Chemical Technology and Materials Science
Delft University of Technology, Leeghwaterstraat 44, 2628 CA Delft, The Netherlands
**DSM Research, P.O. Box 18, 6160 MD Geleen, The Netherlands

Ammonium nitrate (AN), mainly used as a basic chemical for the production of fertilisers and explosives, occurs in several polymorphic crystal phases. The transition temperatures at atmospheric pressure in pure water-free ammonium nitrate are:

$$\text{melt} \xrightarrow{169^\circ C} \text{I} \xrightarrow{125^\circ C} \text{II} \xrightarrow{84^\circ C} \text{III} \xrightarrow{32^\circ C} \text{IV} \xrightarrow{-18^\circ C} \text{V}$$

The crystallisation temperature of an AN melt is decreased by the addition of water. A melt containing 4 to 12% water directly crystallises into phase II at temperatures between 125 and 84°C respectively. *In-situ* microscopic observations show that this temperature region is above the roughening temperature of AN(II), which develops as dendrites. The crystallisation kinetics, as well as the shape and size of the dendrites depend on the difference ΔT between the crystallisation temperature, imposed by the water concentration, and the temperature of the melt, and on the water concentration itself. Additives can have an additional effect on the crystallisation kinetics and the dendritic growth pattern. The influence of ΔT and water concentration on the growth kinetics of AN(II) and on its growth pattern have been determined by optical microscopy.

In addition tablets have been prepared by crystallising water containing melts in a mould at temperatures between 85 and 120°C. After crystallisation the tablets, consisting of dendritic crystals, were dried at 90°C. The drying rate of the tablets clearly depends on the crystallisation conditions (ΔT and water concentration). Tablets prepared at a small ΔT and a high water concentration show a fast drying rate while those prepared at large ΔT and lower water concentrations result finally in a slower drying rate. From these measurements and microscopic observations it follows that the fine structure of the original dendrites, imposed by their crystallisation conditions, determines the pore size distribution of the tablets and therefore the drying rate. This was confirmed by measuring the porosity of the finally cooled tablets.

Apart from the crystallisation conditions also the presence of specific additives affects the dendritic growth pattern of AN(II) and thus determine the final structure of AN granules. The phase II structure influences product characteristics, like the drying behaviour. The final water content and its distribution over the granules affect the kinetics of the phase transition IV-III which has a strong impact on the mechanical strength of the granules.

A52

KINETICS EFFECT ON DENDRITIC GROWTH

Yukio Saito and Tomoko Sakiyama
Department of Physics, Keio University,
3-14-1 Hiyoshi, Kohoku-ku, Yokohama 223, Japan

The dendritic crystal growth under the effect of both interface tension and the kinetics is simulated by solving the quasistationary evolution equation of the interface. The method is an extension of that used for the free dendrite.[1] When the kinetic coefficient is increased with a fixed undercooling, the controlling mechanism changes from the interfacial tension to the interface kinetics, and the growth velocity shows different universal behaviors.

With interface kinetics, the undercooling at the interface u satisfies the relation $\Delta - d\kappa - u = b\upsilon_n$, with Δ being a bulk undercooling, κ a local curvature, υ_n the normal velocity of the interface. The anisotropic capillary length d and a kinetic coefficient b are assumed to have the four-fold symmetry as $d = d_0(1 - d_4 \cos 4\theta)$ and $b = b_0(1 - b_4 \cos 4\theta)$.

We first choose tile diffusion constant $D = 1$, $d_0 = 10^{-4}$, $d4 = 0.1$, $b_4 = 0.01$, and $\Delta = 0.25$, and increase the strength of the kinetic coefficient b_0 from 0 up to 2×10^{-2} to investigate the kinetic effect. The overall profile of the dendrite does not vary much with many side-branches as is shown in Fig. 1, but only the scale of the dendritic structure or the tip radius ρ increases. Simultaneously the growth velocity υ decreases. The product of the tip radius ρ and the growth rate υ is almost independent of b_0, and takes a constant value compatible with the Peclet number p, defined by the Ivantsov relation. In a double logarithmic plot in Fig. 2a, the stability parameter $\sigma = \upsilon d_0/2Dp(\Delta)^2$ remains constant for a small interface kinetics or for a small = $\mu = 2Dpb_0/d_0$, whereas σ decays inversely to μ for large μ. The result agrees with the perturbation analysis.[2]

With a stronger anisotropy in kinetics as $\nu = b_4/d_4 = 1$, the side-branches are strongly suppressed.[3] Furthermore, the tip of the crystal becomes sharp as b_0 increases, and the velocity shows a complicated behavior (Fig. 2b); it first increases before it decreases ultimately for large enough b_0. The increase of the velocity or σ is also expected in the solvability analysis, but no quantitative agreement is obtained. Here the product of the tip radius ρ and the velocity υ is no more constant but decays rapidly for large μ, and due to this deviation from the Ivantsov relation the solvability analysis may not be valid.

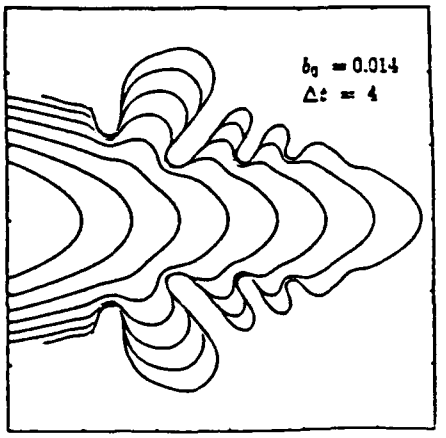

Figure 1. Time evolution of a dendritic crystal with a small anisotropy ratio $\nu = b_4/d_4 = 0.1$.

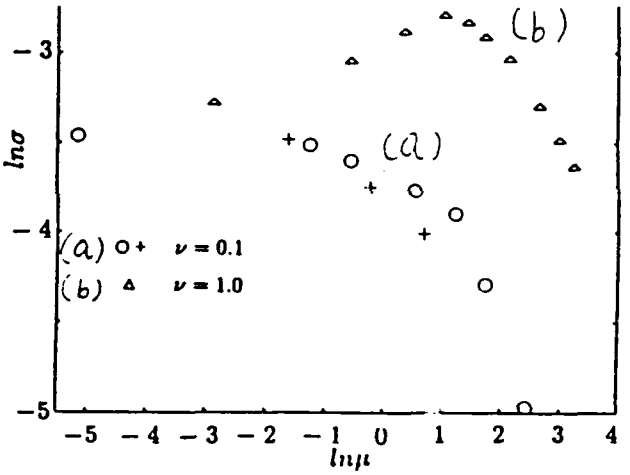

Figure 2. Double logarithmic plot of the stability parameter $\sigma = \upsilon d_0/2Dp^2$ versus the strength ratio $\mu = 2Dpb_0/d_0$.

[1] Y. Saito, G. Goldbeck-Wood and H. Müller-Krumbhaar, *Phys. Rev.* **38** (1988) 2148.
[2] E.A. Brener and V.I. Mel'nikov, *Adv. Phys.* **40** (1991) 53.
[3] A. Classen, C. Misbah, H. Müller-Krumbhaar and Y. Saito, *Phys. Rev.* **51** (1991) 6820.

IN-SITU OBSERVATION OF GROWTH MORPHOLOGIES IN SYSTEMS WITH HIGH MELTING TEMPERATURE

A53

W. Schmidbauer, T. Wilke and W. Assmus
J.W. Goethe-University, Physikalisches Institut
Robert Mayer-Straβe 2-4, D-6000 Frankfurt am Main

Pattern formation with cellular or dendritic morphologies during crystallisation from the melt is observed by optical methods. The investigations are made with different compositions in the KCl-CsCl system (T_m of approx. 750°C) and in the $PbCl_2$-$PbBr_2$ system (T_m of approx. 420°C). A detailed description of the experimental set-up is given. The results of primary dendrite spacing λ_p, secondary dendrite spacing λ'_s and tip radius ρ versus the growth velocity v and temperature gradient G are compared with theoretical predictions.

NOISE REDUCTION EFFECT ON THE PATTERN FORMATION IN THE ELECTROCHEMICAL DEPOSITION SYSTEM

A54

Mu Wang and Nai-ben Ming
National Laboratory of Solid State Microstructures and Department of Physics
Nanjing University, Nanjing 210008, People's Republic of China

Noise reduced electrochemical deposition is performed in agarose gel medium containing $CuSO_4$ solution. Instead of random fractal-like pattern usually observed in aqueous-solution electrodeposition system, the deposit has the morphology of dendrite with evident main stem and relatively stable tip behavior. The agarose gel medium sharply decreases the noise near the growing interface and completely eliminates the convection in the system. As the result, the effective anisotropy during the deposit growth is increased, hence the dendritic pattern is formed. This experimental result is consistent with the theoretical and computational expectations.

IMPURITY INDUCED CHANGE OF THE CRYSTAL HABIT

A55

D. Draganova
University of Sofia, Faculty of Chemistry

More than two centuries have passed since in 1783 Rome de Lisle noticed the effect of habit changing of NaCl in the presence of carbamide. Many investigations were carried out and numerous hypotheses were offered. Our studies concern the dependencies $R_{100}(c_i)$ and $R_{111}(c_i)$ where R is the normal growth rate of the respective face and c_i is the impurity concentration. Potassium halogenides growth in the presence of $(n-1)d^{10}$; $(n-1)d^{10}s^2$ and $(n+1)d^n$ ions was investigated. This allowed us to answer two questions: (i) Conditions at which the impurity stabilizes a certain crystal face because of the strongly passivating effect. This happens within the ranges of mechanism I for all the studied ions on the equilibrial cubic face and for $(n-1)d^n$ ions within the ranges of mechanisms I and II for (100) KX. (ii) The impurity induced habit transition (100) → (111) is marked by the intercept of the curves $R_{100}(c_i)$ and $R_{iii}(c_i)$ i.e. when $R_{100}=R_{111}$. It happens within the ranges of II mechanism for d^{10} and $d^{10}s^2$ ions and within mechanism III for d^n ions. At first the equation was found to be valid

$$\ln C^* = \text{const} \times 1/T + \text{const}' \qquad (1)$$

where C* is the critical habit transition impurity concentration and T is the absolute temperature. Later, on the basis of Lanmuir's phase equation the approximate equation was offered:

$$\ln C^* = 1/2\,(Q_{100} - Q_{111})/RT + \text{const}'. \qquad (2)$$

Here Q_{100} and Q_{111} were determined directly from the temperature dependence of $R_{100}(c_i)$ and $R_{111}(c_i)$. The most precise form of the equation is

$$\ln C^* = Q_o/RT + \text{const}' \qquad (3)$$

where const' has a strictly defined physical meaning. The quantity Q_o is characteristic of the system crystal matrix - impurity and of the impurity induced habit changed (100) → (111), as C* which may be considered as the main critical point in the tri-component water-salt system. Other important characteristics of this critical phenomenon will be considered in other reports.

A56

STRUCTURE OF TETRAPOD-LIKE ZnO CRYSTALS

M. Fujii
Nagasaki Institute of Applied Science, Nagasaki 851-01, Japan
H. Iwanaga
Faculty of Liberal Arts, Nagasaki University, Nagasaki 852, Japan
S. Takeuchi and M. Ichihara
The Institute for Solid State Physics, The University of Tokyo

Tetrapod-like ZnO crystals were grown by oxidation of zinc vapor. A typical scanning electron micrograph of the tetrapod-like crystal is shown in Fig. 1. The crystal is composed of four legs joining at a common juncture. The four legs and the common juncture were examined with the aid of transmission electron microscope (TEM). The four legs A, B, C and D in Fig. 1 have the wurtzite structure growing along the <0001> direction. Fig. 2 shows a dark field image of the common juncture taken by TEM. A nucleus in the shape of the trigonal pyramid is seen on the surface of the common juncture. The nucleus was confirmed to be in the wurtzite structure by an electron diffraction pattern.

Six angles between the four tetrapod-like crystal were legs of a measured accurately by an optical microscope. The measured angles were not the same for each crystal. Table 1 shows the types of set of the six angles and the number of the crystals having the same type of the angles in the last column. The type I crystal with four angles of 102°, a 116° and a 129° was dominant. In the type I crystal every two legs are in twin relationship to each other and the twin planes for two legs with angles of 102°, 116° and 129° $(11\bar{2}4)$, $(11\bar{2}2)$ and $(22\bar{4}3)$ respectively; furthermore, three of the four legs are grown homoepitaxially on the three $(11\bar{2}2)$ planes of the nucleus.

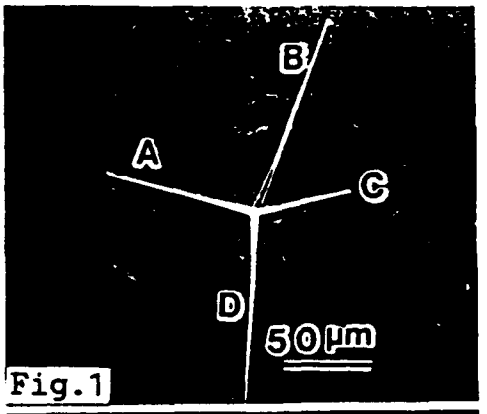

Fig.1

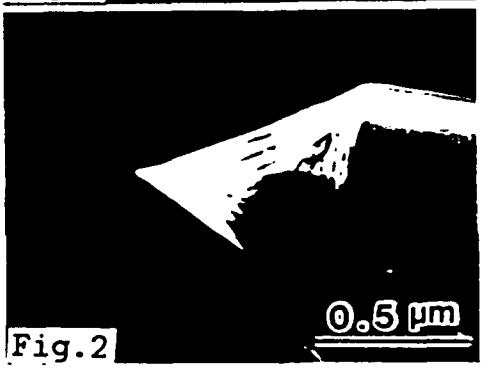

Fig.2

Table 1. Types of set of six angles between two needles.

Angle / Type	96°	99°	102°	107°	110°	116°	127°	129°	131°	No. of Crystals
I			4			1		1		8
II			3		2			1		2
III		1	3			1		1		1
IV		1	3			1			1	1
V	2		2					2		1
VI			1	2	1		2			1

A57

MODELLING THE MORPHOLOGY OF MOLECULAR CRYSTALS IN THE PRESENCE OF BLOCKING TAILOR-MADE ADDITIVES

*G. Clydesdale and K.J. Roberts**
Department of Pure and Applied Chemistry, University of Strathclyde, 295, Cathedral Street, Glasgow G1 1XL, UK
K. Lewtas
Exxon Chemical Ltd, Milton Hill, Abingdon, OXON OX13 6BB, UK
R. Docherty
ICI Specialities Research Centre, Blackley, Manchester, M9 3DA, England, UK
*Also at SERC Daresbury Laboratory, Warrington, WA4 4AD, UK

The morphological control of crystalline materials is commonly effected through the mediation of additives. These can be subdivided into "disrupting", additive molecules which are usually smaller than those of the host and "blocking" additives which are usually larger than the host.

In this paper the methodology behind predicting the morphology of molecular crystals in the presence of tailor-made additives of the *blocking* kind is presented and described. The work is an extension of morphological modelling techniques developed by the authors in which the atom-atom method was applied to:

- calculate the surface attachment energy of crystal surfaces, and hence crystal growth rate, in the case where no additives are present,
- model the effects of *disrupting* tailor-made additives.

The case of blocking additives is complicated by the molecular size effects which results in the need to consider the generation of lattice vacancies in the inter-molecular bonding calculation. The overall approach of the method is illustrated with case examples of host/additive systems including those of α-glycine/L-alanine and docosane/9-methyl-docosane.

A58

F-FACE ANALYSIS AND STRUCTURAL MORPHOLOGY OF THE DIASTEREOMERIC SALT OF THE ALKALOID EPHEDRINE AND A CHLORINE SUBSTITUTED CYCLIC PHOSPHORIC ACID

C.S. Strom
Institute of Earth Sciences, Univ. of Utrecht, P.O. Box 80021, 3508 TA Utrecht, The Netherlands
F.J.J. Leusen
CAOS/CAMM Center, Univ. of Nijmegen, Toernooiveld, 6525 ED Nijmegen, The Netherlands

The goal of this study is to gain detailed insight into the intermolecular interactions governing the resolution of enantiomers via preferential crystallization of diastereomers. Previously studied qualitatively and quantitatively using Computer Assisted Molecular Modeling, the problem is now being tackled utilizing the Hartman-Perdok theory.

The monoclinic unit cell $P2_1$ (a = 19.659 Å, b = 7.208 Å, c = 7.921 Å, β = 100.728° contains two acid and two base ions consisting of a total of 116 atoms. The position coordinates of the molecules $i = 1, \ldots, 4$ were taken as the mass centers of the atoms composing them. Fractional axial coordinates of the acid are x = 0.11721, y = 0.56721, z = 0.732; and of the base x = 0.41874, y = 0.12503, x = 0.3306. The strong bonds depend on the intermolecular distances according to the criterion acid-acid ≤ 8.0 Å, base-base ≤8.0 Å, acid-base ≤9.3 Å, leading to the following adjacency specifications for the unit cell: bonds *i-j* are (1-2, 1-3, 2-3, 3-4).

Based on the above combinatorial information the complete collection of F-slice configurations and their orientations $\{F_i(hkl);\ i = 1, 2, \ldots\}$ were generated by means of Strom's graph-theoretic method. These are infinite two-dimensional networks of strong bonds with thickness md_{hkl} (m is usually 1, occasionally 1/2, but 1/3, 1/4 and 1/6 are also possible). In the spirit of the Hartman-Perdok PBC theory, these are possible elementary growth layers, or F-slices, provided they meet certain preconditions. Furthermore, the slice energy should be as large as possible. The attachment energy, i.e., the interaction energy between slice and semi-infinite structure, is assumed proportional to the growth rate of the (*hkl*) face. The obtained F-slices were d_{hkl} thick, except for (100) where both d_{100} and d_{200} were encountered. Calculation of the slice energies enabled the identification of the configurations corresponding to the maximum slice energy for each (*hkl*) face. Finally, the attachment energies were calculated to derive the growth form.

The energy computations performed were based on both short and long range forces. The short range Van der Waals interactions, which appeared to be important in our previous studies, were computed with the various parametrizations of the CHARMm force field. The long range Coulomb potential was computed by the Ewald method, ensuring sufficient and reasonably rapid convergence. Three independent sets of point charges were used (empirically assigned CHARMm charges, and semi-empirical quantum mechanical charges computed by AMPAC with the AM1 and PM3 parametrizations). The derived morphology is ideal, in the sense that the influence of solvent-crystal interactions and other external factors have been neglected.

A59

MORPHOLOGY OF ROSE QUARTZ BASE SURFACE

I.B. Maxkina, A.A. Mar'in, V.E. Keadzi
Vrissims, Alexandrov, Russia

Morphology of rose coloured synthetic quartz crystals obtained in P doped fluoride solutions has been studied.

It is known /1/ that the base surface of quartz crystals grown in fluoride media shows vivid signs of regeneration. It is all covered with faceted heads of trigonal dipyramides. Even doping the system with various impurities does not remove the regeneration relief from this surface.

Only P-dopant has been found to be a factor defining in a way growth mechanism of this surface. Under effect of this dopant the relief structure changes from the usual pattern to a "cobblestone" one known for the material grown in alkali solutions. The change may be complete or just partial, so the surface relief becomes function of dopant concentration and of temperature in the system.

The change reveals itself first with pinacoid faces appearing on the above mentioned pyramides, whose height becomes smaller accordingly. Then the pinacoid surface grown more round, the side facets diminishing to disappear altogether finally. Now the surface has a characteristic "cobblestone" pattern. Sometimes a hillock has an active summit and we observe a surface with comic growth accessories. It should be noted though that normally there are elements of many stages of relief formation on the changing surface that remains morphologically unstable for some period.

The cobblestone relief is associated with some decrease in the growth rate of the crystal.

A60

SUPERMOBILITY OF CRYSTAL-MELT INTERFACE

V.O. Esin
Institut of Metal Physics, Academy of Sciences
Oral Branch. Ekaterinburg 620219, Russia, USS

The structure particulares of the crystal-melt interface are considered on the basis of the theory of the melting transition in fcc metal crystals and the cluster structure of melts, which was developed in [1], also a study of a surface roughening transition and the mobility of a crystal interface by means of Monte-Carlo computer simulation in the various lattice models. It is shown, that the crystal-melt interface is to be able become the supermobile at the phase transformation and it is determined the conditions of a disappearance of the thermodynamic and kinetic barriers for the interface motion in a condensed system.

It is found, that at the melting temperature the "heat pressure" in the regions of maximum dilation in the cluster-cluster interface in the melt, which are generated by the development of "cavitation density fluctuations" in a condensed system at melting [2], is equal-in-magnitude the theoretical strength of the material. In the regions of the extreme strength (dilatation) the atom jamps over the cluster-cluster interface occurred with the frequency is nearly equal the frequency of them thermal vibrations and the thermodynamic and kinetic barriers for the interface motion between the clusters in the melt vanish at the melting temperature.

At the crystal growth from the melt the transition free volume excess is isolated in the crystal-melt interface, that lead to local stretch (to dilate) of the condensed system in this region and to decrease the kinetic barrier for the atom exchanges between the phases. That lead also to increase of the interfase roughness, which in turn is cause the decrease of the thermodynamic barrier for the interface advance and the increase of the interface mobility. In order for the formation of a gap in the interface (a breakdown of the condensed system) is to be impossible and the extreme dilatation is to be retain, it is necessary a crystal growth carry out under a some excess pressure. It is obtained the expression can be used to estimate the pressure is required for to maintain the supermobility of the crystal-melt interface in the process of the phase transformation.

1. V.O. Esin, *Dokl. Acad. Nauk* SSSR, v.283 (1985) p.89.
2. J.I. Frenkel, Kineticheskaja teorija gidkostej (Leningrad, 1975).

SEGREGATION AND DISTRIBUTIONS OF DOPINGS ALONG THE CRYSTALS LENGTH

A61

Gubenko A. Ya
Moscow Institute of Electronic Machine-building, Moscow, USSR

During crystallization, segregation characterized by distribution coefficient (K_i) is greatly determined by structural state of melt (SM). With changing concentration of component SM is changing non-monotonously as $(\partial \ln K_i/\partial X_i)p = [(1-kg)/k]/S_{cc}(O,X_i)$ where $S_{cc}(O,X_i)$ is a structural factor in the long-wave range of melt. Non-monotony is due to the fact that with changing phase transitions take place even with K_i equal to 10^{-3} - 10^{-1} atm.%. Correspondingly the function $\partial \ln K_i P(X_i)$ is stable out of X_i under which phase transitions take place. It all relates to equilibrium and non-equilibrium. Crystallization of any matter actually occurs from immediate layer of melt (ILM) which is situated between the crystallization from and the main mass of melt. SM and ILM are related to SM of main mass of melt but differ in the following way:

- ILM is under super cooled state that is necessary for growing; the particles of ILM are in the field of forces of surface atoms of growing surface;
- the length of ILM is determined by temperature gradient at the crystallization front.

All these factors tend to order the arrangement of the particles in ILM which are under heat motion and it is followed by intensifying atomic interactions. They are minimal at the crystallization front and decrease with moving from it. Thus atomic interactions in ILM even at stable X_i as well as $S_{cc}(O,X_i)$ depend on conditions of growing and temperature gradient. Experimental data on simulation ILM confirm the substantial role of ILM and SM. When growing crystals by directed crystallization due to changing temperature gradient in ILM and distribution X_i along the length differs greatly from theoretical one. The changes of atomic interactions in ILM are so substantial that they result in different melting temperatures, the parameters of lattice and properties of upper and lower parts of crystal.

THE EFFECT OF MELT STRUCTURAL STATE ON THE STABILITY OF THE GROWING SURFACE

A62

A. Ya. Gubenko
Institute of Electronic Machine-building, Moscow, USSR

The stability of a growing surface depends on the ratio of "embryo" formation rates and growth steps on it. If the latter is essentially higher than the former, then any projection appearing on the surface is bricked out by rapidly spreading growth steps. The surface stability results from it. The steps rate may be essentially raised by increase in the melt disorder degree, other conditions of crystal or epitaxial layers growing being ordinary. The melt disorder degree is determined by the share of free chaotically distributed atoms in it. The more this share the less energy of connection between all the media particles. In the connection energy is the least among all other melts based on the certain component. The disorder degree may be increased by the effect of the external field on the melt, e.g. by ultra-sound vibrations. A cellular structure is formed in the crystal under the accent growing conditions, while it was absent at the crystal irradiation with other conditions being the same. The similar effect was obtained when one more doping was introduced into the melt, the concentration of this doping corresponding to the minimums at the isothermal curves of viscosity, melt density, liquidus curve ($\partial T/\partial x_i = 0$) and function $\partial \ln a_i/\partial x_i$, where a_i denotes the component activity. This effect takes place in all the systems and is indicative of the melt disorder. The doping type determined only the minimums depth and the disorder degree. If $\partial \ln a_i/\partial x_i = 0$, the diffusion coefficients on the surface and in the volume will be the maximum as well as rate. It leads to the increase in the stability and the growth rate. The same doping increases the stability and growth rate in certain concentrations and decreases these parameters in other concentrations. The same regularity takes place at the growth from vapor. In this case, the adlayer disorder degree increases/decreases depending on the composition. The stability and growth rate change in correlation with each other in the corresponding way.

SESSION 4B

MECHANICAL PROPERTIES OF CdTe AT TEMPERATURE APPROACHING THE MELTING POINT

B91

R. Balasubramanian and W.R. Wilcox
Center for Crystal Growth in Space
Clarkson University, Potsdam, New York 13699, USA

Thermal and mechanical stresses play an important part in the formation and multiplication of dislocations during the growth of CdTe. In order to evaluate the effects of thermal stress on crystalline quality, one needs to know the mechanical properties of CdTe at all temperatures that a growing ingot would experience. In this context, we have determined the stress-strain behavior and the critical resolved shear stress (CRSS) of CdTe from 300 K to 1353 K. Single crystal CdTe specimens, oriented along the <132> axis, were uniaxially compressed at a strain rate of 1×1^{-4} s^{-1} at different temperatures. Boron oxide (B_2O_3) was used as the encapsulant to prevent evaporation of CdTe at temperatures above 773 K. The CRSS decreased rapidly with increasing temperature up to 400 K, was nearly constant between 400 K and 800 K, and decreased again beyond 800 K. The value of the CRSS at 1353 K was approximately 0.2 MPa.

EDDY CURRENT DIAGNOSTICS OF THE DIRECTIONAL SOLIDIFICATION OF CADMIUM TELLURIDE

B92

G.J. Rosen and F.M. Carlson
Center for Advanced Materials Processing
Department of Mechanical and Aeronautical Engineering
Clarkson University, Potsdam, NY 13699, USA
J.P. Wallace
Casting Analysis Corporation
Route 2, Box 113, Weyers Cave, VA 24486, USA

The long range goal of this work is to improve the qua ity of cadmium telluride grown by the vertical Bridgman-Stockbarger (VBS) technique. The high melting temperature and volatility of cadmium telluride limit the possible investigative methods. An in-situ technique such as eddy current diagnostics allows direct measurement of various growth parameters.

Eddy current testing is one of a category of methods known as nondestructive evaluation techniques. It is a non-contact, remote technique which can be used to measure a variety of parameters. These parameters include electrical conductivity, material dimensions and solidification phenomena. Eddy current techniques have been used in the metals industry for 30 years. Only recently has it been applied to crystal growth processes.

A custom built high frequency eddy current system was installed in a VBS furnace. The system is being used to measure axial and radial temperature profiles as well as interface shape. In addition, the system is being used to investigate how the crystal separates from the crucible during post-growth cool down.

B93

MACRO AND MICRO DEFECTS IN CdTe, RELATED TO THE THERMAL GRADIENTS NEAR THE INTERFACE

*M. Roth and M. Azoulay**
School of Applied Science and Technology
The Hebrew University, Jerusalem 91904, Israel
*Soreq Nuclear Research Center, Yavne 70600, Israel

The growth of large area CdTe single crystals with high crystalline perfection still faces some difficulties[1]. We have shown recently[2] that it is possible to obtain high quality CdTe single crystals by the seeded vertical gradient freeze technique (SVGF), due to the thermal design of the growth compartment.

In this paper we present a study on the influence of the thermal gradients in the melt on the formation of macro (Grain boundaries and twins) and micro (Dislocations and cellular Structure) defects in the grown crystals. A quantitative analysis has been carried out in order to calculate the energies involved in the formation of defects. It is shown that when the crystals were grown at the highest axial thermal gradient, the volume of single crystal grain was about 15% of the entire volume. In the rest of the solidified mass about 30 grains were counted. On the other hand, in crystals grown at the lowest axial gradient, single grains occupied about 90% of the entire volume on the average. Only few twins were observed at the very top portion of the crystal (10%) in most cases. The microdefect analysis by X-Ray diffraction shows a Full Width at Half Maximum (FWHM) of the DCRC of about 40 arc seconds with symmetrical shape for the best crystals. The highest values of about 250 arcseconds were measured for crystals that were grown under the highest axial thermal gradient (10°C/cm), and the DCRC's exhibit a very significant asymmetry with several clearly marked splits. The above results are explained in terms of the different degree of supercooling near the solidified interface which is proportional to the axial thermal gradient. The latter in conjunction with the growth rate plays a major role in the formation of thermo-mechanical stresses as well as of non-equilibrium defects. It is therefore suggested that high crystalline perfection CdTe crystals can be grown under low axial thermal gradient (3°C/cm or lower) when the interface shape between the grown crystal and the melt is kept near planar.

1. S. Sen, W.H Konkel, S.J. Tighe, L.G. Bland, S.R. Sharma and R.E. Taylor, *J. Crystal Growth* 86, (1988) 111.
2. M. Azoulay, A. Raizman, and M. Roth *J. Crystal Growth* 101, (1990) 256.

B94

THE GROWTH OF (Cd,Zn)Te MIXED CRYSTALS FROM THE VAPOUR PHASE

Sang Wen-bin, K. Durose, J.E. Lewis and A.W. Brinkman*
Department of Physics, University of Durham, South Rd., Durham, DH1 3LE, U.K.

There is growing interest in the bulk crystal growth of the ternary compound $Cd_{1-x}Zn_xTe$ for use as substrate material in the epitaxial deposition of (Hg,Cd)Te. The particular composition where x=0.04 is lattice matched to the important $Hg_{0.8}Cd_{0.2}Te$ material used in long wavelength infrared detection. There is also a need for $Cd_{1-x}Zn_xTe$ crystals (x=0.5) for use as lattice matched substrate material for the growth of CdTe-ZnTe and HgTe-ZnTe strained layer superlattices. In addition, with a band gap varying from 1.45 eV (near infrared) to 2.26 eV (green), (Cd,Zn)Te is also potentially important as an optoelectronic material and is currently under investigation in some solar cell devices. This paper reports on recent attempts to grow single crystals of (Cd,Zn)Te from the vapour phase, over a wide range of composition.

The crystals were grown by two closed tube methods. The first was originally developed for the growth of CdS and has been used with other ternary compounds, notably (Cd,Zn)S and (Cd,Zn)Se. Crystal growth occurred in specially designed silica growth tubes, consisting of a growth capsule (1.5cm in diameter, 10 cm in length) connected to a long narrow tail through a small orifice. The tail tube was loaded with a few grams of one of the principal elements and, during growth, was maintained at an empirically determined temperature such that the partial pressures in the growth capsule were close to optimum values. The second method used similar growth capsules, but without the tail. In both techniques about 20-30 gm of source material (a mixture of crushed ZnTe and CdTe in the desired compositional ratio) was loaded into the capsule which was then evacuated, sealed and placed in a two zone furnace. After equilibration at 1100°C, the tube was gradually pulled through a temperature gradient and when the temperature difference between the source and the growth tip exceeded the threshold value, mass transport and crystal growth commenced.

The as-grown crystal boules were typically about 4-6 cm in length and 1 cm in diameter, and usually contained three or four grains. Wafers were cut from the boules using a diamond saw and used to determine composition and crystal quality. Composition was measured from EDX spectra initially, and then from precise lattice parameter measurements using the Debye-Scherer technique with Nelson-Riley extrapolation. These values were confirmed by determination of the optical band gap from transmission spectra, and revealed that compositional uniformity along the length of the boule was reasonably good, although there was some Zn-enrichment in the closing phase of the growth. The variation in composition along the length of the boule, as deduced from the optical transmission measurements, was of the order of 6% (excluding the Zn-rich end). The structural perfection of the crystals was assessed using Oxford Instruments cathodoluminesence (CL) microscopy apparatus. Grain boundaries, polygonisation walls, isolated dislocations and twins were identified. CL microscopy proved to be a more reliable means of defect assessment than conventional defect revealing etch methods.

*Permanent address: Dept. of Physics, S.U.N.Y. Plattsburgh, NY 12901, USA.

B95

MELT DYNAMICS IN DIRECTIONAL SOLIDIFICATION OF PbSnTe

Krzysztof Grasza and Andrzej Jedrzejczak
Institute of Physics, Polish Academy of Sciences,
PL-02-668 Warsaw, Poland

Several processes of directional crystallization of $Pb_{1x}Sn_xTe$ were performed on the gradient furnace in destabilizing temperature gradient. In order to trace the solid-liquid interface shapes, the crystal pulling velocity was changed rapidly. or the growth was stopped and started again. The temperature at the liquid was recorded versus time. These measurements were correlated with the technological cycles for different values of the ratio of the height of liquid column to its diameter (the aspect ratio) [1.2].

The crystals grown were etched electrochemically and the x-ray microprobe analysis were performed. The hydrodynamics of the melt at destabilizing gradient conditions was discussed and the Rayleigh number versus the aspect ratio was evaluated. Macro-vortical structure present in the melt under turbulent convection was identified. Strong dependencies of a local chemical inhomogeneity of the crystals on the type of melt convection which accompanied crystal growth was observed.

1. K. Grasza and A. Jedrzejczak, *J. Crystal Growth* 110 (1991) 867.
2. G. Müller, G. Neumann and W. Weber. *J. Crystal Growth* 70 (1984) 78.

B96

CRYSTAL GROWTH OF CHALCOPYRITE SEMICONDUCTOR $CuInSe_2$ BY THE METHOD OF HORIZONTAL BRIDGMAN WITH TWO TEMPERATURE ZONES

Hiroaki Matsushita, Saburo Endo, Hisayuki Nakanishi and Taizo Irie
Department of Electrical Engineering, Faculty of Engineering
Science University of Tokyo, Shinjuku-ku, Tokyo, 162 Japan

The chalcopyrite semiconductor $CuInSe_2$ has an energy gap of about 1 eV and large optical absorption coefficient. Therefore, it has the potential to application in photovoltaic cells. It is known that it is easy to prepare the crystals having p- or n-type conduction by controlling the deviation from stoichiometry. In order to control the carrier concentrations, the control pressure is very important.

In order to control the Se vapor pressure, the single crystals of $CuInSe_2$ were prepared by the method of horizontal Bridgman with two temperature zones (2T-HB method) as shown in Fig. 1. The Se composition of the crystals increases with an increase of Se vapor pressure. Figure 2 shows the carrier concentration and the Hall mobility at room temperature as a function of Se vapor pressure. The Hall mobility is maximum and the carrier concentration is minimum at about 20 torr of Se vapor pressure. From the temperature dependence of the carrier concentration, it is found that the carriers have activation energies between 75 and 80 meV for the samples prepared under Se vapor pressure ranging from 10 to 200 torr. All of the crystals show p-type conduction. Therefore, it is considered that the estimated levels are for the acceptor due to V_{Cu}.

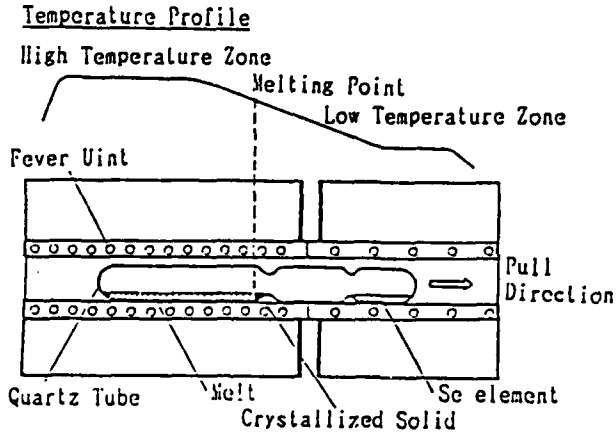

Figure 1. Electric furnace

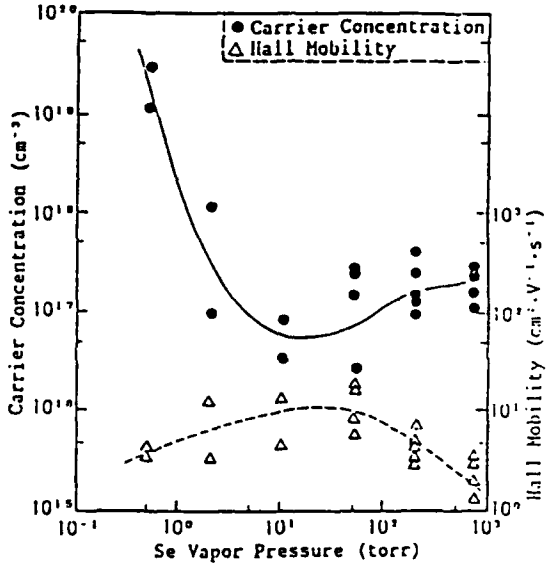

Figure 2. Transport properties

BRIDGMAN-GROWN CRYSTALS OF $CuInSe_2$ FREE OF ADHESION TO AMPOULE

B97

L.S. Yip, Z.A. Shukri, I. Shih and C.H. Champness
Electrical Engineering Dept., McGill University
3480 University Street, Montreal, Quebec, Canada H3A 2A7

The chalcopyrite semiconducting compound $CuInSe_2$ is one of the leading materials for the absorber layer of a thin film solar cell. However, bulk single crystals of this material are also needed to carry out such studies as the development of etching and surface treatments, development of new ohmic contacts, determination of crystal orientation effects, determination of photovoltaic performance limits and determination of the fundamental transport and optical properties of $CuInSe_2$. Such investigations are more conveniently done on bulk material than on thin film samples. In this laboratory, ingots containing centimetre-size single crystals have been prepared by the Bridgman method using both vertical and horizontal growth systems. The growth of good-quality ingots has been hindered in the past by the adherence of the grown ingot to the inner wall of the quartz ampoule. This sticking induces stresses in the material and makes extraction of a complete ingot difficult. However, this problem has been overcome by the introduction into the ampoule of a thick layer of carbon or boron nitride. Titanium has also been found to be effective in avoiding the sticking problem. Such added materials do not have to be in direct contact with the $CuInSe_2$ melt and they appear to act as getters. While the agent causing the sticking has not yet been definitely identified, some evidence suggests that it may be present in the starting element indium, despite its stated 5 nine's purity. In the single crystals, cleavage has been found to occur in {112} and {101} planes and possibly also in {110} planes. Characteristic triangular etch pits are observed on the {112} planes. Studies have been made on bismuth and platinum contacts to single crystal filamentary samples.

STUDY OF MICROSTRUCTURAL CHARACTERISTICS OF Cu Ga Se_2 POLY CRYSTALLINE THIN FILMS

B98

Bahiga Mansour, M.A. Epwagry** and Seham A. Abdel-Hady***
*National Research Center, Dokki, Cairo
**Faculty of Science, Helwan University, Cairo

The structure of deposited films of Cu Ga Se_2 by evaporation is interpreted in terms of line profile analysis of X-ray diffraction patterns. The effects of preparation conditions on the orientation, crystallite size and residual strain were studied. The films are found to be of the tetragonal structure with a=5.611 and c=11.02 Å. All films are found to be preferentially oriented with the <112> fiber texture. The degree of preferential orientation is found to increase slightly with increasing film thickness. The increase of deposition rate (40-60) decrease the percentage of other phases appear. The substrate temperature 320°C during deposition gives the best conditions for crystalline thin films with main composition Cu Ga Se_2.

B99

NEAR-INFRARED ABSORPTION IN $ZnGeP_2$

P.G. Schunemann and T.N. Pollak
Lockheed Sanders, Inc., MER15-1813, P.O. Box 868
Nashua, N.H. 03061-0868
M.C. Ohmer
Wright Laboratory Materials Directorate (WL/MLPO)
Wright Patterson, Ohio 45433-6533
P.J. Drevinsky
Phillips Laboratory (PL/STER), Hanscom AFB, Mass. 01731

$ZnGeP_2$ has long been known as a promising non-linear optical material because of its large d-coefficients (d_{eff} = 75pm/V) and its wide transparency and phase-matching ranges. Its chief limitation for near to mid-infrared frequency conversion applications, however, has been the presence of a broad absorption band extending from the band edge (0.62μm) to ~ 3μm. The goal of this investigation was to identify and eliminate the microscopic origins of this absorption band by correlating the electrical and optical properties with variations in the concentration of native defects. Melt stoichiometry, post-growth annealing, and electron-beam irradiation were used to vary the defect concentration in single crystals grown by the horizontal gradient freeze technique. These samples were characterized using spectrophotometry, calorimetry, photoluminescence, and Hall effect measurements.

The lowest as-grown losses to date have been observed in material grown from nominally stoichiometric melts, whereas both Ge-rich and ZnP_2-rich material exhibited higher near-band-edge absorption. Post-growth annealing (300 hrs, 550°C, in ZnP_2 powder) and e-beam irradiation (1 MeV, 2 x $10^{18}cm^{-2}$ flux) have both been used to reduce losses to as low as $4.5cm^{-1}$ and $0.25cm^{-1}$ at 1μm and 2μm respectively at which point the reduction appears to saturate due to residual non-stoichiometric defects. Hall effect measurements linked the above absorption with a deep acceptor level (denoted AL1) with an energy ranging from 0.3 and 0.6 eV. The identity of this defect is still unknown, but zinc vacancies, cation disorder, and phosphorus anti-site defects have all been proposed.

The most recent results, along with strategies for further reductions in loss, will be discussed.

Work supported by Wright Laboratory Materials Directorate (WL/MLPO), Wright Patterson AFB, Contract No. F33615-88-C-5438.

CRYSTAL GROWTH AND PROPERTIES OF $Ag_{7-x}TaSe_{6-x}I_x$ ($0 \leq x \leq 1$)

B100

H. Wada and A. Sato*
National Institute for Research in Inorganic Materials,
1-1 Namiki, Tsukuba, Ibaraki, 305, Japan

A new type of argyrodite sulfide, Ag_7TaS_6 has recently been prepared at 500°C[1]. This phase is cubic, space group $F\bar{4}3m$, with a=10.51Å and exhibits high Ag^+ ion conductivity. Our interest led us to extend this work to analogous selenide compounds, and we recently succeeded in preparing new compound $Ag_{7-x}TaSe_{6-x}I_x$ ($0 \leq x \leq 1$). Two kinds of crystals have been obtained. In this work, the morphology, crystal structure and transporting properties have been studied.

(1) Phase - I: cubic, a=10.83~10.88Å with S.C. $F\bar{4}3m$. This compound exists in the range 0.1 x 1. $Ag_{6.9}TaSe_{5.9}I_{0.1}$ crystals obtained by prolonged heating at 800°C for 2 weeks show the some morphological features with the development of {III} and {100} faces; cubo-octahedron (Fig. 1).

(2) Phase - II: cubic, a=10.83Å with S.C. $P2_13$. This compound exists in the range $0 \leq x < 0.1$. A precession photograph of Ag_7TaSe_6 is shown in Fig. 2. The observed density is 7.33 g cm^{-3} (Z=4) These both compounds are mixed conductors. Data on the ionic conductivity σ_{Ag+} and transport numbers will be presented.

1) H. Wada and M. Onoda, *J. Less-Common met.*, 175 (1991) 209.

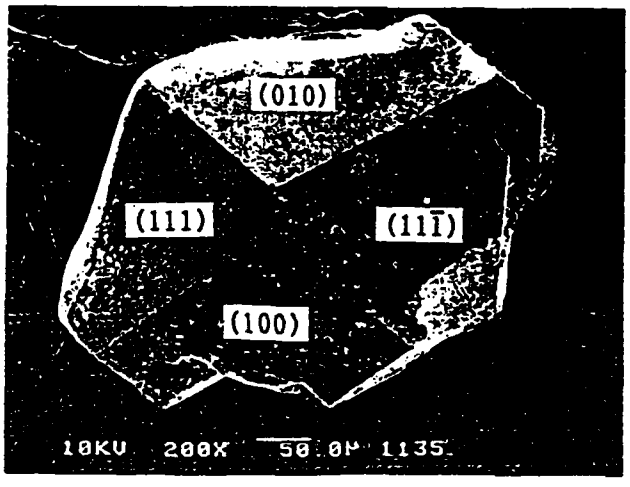

Figure 1

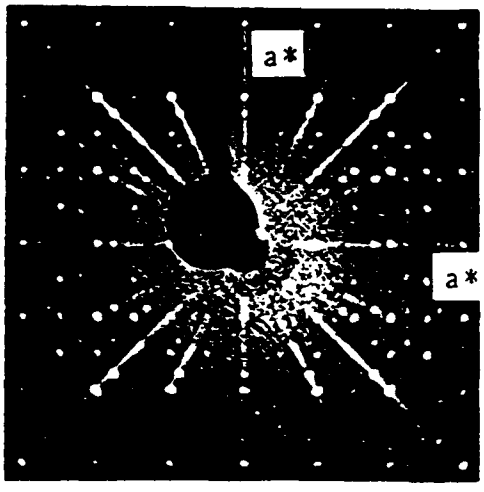

Figure 2

B101

GROWTH AND CHARACTERIZATION OF THE LAYERED STRUCTURE COMPOUNDS InTe AND GaTe

S. Pal and D. N. Bose
Semiconductor Division, Materials Science Centre
I.I.T. Kharagpur-721302, India

The III-VI compounds InTe and GaTe are layer-type semiconductors with strong conductivity anisotropy. Resistivity and Hall effect studies have been carried out on single crystals of InTe and GaTe to examine the nature of carrier scattering along and perpendicular to the layer planes. DLTS measurements on GaTe in two perpendicular crystallographic directions showed anomalous activation energies.

InTe and GaTe crystals were synthesized by fusing the components (6N purity) taken in stoichiometric proportions. Synthesis was carried out in vacuum-baked quartz ampoules evacuated to about 10^{-6} Torr. The resulting melt was mixed thoroughly to ensure homogeneity and kept continuously stirred. The InTe and GaTe monocrystals were grown by the Bridgman technique. A two zone vertical tubular furnace was used for the growth. The reaction vessel (conical-tipped) was heated to about 1000K/1173K, maintained at that temperature for 24 hours and was slowly cooled through the crystallization temperature at the rate of 1.2 mm/hr. The resulting ingots (p-type) were about 2 cm in length and 1.1 cm in diameter.

Samples of InTe cleaved easily in the layer plane at an angle with the growth axis whereas platelets of GaTe cleaved in the layer planes growing in the direction $\perp^r$ to the c-axis. X-ray diffraction studies confirmed that InTe has a tetragonal structure whereas GaTe is monoclinic. For InTe with resistivities of 10^{-3} Ω-cm, the hole mobilities were μ_{11} = 50-60 cm^2/V sec and $\mu_\perp$= 10-15 cm^2/V · sec and were found to vary as $T^{+1.43}$ between 150-300 K in both directions but showed saturation in the c-direction. The conductivity anisotropy factor varied with temperature due to the activation energies being lower (0.012 eV, 0.138 eV) along the layer planes than in the c-direction (0.023 eV, 0.173 eV).

For GaTe (E_g = 1.64 eV at 300K) with resistivities between 30-50 Ω-cm (300K), the hole mobility was found to increase from 35-700 cm^2/V sec between 300-77K with a $T^{-1.9}$ dependence in the layer planes, whereas along the c-axis, the mobility varied from 6-120 cm^2/V sec.

Al/GaTe Schottky devices exhibited large barrier heights (0.8 eV) and were used for DLTS measurements. A hole trap at E = 0.64 eV and another anomalous trap of higher energy were found along the layer plane while two hole traps were found at E = 0.306 eV in the c-direction. This is opposite to the lower shallow acceptor activation energies (23 meV, 72 meV) found along the layer planes compared with 40 meV, 137 meV) in the c-direction. Possible interpretations will be discussed.

B102

ELECTROCRYSTALLISATION BY A PERIODIC PULSE TECHNIQUE

S. Moorthy Babu, R. Dhanasekaran and P. Ramasamy
Crystal Growth Centre, Anna University, Madras-25, India

Binary (CdS, CdSe, CdTe) and ternary ($CdSe_xTe_{1-x}$, $CdxZn_{1-x}S$, $Cd_xZn_{1-x}Se$) of II-VI and ternary ($CuInSe_2$, $CuInTe_2$, $AgInSe_2$) I-III-VI_2 compound semiconductors have been electrodeposited from an aqueous solution by a period pulse technique [1-31]. More compact, uniform and well adhered deposits were obtained by suitably adjusting the duty cycle (pulse to pause width) of the potential. The optimum conditions for good quality deposits are determined. The deposited materials have been characterised with X-ray powder diffractograms, scanning electron micrographs, electron probe microanalysis and voltammetry. Crystalline nature, physical properties, composition and kinetics of the process are explained. The mechanism of charge transfer and the thermodynamic stability of the deposits at the electrode-electrolyte interface have been explained using the charge-mass and potential-current relations respectively.

A kinetic model has been developed for the process of electrocrystallisation by periodic pulse technique. The model considers the oscillation of driving force at the electrolyte interface with the applied frequency of pulses. The role of different kinetic factors, mass transport, convection, diffusion etc., on the electrocrystallisation process by this periodic pulse technique has been analysed. The influence of different parameters such as concentration of the individual species, hydrogen ion concentration, potential, temperature and the duty cycle on the deposit distribution has been studied. The advantage and applicability of this technique are discussed with the results obtained.

[1] S. Moorthy Babu, T. Rajalakshmi, R. Dhanasekaran and P. Ramasamy, *J. Cryst. Growth*, 110 (1991) 423.
[2] S. Moorthy Babu, R. Dhanasekaran and P. Ramasamy, *Thin Solid Films*, 198 (1991) 269.
[3] S. Moorthy Babu, R. Dhanasekaran and P. Ramasamy, *Thin Solid Films*, 202 (1991) 67.

B103

PRESSURE DEPENDENCE OF PROTOTYPE STRUCTURES OF METASTABLE NIOBIUM OXIDES

Kozo Obara
Faculty of Engineering, Kagoshima University
Korimoto, 1-21-40, Kagoshima 890, Japan

Pressure dependence of prototypes of nonstoichiometric metastable niobium oxides were investigated by an electron microscope. Niobium oxides were formed by a conventional magnetron sputtering system. The morphology of derived crystals depended strongly on the argon pressure; when argon pressure P_{Ar}<02 Torr, thin microcrystals were derived and P_{Ar}>03 Torr, super-fine particles with a cubic structure were derived. In thin microcrystals which were formed below 0.2 Torr, we found five types of superlattice structures. Table 1 shows the lattice constants which are directly estimated from the two dimensional lattice images. In lattice constants between five types structure, following relationships were found within 1% error. The lattice constant c=3.19A of type **B** coincides with half of the lattice constant of type **A**, a_0=6.44/2=322A. The product of the lattice constant a=422 and sin(81.15) of type **C** coincides with a=4.16A of type **B**. The product of lattice constant a=4.76A and sin(72.8) of type **D** coincides with $\sqrt{2}$ times of a_0. The lattice constant a=4.72A of type **E** coincides with a=4.76A of type **D**. All types of superlattice structures is related to the lattice constant a_0. Therefore, the cubic lattice (A_0) of a_0=3.22A is considered as a prototype for these five superlattices. The similar relations between lattice constants were found on the niobium oxides which were formed above 0.3 Torr. The agglomerations of oxidized niobium super-fine particles, which have the lattice constant a=3.44A (BCC) and 56 at% oxygen, were transformed to NbO with the lattice constant a=4.22A (FCC) and NbO_2 with a new superlattice structure. Niobium dioxide has structures of three types as listed Table 2. The new superlattice NbO_2 is related to the rutile type and tetragonal type 1. The lattice constant a=4.85A and c=5.125A of the new type NbO_2 coincide with a=4.85A of T1 type and $\sqrt{3}$ times of c=2.96A of the rutile type, respectively. Unique relationships were found within 0.5% error between the lattice constant a=3.44A of niobium oxide super-fine particles, NbO with ordered vacancies and NbO_2 with tetragonal structures. In this case, the lattice structure with a=3.44A (BCC) is seemed to be the prototype. These structural changes due to pressure difference depend on the density of vacancies in as grown crystals. The density of vacancies is related to the condensation rate of the crystals.

Table 1. P_{Ar} < 0.2 Torr

Type	Lattice constants
A	a = 6.44A
B	a = 4.16A, c = 3.19A
C	c = 4.24 A, c = 3.69A, θ = 81.1
D	a = 4.76A, c = 3.10A, θ = 72.8
E	a = 4.72A, c = 289A
Prototype	a = 3.22A

Table 2. PAr > 0.3 Torr

Type	Lattice constants
Rutile	a = 4.78A, c = 2.96A
Tetragonal 1	a = 485A, c = 2.99A
Tetragonal 2	a = 13.71A, c = 5.985A
New type	a = 4.848A, c = 5.125A
Prototype	a = 3.44A

B104

MEASUREMENT OF PHYSICAL PROPERTIES OF LITHIUM BORATE MELT

Y. Anzai and S. Kimura

KIMURA Metamelt Project, ERATO, JRDC, Tokodai 5-9-9, Tsukuba, 300-26, Japan

In a Li_2O-B_2O_3 system, a compound lithium tetraborate ($Li_2B_4O_7$) is used for SAW device and lithium triborate (LiB_3O_5) single crystals show good performance in nonlinear optics. However, it is difficult to grow high quality and large size single crystals because of its high viscosity of melt. The knowledge about physical properties of the Li_2O-B_2O_3 melt was limited. The purpose of this report is to obtain a basic data for molten state of the Li_2O-B_2O_3 system. The density, viscosity and surface tension of lithium borate melt were measured at the temperatures from 1100°C to 800°C. The density was measured on the Archimedean principle using a 15mmϕ Pt sphere. The surface tension was determined by the ring method. The viscosity was measured on the basis of the Stokes' Law. The raw materials were mixed to Li_2O:B_2O_3 = 1:2,1:3,1:4. The sample melt was held in a Pt crucible. All measurements were carried out in air.

The density of $Li_2B_4O_7$ was 1.951g/cm^3 at 917°C and its thermal expansion coefficient was 2.18E-04. The density of LiB_3O_5 was 1.967g/cm^3 at 880°C and its thermal expansion coefficient was 1.95E-04. The surface tension of the molten Li_2O-B_2O_3 system was shown in fig. 1. The surface tension decreased when the ratio of B_2O_3/Li_2O was increased. At the composition of Li_2O:B_2O_3=1 4, the surface tension was almost independent of the temperature. So Marangoni effect does not have be to considered at this composition. Fig. 2 shows the viscosities of molten $Li_2B_4O_7$ and LiB_3O_5. The viscosity of molten $Li_2B_4O_7$ at its melting point was 280mPa•s and this value was about a half as large as the viscosity of LiB_3O_5. In supercooling region the viscosity showed rapid increase.

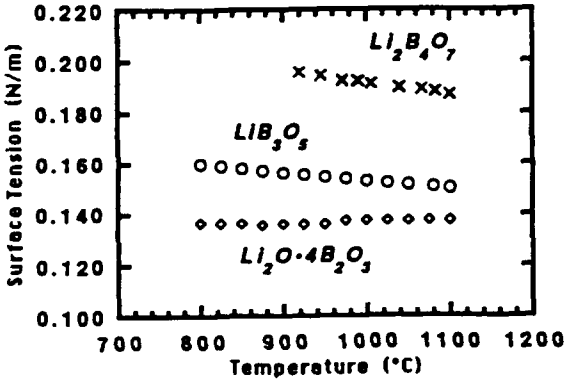

Figure 1. Temperature dependence of surface tension of molten Li_2O-B_2O_3.

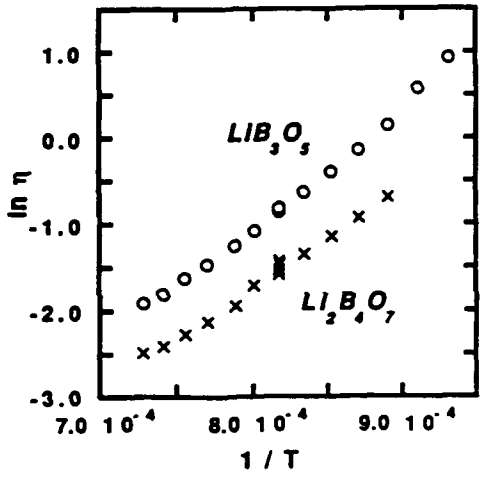

Figure 2. Viscosity of molten $Li_2B_4O_7$ and LiB_3O_5.

B105

MORPHOLOGY OF ROSE QUARTZ BASE SURFACE

I.F. Maxhina, A.A. Mar'in and V.E. Meadei

Vkiisims, Alexandrov, Russia

Morphology of rose coloured synthetic quartz crystals obtained in P doped fluoride solutions has been studied.

It is known /1/ that the base surface of quartz crystals grown in fluoride media shows vivid signs of regeneration. It is all covered with faceted heads of trigonal dipyramides. Even doping the system with various impurities does not remove the regeneration relief from this surface.

Only P-dopant has been found to be a factor defining in a way growth mechanism of this surface. Under effect of this dopant the relief structure changes from the usual pattern to a "cobblestone" one known for the material grown in alkali solutions. The change may be complete or just partial, so the surface relief becomes function of dopant concentration and of temperature in the system.

The change reveals itself first with pinacoid faces appearing on the above mentioned pyramides, whose height becomes smaller accordingly. Then the pinacoid surface grows more round, the side facets diminishing to disappear altogether finally. Now the surface has a characteristic "cobblestone" pattern. Sometimes a hillock has an active summit and we observe a surface with comic growth accessories. It should be noted though that normally there are elements of many stages of relief formation on the changing surface that remains morphologically unstable for some period.

The cobblestone relief is associated with some decrease in the growth rate of the crystal.

GROWTH AND CHARACTERIZATION OF $Li_2B_4O_7$ SINGLE CRYSTALS GROWN BY NOVEL BRIDGMAN TECHNIQUES USING GRAPHITE CONTAINER

B106

T. Katsumata, H. Konoura, A. Konno. K. Takei*, M. Shinohara*, K. Kano** and K. Takahashi***
Toyo Univ.; 2100 Kujirai Nakanodai, Kawagoe 350 Japan
*Tomiyama Pure Chemical; 3-11-1 Mizutanihigashi, Fujimi 354 Japan
**Ohkura Electric Co., Ltd.; 2-9-20 Shirako, Wakoshi 351-01 Japan

In order to grow high quality $Li_2B_4O_7$ (LB) single crystals for the applications of surface acoustic wave devices, it is essentially important to reduce the void defect in crystals. In this paper, we report the growth of high quality LBO single crystals by newly developed vertical and horizontal Bridgman techniques using graphite containers under inert gas atmosphere. The origin and the formation mechanism of voids in the LBO are discussed based on the characterization of crystals grown under various growth conditions of moisture content of raw materials, growth atmosphere, growth rate and temperature gradient.

The graphite is found to be non-wet with LBO melt and a suitable container for Bridgman growth. Crystals were grown using 25 mm wide and 140 mm long, and 75 mm diameter and 200 mm long graphite containers. Void-free crystals have been grown with growth rate of less than 1 mm/hr. Moisture contents of crystals and quenched melt evaluated by a near infrared absorption were about 50 ppm and 200 ppm, respectively. Moisture contents of crystals increased from 40 to 50 ppm with fractional solidification. The void density varied associating with the moisture contents of crystals. Void is suggested to be formed around the solid/liquid interface saturated with water by the segregation of water and large difference in solubility of water between melt and crystal.

CRYSTAL GROWTH AND CHARACTERIZATION OF LBO ($Li_2B_4O_7$) CRYSTAL BY BRIDGMAN METHOD

B107

Mitsuru Ishii, Sinji Makikawa, Toshihiko Ryuoh* and Isao Yamaga***
Shounan Institute of Technology, Fujisawa, 251 Japan
*Shin-Etsu Chemical Co., Ltd., Isobe Annaka, 379-01 Japan
**Futeck Furnace Co. Ltd., Fukuura Kanazawa, Yokohama, 236 Japan

As LBO crystal are zero in temperature coefficient of SAW and comparatively large in electro-mechanical coupling constant, much hope is placed in the fields of SAW devices as a new piezoelectric crystal. Studies on crystal growth of LBO have been made mostly by Cz technique. Recently, large crystal of 3 inches were grown by the Bridgman process by Shi-ji et al. (*J. Cryst. Growth*, 99(1987)37.) Authors made studies on the relations between growth condition and crystal defects by the Bridgman process for LBO.

A vertical type Bridgman furnace with an inner diameter of 90 mm was used for crystal growth of LBO. A boule with 55 mm in dia. and 90 mm in length was grown in 0.2 - 0.5 mm/h. There are 2 kind defects of LBO crystal i.e. void and crack. The voids is produced in the center of boule in growth process to body from corn of boule. It is eliminated at a steady state growth where crystal are grown in the latter half of the body part. The crack is generated in the solidifying part of crystal finally. Dividing the body of grown crystal into 4 equal part, wafers were sampling and measurement on dislocation and lattice parameter by X-rays. A phenomenon of dislocation of developed frequently near voids. About $10^2/cm^2$ of dislocation density was found in the void free body.

The lattice parameter was less than ±0.0002Å* in each and inside of wafer. Measurement was made on absorption of LBO by FTIR. There is a large absorption by -OH in 3600 cm^{-1} in LBO glass prepared by rapid cooling as well as LBO crystal. -OH was decreased to 240 ppm in raw material of LBO and to 30 ppm in crystal. This fact suggests that -OH contained in the raw material of LBO is exhausted at the time of crystallization, resulting in causing voids.

B108

SOLVENTS FOR THE GROWTH OF $BaFe_{12-(x+y)}Co_xSn_yO_{19}$ BULK CRYSTALS FROM HTS

X. Ruiz, V. Nikolov, F. Sandiumenge**, R. Solé, R. Cabré, M. Aguiló and F. Diaz*
Laboratory of Applied Physics and Crystallography, University of Barcelona at Tarragona
*Institute of General and Inorganic Chemistry, Bulgarian Academy of Sciences, Bulgaria
**Institute of Materials Science, CSIC, Bellaterra, Barcelona

The high values of the saturation magnetization and anisotropy ensure a wide application of the different hexaferrites including $BaFe_{12-(x+y)}Co_xSn_yO_{19}$[1,2]. In order to conform the magnetic characteristics of this material to the requirements the x and y must be change in wide regions. The use of suitable solutions is an important condition for successful growth of such multicomponent material. Solvents based on B_2O_3 or Na_2O has usual been performed for HTS growth of barium hexaferrites pure and substituted. From the first type of solutions the hexaferrites crystallizes at moderate temperatures, but high viscosity and relatively low concentration are essential disadvantages[3]. In the case of Na_2O based solutions the crystallization is in the conditions of very high temperature and high volatility is observed[4,5]. The last disadvantages is observed in the some of Na_2O-B_2O_3 systems too[6].

Now we report the results of the investigation of some new solvents. The main characteristics investigated were in the concentration and temperature regions of crystallization of the hexaferrite phase, the temperature dependence of the solubility, the distribution coefficients of the substituting ions, the viscosity, density, volume expansion and surface tension, as the volatility of that solutions.

Comparing all of the above properties the suitable solution of $BaFe_{12-(x+y)}Co_xSn_yO_{19}$ is offered.

1. M. Pernet, X. Obradors, M. Vallet, T. Hernández and P. Germi, *IEEE Trans. Magnetics* MAG-24, 1898 (1988).
2. C. Fucheng, F. Xiaofeng, L. Jun and Y. Liu, *J. Appl. Phys*, 61, 3881 (1987).
3. P. Röschman, M. Lemke, W. Tolksdorf and F. Welz. *Mat. Res. Bull*, 19, 385 (1984).
4. F. Licci, T. Besagni and Y. Lábáz, *Mat. Res. Bull.* 22, 467 (1987).
5. I. Lassau, I. Memessy, F. Winter and D. Becheresсy. *Mater. Constr.* 16, 191, (1986).
6. R. Varadinov, V. Nikolov, P. Peshev, I. Mitov, Kr. Neykov. *J.Cryst. Growth*, 110, 763 (1991).

B109

THE GROWTH MECHANISM OF THE NEW MODIFIED METHOD FOR $Mn_1.\delta\ Zn_\delta\ Fe_2O_4$ SINGLE CRYSTAL

J. W. Chung, J. Y. Uhm and K. K. Orr
Hanyang University, College of Engineering
Department of Inorganic Materials Engineering, Seoul 133-791, Korea

Mn-Zn ferrite has the characteristics of incongruent melting and the zinc oxide evaporation while the crystal is being grown. As a result of these, it comes into existence to be a non-uniform distribution of cations along the crystal growth axis and also Pt particles are usually precipitated into the crystals in Bridgman method. These have bad effects on the magnetic properties of ferrites. But. to overcome these faults and then acquire the better single crystals, new modified growth method was developed. In this method there are such important growth factors as follows melt height in the crucible, surface tension of melt, the behavior of melt at interface, the shapes of crucible and solid-liquid interface, powder feeding rate, and the crystal growing speed. These have intimate relationships with each other when the Mn-Zn ferrite single crystal is grown. Using these factors, we established the growth mechanism of the new modified method. In addition, when we analyzed the compositional fluctuations of crystals, they were suppressed within 1.5 mol% Fe_2O_3, 2 mol% MnO, ZnO respectively with comparing to initial composition of crystal and the etch pits of the crystals on the (110) plane were observed by optical microscope through the chemical etching technique, and the dislocation density was $1.3x10^4 \sim 1.6x10^3\ cm^{-2}$.

FAST SOLID STATE GROWTH OF LARGE HEXAFERRITE CRYSTALS

B110

P. David and C. Maillault
Commissariat à l'Energie Atomique,
Centre D'Etudes de Bruyères-le-Châtel BP 12, 91680 Bruyères-Le-Châtel, France

Hexagonal ferrites with M-structure $BaFe_{12}O_{19}$ are characterized by high values of the saturation magnetization and by large anisotropy fields. This characteristics make them useful in electronic devices such as Faraday rotation isolators, phase shifters, circulators and absorbers.

Hexaferrite compounds have a non congruent melting and therefore these crystals cannot be grown from stoichiometric melts. They can be synthethised by flux technique but generally only small crystals are obtained and solvent inclusions remain.

We have developed a solid state growing technique based on the control of discontinuous or exaggerated grain growth. A seed is welded to a polycrystalline rod and is moved in a furnace. High temperature gradients allow the growth of the seed at the expense of the polycrystals. Rectangular crystals (10 cm x 1 cm x 3 mm) have been obtained with high growth rates (v = 1 cm/h) and with good reproducibility but there is a 5% residual porosity. The influence of different parameters and effects of substitution will be presented.

FLUX GROWTH OF SINGLE CRYSTALS OF $(Nd_{1-x-y}Ce_xSr_y)_2CuO_{4-z}$ CONTAINING VARYING AMOUNTS OF Sr

B111

A.J.S. Chowdhury, B. Wanklyn and F.R. Wondre
National Crystal Growth Facility for Superconducting Oxides
Clarendon Laboratory, Department of Physics
University of Oxford, Oxford OX1 3PU, UK

Single crystals of $(Nd_{1-x-y}Ce_xSr_y)_2CuO_{4-z}$ have been grown by using CuO as flux. Varying amounts of strontium was used to make a comparative study of the series of crystals grown by this method. Electron microscopic studies and X-ray diffraction measurements were used to identify some of the interesting features of these crystals. The calculated lattice parameters were found to be a 3.9514 A°, c=12.0573 A° when (x+y=0.075) and a 3.9505 A°, c=12.0678 A° when (x+y=0.09). Some strontium-rich phases were also identified which were ruby red in colour and were intimately mixed up with the small Nd_2CuO_4 type crystals. Microanalysis identified them as $(Sr,Nd)_{0.6}CuO_x$ type crystal. Dissolution of some of the crystals were observed during hot stage microscopy and due care was taken during the crystal growth to minimise these effects on the size of the crystals.

CRYSTAL GROWTH AND PHOTOELECTRICAL STUDY OF COPPER TUNGSTATE

B112

S.K. Arora and Thomas Mathew
Department of Physics, Sardar Patel University
Vallabh Vidyanagar 388120, Gujarat, INDIA

Copper tungstate single crystals have been grown by flux reaction technique, employing double decomposition reaction in the fluxed melt. Their electrical and optical characteristics have been measured. Interestingly, electrochemical characterization of the grown crystals, as accomplished from the nature and the values of the parameters N_D, E_C, E_F and E_V which are determined by Mott-Schottky plots, reveals the material to be an n-type semiconductor and has been effectively used as photoanode in the fabrication of a photoelectrical solar cell. The value of flat-band potential has been found to be sufficiently negative and consequently, the photoelectrochemical solar cell using $CuWO_4$ does not require cell bias for operation. Thus a concentration cell, entailing self-bias, has been constructed which gives better performance and efficiency than other photoelectrolysed cells.

B113

STUDIES ON THE MORPHOLOGY OF INCLUSIONS IN FLUX-GROWN RUBY

Xiaoyang Wang, Lintang Fu, Weiguo Liu and Mingliang Qin
Research Institute of Synthetic Crystals
P.O. Box 733, Beijing 100018, P.R. China

Characteristics of inclusions in ruby form an important basis in identification of gems. In this paper, ruby crystals were grown by flux method, and their microstructures were studied by means of microscopy. The results show that flux-grown rubies contain typical inclusions in form of fingerprints, dendrites and planes, some of which are similar to those in natural ruby. The size and morphology of inclusions not only relate to growth conditions, but also to type of flux. The formation mechanism of some representative inclusions in the crystals were also discussed.

B114

MICROMORPHOLOGICAL STUDIES ON SOME FLUX GROWN $RCrO_3$ (R=Y, La, Gd, Yb) SINGLE CRYSTALS BY OPTICAL AND SCANNING ELECTRON MICROSCOPY

Ashok K. Razdan, E.M. Wanklyn** and P.N. Kotru**
Department of Physics, University of Jammu, Jammu Tawi 130 001 India
Department of Physics, Clarendon Laboratory, University of Oxford, Oxford OX1 3PU England

Optical and scanning electron microscopic studies have been carried out on a few micromorphologies exhibited by {001} and {110} faces of $RCrO_3$ (R+Y, La, Gc, Yb) single crystals, and the results thereof are presented. These crystals, however, have been grown from a PbO-PbF_2 flux [1]; the study of surfaces of such crystals yields useful information concerning the growth mechanism and the defects. A variety of hillocks and pyramids on different planes of $RCrO_3$ crystals is illustrated. The presence of hillocks suggests their independent growth at the points of emergence of dislocations. However, some growth microstructures are considered to be indications of independent growth taking place on the crystal habits, at least in the later stage of growth, and the process, it may be treated, is mainly due to two-dimensional nucleation and piling up of growth layers. Some observations also suggest that the independent growth at some peculiar sites may occur due to recrystallization of droplets of solute components in the high-temperature solution. And this mode of growth is visualized through the growth hills comprising circular lamellas on the $YbCrO_3$ surfaces. The explanation is based on the mechanisms of closed-loop formations suggested by Krohn and Bethge [2]. Etch patters of varied morphologies are also noticed on as-grown $RCrO_3$ surfaces. The rows of etch pits and etch channels are respectively attributed to the presence of low-angle grain boundaries and enhanced dissolution of impurities along linearly arrayed faults. Also some hillocks exhibiting pits at the centres of initiation are revealed, and is considered the preferential etching at the sites of dislocations. It is suggested that $RcrO_3$ crystals might have got etched by the flux composition in the growth system itself as and when the conditions for their growth become unfavourable.

[1] B.M. Wanklyn, *J. Cryst. Growth* 5 (1969) 323.
[2] N. Krohn and H. Bethge, *Crystal Growth & Materials* (1977) Eds. E. Kaldis & H.J. Scheel, North Holland Pub. pp. 142-165.

B115

MOLECULAR DYNAMICS STUDY ON THE STRUCTURE OF BaB_2O_4 LIQUID JUST AFTER MELTING

Hiroshi Ogawa[1] *and Yoshio Waseda*[2]
[1]Kimura Metamelt Project, ERATO, JRDC (Res. Dev. Corp. Japan),
2-1-1, Yagiyama-minami, Taihaku-ku, Sendai, 982, Japan
[2]Institute for Advanced Materials Processing (AMP), Tohoku University,
2-1-1, Katahira, Sendai, 980, Japan

The beta-Ba_2O_4 (BBO) is a well-known nonlinear optical crystal which is useful in the ultraviolet region. Kouta *et al.*[1] found that a single crystal of beta (low temperature) phase can be grown by the direct Czochralski method by using the starting material in the beta phase unless the melt is heated up to 1200°C. This fact is suggestive of differences in the liquid structures and some further investigation is desired.

The purpose of this paper is to present the structural features of BBO liquids obtained by the molecular dynamic simulation. We determined the interatomic potentials for BaB_2O_4 in the Born-Mayer-Huggins form by modifying the parameters for Na_2O-B_2O_3 system.[2] The simulation was carried out on 4036 atoms at P=10^5Pa and T=27 ~ 1227°C. The densities and structures of the crystals in both alpha and beta phases were properly reproduced by the simulation. The structure in the liquid phase was also in good agreement with the result of X-ray diffraction experiment.

Some structural relaxation phenomena were observed in the simulated BBO liquid after melting. For example, the structure factors on the ab-plane maintain their crystal-like features for more than 20ps after melting from the beta phase crystal. In the figure is shown the time variation of the number of rings in the simulated BBO liquid. The numbers of long rings are increasing even 40ps after melting, and hence the representative size of the structural unit in the liquid is expected to increase as the time passes after melting. This result is consistent with the experimental data on the time variation of shear viscosity after melting[3].

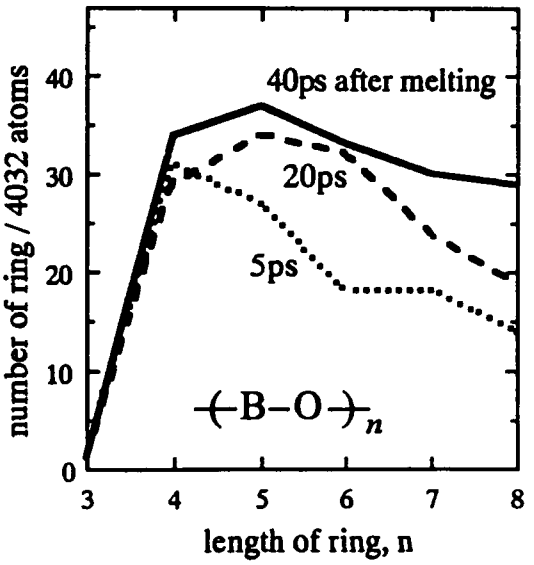

Time variation of the number of rings in BaB_2O_4 liquid.

[1] Kouta *et al.*, *J. Cryst. Growth*, **114** (1991) 676.
[2] Xu *et al.*, *J. Non-Cryst. Solids*, **104** (1987) 261.
[3] Imoto *et al.*, to be submitted to *J. Cryst. Growth*.

B116

PREPARATION OF β-BaB_2O_4 USING A ZONE MELTING TECHNIQUE

*T. Katsumata, H. Ishijima, H. Sugano and K. Takahashi**
Dept. Appl. Chem., Toyo Univ.; 2100 Kujirai, Kawagoe 350, Japan
*Ohkura Electric Co., Ltd.; 2-9-20 Shirako, Wakoshi 351-01, Japan

High quality and large β-BaB_2O_4 (BBO) crystals are required for the non-linear optical applications. In this paper, β-BBO has been successfully synthesized by a zone melting technique using a non-wetting graphite boat under an Ar atmosphere. Composition and zone refining of raw material are found to effect greatly the formation of β-phase, α- and β-phases tend to be formed from the non-stoichiometric and the stoichiometric melt, respectively. The most dramatic result is obtained by using zone refined raw material. In this case, β-phase is found to be formed dominantly all over the ingot.

In order to examine the effects of the melt composition and the zone refining of raw material on the β-phase formation, ingots with various compositions and zone refined ingots were used. Formations of α- and β-phases are detected by (10$\underline{1}$0) and (113) reflections in X-ray powder diffraction patterns.

Solidified ingots in the graphite boat are opaque polycrystals and are partly covered with carbon. In using non-stoichiometric raw materials, Ba/B=0.15 and 0.55, almost all of the ingots are α-phase. While, using stoichiometric raw material, Ba/B=0.5, β-phase, appears at the top part of the ingot. α-phase then, becomes dominant at the tail part of the ingot. In the zone melting using a zone refined raw material, β-phase is demonstrated to be formed over the whole ingot, independent of the composition of the starting mixture. The composition of the raw material is considered to become stoichiometric by zone refining. The results on a rapid cooling and a normal freezing will be also reported in detail.

B117

CRYSTALLIZATION OF SUPERCOOLED BaB_2O_4 MELT

Noriyuki Yoshimoto, Atsushi Yokotani and Shigeyuki Kimura
Kimura Metamelt Project, ERATO, JRDC
5-9-9 Tokodai, Tsukuba 300-26, Japan

BaB_2O_4 crystal has two structural modifications; alpha, a high temperature phase, and beta, a low temperature phase. Only the beta-form has properties for use in application to generate an ultra violet light by a higher harmonic generation. Recently, the successful crystal growth of beta-form by the Czochralski technique from melt was reported(1). However, the mechanism of appearance of low temperature phase directly from the melt has not been specified. To clarify the mechanism, we investigated crystallization of supercooled BaB_2O_4 melt by considering a role of melt structure.

We identified which phase crystallized from the melt as in terms of crystallization temperature, cooling rate and preheating temperature of the melt, by means of X-ray diffraction and DSC techniques.

The effects of crystallization temperature to the appearance of phases were examined by dropping tiny seed crystals into the supercooled melt which was kept at different temperatures below the melting point, 1100°C. Both the starting material and the seed crystals were beta-form. The crystallization temperatures were set at 950°C, 1000°C, 1050°C and 1080°C. After completion of crystallization, the sample was quenched to room temperature. A powder X-ray diffraction method was used to identify the phase of crystals. The result was summarized in Figure 1. The alpha-form crystallized at higher temperatures than 1050°C, but below this temperature the beta-form crystallized. Since the transition temperature of the two forms is 920°C, it is clear that metastable phase crystallized preferentially in the temperature range between 920°C and 1050°C. This means that the readiness of crystallization of the two phases are equivalent at 1050°C. The cause for this balance seat may be understood as the consequence of the difference in free energy between two solid phases falling to the value which corresponds to the difference in surface energy term for crystallization.

To clarify the effects of melt structure on the crystallization, crystallization temperature was measured as a function of preheating temperature of the melt in a furnace of DSC (Figure 2). As a result, only the beta-form was crystallized at around 840°C at any condition. It was found that the preheating effect to the nucleation of BaB_2O_4 was not appreciable in this system.

1) K. Itoh, F. Maruno and Y. Kuwano, *J. Crystal Growth* 106 (1990) 728.

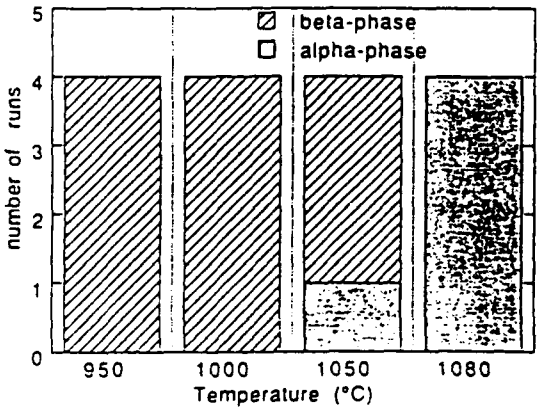

Figure 1. Dependence of phase appearance of BaB_2O_4 crystal on crystallization temperature

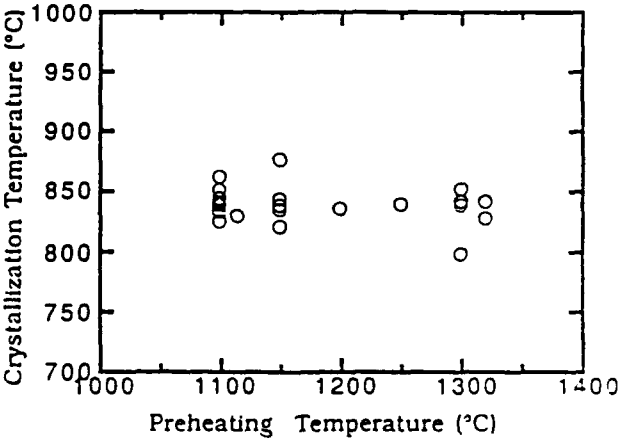

Figure 2. Preheating temperature effect on crystallization temperature of BaB_2O_4

IMPURITY STRIATION AND ITS EVOLUTION IN THE PROCESS OF GROWTH AND ANNEALING OF CORUNDUM SINGLE CRYSTALS

B118

E.R. Dobrovinskaya, V.V. Pishchik and L.A. Litvinov
Institute for Single Crystals Acad. Scie. of the Ukraine, Kharkov

The nature of previously revealed new type defects called as ultramicrostriation did not find a satisfactory explanation. The purposefully carried out experiments on modelling the processes of the advent of the impurity nonuniformity which resided in a local melting-through the crystals with a known distribution of impurity and structural defects showed that a necessary condition for the origin of ultramicrostriation is the presence of specific distribution of point defects in a crystal.

In the process of model experiments crystal zones with different types of ultramicrostriation were obtained. Thus, the width of striae varied in the range of 0.01 - 0.03 μm, the interval between them - from 0.05 to 0.25 μm depending on thermodynamic parameters of the process of local melting-through and type of the impurity. In the same experiments also parameters of microstriation could be varied in rather wide limits (stria width $5x10^{-3}$ - $3x10^{-2}$ mm, interval between them - $1x10^{-2}$ - $1x10^{-1}$ mm).

In the process of high temperature annealing the evolution of both ultra-and microstriation was observed. The width of the impurity striae is broadened with the diffusion coefficient which allowed to develop a principally new method for the determination of the diffusion constants, the method being based on this effect. Unlike conventional methods, expensive and tedious, in this method a sample with a preliminarily measured impurity nonuniformity is placed in a gradient heating zone of the furnace so that one of the ends of the studied sample may be melted. After cooling a repeat measurement of the diffusing impurity distribution along the rest of the sample is made. Melting one of the ends of the sample in the gradient heating zone allows to obtain a precise temperature fixing of the sample's coordinates, to the varying in the annealing process profile of the impurity nonuniformity, i.e. gives the possibility to get in one experiment a series of the distribution curves at various temperatures and to find the dependence D(T). Using this dependence the diffusion constants are determined: preexponential factor (Do) and activation energy of the process (Q). Thus, for example, the diffusion constants for chromium diffusion into corundum single crystals, measured by the suggested method are $Do=4.1x10^{-4}$ $cm^{-2}c^{-1}$; Q-3.5 eV.

EVOLUTION OF DISLOCATION AND GRAIN BOUNDARY STRUCTURE AT GROWTH AND THERMAL-MECHANICAL LOADING OF CORUNDUM SINGLE CRYSTALS

B119

E.R. Dobrovinskaya, V.V. Pishchik and L.A. Litvinov
Institute for Single Crystals Acad. Scie. of the Ukraine, Kharkov

In the growth process of corundum single crystals from melt by either method a nonuniform distribution of structural defects both over the cross-section and length takes place. This results in the variation of physical characteristics of single crystalline articles. Investigation of reasons for the formation and evolution of defects under real conditions of the high temperature oxides growth is a very tedious problem. Therefore, in the present paper such investigation was carried out by modelling the real processes. The idea of the method involves a local melting-through of an already grown crystal using one or several molybdenum or tungsten wires. In the course of the experiment the temperature of the main heater and that of the wire as well as the rate of their mutual displacement varied which allowed to control the thermodynamic conditions of melting-through and crystallization, hydrodynamics of melt fluxes etc. As the model experiments showed the non-uniformity of the structural defects distribution is due to local temperature perturbations of the thermal field. Such local violation of the growth thermal conditions results in the change of the character of the point defects distribution which in its turn defines the possibility of elastic flow in these zones at the relaxation of thermoelastic stresses. If the distribution of point defects is such that they do not impede the elastic deformation (the parameter of point defects' quasilattice does not exceed 400 Å the density of single dislocations in this zone exceeds the critical one and the formation of low-angle dislocation boundaries takes place. But if the quasilattice parameter is about 500-700 Å the elastic deformation in these zones is impeded and the dislocation density is not higher than $1x10^{4}$ cm^{-2}. In the finite case of enormously high parameters of the point defects quasilattice there can be formed zones with few dislocations or free of them. The relaxation of thermoelastic stresses in such zones may result in crack formation.

At thermal and mechanical loading not only formation of low angle dislocation boundaries takes place but also a rotation of block boundaries towards load application. A local melting-through and mechanical loading may lead to the turn of block boundaries by 90°.

The regularities, observed during model experiments, were utilized for the control of structural quality when growing real crystals, specifically corundum with a preset distribution of structural defects.

B120

GROWTH AND PROPERTIES OF NEEDLE-SHAPED CRYSTALS OF BORATE ALUMINUM

E.G. Yarotskaya, V.P. Golenko, M.E. Andreev, E.V. Polyanski, V.A. Vanyshev and V.G. Yarotski
All-Union Research Institute for the Synthesis of Minerals
Alexandrov, USSR

Borate aluminum Al_3BO_9 of the rhombic structure is new perspective crystalline material.

This has shown the highly effective absorbent of the neutron emanation (it contains about 14 mass % B_2O_3), the absorbent is raises double if to add 0.8 mass % B_2O_3 [1].

Prismatic colourless, transparent single crystals of the borate aluminum up to 30 mm in length have been grown from high-temperature solution (the system Y_2O_3-Al_2O_3-B_2O_3-R_2O-MoO_3) [2].

The paper present the result of the growth of the borate aluminum from Al_2O_3-H_3BO_3, SiO_2-B_2O_3-AlF_3, Al_2O_3-B_2O_3-AlF_3 systems in the solid state with participation of the vapour phase.

The synthesis was realized from starting powder materials in the temperature range of 1100-1300°C with using of alundum crusibles.

In systems Al_2O_3-H_3BO_3, SiO_2-B_2O_3-AlF_3, Al_2O_3-H_3BO_3-AlF_3 were obtained prismatic crystals (length about 20 μm, thickness about 5 μm). Needle-shaped crystals of the borate aluminum up to 60 μm in length and 3 to 5 μm in thickness were obtained in system Al_2O_3-H_3BO_3-AlF_3. X-ray powder pattern data for Al_3BO_9 were found to be a=5.6673; b=15.011; c=7.693 Å, z=4.

The bulk density is 0.25-0.30 g/cm^3; the overall specific surface is 20-25 m^2/g; the melting point is 1935°C.

Light weight refractory of the borate aluminum consisting from needle-shaped crystals are obtained by sintering of starting components in the system Al_2O_3-B_2O_3-AlF_3 in the temperature range of 1100-1300°C for 2-20 hrs. The properties of resulting ceramics were found to be up to 30 μm in length and 1 to 3 μm in thickness; the bulk density is 0.8-0.85 g/cm^3, the open porosity is 52-61%; the breaking point is 18-20 MPa, thermal conductivity is 0.42-0.47 W/(m*K).

[1] B.P. Tarasevich a.o., *Glass and Ceramics*, N 5, 17 (1990).
[2] E.V. Sokolova a.o., *Doklady Akademii Nauk* SSSR, 243, N3, 655 (1978).

B121

SCINTILLATOR CRYSTALS ZnSe(Te) - A NOVEL MATERIAL FOR DETECTORS OF IONIZING RADIATION

L.P. Gal'chinetskii, E.K. Lisetskaya, V.D. Ryzhikov and V.I. Silin
Institute for Single Crystals of Acad. Sci. of Ukraine, Kharkov

Thermodynamic, thermal and physico-chemical conditions of growth from the melt using the Bridgman method were studied for the ZnSe single crystals doped with Te up to concentrations of 10^{20} cm^{-3}. The crystals grow (up to 40 mm diameter) are characterized with high intensity of radioluminescence (RL) at the wavelength of emission 640 nm at T=300 K, absence of light storage (afterglow level after 3 ms less than 0.05 %, comparatively high transparency in the region of emission (not worse than 0.1 cm^{-1}). The method of growing and subsequent thermal processing of the crystals which has been worked out allowed to achieve high reproducibility level of the above-mentioned parameters, ensuring thermal (no changes up to 400 K) and radiational (no degradation under γ-radiation doses up to 10^7 rad) stability. RL mechanism of ZnSe(Te) crystals was studied.

Basing on the ZnSe(Te) crystals, fast ionizing radiation detectors of the "scintillator-silicon photodiode" type were produced, ensuring registration of X-ray and gamma-radiation in the energy range from 10 keV to 10 MeV with dose power from 10^{-5} to 10^4 R/hour.

ISOVALENT DOPING AND RADIATION STABILITY OF $A^{II}B^{VI}$ SCINTILLATION CRYSTALS

B122

L.P. Galchinetskii, Yu.N. Dmitriev and V.D. Ryzhikov
Institute for Single Crystals of Acad. Sci. of Ukraine, Kharkov

Irradiation experiments by Co^{60} γ-radiation on ZnSe(Te)-type scintillation crystals show that radioluminescence intensity of the crystals remains practically unchanged up to the absorbed dose of ~10^7 rad; at $1.6 \cdot 10^8$ rad the change does not exceed 20%. Optical transmission spectra were practically unchanged after irradiation by the dose of 10^5 rad. These data together with the absence of change in the luminating kinetics of the intensive radiation after having been submitted to the dose of $2 \cdot 10^4$ rad provide an evidence of the radiation defects instability, i.e. of the sufficiently high radiation stability (RS) of the ZnSe(Te) crystals.

Increased RS of the $A^{II}B^{VI}$-based scintillators can be explained in terms of the model, which requires as the necessary and sufficient condition for high RS of the nonmetallic crystals that the free path of the dynamic crowdion should be less than the instability zone radius in any of the crystallographic directions. Crystals where focusing is suppressed only in some crystallographic directions, as well as crystals where atomic lenses are not destroyed, but distorted are characterized by lower RS, which is higher, however, than that of the ideal crystals. To this type of crystals belong $A^{II}B^{VI}$ semiconductors with isovalent dopants. Similar effect can be caused by lattice vacancies; when ZnSe is doped by the isovalent Te, concentration of vacancies in the cationic sublattice c^{v}_{Zn} is proportional to the concentration of the isovalent dopant c^{Te}_{Se}:

$$c^{v}_{Zn} \equiv (1 - e_{ZnTe} \cdot e^{-1}_{ZnSe}) C^{Te}_{Se}$$

where e_{ZnTe}, e_{ZnSe} are the effective charges of the Zn-Te and Zn-Se bonds, respectively.

With the commonly used $c^{Te}_{Se} = 1 \cdot 10^{-2} c^{V}_{Zn} = 10^{-5}$ which is several orders higher than the equilibrium concentration of the intrinsic defects in ZnSe.

CHARACTERISTIC FEATURES OF THE $ZnSe_{1-x}Te_x$ SOLID PHASE SYNTHESIS

B123

S.N. Galkin, L.P. Gal'chinetskii, K.A. Katrunov, E.K. Lisetskaya and V.D. Ryzhikov
Institute for Single Crystals of Acad. Sci. of Ukraine, Kharkov

Properties of the melt-grown $ZnSe_{1-x}Te_x$ scintillator crystals are affected by the regime of synthesis of the charge material.

In the present work thermodynamic analysis of interaction of the components has been carried out, and kinetics of the $ZnSe_{1-x}Te_x$ solid solution (SS) formation studied in the system ZnSe-ZnTe-Se-H_2 in the temperature range of 800-1300 K.

SS formation proceeds rather intensively, starting from 1000 K. Formation rate and actual SS composition depend mainly on the proceeding of the reactions

$$ZnTe_{sol.} + Se_{liq.} \leftrightarrows ZnSe_{sol.} + Te_{liq.}$$
$$ZnTe_{sol.} + 0.5\ Se_{2\,gas} \leftrightarrows ZnSe_{sol.} + 0.5\ Te_{2\,gas}$$
$$ZnTe_{sol.} + H_2Se \leftrightarrows ZnSe_{sol.} + H_2Te$$
$$ZnO_{sol.} + H_2Se \leftrightarrows ZnSe_{sol.} + H_2O.$$

Influence of the components ratio has been studied in the solid system upon radioluminescence spectra and optical absorption of the crystals grown from the charge prepared.

It is shown that under sintering in the inert medium porous layer of the ZnO film on the surface of ZnSe and ZnTe particles does not hinder the SS formation. ZnO appears to be blocked inside the SS matrix, being partially dissolved therein.

B124

IN SITU UHV REM OBSERVATIONS OF EPITAXIAL GROWTH ON THE SEMICONDUCTOR SURFACES

A.V. Latyshev, A.B. Krasilnikov and A.L. Aseev
Institute of Semiconductor Physics, Russian Academy of Sciences
Siberian Branch, 630090 Novosibirsk, Russia

The use of in situ technique to study epitaxial growth with high spatial resolution has received increasing emphasis in recent years. The present report devoted to the some application of ultra high vacuum reflection electron microscopy (UHV REM) to study of structural transformations on stepped Si(100) and Si(111) during initial stages of MBE growth.

The influence of direct electric current heating the crystal on the behavior of monoatomic steps during sublimation and epitaxy on Si(111) and Si(100) is observed and the conditions of step bunching and debunching are found. The monoatomic step behavior is discussed in terms of diffusion and drift of charged adatoms and their interaction with steps.

The redistribution of about (4-6)x10^{14}cm^{-2} atoms on the clean silicon (111) surface during the reversible (7x7) ⇔(1x1) transition has been revealed by the shift of monoatomic steps and the change in size of two-dimensional sublimation and growth islands.

The dependence of surface step morphology on the surface (7x7), (5x5), (5x1), (3x1) and (2x1) reconstructions during Si, Ge, Au and CaF_2 epitaxy on Si(111) and Si(100) is shown. During surface reconstructions the reversible monoatomic steps clustering due to displacement of segments of monoatomic steps bounded the superstructural domains is observed. The dependence of this process on the initial monoatomic steps density, substrate temperature and rate of superstructural transitions is found. The mechanism of step clustering, including the mass transfer across the reconstructed areas of the surface is proposed. The morphological changes of the surface corresponding to one period of intensity oscillation of diffracted electron beams during epitaxial growth are visualized.

B125

GROWTH AND PROPERTIES OF CERIUM AND PRASEODYMIUM DOPED GADOLINIUM ORTHOSILICATE SINGLE CRYSTALS

V.A. Voloshin, M.B. Kosmyna and B.I. Minkov
Institute for Single Crystals of Acad. Sci. of Ukraine, Kharkov
M.V. Korzhik, V.I. Moroz and A.A. Fedorov
Institute for Nuclear Problems of the Byelorussian State University, Minsk.

Gd_2SiO_5 single crystals doped with Ce^{3+} and Pr^{3+} ions have been obtained. The impurities were introduced both ways separately and together in a wide concentration range. Such crystals were grown from melt onto the oriented seed by the Czochralski method in protective and protective oxidizing gaseous media using iridium crucibles.

The effect of concentration and activator distribution over nonequivalent cation positions on the scintillation properties of crystals has been studied.

Ce^{3+} ion concentration in gadolinium orthosilcate single crystals has been optimized and energy exchange processes between Ce^{3+} and Pr^{3+} ions has been investigated.

The main problem in the crystal growth is their lamination along the cleavage plane (100). Some factors affecting mechanical properties of crystals have been studied.

The main characteristics of the grown crystals are shown in the Table comparatively to the known scintillation crystals.

Material	Density, g/cm^3	Effective atomic number, Z_{ef}	Refractive index	Scintillation efficiency, %	Scintillation time, ns
NaI (Tl)	3.67	50	1.85	100	230
BGO	7.13	74	2.15	10-12	300
GSO:Ce	6.77	59	1.9	21	35-60

SESSION 4C

CS3

ESTIMATION OF THE OPTIMAL CONDITIONS FOR THE CRYSTAL GROWTH FROM THE VAPOUR PHASE WITH NO CONTACT BETWEEN CRYSTAL AND AMPOULE WALL

Krzysztof Grasza
Institute of Physics, Polish Academy of Sciences
Al.Lotników 32/46, PL 02-668 Warsaw, Poland

Crystals grown by method of directional crystal growth with no contact between crystal and ampoule wall [1] are characterized by a low density of dislocations (below 10^4 1/cm^2) and a wide range of ohmic resistance (for CdTe up to 10^8 Ωcm) [2]. The absolute temperature and temperature gradient are the most important parameters in determining the proper conditions of crystal growth. In this study, a simple way of the determination of the optimal temperature and temperature profile suitable for crystal growth is presented.

The growth of long crystals is optimal when the temperature gradient along the axis of symmetry on the lateral surface of the crystal near the crystallization front is smaller or equal to temperature gradient in the furnace at the same place, and the temperature of the crystal is smaller than the temperature of the furnace and ampoule wall. Then the vapour resublimates on the silica or graphite core but not on the ampoule wall. Assuming the domination of radiative heat transfer between the furnace and crystallization front, this condition can be written in the form:

$$\frac{\varepsilon}{k} \le N_{Gs} \overline{T_i}^{-3}$$

$$N_{Gs} = \frac{1}{4} \cdot \frac{1}{\sigma} \frac{1}{T_f T_i} \cdot \frac{dT}{dx}$$

ε - average emissivity of the growing surface

k - heat conductivity of the crystal

T_i - average temperature of the crystallization front

σ - Stefan-Boltzmann constant

$\frac{dT}{dx}$ - temperature gradient in the furnace near the crystallization front

T_f - parameter characterizing the effective average temperature of the elements (furnace, ampoule, source material) "seen" by the crystallization front – this is the temperature of the hypothetical isothermal opaque sphere surrounding the crystallization front

$\frac{\varepsilon}{k}$ characterizes the material, N_{Gs} characterizes the crystal growth system. The unknown factor N_{Gs}, can be determined experimentally. We can use material for which the value $\frac{\varepsilon}{k}$ is a growing function of temperature and find the critical temperature of the growing face $T_{i\ crit}$, for which the slit between the crystal and the ampoule wall vanishes (for this critical temperature $\frac{\varepsilon}{k} = N_{Gs} T_{i_{crit}}^{-3}$. When the value of $|T_f - T_i|$ is reduced, this method of crystal growth can be used for a greater group of materials (especially for low thermal conductivity materials). For this purpose the ampoule has to be located near the temperature plateau of the furnace but where the temperature gradient is still great. Sometimes the temperature profile has to be specially shaped.

For a given experimental system, it is possible to create a graph of temperature vs. ratio of emissivity and heat conductivity, where the region suitable for directional crystal growth from the vapour with no contact between crystal and ampoule wall can be marked. If the curve characterizing the temperature dependence of $\frac{\varepsilon}{k}$ of a given crystal material crosses this region, then the optimal temperature for crystal growth in a given experimental system can be determined.

The correctness of the above considerations was confirmed in experiments of CdTe and $Pb_{1-x}Sn_xTe$ crystal growth. Observations of the growing face and slit between the crystal and the ampoule wall were made during growth in several temperatures that were changed progressively in 20°C intervals.

In crystal growth system used in this experiment the crystal of $Pb_{1-x}Sn_xTe$ always grows with no contact between crystal and ampoule wall.

For CdTe there is critical temperature, for which the crystallization front is flat and the slit vanishes. This is because for CdTe the value $\frac{\varepsilon}{k}$ is a growing function of temperature.

[1] E.V. Markov and A. A. Davydov, *Izv. Akad. Nauk* SSSR, Neorg. Mater. 7 (1971) 575.

[2] K. Grasza, U. Zuzga-Grasza, A. Jedrzejczak, R.R. Galazka, J. Majewski, A. Szadkowski and E. Grodzicka, *J. Crystal Growth*, submitted.

C54

A HISTORICAL VIEW ON THE BRIDGMAN METHOD

M. Mühlberg and M. Pfeiffer
Humboldt University of Berlin, Department of Physics
Institute for Crystallography and Materials Science
Invalidenstraße 110, 1040 Berlin, Germany

A computer analysis of several journals on materials science from 1966 to 1990 has been evaluated and confirms an increasing consideration of the Bridgman method.

From today's knowledge of the essential experimental parameters a discussion of the most important papers, beginning with BRIDGMANs original paper in 1925 [1], is carried out. The role of the temperature field, regarded as more or less insignificant by BRIDGMAN, was noticed early by STOCKBARGER in 1936 [2].

TILLERs criterion of stability [3] to avoid constitutional supercooling has oriented on the use of steep temperature gradients for years. Consequently, the chances of the Bridgman technique to obtain material with a high crystalline quality, have been hided for a long time. Today low gradient configurations normally are used.

The most important stages of modelling since the pioneer work of CHANG and WILCOX [4] are characterized.

Structural perfections and chemical homogenities of several substances grown by the vertical Bridgman method, that are attainable today, are described with respect to the used experimental conditions.

[1] P.W. Bridgman; *Proc. Amer. Acad. Arts Sci.* 60 (1925) 303-383.
[2] D.C. Stockbarger; *Rev. Sci. Instrum.* 7 (1936) 133-136.
[3] W.A. Tiller, K.A. Jackson, J.W. Rutter, B. Chalmers; *Acta Metallurg.* 1 (1953) 428-437.
[4] C.E. Chang, W.R. Wilcox; *J. Crystal Growth* 21 (1974) 135-140B18.

C55

TEMPERATURE MONITORING ON BRIDGMAN CRYSTAL GROWTH PROCESS

Yan Shenghui, Chai Yao, Wang Shiting, Wang Fungyun, Ying Shunhu and Zhu Hongbing
Shanghai Institute of Optics and Fine Mechanics
Academia, Sinica
P.O. Box No. 800-216, Shanghai(201800), China

Bridgman method is one of the techniques widely used in crystal growth from a melt contained in a crucible. For growing refractory crystal, generally the graphite heater, molybdenum crucible and heat shield are supplied. Such a growth arrangement is a sealed system so the situation of the melt can not be seen by neck eyes and the growth temperature is difficult to be judged and modulated at a suitable degree. Too much over heating of the melt always causes many accident,such as to melt the crucible,the heat shield or to melt the seed crystal entirely, so that the growth runs to failure. And as the growth temperature is too low the material will not be melted sufficiently and it does not attain the essential condition for satisfactory growth. Therefore, how to control the growth temperature at an optimum level and how to monitor the growth process are the main problems which have to be solved in this technique.

This paper presents the growth arrangement and growth process of Al_2O_3 crystal by Bridgman method. Some thermocouples were mounted on the different point of the growth arrangement and the variations of the temperature with the time was recorded. As a result, the melting and condensing of the material inside the crucible were well corresponded to the variations of the recorded curves so that it provided reliable data which were good reference for the improvement of the growth parameters and growth technique.

Al_2O_3 single crystals of 120mm in diameter and 50mm in height with good optical quality have been grown successfully by this technique. Being used the monitoring technique, the stability and reproduction of Bridgman method is greatly improved.

C56

A NEW TECHNIQUE FOR MEASURING THE HEAT TRANSFER BETWEEN AN AMPOULE FURNACE

W. Rosch
University of Virginia, Charlottesville VA
W. Debnam, A. Fripp and G. Woodell
NASA Langley Research Center, Hampton VA
T.K. Pendergrass
NASA Marshall Space Flight Center, Huntsville, AL

The amount of heat that is conducted, convected and radiated between an ampoule and the furnace is an important parameter during vertical Bridgman crystal growth. The heat transfer determines how well the crystal matches the temperature profile of the furnace, and is a key factor in the steepness and sharpness of the thermal gradient that can be achieved. Because of these important functions, it is a key variable for doing realistic thermal modelling.

The amount of heat that is transferred depends on the temperature, emissivities and geometries of both the furnace and ampoule, as well as the thermal properties of the ambient atmosphere present. This paper will present a new method for directly measuring this heat transfer. Results using this technique will be used to develop a simple relationship between the heat transferred and the temperature difference for a variety of ampoule surfaces and ambient atmospheres. This paper will also discuss the difficulty and success to date of determining the magnitude of radiation compared to conduction and convection at various temperatures.

C57

APPLICATION OF PRODUCTIVITY FUNCTION IN CLOSED TUBE CHEMICAL VAPOUR TRANSPORT

K. Balakrishnan, B. Vengatesan and P. Ramasamy
Crystal Growth Centre, Anna University, Madras 600 025, India

Chemical Vapour Technique is successfully used for growing crystals of relatively non-volatile materials. To facilitate the selection of an efficient transport reaction Schafer has stated valuable rules supported by countless number of experiments. During the past several years numerous attempts have been made to provide a more accurate prediction of the crystal growth rate. Transport equations on the basis of diffusion-limited vapour transport have been given by Lever and Mandel, Arizumi and Nishinaga, Faktor, Garrett and Heckinbottom and undoubtedly by others. Due to their complexity, these procedures are generally less suited to preliminary evaluation of the efficiency in arbitrary reaction systems.

In the present investigation, the productivity function, $\mathcal{F}$, as defined by Klosse, has been reformulated in terms of Lever-Mandel theory of diffusive closed tube chemical vapour transport, (CT-CVT) in which the efficiency of reaction process has been given by a function involving the mole fractions of the gaseous species and the stoichiometric coefficients. The main advantage in using the productivity function, $\mathcal{F}$, for predicting the maximum efficiency of diffusion CT-CVT process is that only thermodynamic quantities, and no fluid dynamic quantities, are involved in its calculations. The features of such productivity function in the case of ZnS are discussed.

C58

GRAVITATIONAL AND THERMAL EFFECTS IN CHEMICAL VAPOR DEPOSITION

I.O. Clark[1], *L.R. Black*[2], *E.J. Johnson*[3], *P.V. Hyer*[3], *P.W. Culotta*[3], *W.K. Gerdes*[1], *W.A. Jesser*[2], *and J. Kui*[2]
[1]NASA Langley Research Center, Hampton, VA 23665
[2]University of Virginia, Department of Materials Science, Charlottesville, VA 22903
[3]Lockheed Sciences and Engineering Company, Hampton, VA 23666

The flow of gases in chemical vapor deposition (CVD) reactors depends strongly on the geometry of the reactor, its orientation relative to the gravity vector, and the magnitude and orientation of thermal gradients. Other parameters such as overall flow rate, pressure, and the choices of source and carrier materials also play important roles in determining the reactor flow fields. A three-phased approach has been used to investigate the transport phenomena occurring in horizontal CVD reactors: laser velocimetry experimental flow studies, metalorganic chemical vapor deposition (MOCVD) experimental studies, and computational fluid dynamic (CFD) modeling. Laser velocimetry measurements of flow in a horizontal reactor with a cylindrical flow channel and tilted susceptor have demonstrated velocity components arising from thermal expansion and buoyancy effects which significantly exceed the velocity components due to the external applied flow. A commercial computational fluid dynamics code has been used to model the MOCVD of GaAs and InP thin films in a horizontal reactor with a rectangular cross section and a tilted susceptor. Finite-rate chemical reactions have been employed in the model. The numerically predicted deposition profiles have been compared with those determined experimentally under a variety of growth conditions. The interactions of the gravitational and Soret (thermal diffusion) effects over a range of gravity levels from zero- to one-g have also been studied for a horizontal CVD reactor with a rectangular cross section and backward-facing steps using numerical simulations. The status of this research and its implications for the growth of CVD layers will be reviewed.

C59

DEVELOPMENT OF COMPUTATIONAL HOLOGRAPHIC INTERFEROMETRY FOR OBSERVATION AND CONTROL OF VAPOR DEPOSITION PROCESSES

P.R. Griffin and S. Motakef
Massachusetts Institute of Technology, Cambridge, MA 02139

The development of an on-line non-intrusive technique for observation and control of vapor deposition processes is reported. In this approach temperature and compositional variations in the reactor are observed through generation of holographic interferograms. The capabilities of this sensor are being investigated for rotating-pedestal CVD reactors. In the diagnostic mode, the sensor is found to detect the presence of unsteady flow patterns in the reactor. For process control purposes, the interferograms are observed by a video camera and digitally processed to provide quantitative information on the flow structure and density gradients in the reactor. The performance of the sensor in this configuration is found to be case-specific and controlled by the ratio of signal strength to the speckle noise. A computational approach, based on the use of numerical simulation of gaseous convection and generation of synthetic interferograms, aimed at identification of the suitability of this technique for a given growth system is discussed.

C60

DEVELOPMENTS IN FLUX GROWTH

S.K. Arora
Department of Physics, Sardar Patel University,
Vallabh Vidyanagar 388120, Gujarat, India

Flux method of crystal growth has been of great value and potentiality because many materials, right from highly nonconducting dielectrics to good conducting metals and superconducting compounds, have been crystallised using it. In principle, the required supersaturation, appropriate to crystallization, is promoted either by isothermal solvent evaporation, by continuous slow cooling or by a transport process in which the solute is forced to flow from a hotter to a cooler region. The importance of Ostwald-Mier region on the phase diagrams has been demonstrated. Several experimental setups and growth procedures have been reviewed and discussed with a view to obtaining larger and more perfect single crystals. Examples of different materials have been taken to analyse the experimental results.

Flux growth is a suitable method to investigate crystallization kinetics and mechanism which cannot be attempted with other high temperature techniques of crystal growth. Study of such kinetics have been attempted in detail during the growth of single crystals of copper tungstate. Further, certain typical observed microtopographical features, common to most flux-grown crystals, have been described.

A MACINTOSH BASED SYSTEM WITH AUTOMATIC DIAMETER CONTROL FOR CZOCHRALSKI CRYSTAL GROWTH

C61

M.R. Singelenberg, R.A. Manente, C.L. Melcher, C.A. Peterson and J.S. Schweitzer
Schlumberger-Doll Research, Ridgefield, CT 06877-4108, USA
F.J. Bruni
Santa Rosa, CA 95405, USA

A new type of graphics-oriented programming environment has been used to develop a highly versatile automatic diameter control software system for Czochralski crystal growth. The program uses the LABVIEW software system on a Macintosh computer which is interfaced to a Crystalox CGS growth station. The software monitors and controls the rotation rate, pulling rate, crucible load cell, and power level of the induction heater. It implements algorithms which compensate for melt drop and for magnetic levitation of the crucible as a function of input power to determine the true weight of the crucible and contents. The system monitors, displays, and stores all diameter control data throughout the growth run, and any of this data can be graphically displayed without interfering with the control of the growing equipment. An important feature of this system is that several continuously updated graphical displays of data, such as power level, crystal radius or diameter, crucible weight or differential weight, etc., can be viewed simultaneously. In addition, the system resides on a network which allows access to the crystal-growth computer through remote terminals.

This system has been successfully used for the past year for the growth of rare earth oxyorthosilicate crystals. Specific techniques needed to implement the interfaces between the computer and the crystal growing equipment will be presented. Examples will be presented showing the numerous high resolution color graphical displays that are routinely accessible and the quality of crystals that have been obtained from the automatic control provided by the software.

STUDY OF DIRECTIONAL CRYSTALLIZATION PROCESS IN A COLD CONTAINER WITH DIRECT RADIO-FREQUENCY HEATING

C62

V.V. Osiko, D.L. Penyaz and N.P. Khaneev
General Physics Institute, Academy of Sciences, Moscow, USSR

At present there is a problem to obtain large high-quality crystals thus the necessity detailed study of the factors influencing on their growth exists. One of them is the density of power absorbed by the melt - $Q_m = P_m/M$, where P_m is the power absorbed by the melt; M is the weight of the melt. It was noticed in the numerous experiments that the different levels of Q_m during the crystal growth led to the different manifestations of the crystals degradation process, which determined the quantity and, consequently, dimensions of the crystals grown to the top surface of the crystal block.

In the present work it was experimentally investigated the relationship between the degradation process of crystals ZrO_2 stabilized by Y_2O_3 and Q_m at time of the crystallization beginning. The investigation was made on a Kristall-401 apparatus with a power of 60 kW and a frequency of 5.28 MHz. New method for the study of melting and crystallization processes in a cold container (CC), which allows to monitor P_m and heat transport from the CC in different directions was used.

In order to define the degradation process for the whole crystal block it was introduced the degradation coefficient $k_d = (n_1-n_2)/n_2h$, where n_1 is the number of crystals, which began to grow from the molten volume bottom; n_2 is the number of crystals grown to the top surface of the crystal block; h is the height of the crystal block. As have been experimentally established, the degradation coefficient value depends on Q_m. It is explained that the level of Q_m determines the thermal gradients in the melt, which, in turn, determine the conditions of competition between the crystals with different orientations.

Thus, the established dependence between k_d and Q_m gives opportunity altering Q_m to affect the degradation process and, hence, to vary the dimensions of crystals.

C63

THE SINGLE CRYSTAL GROWTH OF SAPPHIRE TUBE BY EFG PROCESS AND THE STUDY ON THE DEFECTS OF THE CRYSTAL

J.H. Lee and K.K. Orr
Hanyang University, College of Engineering
Department of Inorganic Materials Engineering
Seoul 133-791, Korea

The sapphire tube were grown with a diameter of 10 mm, thickness of 1 mm at rate up to 6 mm/min by the EFG process. A large impurity concentration causes constitutional supercooling. The stability of the interface shape is disturbed up to the cellular structure are generated. The voids are distributed in a thin layer at a distance of 50-200μm from the lateral surface at growth rate of 2.5-3 mm/min and the higher the pulling rate the greater is their density and the smaller is their size. The increased density of voids caused stress to generate the dislocation and then generate the subgrain boundary. The dislocation in the as grown {1120} sapphire tube were investigated by chemical etching in fused KOH and by optical microscope. The shape of etch-pit is a distorted pyramid and the dislocation density measured on the tube surface varied, typically, from $2x10^4$ to $3x10^5$. The misorientation of adjacent subgrains increases with distance from the seed, reach a certain limit and then decrease slightly with further growth by a rearrangement of the subgrain structure. The facet of lateral surface of sapphire tube was formed in different orientation and the striation was formed on the lateral surface.

C64

MHOI: MULTIDIRECTIONAL HOLOGRAPHIC INTERFEROMETER FOR CRYSTAL GROWTH EXPERIMENTS IN SPACE

L. Gatti and F. Solitro
Alenia Spazio, S.p.A. - Torino (Italy)
F. Bedarida and G.A. Dall'Aglio
University of Genova, Italy

This paper deals with the development of a device for the application of multidirectional holographic interferometry to Crystal Growth in Space. This technique provides a three-dimensional reconstruction of refractive index gradients in transparent objects.

Alenia Spazio is developing the MHOI (Multidirectional Holographic Interferometer), based on fiber optics, in cooperation with the University of Genova under ESA contract. The instrument's aim is the study of chemico-physical properties of transparent liquids in micro-g conditions. The instrument is essentially an optical tomograph whose most remarkable feature is the optical fiber system, making it not only compatible with but also effective to Space applications. The instrument performances and first experimental results are presented in this paper.

A microgravity environment would guarantee the growth of crystals of large dimensions and high purity, thus the development of such instrument for space applications is to be considered mandatory.

BLOCK STRUCTURES IN SAPPHIRE CRYSTALS PRODUCED BY STEPANOV TECHNIQUE

C65

S.V. Artyomov, V.S. Papkov and V.F. Perov

The application of the sapphire profiled crystals as an optical and structural material is connected with the block structure of the grow crystals.

The block structure of the crystals is determined by two factors: first, by the character and the degree of plastic deformation of the seed, second, by the deformation processes existing in crystals during the growth.

The influence of the first factor has been studied during the crystals growth using earlier deformed seeds with the specified bending radius.

Block structure pattern and misorientation degree of the block (θ) precisely corresponds to the deformation pattern and bending radius value (R) of the seed:

$$\theta \approx c - kR \ ,$$

where k and c are constants.

The significant feature of this dependence at R = 10 cm 8 = 0, i.e. block-free crystals are formed on the deformed seed.

It follows from the relation

$$\rho_{kp} = \frac{\Lambda}{b \cdot R_{kp}}$$

where b is the Burgers vector, dislocation density ρ for R_{kp} = 6.0 cm corresponds to 2 x 10^6 cm^{-2}.

Maximum dislocation density in the block-free sapphire ribbons is 2 - 4 x 10^6 cm^{-2} [1], that differs considerably from $\rho_{kp} \sim 3 \cdot 10^4$ cm^{-2} cited in the work [2].

During the crystal growth on the straightened after bending planar seeds block structure pattern and block misorientation degree correspond to the relief of the seed.

It follows that it is high dislocation density which leads to the block structure formation but having supercritical deformation of the crystallographic planes. The presence of such planes through the crystal grow becomes an disadvantageous state owing to consumption of energy without block boundaries formation in it.

ASPECTS REFERRING TO THE CONTROL OF CRYSTAL - BY ELECTRICALLY MODIFYING THE INTERFACE T

C66

Z. Schlett, A.M. Balint and I. Jadaneant
Department of Physics, University of Timisoara, 1900 Timisoara, Romania
B. Balint
Department of Mathematics, University of Timisoara, 1900 Timisoara, Romania
M. Serbanesco and V. Vanca
I.C.P.M.S. 2000 Bucuresti, Romania

Inspired by Lippman's works who succeeded in electrically modifying the interface tension of Hg-Hg ion solution system, in the Plasma Physics Laboratory of the University of Timisoara, we have carried out an experiment underlining the electrical modification of the interface tension of a Hg-rarefied gas system. Based on this achievement we succeeded in modifying the diameter of a sapphire crystal by changing the interface tension of sapphire-Al_2O_3 vapour system without altering command parameters (pulling speed and temperature) by using a pulling EFG technique.

At the same time the paper presents the admissible manouevres of the crystal-growth process considering interface tension the variable command parametre.

C67

METHOD OF COAXIAL CRYSTAL GROWTH FROM MELT

E.R. Dobrovinskaya, L.A. Litvinov and V.V. Pishchik
Institute for Single Crystals, Acad. Scie. of Ukraine, Kharkov

With the IFG growth method used, the group of crystals is usually located round a circle with the centre on the geometric and thermal axis of the crucible, i.e. in the zone of radial temperature gradient. This results in different wall thickness and a number of other structural defects. To avoid such disadvantages, methods for coaxial growth of crystals have been developed.

The calculation of the temperature fields in the system of thin-wall coaxially grown sapphire tubes, heat exchange between which occurs by radiant energy exchange through the side surface, showed that under such conditions the inner tubes grow at lower temperature gradients and secondary derivatives of temperature with respect to the coordinate which is to affect favourably the quality of the grown crystals [1].

The experiments showed that the inner tubes growing under more favourable conditions are characterized by a lower dislocation density (ρ) shorter block boundary length (ΣP), lower residual stresses (σ) and higher cracking resistance (K_{ic}) (see the table).

1. E.P. Andreyev, A.V. Zykova, O.D. Kolotii, L.A. Litvinov, Temperature fields calculation in the system of coaxial sapphire tubes grown by Stepanov method //Optical and scintillation materials, preparation and research. Collected articles. Institute for Single Crystals, Kharkov, 1984, N12, pp. 55-59.

Table

Parameters	Coaxial Method			Conventional method
	outer tube dia 20 mm	medium tube dia 114 mm	inner tube dia 9 mm	
ρ, cm^{-2}	8×10^5	$4 - 6 \times 10^5$	$1 - 3 \times 105$	$7 - 8 \times 10^5$
ΣP, mm^{-1}	2 - 3	1.5 - 2	0.5	2 - 3
σ, kg/mm^{-2}	2.5 - 3	1 - 1.5	0.8	1.5 - 3
K_{1C}, $MN/m^{3/2}$	2.5 - 3	3 - 3.8	4 - 4.5	2.5 - 3

C68

HETEROPHASE EQUILIBRIA INVESTIGATION METHOD

A.A. Gamazov, A.A. Gamazov jun.
"Invect" Company, Krasnodar, USSR

The knowledge of heterophase equilibria is required for producing of crystals.

Every multicomponent system can be looked upon as a complex of binary and pseudobinary systems with the solid solutions formation, for example, of the $AB_{1-y}C_y$ type.

The method of heterophase equilibria investigation has been elaborated. The essence of it is that a sequence of equilibria states is registered in a conservative heterophase system with the solid solutions formation of the $AB_{1-y}C_y$ type, and measurements of pressure, temperature and liquid phase samples are taken at the equilibria moments, while the solid phase compositions are calculated using the formula:

$$y = [F_c'(T)/F_a'(T)] \cdot [1 - 2F_a(t)] + 2F_c(t),$$

where $F_a(T)$ and $F_c(T)$ are the dependences of the molar concentrations for the components A and C in the liquid phase on the temperature, $F_a'(T)$ and $F_c'(T)$ are their derivatives.

The computer model was undertaken in mathematical analysis of calculation error estimation. The equilibria compositions of the solid and liquid phase were calculated by means of the known liquidus-solidus equations in the GaInP system. The functions $F_a(T)$ and $F_c(T)$ were approximated by the method of the square segment interpolation, then the solid phase compositions were calculated by the formula and the errors relatively to the solid state compositions obtained as a result of the liquidus-solidus equations solution were determined.

It is established that temperature intervals for the first and final points of heterophase equilibria series have to be taken as 1/3 of the interval for medium points (25 K). It provides the accuracy of the calculations for all the points about 0.1-0.2 percent that is comparable with the accuracy of a liquid phase chemical analysis, and it exceeds by an order all the known methods.

The equipment to bring this method of heterophase equilibria investigation into life has been elaborated, and it is based on successive capsulation of liquid phase samples.

THE OBTAINING OF SEMICONDUCTOR CRYSTALS

C69

A.A. Gamazov
"Invect" Company, Krasnodar, USSR

All crystals of semiconductors are in fact solid solutions. Low concentrated solid solutions based on heterovalent replacement make it possible to change structure sensitive properties. Higher concentrated solid solutions based on isovalent replacement make it possible to change fundamental properties.

The increase of components number allows to change the complex of structure sensitive and fundamental properties and the aim of the work is to bring this possibility into life. Crystallization of solid solutions is accompanied by the change of feed phase composition. To compensate these changes and for required change of feed phase composition the subfeed of the feed phase is undertaken. The properties of the subfeeds by the components of liquid, solid and vapour state, the interaction between subfeeds have been studied. The regulations of subfeeds application in isothermal and nonisothermal conditions of crystallization from liquid of epitaxial layers and bulk crystals have been worked out. The accuracy of vapour-gas mixture reproduction was increased and the morphology of growth was stabilized in gas phase epitaxy by separation of the nucleation and growth of layers processes.

The obtaining of homogeneous composition crystals requires the stabilization of outside and inside conditions. The stability of outside conditions is provided by constant temperature on subfeed and crystallization surfaces, by constant amount of crystal feeding liquid and its composition at the surface of crystallization, it is also provided by constant amount of heat taken away from the surface of crystallization. The inside stability is provided by the flat surface of crystallization and by conditions eliminating the effect of concentrational overcooling. The stabilization of outside and inside conditions results in maximum crystallization speed, in homogeneous composition and structure perfection of bulk crystals, profiles and epitaxial layers.

SESSION 4D

SOLUTION CONVECTION EFFECTS ON THE GROWTH OF HEN-EGG WHITE LYSOZYME

D86

Liu Shan, Xiao Wen, Huang Tao and Zhou Yaohe
National Lab of Solidification Processing
Northwestern Polytechnical University, Xi'an
Shaan Xi Province, People's Republic of China, 710072

Solution convection greatly influences the crystal growth process and thus the internal quality of grown crystals. Owing to the urgent need of bioelectronics, protein crystallography and drug design, protein crystal growth has aroused the attention of many researchers, and a lot of studies have been made to determine the nucleation and growth process. Different from the growth of small molecular crystals, protein crystals had the tendency to stop growing when they grow to a definite size which is often too small to be used for structural analyses. Some researchers have noticed the important role solution convection plays, but there is no definite conclusion of whether solution convection has a deleterious effect or not. The authors think it is necessary to understand thoroughly the coupling effects of solution convection with the growth process of protein crystals.

In this paper some experimental observations about the above problem are presented for the growth of a model protein-hen-egg white Lysozyme under isothermal free growth and under constrained solution growth with continuous solution flow. It is found that there is a very close relation of crystal morphologies with solution flow. The upstream side of crystal boundle at its iso-electric point (pH = 10.7) grows much faster than the downstream side, and in some extreme cases the single side crystal boundle forms. The solution flow greatly increases growth velocity of the tetragonal lysozyme, sometimes up to 2.77 μm/hr.

A new explanation to the growth cessation, which attributes to the solute-depletion zone around a growing crystal, has been suggested. The solute-depletion zone results from the low solute diffusivity and electrical double layer around a growing crystal. The former makes it much slower for solute molecules to come to the growing interface, while the latter leads the repulsive electrical force between the growing crystal and solute molecules in the solution, which hinders the movement of solute molecules from the solution to the crystal surface. Based on this explanation, the authors utilized solution exchanging method to ensure the solute supersaturation-driving force for solution crystal growth, and grew triclinic Lysozyme crystals as large as 2.42 x 0.96 mm^2 and iso-electric lysozyme crystals as long as 1.02 cm after changing the solution 3 times and growing 30 days.

PROBLEMS IN GROWING URIC ACID CRYSTALS

D87

C. Aravindakshan, Y.M. Fazil Marickar, T.G. Dhanalakshmi, N. Sylaja, S. Sindhu, H. Krishna Moorthy and Sapna V. Roshni
Department of Surgery, Medical College Hospital, Trivandrum 695 011, S. India

INTRODUCTION: The problems encountered in growing uric acid in silica gel medium are discussed in this paper.

MATERIALS & METHODS: Different concentrations of uric acid solution in 1 M sodium hydroxide, namely 0.1%, 0.2%, 0.3% and 0.4% were prepared. The resulting pH was above 10 in all the solutions. This solution of uric acid was acidified with 1 M acetic acid and the ph was brought down to 8. Silica gel medium was prepared in Hane's tube utilising the modified single diffusion technique at pH 5. The crystal growth was attempted in two ways. In the first method, the uric acid solution was added to the top of the gel. In the second method, the uric acid solution was incorporated in the gel medium and 5 ml of 1 M acetic acid was added on top. Each set of experiments consisted of 6 tubes. The crystals were collected, washed, dried and subjected for light microscopy, IR analysis and SEM.

OBSERVATIONS & DISCUSSION: Uric acid was found to be soluble only in alkaline solutions and as the pH of the solution was reduced, it started precipitating. To avoid precipitation while lowering the pH and to facilitate its incorporation into the silica gel at a lower pH, the solute concentration was reduced considerably to obtain a workable concentration of 0.25%. In the first method, uric acid crystals were seen in size of 400 microns from day 1 onwards and became friable as days passed by. These crystals did not penetrate the gel medium. In the second method, the same type of crystals grew by day 1, but the size of the crystals showed a mean size of only about 200 microns. The crystals grown were found to be pure uric acid on infrared analysis.

D88

GROWTH AND CHARACTERISATION OF SOME URINARY CRYSTALS

T. Irusan, D. Arivuoli and P. Ramasamy*
*Presidency College, Madras-1, India
Crystal Growth Centre, Anna University, Madras-25, India

Crystallization processes of stone minerals are becoming important in understanding stone formation. Hence studies in synthetic systems are predicted on the hypothesis that renal or urinary stone growth is similar to that of crystal growth. Therefore the investigation of factors that inhibit nucleation or modify crystal growth or arrest crystal aggregation are necessary for understanding stone growth prevention. The inhibitors are thought to act at growth sites on the surface of the crystals and if so may exhibit an effect on crystal morphology. Some of the urinary crystals like brushite, newberyite and ammonium urate were grown in silica gel. The growth experiments were carried out by single as well as double diffusion methods. Brushite and newberyite crystals were found to be pH dependent whereas ammonium urate is pH independent.

The effect of several chemical inhibitors and the juices of some medicinal plants viz. phyllanthus niruri, solanum nigrum, osimum sanctum and misa paralislios on brushite, ammonium urate and newberyite have been investigated. The morphology of the crystals has been studied for various concentrations of the inner and outer reactants and pH of the gel medium. The dislocation studies and mechanical properties have been monitored for the different situations investigated above. In the case of crystals grown using juices of medicinal plants, the hardness is found to decrease and size of the crystals also found to decrease. SEM studies revealed that the crystals grow by layer growth mechanisms.

D89

EFFECT OF ENVIRONMENT ON CHOLESTEROL CRYSTAL GROWTH IN VITRO

E. Abdul Salim, Y.M. Fazil Marickar, N. Sylaja, C. Aravindakshan and Narayan Kalkura
Department of Surgery, Medical College Hospital
Trivandrum and Crystal Growth Centre, Anna University, Madras

INTRODUCTION: There is increasing incidence of cholelithiasis in South India. This may he due to some triggering factor in the biliary environment to initiate cholelithiasis. This study was undertaken to see whether environmental factors affect the growth of cholesterol crystal in vitro.

MATERIALS AND METHODS: Silica gel medium was prepared in Hane's tubes using sodium meta silicate in distilled water to a specific gravity of 1.05. pH was adjusted to 5 by adding 3 M acetic acid. This was mixed in a 2:1 ratio with acetone and allowed to set. On top of the gel that formed within 48 hours, 6 test solutions were added, namely 0.5% cholesterol solution in acetone, cholesterol and lithogenic bile in acetone, cholesterol and non lithogenic bile in acetone, cholesterol gall stone dissolved in acetone, cholesterol gall stone and cholesterol crystals dissolved in acetone. Acetone alone was added in the control. The size and number of crystals were assessed every day till the 15th day. Purity of crystals was assessed by infra red analysis. The rate of growth and morphology were compared in the different groups.

OBSERVATIONS AND CONCLUSIONS: The crystals reached the maximum size on the 15th day. Cholesterol alone added on the top layer or added along with powdered cholesterol gall stones produced maximum number of crystals. The size of the crystals was maximum (2.2 cm) on the 15th day on the setup incorporating the cholesterol gall stone powder. The studies indicate that there may he some factor in gall stone responsible for enhancing the growth of cholesterol crystals. Further studies are needed to identify the exact promotor of cholesterol crystal growth.

D90

DOPING IN URINARY OXALATE CRYSTAL GROWTH - AN SEM STUDY

S. Sindhu, Y.M. Fazil Marickar, C. Aravindakshan, Neena Elizabeth and Peter Koshy
Department of Surgery, Medical College Hospital
Trivandrum 695 011 and Regional Research Laboratory, Trivandrum

INTRODUCTION: Pure oxalate crystals can be grown in silica gel medium. However the urinary milieu is not a simple supersaturated nucleating solution for the oxalate crystals to precipitate. Various other chemicals/organic materials are present in the urine. These produce an effect very similar to the doping effect on crystal growth. In this paper we have tried to assess the role of doping on the surface characteristics of the oxalate crystals grown *in vitro*.

MATERIALS AND METHODS: Calcium oxalate monohydrate crystals were grown by single diffusion method using silica gel medium. Two sets of crystal growth were included, the test group incorporating citric acid and tartaric acid as dopants onto the top solution and a control group using distilled water. The crystals were washed and taken up for study under the Jeol JSM 35c scanning microscope after gold sputtering at 100 A thickness. The pictures were compared between the control crystals and dopant added crystals.

OBSERVATION: The mean size of the crystals was lesser in the test group incorporating citric acid (103.33) and tartaric acid (105.67) than control group (138.67). Scanning electron microscopic study showed that the surface morphology of the crystals changed significantly on addition of dopants. The crystals showed blunting of edges and significant distortion of crystal architecture.

CONCLUSION: Doping has definite effect on the morphology of oxalate crystals, as identified by scanning electron microscopy.

D91

CRYSTALLIZATION OF URIC ACID

S. Narayana Kalkura, U.K. Vaidyan, M. Kanakavel** and P. Ramasamy*
Crystal Growth Centre, Anna University, Madras-600 025, India
*Department of Physics, University of Kerala, Trivandrum-695 581
**Analytical Spectroscopy Division, VSSC, Trivandrum-695022, India

Uric acid (2, 6, 8 - trioxy purine, $C_5H_4N_4O_3$) is often found as a constituent of urinary calcui. Increase of uric acid in blood (hyper urecaemia) results in uric acid depositing in the joints with resultant pain and swelling usually in a single joint. Extensive research work is going on in human uric acid stones. Recently there has been an increasing interest in studying the crystal deposition diseases in vitro using gel medium because gel acts as an inert medium during the crystallization process. Uric acid crystallizes with monoclinic unit cell with a = 14.464, b = 7.403, c = 6.208 Å, $\beta = 65.10 \pm 0.05°$, space group $P2_1/a_1$, z=4.

Since uric acid has a very poor aqueous and organic solubilities, it is very difficult to crystallise them in an aqueous medium like silica gel. A method has been suggested to grow uric acid crystals in gels using U-tubes and single tube diffusion techniques. Tetra methoxy silane (TMS) and silica gels were used to grow large single crystals of uric acid. Solution of uric acid in NaOH and dil HCl were taken in different limbs of a U-tube which contained TMS or silica gel. In the single test tube diffusion method a solution of uric acid in sodium hydroxide was allowed to diffuse into the gel medium. The solution was allowed to diffuse into the gel medium for about two weeks and then the supernatant solution was replaced with dil HCl. Flat, platy and transparent single crystals of uric acid was obtained in a week's time. Crystals were characterized by thermal X-ray powder diffraction, scanning electron microscopy and IR analyses.

D92

DIELECTRIC STUDIES OF GEL GROWN NEODYMIUM MOLYBDATE CRYSTALS

Sushma Bhat and P.N. Kotru
Dept. of Physics, Univ. of Jammu, Jammu -180001 (India)
R.P. Tandon
National Physical Laboratory, New Delhi, India

Neodymium molybdate crystals grown by gel technique using the system Na_2SiO_3 - $(NH_4)_2$ $(MoO_4)_3$ - Nd $(No_3)_3$ are characterized using XRD, IR, EDAX & thermoanalytical techniques. The x-ray powder diffraction data of the grown materials does not match with that of the published data on high temperature grown neodymium molybdates (ASTM cards 19-817, 25-1174). Thermoanalytical techniques and IR spectroscopic results suggest that the material is hydrated. It is felt interesting to carry out dielectric studies on these samples. The dielectric constant ε' and loss (tan δ) is observed to be strongly dependent on frequency and temperature. The value of ε' at room temperature (25°C) is 154 at 10^3 Hz which increases abruptly to 360 at 80° and thereafter has a rapid fall. The dependence of dielectric constant and loss on temperature for different frequencies shows almost similar behaviour. An attempt is made to explain the results.

D93

ABSOLUTE CONTROL OF NUCLEATION IN THE GEL GROWTH OF CRYSTALS BY GNGT

G. Sivanesan
Dept. of Physics, RSG College, Thanjavur, T.N., India - 613 005

Control of nucleation is vital in any unseeded system of crystal growth. A nucleation control mechanism that allows the crystal to grow at the heart of the gel system is really advantageous. The absence of such a system was felt deeply in the past. The GRADED NEUTRAL GEL TECHNIQUE (GNGT), evolved recently fulfills the said purpose. A neutral gel incorporating an air wedge in the form of an inverted pyramid was introduced over the gel set. This was possible in four stages using simple devices, without any gel collapse. The top reagent had to diffuse through a nozzle like region in the graded neutral gel. This produced concentration gradients of the crystallising material both along the axial and radial directions. Large and perfect single crystals, very few in number were found grown near the axis of the test tubes. Encouraging results were obtained in all cases except one, when this method was put to acid test over a dozen system of crystals. Crystals were grown successfully both by chemical reaction and by solubility reduction methods. Habit modification was obtained in the case of Potassium tartrate crystals. Increase in size and morphological stability were achieved in TGS and $(NH_4)_2SO_4$ crystals. Nucleation was attained in the growth of Cobalt tartrate and Iron tartrate crystals.

D94

CHARACTERIZATION OF GYPSUM ($CaSO_4 \cdot 2H_2O$) TWINS BY X-RAY TOPOGRAPHY

C. Rinaudo and M. Franchini-Angela
Dipartimento di Scienze Mineralogiche e Petrologiche
Via Valperga Caluso 37 - 10125 TORINO, Italy

Natural and synthetic gypsum crystals twinned following (100) by contact and by penetration and ($\bar{1}$01) by contact have been characterized by X-ray topography, Lang method.

All the examined samples, natural and synthetic, showed an elongated habit, as commonly on gypsum, but the elongation direction of the crystals was the [001] direction in the case of (100) twins and the [101] on the ($\bar{1}$01) twins. X-ray transmission topographs revealed, on all the twins, the presence of numerous linear dislocations running along the elongation direction of the crystals. These defects resulted of mixed type and to their number and character may be ascribed the elongated habit of the gypsum.

The X-ray topographs showed also numerous dislocations with a quite edge character on the (100) twins but with mixed character on the ($\bar{1}$01) twins. The different lateral development of the crystals, poor on the (100) twins and more important on the ($\bar{1}$01) twins, may be therefore ascribed to the different character of the lateral dislocations.

D95

THE INFLUENCE OF ADDITIVES ON THE GROWTH OF POTASSIUMCHLORIDE AND L-ALANINE

R. Lacmann and W. Schröder
Institut für Physikalische und Theoretische Chemie, Technische Universität Braunschweig.
Hans-Sommer Str. 10, D-3300 Braunschweig, Germany

Experimental and theoretical results of different additives on the growth and habit of Potassiumchloride and L-Alanine in aqueous solutions are presented. The used additives are chosen by modeling the additive molecule according to the surface structure of the crystal.

Growth experiments are carried out in a thermostated growth flask. The seed crystals are fixed in a teflon plate which rotates in the supersaturated solution containing one of the additives. The supersaturation of the solution is continuously registered by density measurement. Photographs of each crystal are made at different supersaturations.

The influence of additives on Potassiumchloride are summarized as follows: Additives which adsorb on the {100} faces inhibit very strongly the growth. These are: Alizarine and Potassiumferrocyanide. In the case of Potassiumferrocyanide the Ostwald Miers region is strongly extended (the relative supersaturation is increased from 0,24% to 5,3%). In this region growth is not observed. Additives which adsorb on the {111} faces decrease their growth rate making it lower than the growth rate of the {100} faces. The habit changes from cube to octahedron. A very good example is Sodiumhexametaphosphate (HMP). The picture shows schematically the HMP-ion on the (111) surface of Potassiumchloride.

The crystal faces of L-Alanine grown from an aqueous solution are determined. The faces are {011}, {110} and {210}. The surfaces of the crystallographic faces are visualized on a computer display. We are searching for additives which would adsorb on the (011) or the (001)-face to inhibit the growth in the z-direction of the crystal. Growth rate measurements with such additives have been carried out and the obtained results confirm the expected influence on the growth and habit.

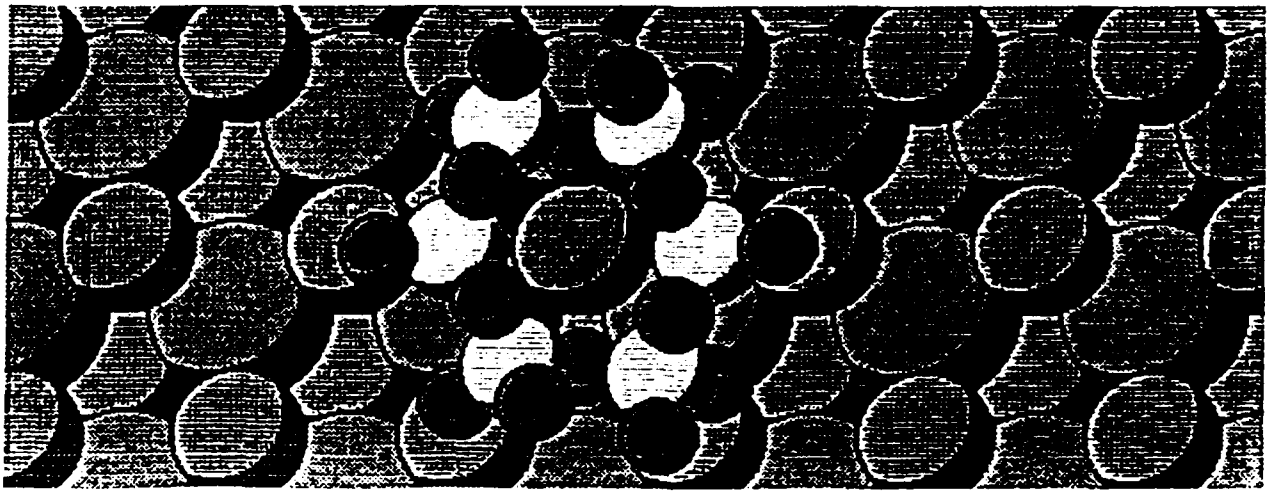

D96

GROWTH OF $LiClO_4$ CRYSTAL AND *IN-SITU* OBSERVATION

C. Chen and A.Y. Xie
Institute of Physics, Chinese Academy of Sciences
P.O. Box 603(83), Beijing 100080, China

Newly singal crystals of $LiClO_4$ have been grown in our laboratory by the low temperature solution method. The solubility of the crystal in the saturated solution has been measured by a weighing method. The in-situ observation of the growing processes has been studied by Holographic Interferometry.

The interferograms of the growing process shown that: (1) The saturated solution of $LiClO_4$ is stratified during the period of crystal growth; (2) The steady-state growth rate could be reach while the distribution of the interfergrams are arrived stable[1]; (3) The boundary layer remained stable while the emergine plume changed from stable to partially oscillatory[2]; (4) The imperfection of $LiClO_4$ is markely influenced on the hydrodynamics[3].

1. C. Chen, W.Y. Ma, D.D. Liu and A.Y. Xie, *J. Crystal Growth*, 84(1987)303.
2. C. Chen, Y.T. Sheng and W.Y. Ma, *Chinese Physics Letter*, 8(1991)906.
3. H.U. Walter, *Fluid Sciences and Materials in Space*, Springer-Verlage Berlin, 1987, p. 430.

D97

CRYSTAL MORPHOLOGY OF BRUSHITE, $CaHPO_4 \cdot 2H_2O$

F. Abbona[1], F. Christensson[2], M. Franchini-Angela[3] and H.E. Lundager Madsen[2]
[1]*Dip.to di Scienze della Terra, Università della Calabria, 87036 Rende (Italy)
[2]Kemisk Institut, K.V.L., 1871 Frederiksberg C (Danemark)
[3]Dip.to di Scienze della Terra via Valperga Caluso 37, 10125 Torino (Italy)

By growing brushite crystals from aqueous solutions at 25 and 40°C under different conditions of concentration and pH, a great variety of morphologies have been obtained: single crystals, twins, aggregates. For each of them the occurrence field has been established. Crystals may be thick tabular, thin platy, prismatic, needle-like, triangular, trapezium-like depending on the relative development of the forms (010), ($\bar{1}$20), (111), (11$\bar{1}$), (12$\bar{2}$), (011). Many crystals are irregular showing rounded borders or incomplete faces at one end. The polar character of brushite reveals in crystal habit only under definite conditions. Morphodromes relating crystal habit to supersaturation and pH are presented.

The theoretical crystal habit derived from the structure by the P.B.C. analysis is compared to the experimental one. The form (111), which has a high frequency, shows morphological instability due to its S character.

Four twin laws have been found and are described.

Finally, the growth mechanisms of the most important faces are discussed.

GROWTH AND CRYSTAL STRUCTURE OF $LiCuO_2$

D98

Katsuhiro Imai, Masayoshi Koike and Humihiko Takei
Institute for Solid State Physics, University of Tokyo
Roppongi, Minatoku, Tokyo 106, Japan

Single crystals of $LiCuO_2$, a new compound of ABO_2 type material, have successfully been grown using a Li-deintercalation from L_i2CuO_2 single crystals, which made by flux-growth technique. The starting Li_2CuO_2 crystals were put into acetonitrile with excess of iodine and tetra-n-butyl ammonium iodide, and were heated at 70°C with stirring over a night. The products were filtered off, washed with acetonitrile, and dried in vacuo, and were analyzed by X-ray powder diffraction method. Careful examinations of the powder diffraction data, as well as the results of chemical analyses, revealed that the products are of single phase with the composition $LiCuO_2$. Single crystals were found in the products in the same shape of Li_2CuO_2 with the maximum size of 0.60x0.07x0.02 mm^3. An example of $LiCuO_2$ single crystal is shown in Fig. 1.

Precession photographs revealed that $LiCuO_2$ has an orthorhombic symmetry with the lattice constants 5.71x9.64x2.71Å. The reflection spots in the photographs indicate considerable broadening, suggesting low crystallinity. Intensity data collection by a four-circle diffractometer for crystal structure analysis had failed because of bad quality in diffraction. Thus, the Rietveld refinement of the powder diffraction data was attempted using an structure model originally suggested by referring the structure of Li_2CuO_2. The final structure determined was; orthorhombic, Cmmm, Z=4, a=5.7078(6), b=9.639(2), c=2.7172(3)Å.

Crystal structure of $LiCuO_2$, as shown in Fig. 2, indicates that $LiCuO_2$ is composed of stacking of the Cu-O edge-shared one dimensional chains along the c-axis. Each chains are connected by the octahedrally coordinated Li. This structure is quite similar to that of $NaCuO_2$, where the edge-shared Cu-O chains are apparent, and is completely different from the other $LiMO_2$ (M : 3d transition metals) compounds having the NaCl-related structure. The fact that the edge-shared Cu-O chains are also seen in the structure of Li_2CuO_2 suggests an advancement of the Li-deintercalation reaction with a topotactic mechanism which provides the growth of $LiCuO_2$ crystal.

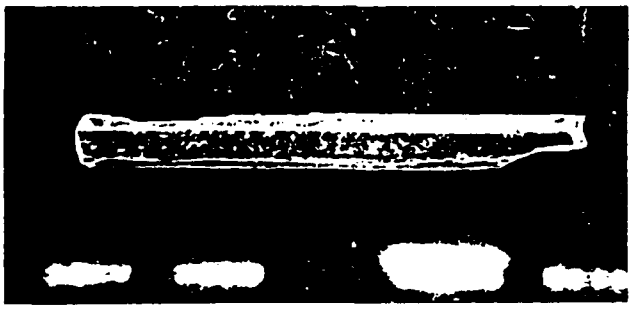

Figure 1. $LiCuO_2$ single crystal (SEM image).

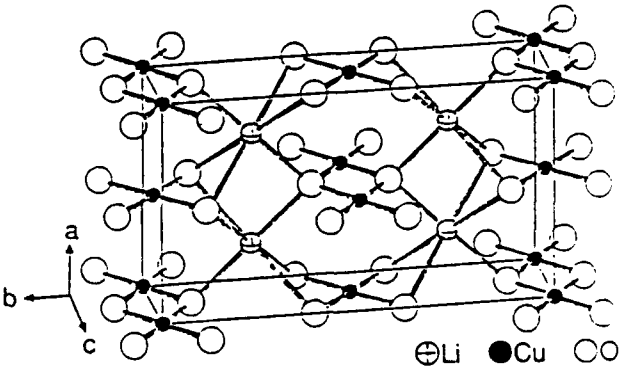

Figure 2. Crystal structure of $LiCuO_2$.

D99

AUTOMATIC FACILITY FOR CRYSTAL GROWTH FROM SOLUTION MICROGRAVITY EXPERIMENTS

Mariusz J. Krasinski, Pawel Kidula and Michal Idzikowski
Institute of Physics, Technical University
Wolczanska 219, 93 005 Lodz, Poland

Many scientists and technologists think that microgravity environment is very interesting and promising for crystal growth from solution. Some experiments performed on the board of space laboratories confirm some of these expectations then many new experiments are in preparation. But from the practical point of view it has appeared that at present time participation of spacecraft crew in experiments should be minimized or even excluded. It is subject for discussion if it is good or not for realization of scientific program but requirement for automatic crystal growth facilities is obvious.

We are describing the automatic crystal growth facility which is actually built in our laboratory. It was planned for crystal growth from solution experiments (growth and dissolution in various conditions) but the modular construction enables to prepare also other experiments.

In the apparatus twelve experimental cells are placed in magazine and mechanical feeding device enables to introduce cells to and abort from the working place. The electronic microprocessor controller assures proper realization of scientific program. It is controlling all functions of the facility and allows to collect some experimental data in the electronic memory. It is also possible to send some commands from the Earth.

The measurement cell is unified block prepared for particular experiment.

The optical observation of the solution near the crystal face and investigation of crystal surface is realized through conventional photography or holographic interferometry in real time. These systems are built as exchangeable modules. All blocks are mounted together in the cage assuring mechanical rigidity.

The main advantage of this facility is open and modular construction what enables to prepare setup for new experiments through exchange of some blocks. This assures very economical use of the apparatus.

D100

VERY LARGE MELTING POINT DEPRESSION OF WATER IN SILICA

J.C. van Miltenburg and J.P. van der Eerden
Laboratory of Interfaces and Thermodynamics
Padualaan 8, 3584CH Utrecht, The Netherlands

Calorimetric measurements of water absorbed in porous silica indicate a large melting point depression. This observation can be understood when it is accepted that the surface tension water/silica is considerably lower than the specific interface free energy ice/silica.

We accurately measured the enthalpy of a silica sample filled with different fractions of water. Between 10K and 100K we did not measure a difference between the heat capacity of bulk ice and of ice in pores. In the temperature range from 100K to 260K we found an algebraic dependence of the excess (as compared to the sample filled with ice) enthalpy ΔH on the undercooling $\Delta T = T_m - T$. Indeed we obtained good fits of the form $\Delta H = B/(\Delta T)^{\beta}$, where the exponent β has the same non-integer value for different degrees of filling.

We propose to interpret the data with the following model. Firstly, we assume that the silica pores have a fractional structure. To this end we define the differential pore density n(r) in m^{-3} such that $Vn(r)dr$ is the total length of pores with diameter between r and r + dr in a sample of total volume V. The fractional character of the structure is then expressed by the assumption $n(r) = Ar^{\alpha}$, where A and α are material parameters.

Secondly we assume that the interfacial interactions are such that ice melts in pores with a radius smaller than a radius r^* which depends on temperature. E.g. when it is assumed that the interfacial free energies, the heat of fusion and the entropy of fusion are temperature independent one finds r^* to be inversely proportional to ΔT. Combining these assumptions indeed leads to an algebraic dependence of ΔH on ΔT.

The model we propose here can, in principle be used in two alternative ways. Firstly, with some plausible assumptions on the thermodynamic parameters of the liquid, one can get information on the pore structure. Secondly, knowing the pore structure one can obtain information on the thermodynamic parameters of the liquid. Especially for undercooled water anomalous behavior of the specific heat is expected in the literature, and we intend to use the present experiments to study this quantitatively.

ORIENTED GROWTH OF SILICA MOLECULAR SIEVE CRYSTALS AS SUPPORTED FILMS

D101

J.C. Jansen and G.M. van Rosmalen***
Delft University of Technology, The Netherlands
*Julianalaan 136, 2628 BL Delft
**Leeghwaterstraat 44, 2628 CA Delft

INTRODUCTION. Recently, the preparation of layers of microporoous tactosilicates, denoted as zeolites, has been reported (1). Polycrystalline material was deposited on various supports with the main objective to create potential applications as catalysts, membranes and sensors. In this work parameters pertaining to a continuous film production of lateral oriented microporous silica crystals on a silicon support are studied as well as the history of formation of the crystals and the crystal film.

EXPERIMENTAL. Silicon supports of 1 cm^2 were, after cleaning procedures, positioned vertically in a Teflon holder. The holder including the support were placed in a Teflon lined autoclave of 35 cm^3. Next an aqueous synthesis mixture containing a Si-source, OH as a mineralizer and an organic template molecule, to obtain a microporous framework, were added. The crystallization behaviour of different mixtures of an MFI-type microporous silica on the silicon support was studied at 160°C as a function of time.

RESULTS AND CONCLUSION. A continuous layer of laterally oriented plate-like crystals, each at least .2x.5x.5 um^3 in size, could be prepared on a silicon [001]/silicondioxide surface of 1 cm^2. It was observed that in the crystallization process first a thin gel layer is formed on the support followed by the nucleation of the microporous silica at the interface of the gel film and the synthesis liquid. This nucleus location comes from the fact that the template is only present in the solution and not in the gel film. The nuclei grow by penetrating into the gel film in a way reported earlier for a comparable system [2]. During this growth the plate-like crystals get oriented parallel to the support surface. Finally the crystals and the support become chemically bonded through condensation reactions.

Crystallizations without the formation of a preceding thin gel film never result into a uniform orientation of crystals on the support surface.

In conclusion it seems that oriented growth of molecular sieve crystals on a support is obtained only when a gel film precedes the crystallization.

[1] Davis, S.P. et al., *Chem. Mat.*, 2 (1990) 712.
[2] Jansen, J.C., et al., ACS Symp. Ser. 398 (1989) 257.

APPLICATION OF THE NUCLEATION KINETICS OF IONIC SYSTEMS*

D102

P. Meenan and K.J. Roberts
Department of Pure & Applied Chemistry
University of Strathclyde, Glasgow G1 1XL, UK

Precipitation from solution is essentially a two-step phase transformation process: the creation of new crystallisation centres followed by the nucleation and growth of these centres in the supersaturated solution. Nucleation kinetics are central in many industrial precipitation processes, nucleation may occur in the wrong part of a process, ultimately leading to scaling etc; excessive nucleation may lead to the formation of undesirable crystal morphologies or crystals that are of the wrong size distribution for a particular process.

This paper will describe the determination of nucleation kinetic parameters using an automated crystallisation cell employing light transmittance and conductivity as means of detecting crystallisation and dissolution of solids from solution. Important "benchmark" parameters such as overtemperature, removal of hetero-nuclei etc are presented and discussed in through detailed studies on the nucleation of potash alum ($AlK(SO_4)_2 \cdot 12H_2O$), ammonium dihydrogen orthophosphate ($NH_4H_2PO_4$), sodium carbonate decahydrate ($Na_2CO_3 \cdot 10H_2O$) and sodium sulphate decahydrate ($Na_2SO_4 \cdot 10H_2O$) from saturated aqueous solutions.

*Work supported by Unilever Research.

D103

THE ROLE OF SOLVENT IN THE NUCLEATION AND GROWTH OF NORMAL ALKANES IN THE HOMOLOGOUS SERIES FROM $C_{18}H_{38}$ TO $C_{28}H_{58}$*

*A.R. Gerson, K.J. Roberts**, J.N. Sherwood and A. Taggart*
Department of Pure and Applied Chemistry
University of Strathclyde, 295, Cathedral Street, Glasgow G1 1XL, UK
**Also at SERC Daresbury Laboratory, Warrington, WA4 4AD, UK

The nucleation and growth of normal alkanes is of significant importance in understanding the formation of wax crystal cakes which can impede and eventually stop the flow of hydrocarbon fuels under cold weather conditions. Over the last few years we have developed an automated technique, using light scattering, for detecting crystal formation from the liquid phase. The technique assesses three important, but related, parameters:

- the solution saturation temperature as a function of temperature thus enabling a test, using the van't Hoff isotherm, of assessing solution ideality,
- the difference between saturation and crystallisation temperatures, ie the meta-stable zone width (MSZW) which indicates the temperature range over which crystal growth will be preferred to spontaneous nucleation,
- the induction time within the MSZW as a function of supersaturation from which fundamental solution properties such as critical cluster sizes, interfacial tension can be deduced.

The paper will overview the techniques and, in particular, present data on the crystallisation of normal alkanes and homologous mixtures from m-xylene and dodecane. These two solvents, respectively, mimic the behaviour of the aromatic and linear components present in commercial fuels. The behaviour of these model systems will be compared to the crystallisation of mixed normal alkanes from the fuels themselves.

*Work supported by Exxon Chemical Ltd, Abingdon, OXON, UK

D104

SYNCHROTRON RADIATION STUDIES OF THE PHASE TRANSFORMATIONS WITHIN OLEIC ACID*

*S.R. Craig, Y. Hayashi, K.J. Roberts** and J.N. Sherwood*
Department of Pure and Applied Chemistry
University of Strathclyde, Glasgow G1 1XL, UK
M. Iwahashi
Department of Chemistry, School of Hygenic Sciences
Kitasato University, Sagamihara, Kanagawa-ken, Japan
**Also at SERC Laboratory, Daresbury, Warrington, WA4 4AD, U.K.

Unsaturated fatty acids are of significant importance in Biophysical Science and Food Science. In particular there is a great interest in Oleic Acid (cis-w-9-octadecenoic acid) where much work has focused on characterising the role of preparative conditions and liquid structure in the formation of the various structural polymorphs.

In this paper we describe *insitu* X-ray studies carried out using beamlines 8.2 and 2.3 at the Synchrtotron radiation source at Daresbury Laboratory. Previous studies have revealed the existence of three polymorphs which have shown that pre-heating/supercooling temperatures, rate of supercooling and phase transformation alter the selective occurrence of the alpha, beta and gamma polymorphs.

Small angle diffraction patterns were obtained for samples prepared from the melt (>99.9% purity) for the various polymorphs and have enabled the lamella thickness and lateral packing of the aliphatic chain to be calculated. The use of time-resolved data collection has enabled us to follow the conversion process between polymorphs leading eventually to a single phase. The meta-stability of the polymorhs in oleic acid has enabled us to follow the phase transformation process from the ordered gamma form to the more disordered alpha form, as well as the reverse process.

Structural order in the liquid phase together with its dependance on temperature was also investigated to assess the transformation of quasi-smectic iostropic liquid crystals to nematic type liquid crystals to an eventual isotropic liquid, with respect to increasing temperature.

*Work supported by Nippon Oils and Fats, and Exxon Chemical Ltd.

GROWTH AND CHARACTERIZATION OF TRIGLYCINE SULPHO - PHOSPHATE MIXED CRYSTALS

D105

G. Ravi, S. Anbukumar and P. Ramasamy
Crystal Growth Centre, Anna University, Madras-600 025, India

Triglycine sulphate (TGS) stands prominent in the list of ferroelectric crystals with transition temperature at 49°C finding application in thermal detection. These crystals are grown from aqueous solution. In the present investigation, the changes in the physical properties of Triglycine sulphate due to the substitution of phosphate ions in the place of sulphate ions in various concentrations have been studied. As the higher concentration of phosphate ion yields only polycrystalline material, phosphate substitution has been restricted to $TGS_{(0.5)}P_{(0.5)}$. The microbes have been eliminated by the addition of H_2O_2. By this way, optically transparent crystals of size 45x25x20 mm^3 have been grown. Vickers microhardness tests carried on TGSP crystals showed that the crystal becomes harder on reducing the phosphate ion concentration. The dislocation density of the TGS and TGSP crystals is found to vary between 10^3 and 10^4 cm^{-2}. The transition temperature and the activation energy for electrical conduction have been determined by dc electrical conductivity studies. The activation energy for a b-cut plate is calculated to be 0.62ev in the ferroelectric region and 0.72ev in the paraelectric phase. The thermal behaviour has also been studied using Differential Scanning Calorimetry (DCS). The values of lattice parameters are calculated from X-ray diffraction studies. The pyroelectric current measurements made on the samples of TGS and TGSP crystals have shown that the thickness of the sample has a profound effect in this study. The pyroelectric coefficient is found to be $2.1x10^{-7}$ c/cm^2 deg for TGS and $17.8x10^{-7}$ c/cm^2 deg for TGSP crystals of thickness ~1 mm. Chemical analyses of the synthesised material and grown crystal have been carried out by Induction Coupled Plasma (ICP) which shows that only small amount of phosphate has been incorporated into the crystal lattice in spite of larger concentration in the mother liquor.

RADIATION EFFECTS IN Ge-DOPED CRYSTALLINE QUARTZ

D106

Harish Bahadur
National Physical Laboratory
Hillside Road, New Delhi-110012, India

Ge^{4+} like Al^{3+} isomorphously replaces Si^{4+} in quartz lattice. While the Al-related effects have been extensively studied the Ge effects have started receiving attention only of late on the performance of quartz-containing devices [1]. In the present work using infrared absorption in the 3100-3700 cm^{-1} region, we have examined radiation effects in Ge-doped quartz crystals grown at Bell Laboratories and Sawyer Applied Research Products, OH. Ge concentration ranged as high as 1000-3000 ppm. We have found that Ge-doped crystals exhibited the presence of a previously unreported IR band at 3656 cm^{-1}. This band appeared in much smaller strength compared to the growth-defect bands in conventionally grown cultured crystals [2,3]. Irradiation at 77K did not remove this band for radiation doses as high as 20 Mrad. Room temperature irradiation (dose = 2 Mrad) reduced this band to about 20% of its as-grown strength.

A new band at 3400 cm^{-1} was found to get produced in both samples at low temperature irradiation provided the sample had been prior irradiated at 300K. Production and annealing studies of radiation-induced 3400 cm^{-1}, Al-OH^- and the growth-defect bands have shown that while the growth-defect band started showing a recovery at about 200K the new 3400 cm^{-1} sharply decayed to about to 12% of its maximum value and remained at this value until room temperature. Al-OH^- bands in Ge-doped quartz exhibit essentially the same character as shown by conventionally grown cultured quartz [3] and also natural quartz [4].

1. F. Euler and A. Kahan, *Phys. Rev.* B35, 4351 (1987).
2. J.J. Martin, Ho B. Hwang, H. Bahadur and G.A. Berman, *J. Appl. Phys.* 65, 4666 (1989).
3. W.A. Sibley, J.J. Martin, M.C. Wintersgill and J.D. Brown, *J. Appl. Phys.* 50, 5449 (1979).
4. Harish Bahadur, *J. Appl. Phys.* 66, 4973 (1989).

*This work was supported by Sandia National Laboratories and RADC U.S. Air Force and done at Oklahoma State University in the laboratory of Professor J.J. Martin.

D107

THIN FILM GROWTH BEHAVIOR OF $YBa_2Cu_2O_{7-\delta}$ IN SEQUENTIAL DEPOSITION WITH A HIGH PURITY OZONE GAS

T. Shimizu, H. Nonaka and K. Arai
Electrotechnical Laboratory, 1-1-4 Umezono, Tsukuba, Ibaraki 305, Japan

The molecular beam epitaxy (MBE) growth of $YBa_2Cu_2O_{7-\delta}$ (YBCO) is observed using reflection high energy electron diffraction (RHEED) in the sequential deposition of constituent metals under continuous pure ozone flow. The intensity of the RHEED specular beam overall oscillates with the period of one unit cell formation. Each oscillation has characteristic structures corresponding to each atomic layer supply. Possible atomic layer formation is discussed.

D108

NONDESTRUCTIVE ANALYSIS OF OXYGEN DISTRIBUTION IN A Cu(1) PLANE OF AN ORTHORHOMBIC $YBa_2Cu_3O_x$ USING AN EXAFS SPECTROSCOPY

Hiroshi Kajiyama, Yasuharu Hirai, Tokuumi Fukazawa, Toshiyuka Aida*, Tatsumi Hirano** and Katsuhisa Usami***
Advanced Research Laboratory, Hitachi, Ltd., Saitama 350-03, Japan
*Central Research Laboratory, Hitachi, Ltd., Tokyo 185, Japan
**Hitachi Research Laboratory, Hitachi, Ltd., Ibaraki 316, Japan

In an $YBa_2Cu_3O_x$ system, it has been clarified that the oxygen content profoundly affects not only crystal structure but also superconducting transition temperature(Tc). Oxygen atoms are known to occupy O(1), O(2), O(3) and O(4) sites in an orthorhombic $YBa_2Cu_3O_x$, and of these sites, an O(1) site plays a most important role in superconductivity. Compared with x-ray photons, neutron has a relatively larger scattering cross section for oxygen atoms. Neutron diffraction measurements, therefore, yield a more reliable measurement of the oxygen distribution in $YBa_2Cu_3O_x$ bulk maretials. For thin films, however, neutron diffraction is not valid, because the signal-to-background ratio from thin films is low. This paper, therefore, reports the use of extended x-ray absorption fine structure (EXAFS) for the nondestructive determination of the occupation probability of an O(1) site in an orthorhombic $YBa_2Cu_3C_x$. EXAFS spectroscopy is a powerful probe for a local atomic arrangement around a atom of a specific element.

An epitaxial $YBa_2Cu_3O_x$ film, which was grown on a (110) $SrTiO_3$ substrate by using a conventional sputtering technique, was investigated in this study. The film thickness is roughly 0.7 μm. The Tc of the film is 89K. The cross sectional TEM image and x-ray diffraction profile reveal that the film has a (110) preferred orientation and a twinned structure with respect to the a and b axes.

An EXAFS spectrum is measured by a fluorescence x-ray mode. Synchrotron radiation is used as a photon source. This mode is sensitive to films with a thickness of less than a few μm. Synchrotron radiation provides an intensive and nearly poralized x-ray beam. Combining these advantages, makes it possible to measure an atomic arrangement along a specific direction of thin films. The polarization vector E was adjusted to the film's a and b axe. Cu K-edge spectrum was measured in air at room temperature. The local atomic arrangement around a Cu atom was extracted by a Fourier transformation of a measured spectrum. The contribution of only CuO bonds was transformed back into k-space so as to obtain the EXAFS oscillation due to Cu(2)-O(2), Cu(2)-O(3), and Cu(1)-O(1) bonds. Both Cu(2)-O(2) and Cu(2)-O(3) contribution are calculated according to a spherical wave approximation using crystal parameters obtained by Izumi et al. and were then subtracted from the original EXAFS oscillation. The final EXAFS oscillation, which is due to a Cu(1)-O(1) bond, was analyzed by a curve-fit method based on a spherical wave approximation.

The Cu(1)-O(1) distance thus determined was 1.85 A and the occupation probability on an O(1) site was 0.90-1.00. Thus the oxygen content x in an orthorhombic $YBa_2Cu_3O_x$ is 6.95-7.0. It should be noted here that an EXAFS spectroscopy can detect all oxygen atoms whether or not they are regularly distributed in a Cu(1) plane. Accordingly the occupation probability on an O(1) site is equal to or greater than that determined by neutron diffraction measurements.

MICROSCOPIC STUDIES OF YBCO SINGLE CRYSTALS

D109

A. Drake, M. Rand, M. Aindow and J.S. Abell
School of Metallurgy and Materials, University of Birmingham, UK

The microstructure of crystals of YBCO grown by the self flux method have been compared with that of crystals grown by an alternative method involving the use of an additive flux. Optical and electron microscopy observations have shown that twin morphologies and interactions, and density of inclusions and other defects depend on the method employed. In some cases, specific twin intersections appear to be avoided with parallel bands of shorter intermediate twins generated in the manner of classic accommodation twins to relieve localized stress concentrations. The crystallography of these twin formations and distribution has been examined by means of high resolution synchrotron x-ray diffraction. In contrast, complex interactions between bands of twins can also be seen, leading to the formation of a regular network of twin intersections. The detailed surface topography of as-grown and cleaved surfaces of crystals has been examined by atomic force microscopy. Fine arrays of growth steps with heights of the order of 10nm are observed which often exhibit significant deviations from linearity where the growth front has apparently been held up or deflected. Nucleation sites for new crystals occur in the surface, round which a recess with interrupted stepped growth fronts can be observed.

ADDENDUM

CRYSTAL GROWTH AND LUMINESCENT PROPERTIES OF NEODIMIUM ACTIVATED LANTHANUM HEXAALUMINATES

M. Namtalishvili, F. Todria, A. Mikaberidze, G. Brodzeli, Z. Khorbaladze and N. Tsorikishvili
Geological Institute, Georgian Academy of Sciences, USSR

Single crystals of neodimium activated lanthanum hexaaluminates $La_{1-x}Nd_xMgAl_{11}O_{19}$ with the magnetoplumbite structure appear as a possible substitute for the YAG:Nd3+, the most widely used solid state laser up till now (1,2).

$LaMgAl_{11}O_{19}$:Nd single crystals have been grown in our laboratory from the melt in the (100) direction through the vertical and horizontal directional crystallization under inert or argon + hydrogen atmospheres.

The investigation of crystal growth conditions has shown that the most perfect crystals are grown by the horizontal directional crystallization. In this case the elements of directional crystallization are combined with those of zone melting.

Crystallization is carried out in the conditions of sufficiently developed mirror of melting, that helps the evaporation of irrelevant impurities. As a result in this case the chemical purity of crystals increases.

We have also studied the spectra-luminescent properties of the grown crystals (3). Thus the Nd-ions $^4F_{3/2}$ metastabile state lifetime has been measured for the crystals grown in different gase areas.

(1) A. Kahn, A.M. Lejus, M. Madsac, J. Thery, and D. Vivien, *J. Appl. Phys.*, **52**(11), 6864 (1981).
(2) A. Kahn, J. Lecome, J. Thery, and D. Vivien, *J. Solid State Chem.* **76**, 192 (1988).
(3) M. Namtalishvili, T. Todria, A. Mikaberidze, N. Tsorikishvili, Z. Khorbaladze, *Bull. Academy of Sciences of the Georgian Republic*, **137**, 61 (1990).

THE IMPROVED MODEL OF STEADY-STATE LPE GROWTH FROM SOLUTION

O.B. Nevsky, I.V. Morgunov and L.V. Kozhitov*
*All-Union Research Institute of Chemical Technology
Kashirskoye Shosse 33, 115230 Moscow, USSR
Moscow Institute of Steel and Alloys
Lenin Prospect 4 117936 Moscow, USSR

The model of steady-state LPE growth by the solution cooling at a constant rate a has been published previously [1,2,3] for the growth period $t > h_s^2 \cdot D$, where: D - solute diffusion coefficient, h_s - distance from the substrate, where the solution supersaturation ΔC_s takes place:

$$\text{Delta}C_s = \frac{\alpha \cdot m \cdot h_s^2}{2D}, \text{ where } m = \frac{dc}{dT} - \text{the slope of liquidus.}$$

An improved model of steady-state LPE growth is based on an assumption that three critical supersaturations or supercoolings of the solution can be formed during LPE growth: the initial ΔT_i, creating the precrystallization clusters in the solution, nucleating ΔT_n, creating the first solid solute nuclei and maximum ΔT_m, creating the second growth plane on the solid nuclei in the solution.

The experimental data on silicon LPE growth from a tin solution between two horizontal substrates allowed to calculate the experimental values ΔT_i, ΔT_n, ΔT_m [4].

The equations for calculations of the epitaxial layer thickness on the upper and lower substrates were proposed.

All the published experimental values ΔT_i and ΔT_m for LPE growth are summarized. These values presumably depend on chemical bonds in the solutions.

1) A.Ju.Malinin, O.B. Nevsky et al.: *J. Electron Mat.*, 1978, 7, 757, 775.
2) O.B. Nevsky, A.I. Noghinov, I.N. Kuznetsov: Kristall und Technik, 1980, 15, 517.
3) A.Ju.Malinin, O.B. Nevsky et al.: Kristall und Technik, 1978, 13, 915.
4) L.V. Kozhitov, M.P. Volkov, A.S. Aristov: Electr. Technika seria 6, Materials, 1986, 6(217), 20 (Russian).
5) O.B. Nevsky, M.S. Minazhdinov et al.: Electr. Technika, seria 6, Materials, 1979, 10(135), 39 (Russian)..

METHOD OF LIQUID-PHASE HETEROEPITAXY IN $C^{IV}A^{III}B^{V}$ SYSTEMS

Vadim A. Mokritski and Vjacheslav S. Shobik
Odessa Polytechnic Institute, Odessa, Ukraine

Phase diagrams of ternary and quaternary systems including C^{IV} and $A^{III}B^{V}$ compounds are of eutectic types. Eutectic epitaxy (i.e. epitaxy from solutions saturated by C^{IV} and $A^{III}B^{V}$ simultaneously) in these systems has some peculiarities and application of tradition cooling technique for $A^{III}B^{V}$ heteroepitaxial growth is not possible because of substrate dissolution [1-3].

We propose to grow such heteroepitaxial layers by special step-cooling of new-eutectic solution. In accordance to this technique solution saturated by C^{IV} and $A^{III}B^{V}$ simultaneously will be prepared. Then solution will be slightly overheated, saturated by desire layer material only, supercooled for some degrees and inserted on the substrate for heteroepitaxy. As usually for step-cooling technique layer's thickness will be depended on degree of solution supercooling and growth time.

For example, proposed method was checked in the Sn-Ge-GaAs quasy-ternary system for growth of GaAs layer on Ge(iii) substrate. Epitaxy temperature was 650-750°C, supercooling did not exceed 5°C, growth time was 2-10 minutes. As a result EBM-analysis revealed a growth of thin (about 1-2 m) layer of GaAs.

Obtained results and possibilities of proposed technique for heteroepitaxy in another systems are discussed.

1. Jordan, A.S., Weiner, M.E., *J. Electrochem. Soc.* 121 (1974) 1634,
2. Zavadski, V.A., Mokritski V.A., Shobik, V.S. *Sov. Phys. Chem. Material Treatment*, N4 (1977) 137.
3. Kazakov, A.I. et al. *Cryst. Res. Techno.* **25** (1990) K114.

AUTHOR INDEX

AUTHOR INDEX (Cont'd)

AUTHOR INDEX (Cont'd)

AUTHOR INDEX (Cont'd)

AUTHOR INDEX (Cont'd)

AUTHOR INDEX (Cont'd)